



Terms and Conditions of Use of Digitised Theses from Trinity College Library Dublin

Copyright statement

All material supplied by Trinity College Library is protected by copyright (under the Copyright and Related Rights Act, 2000 as amended) and other relevant Intellectual Property Rights. By accessing and using a Digitised Thesis from Trinity College Library you acknowledge that all Intellectual Property Rights in any Works supplied are the sole and exclusive property of the copyright and/or other IPR holder. Specific copyright holders may not be explicitly identified. Use of materials from other sources within a thesis should not be construed as a claim over them.

A non-exclusive, non-transferable licence is hereby granted to those using or reproducing, in whole or in part, the material for valid purposes, providing the copyright owners are acknowledged using the normal conventions. Where specific permission to use material is required, this is identified and such permission must be sought from the copyright holder or agency cited.

Liability statement

By using a Digitised Thesis, I accept that Trinity College Dublin bears no legal responsibility for the accuracy, legality or comprehensiveness of materials contained within the thesis, and that Trinity College Dublin accepts no liability for indirect, consequential, or incidental, damages or losses arising from use of the thesis for whatever reason. Information located in a thesis may be subject to specific use constraints, details of which may not be explicitly described. It is the responsibility of potential and actual users to be aware of such constraints and to abide by them. By making use of material from a digitised thesis, you accept these copyright and disclaimer provisions. Where it is brought to the attention of Trinity College Library that there may be a breach of copyright or other restraint, it is the policy to withdraw or take down access to a thesis while the issue is being resolved.

Access Agreement

By using a Digitised Thesis from Trinity College Library you are bound by the following Terms & Conditions. Please read them carefully.

I have read and I understand the following statement: All material supplied via a Digitised Thesis from Trinity College Library is protected by copyright and other intellectual property rights, and duplication or sale of all or part of any of a thesis is not permitted, except that material may be duplicated by you for your research use or for educational purposes in electronic or print form providing the copyright owners are acknowledged using the normal conventions. You must obtain permission for any other use. Electronic or print copies may not be offered, whether for sale or otherwise to anyone. This copy has been supplied on the understanding that it is copyright material and that no quotation from the thesis may be published without proper acknowledgement.

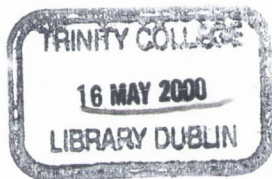
***ON THE MOLECULAR GENETICS OF RETINAL
DYSTROPHIES AND GLAUCOMA***

A Thesis Submitted to the University of Dublin for the Degree of Doctor of
Philosophy

by

Avril Maria Kennan
Department of Genetics
University of Dublin
Trinity College
Dublin

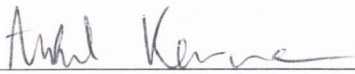
November 1999



THESIS
5628

DECLARATION

This thesis has not been previously submitted to this or any other university for examination for a higher degree. The work presented here is entirely my own except where noted. This thesis may be made available for consultation within the university library. It may be photocopied or lent to other libraries for purposes of consultation.



Avril Kennan

November, 1999

Dedicated to Jim

❖ *Acknowledgements* ❖

I would like to give sincere thanks to my supervisor, Pete for his constant support and guidance from day one of this thesis. I feel privileged to have been part of the lab and to work alongside all the wonderful people in it; Jane, Paul, Sophia, Gearoid, Denis, Marian, Denise, Mary, Sophie, Fiona, Alex and Michael. There isn't one of them who didn't help at one time or another. Thanks also to the guys in the prep room. In particular I want to thank my dear friends Niamh and Brian with whom I was very lucky to share the whole PhD experience with.

There are a number of other people in the science world who deserve particular thanks: Catherine Winchester in Glasgow for giving so generously of her time to show me the in situ technique and for introducing me to the Scottish Ceile; our collaborators in the States, Steve Daiger and colleagues, in particular Sara for her many informative e-mails; Carmen Ayuso in Spain for supplying DNA and clinical data and most importantly, all the families who participated in these studies.

Thanks to my many wonderful friends for putting up with me not being able to afford them pints; particularly to Pauline and Anne for frequent warm dinners and lifts and the girls in the house for seeing me through it. Thanks also to my family and extended family who have always been so encouraging. My parents are particularly amazing and I couldn't possibly mention all the ways they should be thanked. Even when I make the occasional wild suggestion such as becoming an archaeologist, they are still incapable of being anything but supportive!

Thanks beyond compare must go to Kieran for his ever eagerness to repay those many evenings in the biomechanics lab in Jordanstown! I don't think you quite clocked up the hours but you more than made up for it with your never failing support and love. It won't ever be forgotten.

TABLE OF CONTENTS

| | Page |
|-------------------|-------------|
| Title page | I |
| Declaration | II |
| Acknowledgements | IV |
| Table of contents | V |
| List of tables | XII |
| List of figures | XIII |
| Summary | XVI |
| Publications | XVIII |
| Abbreviations | XIX |

CHAPTER 1: GENERAL INTRODUCTION

| | | |
|-------|--|----|
| 1.0 | INTRODUCTION | 2 |
| 1.1 | The eye | 2 |
| 1.1.1 | The retina | 3 |
| 1.1.2 | The photoreceptors | 4 |
| 1.1.3 | Visual transduction | 5 |
| 1.2 | HEREDITARY EYE DISORDERS | 8 |
| 1.2.1 | Retinitis pigmentosa and related disorders | 9 |
| 1.2.2 | Congenital stationary night-blindness | 10 |
| 1.2.3 | Macular dystrophies | 10 |
| 1.2.4 | Cone-rod and cone dystrophies | 12 |
| 1.2.5 | The role of apoptosis in the retinal dystrophies | 12 |
| 1.2.6 | Glaucoma | 13 |
| 1.3 | IDENTIFICATION OF DISEASE GENES | 13 |
| 1.3.1 | Genetic mapping | 14 |
| 1.3.2 | Physical mapping | 17 |
| 1.3.3 | Identifying candidate genes | 18 |
| 1.3.4 | Screening candidate genes | 19 |

CHAPTER 2: RE-EVALUATION OF THE RP10 LINKAGE DATA AND THE SCREENING OF TWO CANDIDATE GENES FOR THE RP10 MUTATION

| | | |
|--------|--|----|
| 2.1.1 | INTRODUCTION | 23 |
| 2.1.2 | Clinical features of RP | 23 |
| 2.1.3 | The diagnosis of RP | 24 |
| 2.1.4 | Genetics of RP | 25 |
| 2.1.5 | Autosomal dominant RP loci | 26 |
| 2.1.6 | Autosomal recessive RP loci | 29 |
| 2.1.7 | X-linked RP loci | 31 |
| 2.1.8 | Syndromic RP | 32 |
| 2.1.9 | A locus for adRP on chromosome 7q | 32 |
| 2.1.10 | Candidate disease genes on 7q | 34 |
| 2.1.11 | Metabotropic glutamate receptors and GRM8 | 36 |
| 2.1.12 | RT-PCR on illegitimate transcripts | 38 |
| 2.1.13 | Diacylglycerol Kinases and DGK ₁ | 39 |
| 2.1.14 | Study Aim | 41 |
| 2.2 | MATERIALS AND METHODS | 42 |
| 2.2.1 | Patient clinical assessment and DNA extraction | 42 |
| 2.2.2 | PCR amplification | 42 |
| 2.2.3 | Microsatellite analysis | 43 |
| 2.2.4 | Linkage analysis | 43 |
| 2.2.5 | Large scale plasmid purification (maxiprep) | 43 |
| 2.2.6 | Single stranded conformational polymorphism electrophoresis (SSCP) analysis. | 44 |
| 2.2.7 | Sepharose columns | 45 |
| 2.2.8 | PCR purification for sequencing | 45 |
| 2.2.9 | Automated sequencing | 45 |
| 2.2.10 | End-labeling of primers for direct sequencing | 46 |
| 2.2.11 | Direct sequencing | 46 |
| 2.2.12 | RNA preparation | 46 |
| 2.2.13 | RT-PCR and nested PCR on illegitimate transcripts | 47 |
| 2.2.14 | PCR digestion | 48 |

| | | |
|-------|--|----|
| 2.3 | RESULTS AND DISCUSSION | 49 |
| 2.3.1 | Re-haplotyping of the 7q interval in family FA-84 | 49 |
| 2.3.2 | Elucidating the genomic structure of GRM8 | 53 |
| 2.3.3 | Mutational screening of GRM8 in family FA-84 | 54 |
| 2.3.4 | Mutational screening of portion of GRM8 using illegitimately transcribed RNA | 55 |
| 2.3.5 | Screening of GRM8 in family CVRP4 | 56 |
| 2.3.6 | Screening of DGK ι in family FA-84 | 57 |
| 2.4 | CONCLUSION | 59 |

CHAPTER 3: METHODS TO IDENTIFY CANDIDATES FOR THE RP10 GENE

| | | |
|--------|--|----|
| 3.1 | INTRODUCTION | 61 |
| 3.1.1 | Introduction | 61 |
| 3.1.2 | Long range PCR | 61 |
| 3.1.3 | ESTs | 62 |
| 3.1.4 | The rhodopsin knockout mouse | 64 |
| 3.1.5 | <i>In situ</i> hybridization on tissue sections | 65 |
| 3.1.6 | Study aim | 70 |
| 3.2 | MATERIALS AND METHODS | 71 |
| 3.2.1 | Phage library titration | 71 |
| 3.2.2 | Phage library amplification | 71 |
| 3.2.3 | Phage DNA extraction | 72 |
| 3.2.4 | Long range PCR amplification | 73 |
| 3.2.5 | Reverse transcriptase - PCR (RT-PCR) | 73 |
| 3.2.6 | Preparation of the template DNA for ISH riboprobe | 73 |
| 3.2.7 | Transcription of riboprobe from template DNA | 74 |
| 3.2.8 | Dot blot to test labeling of riboprobe | 74 |
| 3.2.9 | Coating slides for ISH | 75 |
| 3.2.10 | Tissue Preparation for cryosections | 75 |
| 3.2.11 | <i>In situ</i> hybridization protocol for cryosections | 75 |
| 3.2.12 | <i>In situ</i> hybridization protocol for paraffin embedded sections | 78 |

| | | |
|-------|--|----|
| 3.3 | RESULTS AND DISCUSSION | 82 |
| 3.3.1 | A novel method involving long range PCR in an attempt to isolate RP10 | 82 |
| 3.3.2 | Expressed sequence tags (ESTs) mapping to the RP10 disease interval | 83 |
| 3.3.3 | A novel method to determine whether candidate genes are rod photoreceptor specific | 86 |
| 3.3.4 | Testing 7q ESTs for rod photoreceptor specificity | 87 |
| 3.3.5 | Development of the ISH technique on tissue sections | 88 |
| 3.3.6 | ISH on human eye sections | 90 |
| 3.4 | CONCLUSION | 92 |

CHAPTER 4: THE IDENTIFICATION OF A NOVEL ASP380ALA MUTATION IN THE MYOCILIN GENE IN A FAMILY WITH JUVENILE ONSET PRIMARY OPEN ANGLE GLAUCOMA

| | | |
|-------|--|-----|
| 4.1 | INTRODUCTION | 95 |
| 4.1.1 | Introduction | 95 |
| 4.1.2 | Glaucoma | 95 |
| 4.1.3 | Primary open-angle glaucoma | 96 |
| 4.1.4 | Genetic loci implicated in glaucoma | 97 |
| 4.1.5 | The GLC1A locus | 99 |
| 4.1.6 | The TIGR/myocilin gene | 100 |
| 4.1.7 | The involvement of myocilin in POAG | 101 |
| 4.1.8 | Family TCD-POAG1 | 102 |
| 4.1.9 | The aim of the study | 102 |
| 4.2 | MATERIALS AND METHODS | 103 |
| 4.2.1 | Patient diagnosis | 103 |
| 4.2.2 | DNA extraction | 103 |
| 4.2.3 | PCR digestion | 104 |
| 4.3 | RESULTS AND DISCUSSION | 105 |
| 4.3.1 | Screening of the myocilin gene in family TCD-POAG1 | 105 |

| | | |
|-------|--|-----|
| 4.3.2 | Screening of all family members and control individuals for the Asp380Ala mutation | 105 |
| 4.3.3 | Anomalies in diagnostic status | 106 |
| 4.3.4 | The effects of the Asp380Ala mutation at the molecular level | 106 |
| 4.4 | CONCLUSION | 108 |

CHAPTER 5: RETINITIS PIGMENTOSA AND PROGRESSIVE SENSORINEURAL HEARING LOSS CAUSED BY A C12258A MUTATION IN THE MITOCHONDRIAL MTT2 GENE.

| | | |
|-------|--|-----|
| 5.1 | INTRODUCTION | 110 |
| 5.1.1 | Introduction | 110 |
| 5.1.2 | Usher syndrome | 110 |
| 5.1.3 | Family ZMK | 112 |
| 5.1.4 | The search for the ZMK disease gene | 113 |
| 5.1.5 | The mitochondria | 114 |
| 5.1.6 | Mitochondrial mutations | 116 |
| 5.1.7 | Mitochondrial diseases involving RP and/or sensorineural deafness | 118 |
| 5.1.8 | The aim of the study | 121 |
| 5.2 | MATERIALS AND METHODS | 122 |
| 5.2.1 | Patient Clinical assessment | 122 |
| 5.3 | RESULTS AND DISCUSSION | 123 |
| 5.3.1 | Evidence implicating the mitochondria in the disease in family ZMK | 123 |
| 5.3.2 | Sequencing the mitochondria | 124 |
| 5.3.3 | Evidence of the pathogenicity of the C12258A mutation | 125 |
| 5.3.4 | Analysis of levels of heteroplasmy of the C12258A mutation and correlation with disease symptoms | 127 |
| 5.3.5 | Influences on the expression of the disease in family ZMK | 130 |
| 5.3.6 | Effects of the C12258A mutation at the molecular level | 131 |
| 5.3.7 | The identification of the C12258A mutation in a second family | 133 |

| | | |
|-------|---|-----|
| 5.3.8 | Screening of Usher syndrome patients for the C12258A mutation | 133 |
| 5.4 | CONCLUSION | 136 |

CHAPTER 6: INVESTIGATIONS INTO THE ETIOLOGY OF AMD IN THE IRISH POPULATION

| | | |
|--------|--|-----|
| 6.1 | INTRODUCTION | 138 |
| 6.1.1 | Introduction | 138 |
| 6.1.2 | The macular degenerations | 138 |
| 6.1.3 | Age related macular dystrophy | 139 |
| 6.1.4 | Risk factors for AMD | 140 |
| 6.1.5 | The involvement of ABCR in STGD | 141 |
| 6.1.6 | The involvement of ABCR in RP and CORD | 142 |
| 6.1.7 | The involvement of ABCR in AMD | 143 |
| 6.1.8 | Speculation on the role of ABCR in AMD | 144 |
| 6.1.9 | The ABCR protein and disease etiology | 145 |
| 6.1.10 | The role of apoptosis in photoreceptor cell death | 146 |
| 6.1.11 | Light-induced apoptosis | 147 |
| 6.1.12 | The role of the RPE65 gene in a protective effect against light-induced apoptosis | 148 |
| 6.1.13 | The RPE65 protein | 149 |
| 6.1.14 | The role of RPE65 in retinal dystrophies | 150 |
| 6.1.15 | The aim of the study | 150 |
| 6.2 | MATERIALS AND METHODS | 152 |
| 6.2.1 | Patient Clinical assessment and DNA extraction | 152 |
| 6.2.2 | Control DNAs | 152 |
| 6.2.3 | PCR digestion of RPE65 PCRs | 152 |
| 6.3 | RESULTS AND DISCUSSION | 153 |
| 6.3.1 | Screening of the ABCR gene in AMD patients | 153 |
| 6.3.2 | Results of screening human RPE65 gene | 155 |
| 6.4 | CONCLUSION | 157 |

| | |
|--|-----|
| REFERENCES | 158 |
| APPENDIX A: stock solutions | 203 |
| APPENDIX B: primer sequences | 211 |
| APPENDIX C: cloned and/or mapped genes causing retinal diseases | 222 |

LIST OF TABLES

| | | |
|------------------|---|-----|
| Table 2.1 | A comparison of lod scores obtained with particular 7q microsatellite markers in the original linkage study and the recently re-calculated lod scores for the same markers. | 52 |
| Table 2.2 | The order and distances of microsatellite markers used in this study on chromosome 7q. | 53 |
| Table 3.1 | Details of the ESTs mapping to the 7q critical disease interval which have been identified as candidates for the RP10 gene. | 85 |
| Table 5.1 | Sequence variations found in family ZMK members. | 125 |
| Table 5.2 | CLUSTAL W (1.7) multiple sequence alignment of the MTTTS2 gene in various species. | 126 |
| Table 5.3 | Estimated levels of heteroplasmy of the C12258A mutation for members of family ZMK | 129 |
| Table 5.4 | The number and percentage of the tRNA serine AGU/C codons within each of the protein coding genes of the mitochondrion. | 132 |
| Table 5.5 | Summary of known clinical symptoms of Usher syndrome patients screened for the C12258A mutation. | 135 |

LIST OF FIGURES

- Figure 1.1** Schematic diagram of rod and cone photoreceptors.
- Figure 1.2** Schematic diagram of the visual transduction process.
- Figure 2.1** Fundus photographs of a normal and an RP retina.
- Figure 2.2** Electroretinogram responses from healthy and RP individuals.
- Figure 2.3** Family FA-84 pedigree.
- Figure 2.4** Microsatellite D7S686 typed through members of family FA-84.
- Figure 2.5** Microsatellite D7S530 typed through members of family FA-84.
- Figure 2.6** Haplotype analysis of family FA-84 across the RP10 interval on chromosome 7q.
- Figure 2.7** Schematic diagram of the structure of the GRM8 gene.
- Figure 2.8** Schematic representation of primers used in RT-PCR of illegitimate GRM8 transcripts
- Figure 2.9** Amplification products following RT-PCR on GRM8 illegitimate transcripts.
- Figure 2.10** Family CVRP4 pedigree.
- Figure 2.11** Typing of an intragenic intron 31 DGK ι polymorphism using SSCP analysis.

- Figure 2.12** sequence analysis of the DGK ι intron 31 polymorphism identified by SSCP.
- Figure 2.13** *EcoRI* digest of PCR products spanning the DGK ι intron 31 polymorphism.
- Figure 2.14** Genotyping of the DGK χ intron 31 polymorphism in family FA-84.
- Figure 3.1** PCR analysis of 20 fractions of a human total genomic library using marker D7S680 primers.
- Figure 3.2** RT-PCR on RNA extracted from Rho $^{+/+}$ mice and Rho $^{-/-}$ mice using cGMP and mGluR8 primers.
- Figure 3.3** A cross-section of a normal mouse retina, stained with haematoxylin and eosin.
- Figure 3.4** *In situ* hybridizations on mouse retinal cryosections with rhodopsin and peripherin/rds probes.
- Figure 3.5** Mouse rhodopsin antisense probe hybridised to a rat eye section shown alongside controls.
- Figure 3.6** Histological features of human retinal sections used in *in situ* hybridizations.
- Figure 4.1** Family TCD-POAG1 pedigree.
- Figure 4.2** Fundus photograph of TCD-POAG1 individual.
- Figure 4.3** Partial nucleotide sequence from a genomic PCR amplification product of exon 3 of the myocilin gene showing a heterozygous C to A substitution.

- Figure 4.4** *Sty I* digestion of genomic 197bp PCR amplification product of exon 3 of the myocilin gene.
- Figure 5.1** Family ZMK pedigree.
- Figure 5.2** Fundus photographs from affected ZMK individuals.
- Figure 5.3** Mitochondrial sequence analysis of family ZMK individuals showing the C12258A mutation.
- Figure 5.4** SSCP analysis using PCR products spanning the C12258A mutation from members of family ZMK.
- Figure 5.5** Automated sequence analysis of mitochondrial samples from an Usher syndrome patient, shown alongside an affected ZMK individual.
- Figure 6.1** Sequence analysis of the ABCR gene of an Irish AMD patient; individual AMD 6.
- Figure 6.2** Fluorescein angiogram of AMD individual 6 shown alongside fluorescein angiogram of normal individual.
- Figure 6.3** Multiple sequence of exon 13 of the RPE65 gene in five different species including human.
- Figure 6.4** *Alu I* digest of the RPE65 exon 13 PCR product.
- Figure 6.5** Schematic representation of assay to determine the presence or absence of a leucine to methionine substitution at amino acid position 450 of the RPE65 gene.

SUMMARY

The central aim of this thesis was the elucidation of the underlying molecular pathologies of inherited diseases of the eye. Previous linkage studies on a large Spanish kindred (family FA-84), segregating adRP, resulted in the localisation of an adRP gene (RP10) to chromosome 7q31.3 (Jordan *et al.*, 1993). Linkage and haplotype data were re-evaluated in this family and two novel genes were adopted as candidates. These genes encoded a metabotropic glutamate receptor, GRM8, and a diacylglycerol kinase, DGK ι . Prior to mutation screening it was necessary to determine much of the structure of GRM8. The gene was screened using both single-stranded conformational polymorphism (SSCP) analysis and direct sequencing. A small portion of the gene for which the intron/exon structure was unknown was screened following RT-PCR on illegitimate transcripts in blood. No mutations were identified in GRM8. SSCP analysis of the DGK ι gene resulted in the identification of a two-allele polymorphism which also allowed exclusion of this gene as RP10.

Following exclusion of these two genes as candidates it was necessary to search for novel genes mapping to the RP10 interval. A number of approaches were taken. The first involved the use of long range PCR in an attempt to generate a PCR fragment contig across the RP10 interval. However, difficulties inherent in the use of long range PCR rendered this technique unsuccessful. Attention was then directed toward the developments in the identification and mapping of human expressed sequence tags (ESTs). Owing to the large number of ESTs mapping to the RP10 interval on chromosome 7q it was necessary to prioritise particular ESTs for further examination as RP10 candidates. Methods to learn more of expression patterns of ESTs were therefore developed, involving both RT-PCR on RNA extracted from normal and knockout rhodopsin mice and *in situ* hybridizations on eye tissue sections. *In situ* hybridisation experiments with DIG-labelled ribprobes were demonstrated to be an appropriate approach. While successful with a rhodopsin probe on mice eyes, these experiments were hindered by difficulties in ascertaining human eye sections with well preserved RNA transcripts.

A gene for juvenile onset primary open-angle glaucoma (JOAG), encoding the so-called trabecular meshwork induced glucocorticoid (TIGR, also known as myocilin), has recently been identified on 1q21-31. Family TCD-POAG1 is a Spanish kindred which segregates JOAG in an autosomal dominant fashion and had previously been

found to be linked to the myocilin region of chromosome 1 (Mansergh, 1997). Direct sequencing of the gene was carried out in this family and revealed a heterozygous A to C transition in codon 380, resulting in the substitution of alanine for aspartic acid (Asp380Ala). This substitution created a *StyI* restriction site, which segregated with the JOAG phenotype and permitted rapid screening of all members of the family and control individuals. The results indicated that this substitution is causative of the disease in family TCD-POAG1.

Family ZMK is a large Irish kindred segregating RP and sensorineural deafness. The absence of a definitive genomic disease locus in family ZMK and the similarity of the disease in the family to documented mitochondrial disorders led to the consideration of mitochondrial inheritance. Screening of the mitochondrial genome, in conjunction with other members of the laboratory, was therefore carried out. This resulted in the identification of a C to A transversion at position 12258 of the mitochondrial genome, within the second mitochondrial serine tRNA, MTTS2 which was demonstrated to be heteroplasmic in the family. This, together with its absence from 270 normal controls and the conservation of the C residue in 12 species, indicates that the mutation is very likely responsible for the disease phenotype in family ZMK. The MTTS2 gene was also screened in 19 Usher syndrome patients but no mutations were identified.

Recently a retina specific member of the ABC transporter family of genes, ABCR, has been implicated in age-related macular dystrophy (AMD). The initial stages of screening the ABCR gene in AMD individuals from the Irish population revealed a variant in exon 48 of the gene in a patient with exudative (wet) AMD. This variant had been previously reported in non-exudative (dry) AMD sufferers of the American population. Its identification in an Irish AMD patient provides further evidence that this variant may be AMD-associated, and significantly, that it may be involved in wet, as well as dry, AMD.

Of further reference to AMD, a variant at codon 450 of the RPE65 gene has recently been associated with a protective effect against light-induced apoptosis of the photoreceptor cells in a strain of albino mice. Sunlight has been reported as a risk factor for AMD. Thus, screening of the RPE65 gene codon 450 was carried out in both AMD and normal individuals in order to investigate any potential role of the RPE65 gene in susceptibility to light damage in humans. The results of the analysis revealed that the site in question is not polymorphic in humans and therefore not connected to AMD susceptibility in man.

PUBLICATIONS ARISING FROM WORK DURING THIS THESIS:

Kennan AM, Mansergh FC, Fingert JH, Clark T, Ayuso C, Kenna PF, Humphries P, Farrar GJ (1998). A novel Asp380Ala mutation in the GLC1A/myocilin gene in a family with juvenile onset primary open angle glaucoma. *J Med Genet* **35**(11):957-60

Mansergh FC, Millington-Ward S, Kennan A, Kiang AS, Humphries M, Farrar GJ, Humphries P, Kenna PF (1999). Retinitis Pigmentosa and Progressive Sensorineural Hearing Loss Caused by a C12258A Mutation in the Mitochondrial MTT2 Gene. *Am J Hum Genet.* **64**(4):971-985

Bowne SJ, Sullivan LS, Ding L, Traer E, Prescott SM, Birch DG, Heckenlively JR, Kennan AM, Humphries P, Daiger SP (1999). Evaluation of human diacylglycerol kinase iota, a homolog of *Drosophila rdgA*, in inherited retinopathy mapping to 7q. In preparation.

Millington-Ward S, O'Neill B, Tuohy G, Al-Jandal N, Kiang AS, Kenna PF, Palfi A, Hayden P, Mansergh F, Kennan A, Humphries P, Farrar GJ (1997). Strategems in vitro for gene therapies directed to dominant mutations. *Hum Mol Genet.* **6**(9):1415-26

ABBREVIATIONS

| | |
|------|--|
| ABC | ATP-binding cassette |
| adRP | Autosomal dominant retinitis pigmentosa |
| AMD | Age-related macular dystrophy |
| ANT | Adenine nucleotide translocator |
| APES | 3-aminopropyl-triethoxysilane |
| arRP | Autosomal recessive retinitis pigmentosa |
| ATCC | American Type Culture Collection |
| ATP | Adenosine tri-phosphate |
| BAC | Bacterial artificial chromosome |
| BCIP | 5-Bromo-4-chloro-3-indolyphosphate |
| cDNA | Complementary DNA |
| CEPH | Centre d'Etude du Polymorphisme Humain |
| cGMP | Cyclic guanosine monophosphate |
| cM | Centimorgan |
| COAG | Chronic open angle glaucoma |
| CORD | Cone-rod retinal dystrophy |
| CPEO | Chronic progressive external ophthalmoplegia |
| CSNB | Congenital stationary night-blindness |
| CSRD | Childhood-onset severe retinal dystrophy |
| DAG | Diacylglycerol |
| DEPC | Diethylpyrocarbonate |
| DGGE | Denaturing gradient-gel electrophoresis |
| DGK | Diacylglycerol kinase |
| DIG | Digoxygenin |
| dNTP | Di-nucleotide phosphate |
| DTT | Dithiothreitol |
| EDTA | Ethylenediaminetetra acetic acid |
| ERG | Electroretinogram |
| EST | Expressed sequence tag |
| ETC | Electron transport chain |
| FFM | Fundus flavimaculatus |
| FISH | Fluorescent <i>in situ</i> hybridization |
| GC | Guanylate cyclase |
| GDP | Guanosine diphosphate |
| GRM | Metabotropic glutamate receptor |
| GTP | Guanosine triphosphate |
| HCl | Hydrochloric acid |
| IGDA | Iridogoniodysgenesis anomaly |
| IGDS | Iridogoniodysgenesis syndrome |
| IOP | Intraocular pressure |
| ISH | <i>In situ</i> hybridization |

| | |
|--------|---|
| JOAG | Juvenile onset primary open-angle glaucoma |
| KSS | Kearns-Sayre syndrome |
| LCA | Leber congenital amaurosis |
| LDB | Genetic Location Database |
| LHON | Leber hereditary optic neuropathy |
| LOD | Log of the odds |
| MELAS | Mitochondrial encephalomyopathy, lactic acidosis and stroke-like episodes |
| MERRF | Myoclonic epilepsy and ragged-red fibre syndrome |
| mRNA | Messenger RNA |
| mtDNA | Mitochondrial DNA |
| NBT | Nitro-blue tetrazolium |
| NARP | Neuropathy, ataxia and retinitis pigmentosa |
| NHGRI | National Human Genome Research Institute |
| NIDDM | Non-insulin dependant diabetes mellitus |
| ORF | Open reading frame |
| PA | Phosphatic acid |
| OXPHOS | Oxidative phosphorylation |
| PBS | Phosphate buffered saline |
| PCR | Polymerase chain reaction |
| PDE | Phosphodiesterase |
| PKC | Protein kinase C |
| POAG | Primary open-angle glaucoma |
| QTL | Quantitative trait locus |
| RBP | Retinal binding protein |
| RCS | Royal College of Surgeons |
| RD | Retinal degeneration |
| RDS | Retinal degeneration slow |
| RFLP | Restriction fragment length polymorphism |
| ROS | Rod outer segment |
| ROS | Reactive oxygen species |
| RP | Retinitis pigmentosa |
| RPE | Retinal pigment epithelium |
| RT-PCR | Reverse transcriptase PCR |
| SDS | Sodium dodecyl sulphate |
| SRC | Subrhabdomeric cisternae |
| SSCP | Single stranded conformational polymorphism |
| STGD | Stargardt disease |
| STS | Sequence tagged site |
| THCs | Tentative human consensus sequences |
| tRNA | Transfer RNA |
| UTR | Untranslated region |
| UV | Ultra violet |
| VNTR | Variable number tandem repeat |

xlRP
YAC

X-linked retinitis pigmentosa
Yeast artificial chromosome

CHAPTER 1

GENERAL INTRODUCTION

1.0 INTRODUCTION

The primary aim of this thesis was the identification of genes involved in the etiology of a number of retinal dystrophies and glaucoma. The purpose of this introductory chapter is to place these studies in the context of the broad field of research into retinopathies and glaucoma. Since many of the genes which have been implicated to date in these diseases play a role in the process of visual transduction, or maintenance of the retina, the eye and the process of visual transduction are discussed in detail. An overview of the many hereditary retinopathies and glaucoma is also presented. Many of these diseases are discussed in great detail in subsequent chapters and so in order to avoid repetition they are mentioned only briefly in this introductory chapter. Finally, a discussion of the various methods applied to the mapping of disease genes and their identification is presented, with particular emphasis on methods used throughout the course of the present studies.

1.1 The eye

The eye is responsible for focusing incoming light on the retina and subsequently transducing that light into electrical impulses, the medium of the brain. It is comprised of three distinct layers: the sclera, the choroid and the retina. The sclera is the outermost, protective layer of the eye which is formed of opaque connective tissue. At the front of the eye the sclera joins with the protective transparent layer known as the cornea. Beneath the sclera lies the choroid. This is a layer of connective tissue which is highly vascularised and forms the ciliary body and iris to the front of the eye. Between the cornea and the iris lies the anterior chamber which is filled with a fluid referred to as aqueous humour. In the center of the highly pigmented iris is an opening known as the pupil which is responsible for allowing light into the eye. By virtue of its muscular tissue the iris adjusts the diameter of the pupil to allow more or less light to enter the eye, depending on the brightness of the environment.

Behind the iris lies the lens, a biconvex structure responsible for focusing light on the innermost layer of the eye, the retina. The lens is a crystalline, transparent

structure, the shape of which can be altered by the smooth muscles of the ciliary body (Newell, 1982). The area between the iris and the lens is known as the posterior chamber. This chamber is connected to the anterior chamber via the pupil. The ciliary process, which is part of the ciliary body, is responsible for the secretion of the aqueous humour into the posterior chamber. Encircling the circumference of the anterior chamber of the eye is the trabecular meshwork which filters the aqueous humour as it passes to the canal of Schlemm. From here the fluid passes into the anterior ciliary and the episcleral veins (Newell, 1982).

The interior chamber of the eye is known as the vitreous chamber and is filled with a transparent, gelatinous solution. This solution is referred to as the vitreous humour and is comprised of water, collagen, various proteins and a polysaccharide known as hyaluronic acid (Djamgoz *et al.*, 1995; Junqueira *et al.*, 1995).

The cornea, lens, aqueous and vitreous humour all play a role in angling and focusing light onto the retina. They possess different refractive indices to that of air and the refractive index of the lens is adjustable, making the focusing of images onto the retina possible (Newell, 1982).

1.1.1 The retina

The retina is a multi-layered tissue within which the process of visual transduction takes place. The layers of the retina are comprised of neural cells, responsible for the transduction of light to the optic nerve in the form of electrical signals. Contrary to what one might expect, the photoreceptor cells, which initiate the biochemical process of phototransduction, are at the back of the retina, meaning that light must pass through all other layers of the retina before it reaches them. The photoreceptor outer segments, inner segments and nuclei are clearly distinguishable as three distinct retinal layers. The cells which lie next to the photoreceptors are the bipolar cells. These cells form synapses with the photoreceptors on one side, in the outer plexiform layer, and with ganglion cells on the other, in the inner plexiform layer (Djamgoz *et al.*, 1995; Junqueira *et al.*, 1995). The cell bodies of the bipolar neurons are located in the inner nuclear layer. Dispersed among the bipolar cells are the amacrine and horizontal neurons. These cells are responsible for communication between adjacent bipolar cells and ganglion cells by way of lateral interactions (Newell, 1982; Dowling, 1987). The

innermost layer of the retina, adjacent to the vitreous humour, is formed by the ganglion cells, the axons of which form the optic nerve.

Another neuron type found in the retina are the glial cells. The glial cells may be divided into three classes: muller cells, astrocytes and microglia. The muller cells are found in all layers of the retina and play a role in supporting the other cell types (Djamgoz *et al.*, 1995; Junqueira *et al.*, 1995). They are involved in the mopping up of potassium ions which are released into the extracellular space following phototransduction, and they may play a role in vitamin A metabolism (Skatchkov *et al.*, 1999; Das *et al.*, 1992).

Lying directly behind the retina is the retinal pigment epithelium (RPE). The RPE is essential in the maintenance of the retina and the photoreceptors are partially embedded in it (Djamgoz *et al.*, 1995; Junqueira *et al.*, 1995). Because the RPE is heavily pigmented it absorbs excess light, helping to maintain high visual acuity (Djamgoz *et al.*, 1995; Junqueira *et al.*, 1995). It also plays more active roles in supplying nutrients to the photoreceptors and in the recycling of outer segment discs and components of the visual transduction pathway.

1.1.2 The photoreceptors

All visual responses in the retina are initiated by the photoreceptor cells. When light strikes a photoreceptor it sets in motion a sequence of events which finally results in the formation of an image in the brain. There are two types of photoreceptor cells: the rod photoreceptors, which govern dim light vision, and the cone photoreceptors, which mediate colour vision. The photoreceptors are elongated cells possessing a cell body, an inner segment and an outer segment (Figure 1.1). Rod and cones can be distinguished from each other on the basis of their shape. The rod outer segments are long and cylindrical while the cone outer segments are shorter and often tapered or conical (Molday, 1998). The cones are located most densely in the macula lutea, an area within the center of the retina which is yellow in colour. The fovea, the region of highest visual acuity in the retina is located within the macula and is completely devoid of rod photoreceptors. The design of the retina at this point is such that the various neural cell layers of the retina do not overlies the photoreceptors, thereby allowing light to hit the photoreceptors directly. Extending outwards from the fovea the concentration of the rod

cells increases and the cone cells are found in much lower numbers in the periphery of the retina (Newell, 1982; Dowling, 1987).

The rod photoreceptor cell body possesses the cell nucleus and extends into a terminal which synapses with the bipolar cells. Adjoining the cell body is the inner segment which contains organelles necessary for cellular function including endoplasmic reticulum, golgi apparatus and high numbers of mitochondria (Molday, 1998). Connected to the inner segment by a thin, non-motile cilium is the outer segment, where the process of visual transduction takes place.

Within the rod outer segment is a column of hundreds of membranous, flattened discs, surrounded by plasma membrane. At the base of the outer segment newly formed discs evaginate from the ciliary membrane (Steinberg *et al.*, 1980). Each rod disc possesses a lumen, distinct from the cytoplasm and is stitched together by two membrane proteins, peripherin/RDS and rod outer segment membrane 1 (ROM1). The discs are continuously being shed from the tip of the rod outer segments from where they are phagocytosed by the cells of the RPE (Newell, 1982). The cone cells are similar in structure to the rod cells, but unlike the case in the rod cells the cone outer segment discs remain open and are attached to the membrane (Molday, 1998; Djamgoz *et al.*, 1995).

The rod photopigment, rhodopsin, accounts for more than 70% of the total rod outer segment protein (Molday, 1998). The cone cells possess not rhodopsin but one of three photopigments which respond to different light wavelengths. Depending on the visual pigment they possess, the cone photoreceptors are classified as either blue, green or red photoreceptors.

1.1.3 Visual transduction

The visual pigment rhodopsin is embedded in the outer segment discs of the rod photoreceptors. It consists of an opsin molecule to which the chromophore 11-*cis* retinal, an aldehyde of vitamin A, is bound. When the visual pigment absorbs a photon of light, the isomeration of the chromophore from the 11-*cis* to the all-*trans* form occurs (Wald, 1968). This reaction leads to a series of conformational changes in the rhodopsin molecule and its conversion to the active Meta II rhodopsin (R*) (Palczewski

and Saari, 1997). R* is now capable of interacting with the G-protein, transducin (Figure 1.2).

Transducin is comprised of α , β and γ subunits and in its inactive state possesses non-covalently bound guanosine diphosphate (GDP). When R* binds to transducin the GDP is exchanged for guanosine triphosphate (GTP) which causes the α subunit (T*) to lose its affinity for the inhibitory β and γ subunits and also for R*. The release of R* allows it to interact with and activate as many as 500 transducin molecules, resulting in significant amplification of the signal (Djamgoz *et al.*, 1995). The molecule phosducin interacts with the β and γ subunits and prevents them from reforming the transducin molecule, thereby preventing continual activation of transducin by R* (Palczewski and Saari, 1997).

T* can now activate the enzyme phosphodiesterase (PDE). PDE is a membrane associated protein comprised of catalytic α and β subunits along with two inhibitory γ subunits. T* binds to the γ subunits and brings about their dissociation from the PDE core. The active PDE can now hydrolyse 3',5'-cyclic guanosine monophosphate (cGMP) to 5'GMP. In the resting state, the cGMP binds to the cGMP-gated channel proteins which maintain cation channels in the cell membrane in an open configuration. These cGMP-gated ion channels allow the cations Na^+ and Ca^{2+} to enter the rod outer segment. K^+ ions simultaneously flow out of the cell from K^+ channels in the inner segment (Molday, 1998). Ion pumps counteract the flow of ions, maintaining high levels of Na^+ and Ca^{2+} outside the cell and K^+ inside the cell. Under these conditions the rod cell is considered to be in a depolarized state and the photoreceptor continuously emits the neurotransmitter glutamate.

The reduction in the levels of cGMP, as a result of hydrolysis by active PDE, cause the closure of the ion channels. The Na^+ and Ca^{2+} are now prevented from entering the cell. The ion exchangers continue to extrude the positive ions from the cell however resulting in a build up of positive charge in the extracellular space. This results in hyperpolarization of the cell and consequently the inhibition of glutamate release (Molday, 1998). In this way a nerve impulse is sent to the brain.

Restoration of the cell to the depolarized state is essential in order to allow the detection of continual changes in light. The restoration of the rhodopsin molecules must be brought about in order that the process of visual transduction can occur again. The binding of R* to transducin results in a conformational change of the rhodopsin,

allowing the C-terminus to be phosphorylated by rhodopsin kinase and subsequently allowing the binding of arrestin (also called S-antigen) (Djamgoz *et al.*, 1995). Arrestin competes with transducin for this binding site on rhodopsin and prevents activation of further transducin proteins. This sequence of events results in the separation of the all-*trans* retinal, which is hydrolysed to all-*trans*-retinol, from the phosphorylated opsin and the disassociation of arrestin (Djamgoz *et al.*, 1995; Palczewski and Saari, 1997). Phosphatases cleave the phosphates from the C-terminus and the regenerated rhodopsin molecules can once again bind to 11-*cis*-retinal to form photosensitive rhodopsin.

The regeneration of 11-*cis*-retinal from the all-*trans* isomer, which has been formed in this process, must be brought about in order to complete the cycle. The all-*trans*-retinol is released into the extracellular space where it is picked up by the interphotoreceptor retinoid binding protein (IRBP) and transported to the RPE. In the cells of the RPE the all-*trans*-retinol is esterified to produce all-*trans*-retinyl palmitate and may be stored in this form (Palczewski and Saari, 1997). The retinyl ester is subsequently isomerized and hydrolyzed to form 11-*cis*-retinol in a process which may involve the RPE microsomal protein, RPE65 (Eriksson, 1997; Redmond *et al.*, 1998) (see chapter 6). The cellular retinaldehyde binding protein (CRALBP) can then bind the 11-*cis*-retinol where it is oxidised by 11-*cis* retinol dehydrogenase to form 11-*cis*-retinal (Strecher, 1999). The transportation of the 11-*cis*-retinal back to the photoreceptors is probably once again mediated by the IRPB (Palczewski and Saari, 1997). Within the photoreceptors it is possibly the retinal ATP-binding cassette protein, ABCR, which is responsible for the transportation of the retinal (Sun *et al.*, 1999) (detailed in Chapter 6).

Despite the fact that the levels of R* have been depleted, there still remains active transducin within the cytosol, which is capable of activating PDE. Transducin has intrinsic GTPase activity however, which brings about the hydrolysis of GTP to GDP on the T* surface (Molday, 1998). The transducin α subunit can now re-associate with the inhibitory β and γ subunits, thereby halting the activation of PDE.

The low levels of Ca^{2+} , brought about by the closing of the ion channels, play an important role in a negative feedback mechanism in the process of visual transduction. High levels of Ca^{2+} both enhance the activity of PDE and inhibit the activity of the enzyme guanylate cyclase (GC1), which is responsible for the synthesis of cGMP. The drop in Ca^{2+} levels bring about the activation of the calcium binding protein GCAP. GCAP activates GC1 and stimulates it to form cGMP from GTP (Molday, 1998; Dizhoor and Hurley, 1999). PDE is no longer hydrolysing cGMP and therefore, the

increased levels of cGMP bring about the re-opening of the cGMP-gated ion channels and the depolarisation of the cell. The rod photoreceptor cell is in this way restored to its resting state and is once again ready for stimulation.

Most research to date has focused on the biochemical pathways of the rod photoreceptors. This is due, to a large degree, to the many rod specific proteins which have been associated with retinal disease. Transducin, PDE, recoverin, cGMP-gated channel and guanylate cyclase proteins have all been identified within the cone pathways however, and a phototransduction cascade similar to that described above has also been proposed for the cone photoreceptors (Evans and Bhattacharya, 1998)

1.2 HEREDITARY EYE DISORDERS

Systematic observations and classifications of hereditary eye diseases began in the late 19th and early 20th centuries. Advances in the fields of clinical ophthalmology and the study of animal models for hereditary diseases of the eye have contributed greatly to our knowledge. More recently however, the identification of etiological genes for retinal dystrophies has provided insight into both the mechanisms of disease pathology and the biochemistry of the eye.

The most commonly encountered group of hereditary eye diseases are those of the retina, which usually involve the photoreceptors or the retinal pigment epithelium (Evans and Bhattacharya, 1998). This is also the group of eye diseases which has been the most studied to date. Diseases of the retina can be classified into those in which either the peripheral retina, or the central retina is affected first (Evans and Bhattacharya, 1998). Those of the peripheral retina are generally due to primary defects of the rod photoreceptors while those of the central retina are usually the result of primary defects of the cone photoreceptors. Most of the diseases initially affecting the peripheral retina are grouped under the blanket term retinitis pigmentosa (RP). Those diseases which are primarily of the central retina include the macular dystrophies and also those which initially affect the macula but subsequently affect the peripheral retina also. Examples of the later group include cone-rod and cone dystrophies.

It should be noted however, that the classification of retinal dystrophies on the basis of clinical symptoms alone can be misleading. Many similar diseases are caused by different genes and conversely different genes can cause diseases of similar

phenotype. Also, the function of both rod and cone cells is compromised in most of the progressive retinal dystrophies, further complicating classification (Bird, 1995). As knowledge of the genes underlying these diseases emerges, classification emphasis is increasingly placed on the underlying molecular pathology (van Soest *et al.*, 1999). For the purposes of simplicity however, the retinal dystrophies are discussed in terms of clinical classifications in this chapter, as there remain many retinopathies for which the underlying genes have not been identified. A complete list of the loci and genes involved in retinal dystrophies is given in Appendix C.

1.2.1 Retinitis pigmentosa and related disorders

RP is the most widely known of the retinal dystrophies. It is characterised by progressive bi-lateral retinal degeneration. Patients initially experience night blindness, followed by the onset of peripheral vision loss and eventually blindness. RP may be inherited in an autosomal dominant (adRP), autosomal recessive (arRP) or X-linked (xlRP) fashion, which is broadly indicative of its genetic heterogeneity. The disease is also clinically heterogeneous, patients experiencing varying degrees of severity and age of onset. A family segregating adRP is the central subject of Chapter 2 of this thesis and a detailed discussion of the disease is presented there.

RP also occurs as one of a number of symptoms in certain hereditary syndromes. It has been noted as one of the symptoms in at least 50 documented syndromes (Heckenlively, 1998). One of the most widely known of these is Usher syndrome, a genetically heterogeneous disease characterised by progressive RP along with varying severities of sensorineural deafness. A large Irish family presenting with a disease very similar to Usher syndrome is the central focus of Chapter 5 and a more in-depth discussion of the syndrome is presented there.

A particularly severe retinal dystrophy, which is clinically very similar to RP, is Leber congenital amaurosis (LCA). Unlike RP however, LCA patients are blind at birth or within a few months of birth (Morimura *et al.*, 1998). A membrane bound guanylate cyclase gene (RETGC1) has been found to be involved in cases of LCA (Perrault *et al.*, 1996). This gene is preferentially expressed in cone photoreceptors. Mutations of the gene may lead to considerably reduced levels of cGMP and therefore desensitization of

the photoreceptors (Evans and Bhattacharya, 1998). Mutations of the RPE65 gene have also been detected in LCA (Morimura *et al.*, 1998) (detailed in Chapter 6).

1.2.2 Congenital stationary night-blindness

Congenital stationary night-blindness (CSNB) is another retinal dystrophy of the rod photoreceptors. Unlike RP however, it is non progressive and affects only night time vision. It is most frequently transmitted in an autosomal dominant fashion and patients experience early onset of symptoms (Evans and Bhattacharya, 1998).

Three rhodopsin mutations have been identified in CSNB and the constitutive activation of transducin has been proposed as a disease mechanism in these cases (Rao *et al.*, 1994; Dryja *et al.*, 1993; al-Jandal *et al.*, 1999). A mutation in the N-terminal region of the β subunit of the PDE protein (PDEB) has also been shown to result in CSNB in a single family of Danish origin (Gal *et al.*, 1994). It has been postulated that this mutation may prevent the complete inactivation of PDE which would bring about a desensitization of the rod cells (Evans and Bhattacharya, 1998). A single mutation in a third gene, the α subunit of the transducin protein (GNAT1), has also been associated with the disease (Dryja *et al.*, 1996).

Oguchi disease is a rare autosomal recessive form of stationary night-blindness which is accompanied by a light-dependant discolouration of the fundus. This disease has been associated with null mutations of both arrestin and rhodopsin kinase (Fuchs *et al.*, 1995; Yamamoto *et al.*, 1997). Involvement of these two genes indicates that it is a delay in dark adaptation that is responsible for the phenotype in this disease

1.2.3 Macular dystrophies

In contrast to RP, the macular dystrophies are associated with loss of central vision and preservation of the peripheral visual field. The term macula dystrophy encompasses a range of diseases associated with the macular region of the retina.

Stargardt disease (STGD) is the most frequently observed autosomal recessive form of macular dystrophy and affects patients in childhood or early adulthood (Lewis *et al.*, 1999). Histopathologically, STGD is characterised by the build up of lipofuscin-

like debris in the RPE. Mutations of the ABCR gene on chromosome 1p have been shown to cause STGD (Allikmets *et al.*, 1997).

Age-related macular dystrophy (AMD), which as its name suggests, is a disease of the elderly, is the most common cause of retinal blindness in the Western world (Evans and Bhattacharya, 1998). AMD has also been linked to the ABCR gene (Allikmets *et al.*, 1997b). A more in-depth discussion of STGD, AMD and the ABCR gene is given in Chapter 6.

Vitelliform macular dystrophy (also known as Best Macular dystrophy) is an autosomal dominant form of macular degeneration. A yellow mass resembling the yolk of an egg is apparent in the macular region of patients and later in life this "scrambles" becoming deeply and irregularly pigmented (Braley, 1966). A retina-specific gene designated vitelliform macular dystrophy 2 (VMD2), on chromosome 11q has been found to be mutated in cases of this disease (Petrukhin K *et al.*, 1998). The corresponding protein is sometimes referred to as *bestrophin* and may be involved in the metabolism or transportation of poly-unsaturated fatty acids (Petrukhin *et al.*, 1998). Mutations of the peripherin/RDS gene have also been associated with this form of macular dystrophy (Wells *et al.*, 1993). An in-depth discussion of the peripherin/RDS gene is given in Chapter 2.

Sorsby fundus dystrophy is a rare, autosomal dominant disease causing central vision loss. Loss of vision occurs as a result of sub-macular neovascular scarring or geographic atrophy of the macula. It is associated with a thickening of Bruch's membrane (a layer of connective tissue lying between the RPE and the choroid) and with abnormal subretinal deposits (Evans and Bhattacharya, 1998). Mutations in one of the tissue inhibitors of metalloproteinase, TIMP3, have been associated with this disorder (Weber BHF *et al.*, 1994). TIMP3 is an extracellular matrix-bound glycoprotein which is found in the RPE. It plays a role in controlling the activity of the matrix metalloproteinases which are involved in the continuous remodeling of the extracellular matrix (Evans and Bhattacharya, 1998).

There are quite a number of other macular dystrophies which have been classified as distinct disorders. These include North Carolina macular dystrophy (Small, 1998) and a dominant Stargardt-like macular dystrophy (Kniazeva *et al.*, 1999).

1.2.4 Cone-rod and cone dystrophies

The cone-rod dystrophies are a heterogeneous group of disorders involving both the cone and the rod photoreceptors. Cone-rod retinal dystrophy (CORD) differs from RP in that loss of colour vision and a reduction in visual acuity precede night blindness and loss of peripheral vision. Patients generally experience early onset of visual impairment. Mutations in the cone-rod homeobox gene (CRX) gene have been associated with a progressive form of CORD (CORD2) (Freund *et al.*, 1997; Swain *et al.*, 1997). CRX is a homeobox gene which is involved in the regulation of photoreceptor differentiation (Furukawa *et al.*, 1997). In the adult retina it plays a role in the expression of a number of photoreceptor outer segment proteins (Freund *et al.*, 1997). The rod specific ABCR gene has also been implicated in a form of CORD (Cremers *et al.*, 1997).

There are also cone dystrophies in which the presence of night blindness and loss of peripheral vision are rare (Krill *et al.*, 1973). Defective colour vision and loss of visual acuity are the main complaints in these cases. A form of autosomal dominant cone dystrophy is caused by a mutation of the guanylate cyclase activating protein 1A (GCAP1) gene (Payne *et al.*, 1998). This is a constitutively active mutant which leads to elevated levels of cytoplasmic cGMP in cone photoreceptors (Sokal *et al.*, 1998)

Mutations in the photopigments of the cone cells also cause visual defects, although their severity tends to be less than mutations of rhodopsin. The usual symptoms of such mutations are disturbances of colour vision. The red and green opsin genes are located side by side on the X chromosome and in rare cases a total inactivation of both genes causes blue cone monochromy (Nathans *et al.*, 1993). Mutations of the blue cone pigment gene on chromosome 7 cause dominant tritanopia (defects in blue cone vision) (Weitz *et al.*, 1992).

1.2.5 The role of apoptosis in the retinal dystrophies

Despite the extreme genetic heterogeneity observed in the retinal dystrophies, there is surprisingly little variety observed in the histopathological changes of the retina. The observation that mutations of the rod photoreceptors not only bring about cell death of the rods but also of the cones is also surprising. In the last number of years it has

become apparent that photoreceptors of compromised structure or function die by a final common pathway of apoptosis (Evans and Bhattacharya, 1998).

Metabolic defects, caused by mutations of retinally expressed genes, do not therefore cause death of the photoreceptors directly but do so by inducing apoptotic cell death. Because of this, despite differences in the underlying causes of cell death in retinopathies, the appearance of photoreceptor cell death is remarkably similar.

All cells have an intrinsic ability to undergo apoptosis and it plays a fundamental role in development and in tissue homeostasis. Morphologically it can be characterised by the internucleosomal fragmentation of the nuclear DNA and its condensation into bands of DNA with lengths in multiples of 200 base pairs (Wyllie AH, 1980).

All cases of animal retinal dystrophy examined to date have been shown to undergo retinal degeneration as a result of apoptosis (Portera-Cailliau *et al.*, 1994; Tso *et al.*, 1994; Hobson *et al.*, in press). Apoptosis in a human retinal degeneration has also been observed in the postmortem ocular analysis of a man carrying a mutation of the rhodopsin gene. The death of the cells at the boundaries between dying and healthy photoreceptors in this case, was clearly due to apoptosis (Li *et al.*, 1994). Apoptosis is discussed in greater detail in Chapter 6.

1.2.6 Glaucoma

The term glaucoma describes a group of disorders of the eye that are distinct from the retinopathies. Glaucoma is a clinically and genetically heterogeneous disease causing optic neuropathy and progressive loss of visual fields. It is typically characterised by high intraocular pressures and an abnormal appearance of the optic nerve head. An in-depth discussion of glaucoma is presented in Chapter 4.

1.3 IDENTIFICATION OF DISEASE GENES

The identification of the genes underlying genetic disorders is a key step in the understanding inherited ocular disorders. Once the gene has been identified it is possible to begin elucidating the disease mechanism, which may eventually lead to the development of suitable therapies for the disease.

A number of genes have been identified in the past by what is known as a functional cloning approach (forward genetics). This approach requires prior knowledge of the biochemical defect which brings about the disease pathology. The polypeptide sequence of the protein mutant in the disease can be used to decipher the DNA nucleotide sequence and in this way the gene can be isolated. An example of a gene identified by functional cloning is the hypoxanthine-guanine phosphoribosyltransferase (HPRT) gene which is involved in Lesch-Nyhan syndrome (Caskey, 1979). For the majority of diseases however, including all the retinal dystrophies and the different forms of glaucoma, there is no prior knowledge of the biochemical defect in patients and an approach traditionally known as positional cloning (reverse genetics) must be taken.

Positional cloning relies on the localization of a disease gene to a chromosomal location in the genome, which is generally achieved by the process of genetic mapping. The next stage in this approach is physical mapping, which usually involves the generation of contiguous clones spanning the disease interval. Once physical mapping is complete a variety of approaches can be taken to identify gene-based sequences of interest within the interval. Having identified a candidate gene it is then subjected to mutation screening in disease patients.

Since various aspects of the positional cloning approach are relevant to this thesis, they are discussed in further detail below.

1.3.1 Genetic mapping

The first stage in the identification of a disease gene generally involves the assignment of the gene to a specific subchromosomal region. The human genome possesses many regions of DNA which differ between individuals and can be employed as genetic markers. Genetic mapping involves the mapping of these polymorphic markers to discrete chromosomal positions within the genome. The availability of mapped polymorphic markers allows the correlation of genotypes with disease status and such markers are therefore invaluable in the localization of disease genes.

In the history of genetic mapping several types of DNA-based markers have been used. The first type to be employed were restriction fragment length polymorphisms (RFLPs). RFLPs allow the detection of a polymorphism on the basis of

the presence or absence of a restriction site. The information content at such sites is limited however and therefore, RFLPs have largely become redundant. Another type of genetic marker is the variable number tandem repeat (VNTR). VNTRs are comprised of repeated blocks of sequence that are variable in length. The number of VNTRs throughout the genome is relatively limited however, which is a serious drawback when trying to map genes to specific locations. The most frequently used DNA markers are the microsatellites. Microsatellites are highly polymorphic, consisting of di-, tri- or tetranucleotide repeats. They are found in blocks of 5 to 30 repeats and the number of repeats is generally very variable among different members of the population. Over 5000 of these microsatellites have been characterised within the human genome (Dib *et al.*, 1996). The applicability of the polymerase chain reaction (PCR) to microsatellite analysis makes these markers particularly attractive in genetic mapping.

The phenomenon of homologous recombination allows the specific order of markers, which have been mapped to a particular chromosome, to be determined. During the first division of meiosis, homologous chromosomes align and exchange regions of DNA through the process of recombination. The probability of a recombination event occurring between two loci on a chromosome is a function of the distance between them. In other words, two loci which occur very close to one another on a chromosome are less likely to be separated by a recombination event than two loci which lie a distance apart.

The observation of recombination events in families allows the specific ordering of polymorphic markers on a chromosome. In a collection of families known as the CEPH (Centre d'Etude du Polymorphisme Humain) families, large scale studies have been undertaken to create genetic maps of the human genome on the basis of recombination events within the families (Dib *et al.*, 1996). Recombination events are often also used to determine genetic distances. Genetic recombination loosely relates to physical distance, with a unit known as a Morgan corresponding to a distance over which there is an average of one recombination event per chromatid. It has been estimated that one centimorgan (cM) is equivalent to one megabase (Mb) of DNA (one million base pairs) (Terwilliger and Ott, 1994).

The principles used in genetic mapping can also be applied to the search for disease genes. In attempting to localize a disease gene, the number of recombinations between polymorphic markers and the disease phenotype is observed, rather than the

frequency of recombination events between two markers. This process is referred to as linkage analysis.

The first step in the localization of a disease gene is the ascertainment of DNA samples from affected individuals. In some cases the detection of a large scale chromosomal rearrangement following karyotype analysis is possible. However, the majority of genetic disorders result from DNA mutations at the molecular level and these cases rely on linkage analysis to localize the disease gene. Large families segregating a disease are ideal for linkage studies. The genotype for each individual at a given polymorphic marker must first be obtained. With microsatellite markers this involves the use of PCR to amplify across the marker and the subsequent observation of the alleles possessed by each individual on acrylamide gels. If the disease gene and the marker are located on separate chromosomes, or at a great distance from one another on the same chromosome, they will segregate independently. Such a situation is observed by the random distribution of alleles in affected and unaffected individuals. If the marker and disease locus are located close to one another however, Mendel's law of independent assortment will not apply. All affected individuals will possess the same allele therefore, and the marker and disease locus are said to be linked.

In order to assess the significance of linkage results, statistical methods of inferring linkage are applied. A test known as the log of the odds (LOD) test is used. This test is based on the recombination fraction (θ) which is an estimation of recombination between two loci. When $\theta = 0.5$ it is indicative that the two loci are segregating independently. If θ is less than 0.5 then the loci are said to be linked at a distance of θ ($\theta = 0.01$ corresponds closely to 0.01M or 1 cM) (Terwilliger and Ott, 1994). The lod score is calculated by the equation:

$$Z(\theta) = \log_{10}[L(\theta)/L(0.5)]$$

where Z = LOD score and L = likelihood of observing the patterns of inheritance at the given θ (Taylor *et al.*, 1997). This equation compares the likelihood of any test θ less than 0.5 with the likelihood that the two loci are segregating independently. There are many computer packages available which use this formula as a basis to calculate a range of LOD scores for recombination fractions that range from 0 - 0.5 for a given data set (Bryant, 1997). Proof of linkage is generally accepted when the maximum lod score

(Z_{max}), for θ values of 0.00 to 0.5, is greater of equal to 3. This is equivalent to a situation where the chance of independent segregation is less than 1 in 1000. The possibility of linkage is excluded for any θ which has a Z_{max} of less than minus 2 (Ott, 1991).

Having established a linkage attempts are made to narrow the disease interval as much as possible. The exclusion of tight linkage to flanking markers helps in this aim. All available markers in the region are typed through the family with the aim of identifying family members which show recombination events between these markers and the disease locus, thereby narrowing the disease interval.

1.3.2 Physical mapping

Having established an interval on a chromosome in which a disease gene lies, the role of physical mapping comes into play. Disease intervals which have been defined by linkage studies are still rather large and may span millions of base pairs. Because of this, a series of overlapping genomic clones (a contig) which span the interval is often generated. These clones can be used to correlate genetic distances with physical distances and to isolate candidate genes.

The generation of a physical map depends on an array of markers across the interval, preferably formatted as sequence tagged sites (STSs). The term STS encompasses any stretch of PCR amplifiable, mapped DNA which is unique in the genome (Green and Olson, 1990). STSs include polymorphic markers, expressed sequence tags (ESTs) and random DNA sequences. Each clone can be marked for the presence or absence of a particular STS and in this way the order of the clones within the contig can be defined.

As the size of disease intervals tends to be large, vectors which can only accept small inserts, such as those based on plasmid and phage, are generally avoided in the initial stages of a physical mapping exercise. Yeast artificial chromosome (YACs), which are capable of accepting inserts of up to 2Mb, are frequently employed (Horrigan and Westbrook, 1997). YACs possess the minimal elements required for replication of yeast chromosomes, into which is inserted exogenous DNA. The DNA used to generate human YAC libraries may either come from total genomic DNA, from human-rodent hybrid cell lines which carry one or more human chromosome, or from individual

chromosomes separated by flow sorting. YACs have a number of limitations however, including low copy number, frequent chimerism and instability (Horriagan and Westbrook, 1997).

Because of difficulties in the manipulation of YAC DNA, smaller vectors are regularly used as stepping stones between the generation of the physical map and further investigation of a region of interest. Bacterial artificial chromosomes (BACs) are a cloning vector which are becoming increasingly popular. BAC vectors are based on the *E. coli* fertility plasmid and can take inserts of up to 300kb. PAC vectors which are created from BAC and the bacteriophage P1 clones are also commonly used (Ioannou *et al.*, 1994). Cosmids are frequently employed owing to the relative ease of library construction. They are capable of accepting inserts of 40kb (Valdes and Tagle, 1997).

There is less need than there once was to generate YAC and BAC libraries spanning a particular interval as such contigs are often commercially available, frequently over the internet (Leaving Kansas, 1997; Green *et al.*, 1995). The large scale sequencing being carried out by the human genome project can also mean that the time consuming generation of contigs across a disease interval is increasingly becoming redundant.

1.3.3 Identifying candidate genes

The identification of the causative gene for a disorder, within a chromosomal disease interval, is often the rate-limiting step in positional cloning projects. Any gene which maps within a disease interval as defined by linkage may be considered a candidate for the disease gene on the basis of its position. In situations where there are a large number of known genes mapping within a particular interval, it is unfeasible for investigators to adopt each one as a candidate. Knowledge of the function or expression of a gene is often used in the selection of candidates. If a retina-expressed gene maps to the same region as a retinal degeneration, then this gene will be considered a candidate and screened in affected individuals. Conversely, if genes in the disease interval are known not to be expressed in the disease tissue or have a function which is unrelated to the disease phenotype, they may be excluded on this basis.

It is often necessary to identify novel genes within the interval in order to isolate candidate genes. Many methods have been developed for this purpose. Methods which

identify genes on the basis of gene specific structures are frequently used. Such methods include exon trapping and the identification of CpG islands. These methods identify genes regardless of levels or patterns of expression.

Exon trapping involves the identification of gene based sequences on the basis of splicing signals at exon junctions. This is accomplished by the subcloning of genomic clones into a plasmid-based trapping vector which is transfected into cells that support vector transcription. Transcription of the insert and subsequent mRNA splicing results in any internal exons present being trapped between two vector exons (Krizman, 1997).

CpG islands are frequently associated with the 5' ends of genes and can therefore be used as a means of identifying genes. These islands appear to be found in 40% of genes with a tissue specific expression pattern and in almost all house-keeping genes (Larsen *et al.*, 1992). They can be isolated by either PCR or through the use of rare-cutting enzymes and can subsequently be used as hybridization probes against cDNA libraries (Valdes and Tagle, 1997).

Hybridization based methods are the other main approach to the identification of genes within large areas of genomic sequence. Regions of coding DNA can be identified by using labeled cDNAs as hybridization probes in a method referred to as direct selection. Alternatively genomic clones can be used as probes against cDNA libraries (Valdes and Tagle, 1997). These approaches are generally tissue-specific which has the advantage that they avoid the genes transcribed in other tissues of the body. However, because they are hybridization-based, they result in a surprisingly high number of false positives (Snell, 1996).

Sequencing is perhaps the most straightforward method of identifying genes. As a first step, sequence generated across a contig can be screened against the sequence and protein databases with the aim of identifying gene based sequence and inferring gene function. It can also be analysed using publicly available software to identify open reading frames (ORFs), functional motifs etc. Sequencing is both time consuming and expensive however. Unless the disease interval is small therefore, it is a somewhat impractical approach.

A critical development in the evolution of gene identification methods is the concerted effort to develop a transcript map of the human genome. This involves the identification and mapping of ESTs. ESTs are short, gene based sequence tags derived from single pass sequencing of cDNA libraries. The information they provide is limited

in many respects, but the mapping of such cDNA markers allows the identification of candidate genes on the basis of two important factors: map position and tissue expression. The existence of publicly available EST data means that the process of positional cloning is gradually changing to a positional candidate approach.

Having identified an EST (or a region of coding sequence) of interest, it will still be necessary to screen a cDNA library or use direct extension methods to obtain the entire sequence of the gene. Alternatively it may be possible to retrieve complete genomic sequence for the gene from the large amounts of sequence data which have been generated by the human genome project to date. A number of ESTs have been adopted as candidate genes in this thesis and a detailed discussion of ESTs is given in Chapter 3.

1.3.4 Screening candidate genes

Having identified a candidate gene it must be explored for mutations that segregate in families. When undertaking to screen a gene a number of factors must be considered in choosing a mutation detection method. These factors include the size of the gene and the accuracy and cost of the method. There are a number of techniques available including single stranded conformational polymorphism (SSCP) analysis, heteroduplex analysis, cleavage mismatch detection, denaturing gradient-gel electrophoresis (DGGE) and sequencing (Cotton, 1996). There is generally a conflict between high cost, high accuracy sequencing and the lower cost, less accurate methods.

In general only the coding sequences of a gene are screened for mutations. This involves the PCR amplification of exons, including splice sites and their subsequent subjection to scanning methods. SSCP analysis is widely used in the screening of DNA sequence. It is based on the theory that a single base change will result in a change in secondary structure in DNA which has been denatured and allowed to reanneal. Such changes in secondary structure can be detected on non-denaturing acrylamide gels as band shifts. The PCR product must then be sequenced in order to precisely determine the sequence change. This method only detects approximately 80% of sequence changes and can therefore be of limited use (although electrophoresis under different conditions can increase this percentage) (Cotton, 1996). It is cheap and relatively quick

to carry out however, and for this reason it has been used as a method of initial screening throughout this thesis.

Sequencing is time consuming and expensive but is 100% effective in the detection of mutations. Therefore, when it is essential to confirm the presence or absence of a DNA mutation, it is the method of choice.

Once a sequence variant has been identified in an affected individual a number of criteria must be fulfilled in order to be sure that it is a disease causing mutation. The first indication that a DNA change is a disease mutation is if it results in a change in protein structure e.g. an amino acid substitution. The demonstration that the mutation results in a change in a highly conserved region of the protein is even more convincing. The segregation of a sequence variant with the disease phenotype in a family is also indicative of the pathogenesis of the variant. The confirmation of its absence among normal individuals of the population consolidates the likelihood of pathogenesis. Finally, the ability to show a precise disease mechanism resulting from the mutation is not always necessary but provides even more convincing evidence of its role in the disease.

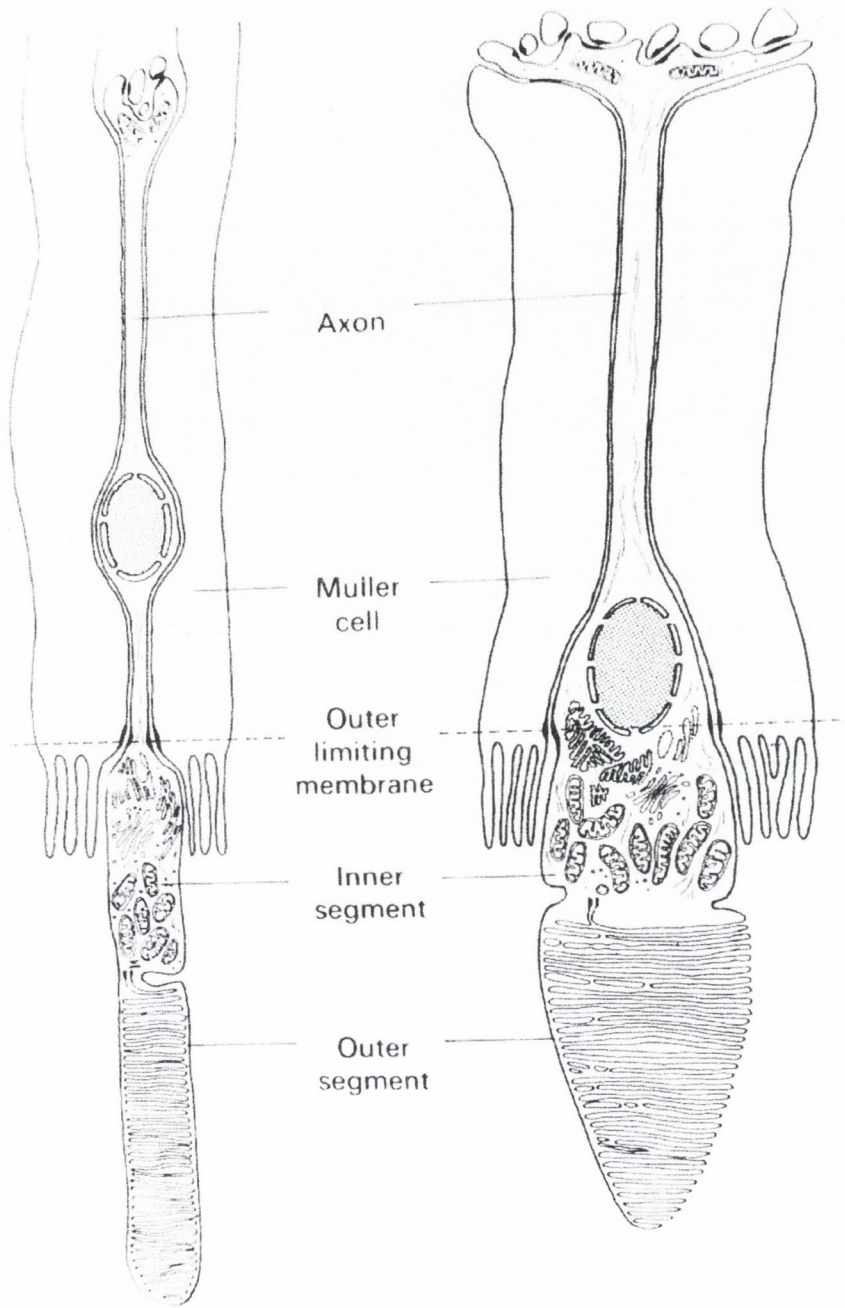


Figure 1.1 Schematic diagram of rod and cone photoreceptors (from Wheater's Functional Histology, Third Edition, 1993).

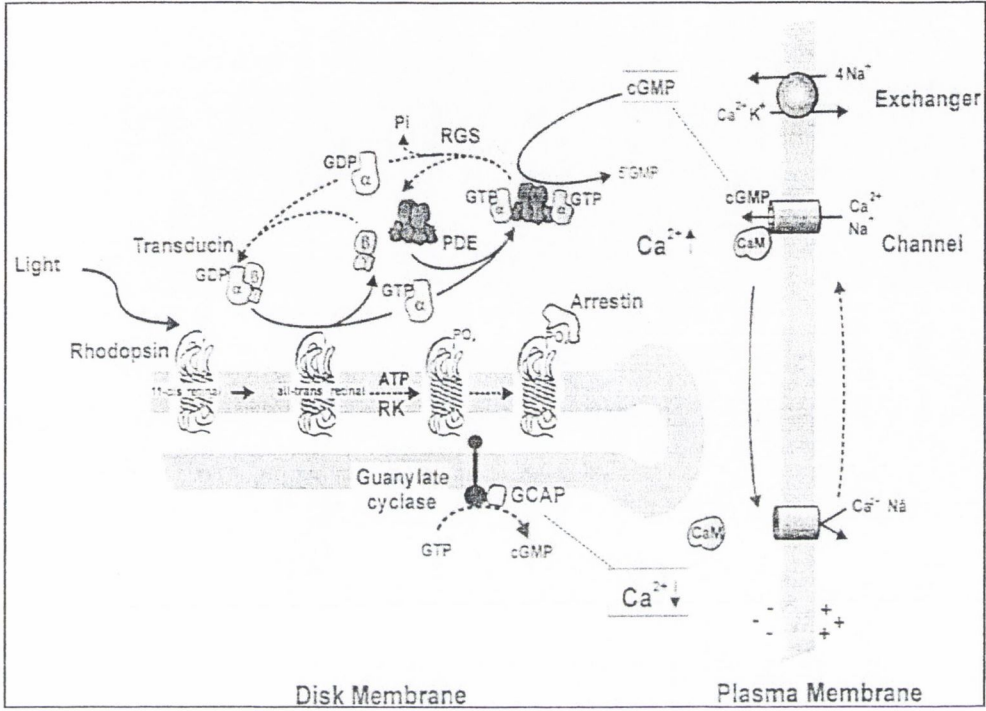


Figure 1.2 Schematic diagram of the visual transduction process.

CHAPTER 2

RE-EVALUATION OF THE RP10 LINKAGE DATA AND THE SCREENING OF TWO CANDIDATE GENES FOR THE RP10 MUTATION

2.1 INTRODUCTION

2.1.1 Introduction

As a result of previous research at this laboratory an adRP gene was localized on the long arm of chromosome 7 (Jordan *et al.*, 1993). These studies involved a large Spanish family, FA-84. Independent investigators have since reported other adRP families which also show linkage to the same region of 7q, the locus being referred to as RP10. Since the mapping of RP10 in 1993, ongoing attempts have been made to identify the disease gene but none have succeeded to date. Therefore, the main aim of the present study was to identify the adRP gene on 7q.

A review of the clinical nature of RP along with our current knowledge of its genetic etiology is presented. The history of the linkage studies which identified the RP10 disease interval and the genes which have previously been excluded as candidates are also given. Two candidate genes were analysed in this study, GRM8 and DGK1. The reasons for adopting these genes as candidates are detailed. The results of a re-evaluation of the linkage and haplotype data used to define the disease interval are also presented. The elucidation of the structure of GRM8 and exclusion of both GRM8 and DGK1 as candidate genes, through the use of various methods, is also detailed.

2.1.2 Clinical features of RP

Retinitis Pigmentosa (RP) is the term given to describe a group of degenerative diseases of the retina. It represents a prevalent form of hereditary visual handicap affecting one in four thousand people, with approximately 1.5 million people affected world-wide (Shastry, 1995). A great degree of clinical heterogeneity is observed among RP patients, but typically a patient will first experience the onset of night blindness during childhood. A restriction of the visual fields generally ensues in the early twenties, with a serious impairment of vision during the forties and often the loss of all effective sight by the sixties.

The clinical manifestations of the disease are due initially to the death of the rod photoreceptor cells. The rod cells are dispersed mostly throughout the periphery of the

retina and govern dim light vision. Patients initially experience night blindness and subsequently develop "tunnel vision". The death of the rod photoreceptors also leads to more extensive tissue degeneration. The cones cells, most of which are located in the macula and responsible for colour vision, begin to die off. The retina becomes visibly thinner and the blood vessels which supply the retina become attenuated. The death of the rods also results in a de-pigmentation of the retinal pigment epithelium and consequently there is a distinct build-up of pigment on the retinal surface (Heckenlively, 1988). This pigment deposition has a characteristic pattern which is best described as a bone spicule pattern (Figure 2.1). The changing morphology of the retina gradually, but progressively, leads to blindness in the patient.

There are also a number of atypical forms of RP which include RP *punctata albescens*, in which scattered white dots are apparent in the mid-periphery, RP *sine pigmento*, in which there are no pigmentary disturbances (Pearlman *et al.*, 1976) and sectorial RP where the disease symptoms are restricted to only a particular area of the retina (Krill *et al.*, 1970).

2.1.3 The diagnosis of RP

The electroretinogram (ERG) is used with great success in the diagnosis of RP. The ERG measures the electrical potential of the retina following stimulation by light. A contact lens with gold foil electrodes allows the detection of the retinal response during exposure to a series of light flashes (Heckenlively, 1988). The ERG can be recorded following either dark adaptation (scotopic ERG) or light adaptation (photopic ERG) of the patient (Heckenlively, 1988) (Figure 2.2). The scotopic ERG uses light waves below the cone threshold and therefore records the responses of the rod photoreceptors. In contrast, the photopic ERG records the responses of the cone photoreceptors only, as the rods have been photobleached and hence are unresponsive. The ERG is biphasic and two types of responses, the a- and b-waves, can be recorded. The a-wave is a negative response due to the repolarisation of the photoreceptor cells and the b-wave is a positive response generated in the inner nuclear layer (Heckenlively, 1988).

Patients with RP show abnormal ERG responses. The fact that abnormalities of the ERG response can be recorded prior to the onset of

discernible symptoms means that it can be used in the pre-symptomatic diagnosis of RP (Humphries *et al.*, 1992). The rod responses in an RP patient are reduced in amplitude and often delayed while the cone responses may be normal or abnormal. In advanced cases of the disease ERG responses are completely extinguished (Humphries *et al.*, 1992). Non-invasive tests such as best-corrected Snellen visual acuity, visual field assessment and dark adaptometry are also used in the clinical diagnosis of RP patients (Newell, 1982).

2.1.4 Genetics of RP

The extreme clinical diversity observed in RP can, to a large extent, be explained by the genetic heterogeneity of the disease. RP can be inherited in an autosomal dominant (adRP), autosomal recessive (arRP) or X-linked (xlRP) form. There are also simplex cases in which no family history can be identified, although the majority of these are believed to be arRP (Heckenlively, 1988).

Autosomal dominant pedigrees are recognized by the vertical transmission of the disease through at least three generations (Heckenlively, 1988). To date twelve loci have been implicated in adRP, with six of the causative genes at these loci identified. The autosomal dominant form of the disease is sometimes divided into type I (early onset) RP, with night blindness evident before ten years of age and type II (late onset) RP, with night blindness beginning in the third decade (Massof and Finkelstein, 1981). Type I is also known as the diffuse type (type D) on the basis of the diffuse distribution of pigmentation of the retina in the early stages of the disease. Rod cell degeneration is also diffuse and leads to extensive loss of cone sensitivity (Lyness *et al.*, 1985). Type II adRP is also known as the regional type (type R) due, once again, to the retinal pigmentation pattern. This subtype shows a regional loss of sensitivity in both rods and cones (Lyness *et al.*, 1985).

Autosomal recessive RP is the most frequently observed form of the disease. At least 15 loci have been implicated in arRP. In this form of the disease unaffected parents have one or more affected children and in some cases it is associated with consanguinity.

X-linked RP is the most rare form of the disease but has the most severe phenotype (Humphries *et al.*, 1990). Males are severely affected, with early onset of the disease and rapid progression of symptoms (Heckenlively, 1988). Female carriers are generally not affected, but may show symptoms later in life, and a small number are severely affected at a younger age (Heckenlively, 1988). The variation in levels of expression of the disease in female carriers may be partly due to the effects of X-chromosome inactivation (Cideciyan and Jacobson, 1994).

The discernment of the mode of inheritance of RP in an affected pedigree is sometimes complicated by the phenomenon of incomplete penetrance. In some families individuals inheriting the disease gene can be asymptomatic and the disease can even appear to skip generations. Cases where female carriers of an X-linked RP gene are severely affected can also cause confusion and may be mistaken for adRP.

Progress in the identification of RP loci, and in many cases the causative genes themselves, has meant that the different forms of RP are increasingly referred to by the loci they have been mapped to. The RP genes which have been identified at these loci are discussed below (see also Appendix C).

2.1.5 Autosomal dominant RP loci

A total of twelve loci have been implicated in the causation of adRP. For a number of these loci the RP genes have been identified; the rhodopsin gene on chromosome 3q (Dryja *et al.*, 1990), the peripherin gene on chromosome 6p (Kajiwara *et al.*, 1991), the ROM1 gene on 11q (Kajiwara *et al.*, 1994), the cone-rod homeo box-containing (CRX) gene on 19q (Sohocki *et al.*, 1998), the Nrl gene on 14q (Bessant *et al.*, 1999) and a gene of unknown function on 8q (Sullivan *et al.*, 1999). However, there are a number of loci for which the RP genes have not been identified.

In 1993, Inglehearn *et al.* used a British adRP family to identify an RP locus on chromosome 7p15.1-p13; RP9. Later that year, an adRP Spanish family, which is the subject of this chapter, were shown to be linked to a separate locus on chromosome 7 at 7q31.3 (Jordan *et al.*, 1993). A form of the disease referred to as RP13 has been linked to chromosome 17p13.3 in a large South African kindred

(Greenberg *et al.*, 1994) and another locus on chromosome 17, at 17q21, has also been mapped in a separate South African family; RP17 (Bardien *et al.*, 1995). A form of adRP which shows frequent incomplete penetrance has been mapped in a number of families to 19q13.4; RP11 (Al-Maghteh *et al.*, 1994; Xu *et al.*, 1995; McGee *et al.*, 1997). The most recent adRP locus to be identified, RP18, was linked to 1p13-q23 in a large Danish family of 7 generations (Xu *et al.*, 1996). None of the RP genes at these loci have been identified to date, although considerable efforts are underway to that aim.

The first RP gene was identified in 1990 (Dryja *et al.*, 1990). Linkage studies in a large Irish family segregating adRP localized the gene to the long arm of chromosome 3 with a lod score of 14.4 at 0% recombination to the marker D3S47 (McWilliam *et al.*, 1989). The rhodopsin gene had previously been mapped to this region of the chromosome and because of this and its role in the visual transduction cascade it was an obvious candidate for the disease gene. The first mutation within rhodopsin to be reported was the Pro23His mutation which was identified in an American family (Dryja *et al.*, 1990). Since the identification of this mutation over 80 further rhodopsin mutations have been identified (Sullivan and Daiger, 1996). Most of these are missense mutations but there are also a number of deletions and splice site mutations (Keen *et al.*, 1991). Two of the rhodopsin mutations result in congenital stationary night blindness (Al Jandal *et al.*, 1999). All other mutations result in RP, most cases of which are dominant but three of which are recessive (Rosenfeld *et al.*, 1992; Dryja and Li, 1995).

The precise mechanisms by which mutations in the rhodopsin gene bring about degeneration of the retina are unclear. The generation of a rhodopsin knockout mouse has revealed that rho^{-/-} mice do not develop photoreceptor outer segments indicating that rhodopsin is essential in the development and maintenance of the photoreceptors (Humphries *et al.*, 1997). Carriers of arRP mutations are phenotypically normal despite the fact that these mutations are believed to result in non-functional rhodopsin proteins (Dryja and Li, 1995). This would suggest that haploinsufficiency is not the means of adRP pathogenesis but that adRP mutations are gain of function mutations (Dryja and Li, 1995).

Studies on the expression of rhodopsin in tissue culture suggest that many of the mutations in the gene interfere with either or both the folding and stability of the protein (Sung *et al.*, 1993). Misfolding mutations appear to interfere with the

transportation of the protein and result in its accumulation within the endoplasmic reticulum (Shastry, 1994). Other mutations within the rhodopsin gene do not interfere with transport of the protein but may bring about pathogenic effects by causing destabilization of the rod outer segments discs or interfering with phototransduction (Bird, 1995; Humphries *et al.*, 1992).

A large number of adRP families did not show linkage to the rhodopsin gene on chromosome 3 which indicated the existence of genetic heterogeneity within the disease. A second RP gene was identified following the demonstration of linkage to chromosome 6p, near the major histocompatibility locus, in a large Irish adRP pedigree (Farrar *et al.*, 1991). A photoreceptor specific gene, the peripherin/RDS gene, has previously been mapped to this region of the human genome (Travis *et al.*, 1989). A mutation in this gene is known to cause a retinal degeneration in the retinal degeneration slow (*rds*) mouse (Travis *et al.*, 1989). Mice which are homozygous for this mutation fail to develop photoreceptor outer segments and the remainder of the photoreceptor cells degenerate over the course of the year after birth (Jansen and Sanyal, 1984). The screening of the human peripherin/RDS gene in RP families linked to chromosome 6p revealed disease causing mutations (Farrar *et al.*, 1991; Kajiwara *et al.*, 1991). Other mutations in the gene have been implicated in a variety of retinal dystrophies including macular degeneration and pattern dystrophies (Wells *et al.*, 1993; Nichols *et al.*, 1993; Weleber *et al.*, 1993; Fishman *et al.*, 1997).

Peripherin/RDS is a 39kDa protein which has been localized to the rim of the photoreceptor outer segment disc membrane (Connell and Molday, 1990). Unlike rhodopsin it is not involved in phototransduction and its location suggests a structural role for the protein. It may be responsible for anchoring outer segment discs to the cytoskeleton (Connell and Molday, 1990).

A digenic form of RP has also been reported involving a L185P peripherin/RDS mutation and a null mutation within the photoreceptor outer segment specific gene ROM1 (Kajiwara *et al.*, 1994; Dryja *et al.*, 1997). Only individuals who co-inherit both mutations develop an RP phenotype. The structure and size of the ROM1 protein is similar to that of the peripherin/RDS protein (Bascom *et al.*, 1993). Unlike peripherin/RDS however, immunocytochemical studies have revealed that ROM1 is expressed only in the rod photoreceptors and not in the cones (Bascom *et al.*, 1992). Both peripherin/RDS and ROM1 form

covalently linked homodimers which interact with each other to form tetramers in the rod outer segment disc membrane (Goldberg and Molday, 1996a). Peripherin/RDS with the L185P mutation fails to form the tetramer complex in the absence of ROM1 and remains in a dissociated state (Goldberg and Molday, 1996b). This affects the stability of the outer segment discs and leads to photoreceptor degeneration (Goldberg and Molday, 1996b).

Another photoreceptor gene, the CRX gene, which maps to 19q13.3, has been implicated in adRP. This is a transcription factor for several of the retinal genes and a mutation has been identified in one adRP family (Sohocki *et al.*, 1998). Mutations in another retina specific transcription factor, the Nrl gene mapping to 14q11.1-q11.2, have also been shown to cause adRP. Unlike the CRX gene which is expressed exclusively in the photoreceptors, this gene is expressed in all the cellular layers of the retina (Molday, 1998; Liu *et al.*, 1996). A single mutation in this gene has been reported in a large adRP family (Bessant *et al.*, 1999). It is hypothesized that the Nrl protein may play a role in the expression of rod photoreceptor genes in both the developing and adult retina (He *et al.*, 1998). Very recently the adRP gene at the RP locus on 8q11-8q13, referred to as the RP1 locus, has been identified. Mutations in this gene were identified in two different families in independent research groups (Sullivan *et al.*, 1999; Guillonneau *et al.*, 1999). This is a photoreceptor specific gene of unknown function.

2.1.6 Autosomal recessive RP loci

Large arRP pedigrees are by their nature difficult to attain for the purpose of linkage studies and therefore investigators frequently depend on consanguineous families in undertaking to localize the genes involved. Candidate gene studies, where investigators examine the possible involvement of a gene based on knowledge of its function, are also employed. Despite the limitations of arRP pedigrees a considerable number of genes have been found to cause arRP.

As previously mentioned three of the mutations identified within the rhodopsin gene to date bring about arRP (Rosenfeld *et al.*, 1992; Dryja and Li., 1995). The gene responsible for the highest percentage of arRP cases is the β -subunit of the rod cGMP dependant phosphodiesterase (PDE) (McLaughlin *et al.*, 1993; Bayes *et al.*, 1996). The

genes of subunits of this protein were adopted as candidates following the observation that a mutation in the β -subunit (PDEB) of the gene brings about a fast retinal degeneration in the retinal degeneration (rd) mice (Pittler *et al.*, 1993). Screening of the human gene on 4p16 in arRP patients has led to the identification arRP specific mutations (McLaughlin *et al.*, 1993; Bayes *et al.*, 1996). The reports of the involvement of the β -subunit of the cGMP phosphodiesterase in arRP led also to the screening of the α -subunit (PDEA) of the gene in RP patients. Three point mutations within the PDEA gene have been identified in individuals with arRP (Huang *et al.*, 1995). Mutations with the PDE subunits are believed to affect the catalytic activity of the protein, bringing about raised levels of cGMP which may be deleterious to the cell (Huang *et al.*, 1995).

Mutations in α -subunit of another key protein of visual transduction, the rod cGMP-gated cation channel (CNCG1), also bring about arRP (Dryja *et al.*, 1995). This gene maps to 4p14-q13 and following its screening in 94 unrelated patients, has been associated with arRP in four families (Dryja *et al.*, 1995).

In 1997 the involvement of the cellular retinaldehyde-binding protein (CRALBP), which maps to 15q26, in arRP was reported (Maw *et al.*, 1997). Unlike most of the RP genes known to date CRALBP is not expressed in the photoreceptor cells but is abundant in the RPE and the muller cells of the retina, where it is a carrier for both 11-cis-retinol and 11-cis-retinaldehyde. In the RPE it is believed to bind 11-cis-retinol while it is used as a substrate for a dehydrogenase to form 11-cis-retinaldehyde (Stecher *et al.*, 1999). A single substitution in this gene in an Indian family has been shown to be responsible for arRP (Maw *et al.*, 1997).

A retina-specific member of the tubby-like gene family, TULP1, was simultaneously reported by independent investigators to cause arRP (Hagstrom *et al.*, 1998; Banerjee *et al.*, 1998). This gene which maps to 6p21.3 is related to the tub gene which causes obesity, deafness and a retinal degeneration in "tubby" mice (Ohlemiller *et al.*, 1995). Five different mutations have been identified within the gene, although how they bring about the disease pathology is as yet unclear (Hagstrom *et al.*, 1998; Banerjee *et al.*, 1998).

Autosomal recessive RP mutations have also been found in a retinal specific member of the ABC transporter family, ABCR (Martinez-Mir *et al.*, 1998) and in the RPE specific RPE65 gene (Morimura *et al.*, 1998) For an in-depth discussion of these genes see chapter 6.

A number of other genes involved in the etiology of arRP have yet to be identified. Loci for the disease have been linked to 1q31-q32 (van Soest *et al.*, 1994), 6cen-q15 (Ruiz *et al.*, 1998; Khaliq, 1999), 16p12.1-p12.3 (Finckh *et al.*, 1998), 2p11-p16 (Gu, 1999) and 2q31-q33 (Bayes, 1998).

2.1.7 X-linked RP loci

The first RP locus to be identified was the RP locus on the X chromosome at Xp11.3-p11.23 (Bhattacharya *et al.*, 1984). This form of the disease is referred to as RP2 and is associated with early onset and severe myopia (Kaplan *et al.*, 1992a). The RP2 gene was identified following a positional cloning approach (Schwahn *et al.*, 1998). The gene encodes a 350 amino acid protein of unknown function. It shows homology however, to the human cofactor C protein which is known to play a role in beta-tubulin folding (Schwahn *et al.*, 1998).

In the year following the identification of the first xLRP locus, a second locus was identified on the X chromosome at Xp21.1-p11.4 (Nussbaum *et al.*, 1985). This locus is referred to as RP3 and is associated with later onset of night blindness than the RP2 locus. Carrier females of this form of RP have an unusual tapetal reflex (metallic sheen of the retina) (Kaplan *et al.*, 1990). Loss of function mutations in a gene known as the retinitis pigmentosa GTPase regulator (RPGR) have been shown to be responsible for this form of xLRP (Meindl *et al.*, 1996). The amino-terminal half of this protein shows homology to the regulator of chromosome condensation gene, which is the nucleotide exchanger for the small GTP-ase, Ran. The RPGR protein has been shown to interact with the delta subunit of the rod cGMP PDE and it has been suggested that RPGR mutations may bring about pathogenic effect by disrupting certain intracellular processes that are involved in protein transport and localization (Linari M *et al.*, 1999). RPGR is unusual among the RP genes, as it appears to be expressed ubiquitously (Meindl *et al.*, 1996). Within the retina the protein is localized to the rod cells (Yan *et al.*, 1998). It is not clear how a ubiquitously expressed protein brings about a tissue specific disease such as RP but an alternatively spliced retina-specific transcript of the gene has been reported and may go toward explaining this (Kirschner *et al.*, 1999).

On the basis of different linkage relationships a third xLRP locus, designated RP6, has been predicted (Ott *et al.*, 1990; Musarella *et al.*, 1990). This locus has been

placed at Xp21.3-21.2, between the RP2 and RP3 genes. A putative locus for cone-rod degeneration, RP15, has also been placed on the short arm of the X chromosome at Xp22.13-22.11 (McGuire *et al.*, 1995a). There has been some speculation however, that RP15 may in fact be allelic to RP6 (Inglehearn and Hardcastle, 1996). It will not be possible to determine whether or not this is the case however, until the genes are cloned.

An RP locus has also been linked to the long arm of the X chromosome at Xq26-q27 (Gieser *et al.*, 1998). Affected males of the 5-generation pedigree used to localize this gene show classic RP symptoms. This gene has been designated RP24.

2.1.8 Syndromic RP

A number of systemic diseases exist for which RP is one of the symptoms. The most widely known of these is Usher syndrome (discussed in chapter 5). Because of the high energy demands of retinal tissue, RP is often a feature of mitochondrial based diseases such as NARP and Kearns-Sayre syndrome (discussed in chapter 5). RP is also a feature of Bardet-Biedl syndrome and can be associated with autosomal dominant cerebellar ataxia and X-linked mental handicap (Beales *et al.*, 1997; Mainzer *et al.*, 1970; Aldred *et al.*, 1994).

2.1.9 A locus for adRP on chromosome 7q

A major linkage study, carried out by members of this research unit resulted, in 1993, in the localization of an adRP gene to the long arm of Chromosome 7 (Jordan *et al.*, 1993). This gene is referred to as the RP10 gene. The investigation involved a genome wide search of DNA from 36 members of a large Spanish family, FA-84, segregating the disease. Autosomal dominant RP has been traced through five generations of this kindred. The mean age of onset of the disease within the family is early at approximately 13 years of age with a range of age of onset from 5-28 years. Patients initially experience night blindness and subsequently suffer from severe constriction of visual fields. A number of individuals have presented with cataracts, debilitating enough to merit surgery. All affected individuals show the classic clinical symptoms of RP, including optic disc

pallor, bone spicule pattern pigmentary deposits, and retinal vascular attenuation. They also show either diminished or extinguished cone and rod ERGs. A number of family members have been declared legally blind by the age of 40 (Jordan *et al.*, 1993).

Positive lod scores were obtained with fifteen chromosome 7 microsatellite markers, placing the disease locus at 7q31-35 (Jordan *et al.*, 1993). These lod scores indicated that the disease gene was most closely linked to markers D7S480, D7S466 and D7S514 with a maximum lod score of 7.22 at $\theta = 0.00$ to the marker D7S480. Multipoint analyses gave a lod score of 7.51 which maximized at D7S480 (Jordan *et al.*, 1993).

An unrelated American adRP family, UTAD045, exhibiting a later onset and a slower progression of symptoms has also been reported to show linkage to 7q31-35 (McGuire *et al.*, 1995b). The marker D7S480 gave a positive lod score of 4.3 at $\theta = 0.05$ in this family. Out of an additional eleven markers used to more precisely locate the disease gene, a maximum lod score of 5.26 at $\theta = 0.00$ was obtained to the marker D7S514. Multipoint analyses carried out in this family indicates that there is a high probability of the RP10 gene being located between the markers D7S480 and D7S514, with its most likely location being 3cM distal to D7S480 (McGuire *et al.*, 1995b).

Data from both families were combined in an attempt to further delimit the disease interval (McGuire, 1996a). The highest combined lod score occurs with the marker D7S514. Affected individuals in both families showed recombination events between the disease locus and a microsatellite marker within the seventeenth intron of the cystic fibrosis transmembrane gene (CFTR), thereby placing the gene distal to CFTR (McGuire, 1996a). Haplotype analysis subsequently indicated that the marker D7S686, which is distal to CFTR, can in fact be considered as the proximal boundary (McGuire, 1995a). The distal marker D7S530 had one recombinant individual in family UTAD045, thereby narrowing the disease interval to ~5cM (McGuire *et al.*, 1996a).

A second adRP Spanish family, CVRP4, has also been reported to show linkage to 7q (Millan *et al.*, 1995). This pedigree is smaller in size than the Spanish pedigree (FA-84) but the disease shows similar clinical features in both. Genotype analysis at the D7S480 locus has indicated that this family is not related to family FA-84 (Millan *et al.*, 1995). However, comparisons of detailed haplotyping of the interval in both families would be necessary to be entirely confident that the families are not related. Multipoint

analyses in this family achieved a maximum lod score of 3.01 by placing the disease locus at $\theta = 0.00$ from D7S480 (Millan *et al.*, 1995). It has since been reported however that if corrected for reduced penetrance this lod score is actually less than 2.0. (McGuire, 1996b).

A 44-year-old unaffected male from the smaller Spanish family (CVRP4) shows a recombinational event between the RP10 locus and the marker D7S514. If this recombinational event is taken into consideration the disease interval is significantly reduced to a physical distance of approximately 1.7cM on 7q31.3. However, further analyses carried out on DNAs from members of CVRP4 indicate that this result may be in error (McGuire, 1996b). It has in fact been suggested that due to the small family size of CVRP4, the young age of some of the individuals and the non significant lod scores that the linkage to 7q may not be true (McGuire, 1996b). Therefore, in order to be entirely confident of delimiting the disease interval, the markers D7S686 and D7S530 should be considered as the RP10 flanking markers.

A fourth adRP family, of Scottish origin, have been reported to show linkage to 7q31.3 with a maximum two point lod score of 3.31 at $\theta = 0.00$ with the marker D7S514 (Mohamed *et al.*, 1996).

It is difficult to estimate the percentage of cases of RP that the gene on 7q is responsible for. This is partly due to the fact that many RP families are too small to carry out linkage surveys on and will only be screened for a mutation on 7q following the identification of a disease gene. One study however, investigated the frequencies of the nine known adRP loci in 20 RP families but did not identify any further families mapping to the 7q locus (Inglehearn *et al.*, 1998).

2.1.10 Candidate disease genes on 7q

With the identification of a chromosomal location for the disease gene in families FA-84 and UTAD045, the screening of candidate genes on chromosome 7q began. In the history of the search for the RP10 gene a number of genes have been considered as candidates. The obesity (OBS), paired-box 4 (Pax4) and inosine-5-prime-monophosphate dehydrogenase type 1 (IMPDH1) genes have all been mapped to the RP10 region of 7q (McGuire, 1996b). PAX4 is a member of the paired-box gene transcription factor family. Transcripts of this gene have never been isolated in humans

however, and on the basis of its structure it is believed to be a pseudogene (Walther *et al.*, 1991). Based on knowledge of their predicted protein functions, together with the fact that neither the OBS or the IMPDH1 genes appear to be expressed in the retina, it was considered appropriate to also exclude each of these genes as RP10 (McGuire, 1996b).

The gene encoding ARF5, an ADP ribosylation factor which maps within the critical region and is expressed in the retina as well as other tissues, was also adopted as a candidate gene. However, it has also been excluded more recently, as the disease gene by direct sequencing of the coding regions (Daiger *et al.*, 1997).

Genes which are known to be expressed in the disease tissue obviously make more attractive candidates in the search for a disease gene. Three genes which are expressed in the retina and play a role in visual transduction also map to 7q. The inhibitory subunit of the protein complex transducin (GNTG1) was mapped to 7q by fluorescent *in situ* hybridization (Scherer *et al.*, 1996a). Linkage studies on the affected families, using a microsatellite marker mapping within the 1-2 Mb of the GNGT1 gene, however, excluded tight linkage between GNGT1 and RP10 (McGuire, 1996b). The gene encoding acetylcholinesterase (ACHE) has also been mapped to 7q by fluorescent *in situ* hybridization (Elrich *et al.*, 1992). ACHE is responsible for cleaving the neurotransmitter acetylcholine and hence plays an essential role in the termination of signal transmission in the retina (Elrich *et al.*, 1992). ACHE has since been mapped centromeric to the RP10 critical region however, and can therefore be excluded as the disease gene. (Getman *et al.*, 1992). A third retinal specific gene, which encodes the blue cone pigment (BCP), maps near the critical disease interval (Fitzgibbon *et al.*, 1994). Despite the fact that RP primarily affects the rod photoreceptors, which makes BCP an unlikely candidate, it was excluded as the RP10 gene by direct sequencing of the coding regions of the gene in affected individuals of both the Spanish and America families (McGuire, 1996b).

During the course of my involvement in the project to identify the 7q adRP gene, two novel genes were identified by other investigators which map to the disease region of chromosome 7q. These genes encode a metabotropic glutamate receptor and a diacylglycerol kinase. Their physical location, together with the nature of their protein function, led us to adopt them as candidates for the 7q RP gene and to screen them for disease mutations.

2.1.11 Metabotropic glutamate receptors and GRM8

The effects of glutamate, the main excitatory neurotransmitter of the brain, are modulated by the glutamate receptors. The glutamate receptors are a highly heterogeneous group of proteins and may be classified as either ionotropic or metabotropic proteins (Duvoisin *et al.*, 1995). The ionotropic receptors are ligand-gated ion channels which are assembled from a number of subunits. The metabotropic receptors (GRMs) are signal polypeptides, which are coupled to G-proteins and bring about various functions through the modulation of intracellular effectors. They are single polypeptides predicted to span the plasma membrane seven times (Duvoisin *et al.*, 1995). To date eight metabotropic receptors have been identified; mGluR1 through to mGluR8 (Duvoisin *et al.*, 1995).

In 1996 the localization of a GRM, GRM8, to the long arm of chromosome 7 was reported (Scherer *et al.*, 1996b). This gene was originally identified from a mouse retina cDNA library. Using somatic cell hybrids and fluorescent *in situ* hybridization (FISH), GRM8 was mapped to 7q31.3-q32.1 (Scherer *et al.*, 1996b). The coding sequence is 2727 nucleotides in length but the entire gene is particularly large with an estimated size of 1Mb (Scherer *et al.*, 1997).

Information processing in the retina occurs in two distinct pathways, known as the ON and OFF channels. Ganglion cells respond to both the onset and offset of light and may be divided into either ON center or OFF center cells (Daw, 1990). The first of the intermediate cells between the rod photoreceptor and the ganglion cell is the ON bipolar cell. This bipolar cell connects to the ON pathway via synapses with the cone bipolar cells and to the OFF pathway via synaptic junctions with the OFF ganglion cells (Schiller, 1992).

The photoreceptors are believed to use the neurotransmitter glutamate which acts on bipolar cells, causing their depolarisation. In the dark glutamate is released from photoreceptor cells. Current evidence suggests that neurotransmission is accomplished when the glutamate receptors of the ON bipolar cells increase the rate of cGMP hydrolysis, via a G-protein mediated process and in this way cause the closure of the ion channels. This results in the hyperpolarization of the bipolar cell (Nawy and Jahr, 1990). Signal transduction of the ON bipolar cell is therefore remarkably similar to the light induced transduction of the photoreceptor cells.

The mouse receptor, mGluR6, has been proposed as the postsynaptic glutamate receptor of the retinal ON bipolar cells (Nomura *et al.*, 1994). The mouse homologue of GRM8, mGluR8, shows 70% homology to mGluR6 and it was considered possible therefore, that it plays a similar role in the retina to mGluR6. *In situ* hybridization studies have shown, that mGluR8 is expressed at high levels in the olfactory bulb, the accessory olfactory bulb and the mammillary body, along with a lower level of expression in the retina (Duvoisin *et al.*, 1995). Preliminary studies showed that within the retina mGluR8 is expressed in both the inner nuclear layer and the ganglion cell layer (Duvoisin *et al.*, 1995). However, at the time of the present study it had not been determined in precisely which cell types of the retina mGluR8 is expressed.

Since the completion of this study immunocytochemistry has been used to locate rat mGluR8 to both plexiform layers of the retina as well as the inner nuclear layer and the ganglion cell layer (Koulen *et al.*, 1999). Within the outer plexiform layer it has been demonstrated to be located in the terminals of the photoreceptors where it is responsible for the presynaptic modulation of intracellular calcium concentration (Koulen P *et al.*, 1999). The calcium concentration in presynaptic nerve terminals is intimately linked to neurotransmitter release. It is believed therefore, that mGluR8 is involved in an inhibitory feedback loop which controls glutamate release from the photoreceptors (Koulen *et al.*, 1999). The mGluR8 protein has also been located presynaptically in the projection neurons of the main olfactory bulb in rat (Kinoshita, 1996)

Evidence that mGluR8 is expressed in the retina, together with the fact that GRM8 has been shown to map to the RP10 interval, led us to embark on a collaborative study with Dr. Lap Tsui's group in the Hospital for Sick Children, Toronto in order to determine the genomic structure of GRM8 and subsequently to screen the gene for a disease mutation in the adRP Spanish pedigree. Significantly, the gene spans much of the RP disease interval, encompassing the microsatellite markers D7S1873, D7S1822, D7S1874 and D7S680, all of which are located within or close to the region of 7q previously shown to map at zero recombination to the disease locus (Scherer *et al.*, 1997).

2.1.12 RT-PCR on illegitimate transcripts

All but two of the ten GRM8 exons have been screened by conventional methods. However, a small portion of the gene proved refractory to cloning and hence the precise structure of the gene in this region has not been determined. The coding sequence in this region was therefore screened for disease mutations using a relatively new technique. This technique uses RT-PCR to detect the transcripts of tissue specific genes in tissues which would not be expected to express these genes, by making use of a phenomenon referred to as illegitimate or ectopic transcription (Chelly *et al.*, 1989). It appears to be a general phenomenon, with all genes so far analysed being expressed at a basal level in all cell types (Roberts *et al.*, 1991). For example, genes which have been noted to exhibit the phenomenon include those of the anti-mullerian hormone, beta-globin, retinal blue pigment, phenylalanine hydroxylase etc. (Roberts *et al.*, 1991).

The level of transcription in "non-expressing" tissue types is very low - probably in the range of 1 transcript per 100-1000 cells (Kaplan *et al.*, 1992b). Illegitimate transcripts have been shown to be identical to the transcripts expressed in tissues for which they are specific (Chelly *et al.*, 1991) and they therefore provide a useful tool for the analysis of mRNA specifically expressed in non accessible tissues. Accordingly, illegitimate transcription potentially allows the screening of transcripts for RP mutations, which are only expressed at a significant level in the eye. While samples of mRNA from the eye cannot be readily obtained from patients for research purposes, it is possible to use total RNA from peripheral blood lymphocytes as a template for an RT-PCR based system to isolate segments of coding region from the candidate gene. Following successful PCR amplification, products are of a quantity and quality sufficient for direct sequencing. The lack of requirement for cloning, or for the laborious determination of the structure of the gene, make this a very attractive system for mutation detection. It is particularly attractive for genes with a large number of exons. Furthermore, as mRNA has undergone transcription and splicing, comparison with controls may allow the detection of splice site mutations (Roberts *et al.*, 1991).

2.1.13 Diacylglycerol Kinases and DGK ι

Diacylglycerol (DAG) plays a complex role in the cell which has yet to be fully elucidated. It occupies a central position in the pathways which lead to the biosynthesis of triglycerides and phospholipids and also functions as an intracellular messenger in stimulated cells. How DAG can serve two such distinct cellular functions has yet to be resolved but its relative levels within the cell at a given time are of critical importance. The concentration of DAG is controlled by the rates of both its synthesis and degradation. Upon stimulation of the cell membrane, activation of phospholipases bring about the cleavage of the membrane phospholipid, phosphatidylinositol 4,5-biphosphate into inositol-1,4,5-triphosphate and DAG. This results in an increase in the intracellular levels of DAG, thus making more available for use in the biosynthetic pathways and also, in the presence of CA^{2+} , bringing about the activation of protein kinase C (PKC) (Kanoh *et al.*, 1990). PKC is responsible for phosphorylating target proteins and the regulation of many cellular functions (Kikkawa *et al.*, 1989).

Diacylglycerol kinase (DGK) plays an important role in the cell by catalysing the conversion of DAG, in the presence of ATP, into phosphatic acid (PA), thus bringing about a reduction in the levels of DAG (Kanoh *et al.*, 1990). The reduction in DAG levels results in an attenuation of both the activation of PKC and of phospholipid synthesis. The increase in amounts of PA has further knock-on affects as it functions as a lipid messenger (Knauss *et al.*, 1990) and initiates the re-synthesis of phosphatidylinositols which is essential for phospho-lipid turnover (Holub and Kuksis, 1978).

The role of DGK in reducing the levels of DAG is therefore of critical importance in a number of cellular functions. Multiple DGK isozymes have been identified in animal cells. These isoforms, which have been designated as DGK α (Sakane *et al.*, 1990), DGK β (Goto and Kondo, 1993), DGK γ (Kai *et al.*, 1994), DGK δ (Sakane *et al.*, 1996), DGK ϵ (Tang *et al.*, 1996), DGK ξ (Bunting *et al.*, 1996) and DGK η (Klauck *et al.*, 1996), differ in their cell type specificity, structural domains and substrate specificities.

A DGK gene has been shown to be responsible for the visual defects in the *Drosophila* retinal degeneration (rdgA) mutant (Masai *et al.*, 1993). This DGK gene, which is expressed almost exclusively in the retina, has been designated DGK2 (Masai

et al., 1993). In the *rdgA* mutant the photoreceptor cells differentiate normally but degenerate rapidly within the first week after eclosion (Hotta and Benzer, 1970). The DGK2 protein has been demonstrated experimentally to be a membrane associated protein (Masai *et al.*, 1993). It has four ankyrin repeats which in other proteins have been implicated in protein interactions, gene regulation and cell-cycle control (Ding *et al.*, 1998). Morphologically it has been observed that the subrhabdomeric cisternae (SRC), which are responsible for the transport of phospholipids to the photoreceptor membranes, are disrupted in the *rdgA* mutant (Matsumoto *et al.*, 1988; Masai *et al.*, 1997). It is not exactly clear as to how the defective DGK2 protein brings about the visual defects but it has been postulated that the lack of a functional DGK results in a deficiency of PA and consequently causes defects in phospho-lipid turnover (Masai *et al.*, 1997).

Recently a novel human DGK gene has been cloned and mapped very near to the RP10 region at chromosome 7q32.3-33 (Ding *et al.*, 1998). This gene is the ninth member of the DGK family to be identified and has been designated DGK ι . It was identified by performing a BLAST search on an EST database using cDNA DGK ξ sequence. A retinal EST, which was derived from a novel DGK gene (DGK ι), was identified in this manner. It was sequenced and used to probe other libraries in order to retrieve the entire coding sequence of the gene (Ding *et al.*, 1998).

DGK ι is expressed only in the retina and brain (Ding *et al.*, 1998). It has been assigned to the group IV DGKs which includes the DGK ξ and DGK2 genes and it shares a number of domain motifs with the other members of this group including two cysteine-rich repeats, four ankyrin repeats at the C terminus and a catalytic domain within which there is a putative ATP binding site (Ding *et al.*, 1998). It also possesses a motif which resembles a phosphorylation site and has previously been shown to serve as a nuclear localization signal and PKC phosphorylation site in DGK ξ . The role of a DGK gene in the *rdgA* mutant, its expression in the retina and its chromosomal location made the DGK ι gene a plausible and exciting candidate for the *adRP* gene (RP10). Screening of this gene for a disease mutation was undertaken in family FA-84.

2.1.14 Study Aim

The aim of this study was firstly to review the linkage and haplotype data which initially defined the RP10 disease interval and secondly to screen candidate genes for the 7q adRP mutation in order to confirm their involvement in RP10 or to exclude them as candidates. These candidate genes were GMR8 and DGK ι . It was necessary to first elucidate the genomic structure of GRM8 before the coding sequences could be screened in affected individuals. Different methods including SSCP, direct sequencing, RT-PCR on illegitimate transcripts, typing of a polymorphic marker and PCR digestion were used to evaluate these genes as the RP10 gene.

2.2 MATERIALS AND METHODS

All reagents were purchased from BDH unless otherwise stated.

2.2.1 Patient clinical assessment and DNA extraction

Patients were clinically assessed in detail by Dr. Carmen Ayuso, Fundacion Jimenez Diaz, Madrid. Best corrected visual acuity, Goldmann perimetry, Octopus 500 automated perimetry, slit-lamp biomicroscopy and electroretinography were used to assess family members. Fundus visualizations by direct and indirect ophthalmoscopy was also performed on patients.

DNA was extracted from lymphocytes using standard methods involving SDS lysis, proteinase K digestion and phenol extraction by Dr. Carmen Ayuso.

2.2.2 PCR amplification

In a standard PCR, 1µg of template DNA extracted from blood was added to 10µl 10x PCR reaction buffer (Appendix A.3), 200µM dATP, dTTP, dGTP and dCTP (Boehringer), 50pmol of each primer and 2.5U Taq Polymerase in a total volume of 100µl. After an initial denaturation (94°C/7 min), 30 cycles of PCR amplification were performed, with each cycle consisting of denaturation (94°C/1 min), primer annealing (55°C/1 min) and extension (72°C/1 min 20 sec). Magnesium curves were often carried out to determine the appropriate magnesium concentration for a particular PCR. Other conditions such as annealing temperature, extension time and concentration of reagents were occasionally modified to optimize amplification with particular primer pairs. PCR reactions were carried out on a DNA Engine PTC-200 (MJ Research).

Radioactive PCRs were performed in a volume of 25µl with the same final concentration of components but with dATP at a concentration of 2.5µM and with the addition of 0.1µCi [alpha-³²P] ATP (Amersham). Radioactive PCRs were carried out on a DNA Thermal Cycler (Perkin Elmer).

2.2.3 Microsatellite analysis

Primer sequences (Appendix B.1) of microsatellites were obtained through an NIH chromosome 7 web site based on the Genethon map (National Human Genome Research Institute, 1999). Radioactive PCRs on family DNAs were carried out as above. Following amplification, 25 μ l of formamide loading dye (Appendix A.1) was added to each sample. Samples were then denatured for 5 minutes at 94°C and 3-5 μ l of each loaded onto 8% acrylamide gels (Appendix A.1). Electrophoresis was performed at a maximum current of 40mA and a maximum voltage of 2000V. Gels were subsequently dried and exposed to X-ray film (Agfa).

2.2.4 Linkage analysis

The microsatellite data was compiled using the LINKSYS version 4.11 data management package (Attwood and Bryant, 1988). Two-point lod scores were subsequently calculated using LIPED, run on a 512K PC. Full penetrance of the disease in family FA-84 was assumed. The frequency of the RP phenotype was set at 0.0001 and the frequency of the unaffected phenotype was set at 0.9999. The frequencies of the microsatellite marker alleles were presumed to be equal.

2.2.5 Large scale plasmid purification (maxiprep)

10mls of LB broth (Appendix A.2) with 75 μ g/ml ampicillin (Sigma) was inoculated with a bacterial stab culture and incubated at 37°C overnight with shaking. 1L of LB broth was inoculated with this overnight culture and allowed to reach an OD₆₀₀ of 0.7-0.8. 0.1g of chloramphenicol (Sigma) was added to this culture and it was incubated at 37°C overnight with shaking. The overnight culture was divided into four 250ml centrifuge tubes (Sorvall) and the cells harvested at 10,000rpm at 0°C for 10 minutes. The pellets were re-suspended and pooled in 50ml of 0.05M Tris HCl pH 8.0 (BDH). The cells were harvested at 7,000 rpm at 4°C for 30 minutes. The pellet was re-suspended in 50ml lysis solution I (Appendix A.4) and left on ice for 10 minutes. 80ml

of lysis solution II (Appendix A.4) was added, the solution mixed well and left on ice for 5 minutes. 40ml of cold lysis solution III (Appendix A.4) was added and the solution left on ice for 15 minutes. The solution was centrifuged at 8,000rpm at 0°C for 15 minutes and the supernatant decanted into a fresh centrifuge tube through sterile gauze. 0.6 volumes of ice cold isopropanol was added and the pellet was harvested at 8,000 rpm at 0°C for 5 minutes. The supernatant was drained off and the pellet air dried. The pellet was re-suspended in 8ml of Tris-HCl, pH 8.0. Precisely 8.8g of CsCl (Gibco-BRL) was dissolved in 8.7ml plasmid solution and 700µl of 10mg/ml EtBr (Sigma) added. This solution was then placed in an ultracentrifugation tube (Beckman), using a Pasteur pipette, and top up solution (Appendix A.4) was used to fill the tube and also a balance tube. Stoppers and metal caps were very carefully used to seal the tubes and the sample was spun at 45,000 rpm in an ultracentrifuge (Beckman) overnight. Following ultracentrifugation, the plasmid band was visible in the solution and was extracted through the side of the tube using a needle and syringe. The extracted DNA was washed 5-6 times in an equal volume of H₂O-saturated butanol to remove the ethidium bromide. The DNA solution was then placed in a collodium bag (Sartorius) which had been soaked in dH₂O for at least an hour and dialysed against 5mM Tris-HCl, pH 7.6 for at approximately 10 hours to remove the salt. The buffer was changed regularly. This also pressure concentrated the solution down to approximately 1ml. The concentration and quality of the DNA were determined by OD readings and observation on agarose gels (Appendix A.1).

2.2.6 Single stranded conformational polymorphism electrophoresis (SSCP) analysis.

25µl radioactive PCRs were carried out as above. 14.5µl of formamide dye (Appendix A.1) was added to each PCR. Prior to electrophoresis, samples were denatured at 95°C for 5 minutes and placed on ice. Electrophoresis was performed on a non-denaturing acrylamide gel (Appendix A.1) at approximately 6W, without pre-heating, and fans were used to ensure gels remained cool. 6% gels with 10% glycerol were used. Gels were subsequently dried and exposed to X-ray film (Agfa).

2.2.7 Sepharose columns

0.6ml eppendorphs were pierced at the bottom using a needle. 20 μ l of glass beads (Sigma) were placed in the eppendorph and the eppendorph then filled to the top with CL-6B sepharose (pharmacia). The eppendorphs were placed in collecting tubes and spun at 2,000 rpm for 2 minutes to form the columns.

2.2.8 PCR purification for sequencing

PCRs were purified prior to sequencing to remove proteins and primers. A chloroform step was performed to remove the last traces of mineral oil. Samples were then incubated at 55°C for an hour with 5 μ l 200 μ g/ml proteinase K (Sigma) solution per 100 μ l PCR. Samples were then loaded onto sepharose columns and retrieved by spinning at 2000 rpm for 2 minutes. The concentration of the purified product was estimated by eye following electrophoresis on a 2% agarose gel.

2.2.9 Automated sequencing

250ng of purified PCR product and 5pmols of sequencing primer was added to 8 μ l reaction mix from the DNA Sequencing, Dye Terminator Cycle Sequencing Ready Reaction Kit (Perkin Elmer). Sequencing reactions were performed in an MJ Research Inc. PCR block. The reactions were precipitated with ethanol and washed with 70% ethanol. They were then re-suspended in 3.5 μ l of suspension buffer (Appendix A.3). Sequencing reactions were resolved on an ABI 373A DNA sequencer according to the manufacturers instructions. The data was processed using ABI data collection and analysis software.

2.2.10 End-labeling of primers for direct sequencing

5pmol of primer was end-labeled by incubating for at least 1 hour at 37°C in the presence of 0.1U T4 polynucleotide kinase (NE Biolabs), 1µl of 10x T4 polynucleotide kinase buffer and 2µCi [γ -32P] ATP, in a total volume of 10µl. The mixture was then heated to 94°C for 5 minutes to deactivate the enzyme.

2.2.11 Direct sequencing

The DNA template was denatured with 2µl of end-labeled primer at 94°C for 5 minutes in a total volume of 10µl. The mixture was snap chilled on ice and held there for 2 minutes. 8µl of sequencing buffer (Appendix A.3) and 2µl sequenase, (USB) diluted in a ratio of 1:8 in sequenase buffer (USB), was added. 4.4µl of this mixture was added to 3µl of each of the G, A, T and C dideoxy termination mixes (USB) at 37°C. The mixtures were incubated at 37°C for 10-15 minutes after which time the reactions were stopped by adding 5µl of formamide dye (Appendix A.1). Samples were overlaid with mineral oil and denatured at 94°C. 3-5µl was loaded on an 8% polyacrylamide gel (Appendix A.1) for analysis. Gels were subsequently dried and exposed to X-ray film (Agfa).

2.2.12 RNA preparation

All solutions were pretreated with DEPC (Appendix A.5) prior to RNA work and all glassware was baked at 180°C for at least eight hours or treated with RNase Away (Molecular Bio Products). Sterile plastic-ware was presumed to be RNase free.

10ml samples of peripheral blood were collected in tubes containing EDTA at a final concentration of 3.9mM/L. 35mM NaCl was added in order to bring about erythrocyte lysis. Lymphocytes, which were used as the source of RNA, were separated by centrifugation at 2500rpm for 15 minutes. 10.8µl of β -Mercaptoethanol (Sigma) was added to 1.5ml guanidinium thiocyanate solution (Appendix A.5) in the fume hood.

750µl of this solution was then added to the lymphocyte pellets. To the resulting lysate, 75µl of 3M sodium acetate, pH 4.0, 750µl phenol (Gibco-BRL) and 150µl chloroform/isoamyl alcohol (49:1) was added and mixed by inversion. The mixture was kept on ice for 30 minutes. It was then divided into two eppendorphs and each centrifuged at 13,200 rpm for 20 minutes. The supernatant was removed to a fresh eppendorph. An equal volume of isopropanol and 1µl of glycogen (Boehringer Mannheim) was added and the RNA allowed to precipitate at -20°C. The samples were spun at 13,200 rpm for 20 minutes, the supernatant removed, and the pellets dried at 80°C for 3 minutes. The pellets were re-suspended in 20-30µl of sterile H₂O. RNA samples were stored at -70°C following purification.

The quality of the RNA was estimated by observation on ethidium stained agarose gel and by calculating the OD 260/280 ratio which should approximate 1.5 (Maniatis *et al.*, 1992). A DNaseI step was then performed. 1U DNaseI (Gibco-BRL) and 1.2µl 10x DNaseI Buffer was added to 2µg RNA in a total volume of 12µl. The reaction was held at room temperature for 15 minutes after which time the enzyme was heat inactivated at 65°C for 10 minutes. The sample was made up to 15µl with H₂O.

2.2.13 RT-PCR and nested PCR on illegitimate transcripts

350ng - 3µg of RNA was incubated at 65°C for 10 minutes with 50pmol of the RT primer in a total volume of 7.5µl, overlaid with mineral oil. This mixture was snap-chilled on ice and made up to a total volume of 20µl with a mix containing 10mM dNTPs (BoehringerMannheim), 4µl 5x RT buffer, 100mM DTT (Gibco-BRL), 200U MMLV RT (Gibco-BRL) and 25U RNase inhibitor (Promega). This reaction was incubated at 42°C for one hour.

Following the incubation step, 30µl of a mixture containing 5µl of 10x Expand high fidelity buffer with 15mM MgCl₂ (BoehringerMannheim), 50pmol forward primer and 3.5U Expand high fidelity polymerase (BoehringerMannheim) was added and 30 cycles of PCR amplification were performed with each cycle consisting of denaturation (94°C/1min), annealing (60°C/1min) and extension (72°C/3min) followed by an incubation time of 72°C for 5min.

1 μ l of this amplified sample was then added to a standard 50 μ l PCR mix containing nested primers and 1.75U Expand high fidelity polymerase. 40 PCR cycles were then performed as above.

2.2.14 PCR digestion

A 15 μ l aliquot of each DGK ι exon 29 PCR product was digested with 20 units of *EcoRI* (New England Biolabs) at 37°C overnight, with the buffer supplied by the manufacturers. Samples were analysed on 2.5% ethidium bromide stained agarose gels.

2.3 RESULTS AND DISCUSSION

2.3.1 Re-haplotyping of the 7q interval in family FA-84

A number of factors necessitated a re-evaluation of the linkage data on family FA-84. These are listed below.

A). DNA was obtained from a further eight family members who had not been included in the initial linkage study. Seven of these were from a family unit within the extended pedigree; from individual III -2, her children and grandchildren. DNA from the unaffected individual V-21 was also obtained (Figure 2.3).

B). Some of the younger members of the pedigree have been re-evaluated clinically and the affected status of each re-assessed, as far as possible.

- ◆ Family member V-12 is a 13 year-old girl, originally classified as unaffected and included in the linkage study as such. Based on recent ophthalmic examination her affected status is no longer clear and it is possible that she may develop RP. In the re-evaluation of the linkage data she has been classified as of unknown disease status.
- ◆ Individuals V-13, V-14, V-15 and V-16 were all included in the original linkage study and their disease status, as it was in the original study, has been confirmed
- ◆ V-17 is a 6 year old boy. Due to his young age he was not included in original linkage study and his clinical status can still not be confirmed.

The change in the clinical status of individual V-12 necessitated a re-calculation of the lod scores generated in the original linkage study.

C). A thesis by Rachel McGuire (1996b) raises the possibility that some of the FA-84 linkage results may be in error due to the lack of molecular weight standards on the microsatellite gels.

D). The order of the microsatellites used to haplotype the family across the disease interval has changed.

Due to the reasons outlined above, it was decided to re-analyze the proximal and distal markers which flank the disease interval. Critical recombinants in both families have placed the disease between D7S686 and D7S530 on 7q31.1 (The order of the microsatellite markers on the chromosome are given in Table 2.2). One affected individual in family UTAD-045 does not carry the disease allele for D7S530 which places the disease proximal to this marker (McGuire, 1996b). Haplotype analysis previously revealed that affected FA-84 individual IV-27 does not appear to carry the disease haplotype at and proximal to the marker D7S686, thereby placing the disease distal to D7S686 (McGuire, 1995b).

Markers D7S686 and D7S530 were re-typed in the family FA-84 (Figures 2.4 and 2.5). The 2-point lod scores for these markers were re-calculated with the inclusion of the new FA-84 DNAs and the changed status of the VI-12 taken into consideration. The lod scores for other markers in the region which had been previously typed were also re-calculated with individual VI-12 classed as having unknown status. The original and new 2-point lod scores are listed in Table 2.1. The re-typing of flanking marker D7S530 did not reveal any recombinants in the family and the results complied with those of the original linkage study (unpublished data).

The re-typing of the flanking marker D7S686 did not reveal any new recombinants either but the alleles at this locus, for a number of the individuals, did not appear to be the same as those typed in the original linkage study. These included the alleles for the critical recombination IV-27. In subsequent attempts to type D7S686 in the family the results did appear to comply with the original results. The alleles for this marker do not resolve on gels very well however, despite the re-amplification of the microsatellite and the re-running of acrylamide gels. There therefore remains some ambiguity regarding whether or not individual IV-27 possesses the disease allele or not. The allele which segregates with the disease at this locus in affected individuals is allele 4. In one of the attempts at re-typing this marker it appears that individual IV-27 has inherited allele 4 along with allele 2. His affected mother does not possess an allele 2 at this locus and therefore allele 2 must have come from the unaffected father, whose DNA is not available. If this typing is correct individual IV-27 does possess the disease haplotype at this locus. The original typing results at this locus indicated that IV-27 possesses alleles 3 and 4. The affected mother possesses allele 3 on her unaffected chromosome and therefore, without the fathers haplotype, it is not possible to tell whether affected individual IV-27 inherited the affected or unaffected haplotype at this

locus. It appears therefore regardless of which of the two alleles this individual possesses, D7S686 cannot now be considered the flanking marker.

At the time of the original linkage study the marker D7S648 was placed immediately proximal to D7S686. This marker was retyped through the family confirming that individual IV-27 possesses the unaffected haplotype at this position. This indicates that a recombination event has definitely occurred distal to this marker. As many new microsatellite markers have been characterised since the original study it was possible to obtain markers between D7S686 and D7S648. A number of genetic maps were consulted in order to obtain data on chromosome 7 polymorphic markers. The chromosome 7 summary map on the Genetic Location Database (LDB) website, provided by the University of Southampton, is a good resource although the genetic map distances are not sex averaged (Collins *et al.*, 1996). This map was generated by integrating data of different types such as genetic linkage maps, radiation hybrid maps, physical maps and cytogenetic data. The comprehensive human chromosome 7 genetic linkage map provided by the Marshfield Center for Medical Genetics is based on linkage data generated from CEPH families at three different sites including Genethon (Marshfield Center for Medical Genetics homepage, 1999). The genetic map distances are sex averaged in this map. A third website, provided by the National Human Genome Research Institute (NHGRI), details the physical location of markers on the chromosome 7 Généthon genetic map and provides links to GenBank which were used to obtain microsatellite marker primer information (National Human Genome Research Institute, 1999).

A microsatellite marker, D7S1874 which is placed at the same map position as D7S686 in the Marshfield genetic linkage map has also been typed through the family. This marker showed only two alleles in the family however, and was uninformative for individual IV-27. The next available microsatellite marker proximal to D7S686 on the chromosome is D7S2471. This marker was typed through the entire family. The results indicated that IV-27 possesses the unaffected allele and, therefore, the unaffected haplotype at this locus. According to the Marshfield genetic linkage map this marker is 0.59 cM from D7S686 and should now be considered as the flanking marker.

More markers have been characterised across the critical interval since the original linkage study. However, the haplotype results indicate that there are unlikely to be recombinants within the family between the presently identified flanking markers

and therefore, for the purpose of refining the disease interval, typing these markers is unnecessary.

With the results from the re-typed markers and the results from the original gels the haplotypes across the region for all the individuals for whom DNA was available were re-constructed (Figure 2.6). With the exception of IV-27 the new haplotypes complied with the previous results for most FA-84 individuals and no new recombinants which would further refine the disease interval were identified.

Table 2.1 A comparison of lod scores obtained with particular 7q microsatellite markers in the original linkage study and the recently re-calculated lod scores for the same markers. In the generation of the new lod scores individual VI-12 was classed as having unknown status instead of unaffected status as in the original study.

| Marker | Original Lod Score | | New Lod Score | |
|--------|--------------------|----------|---------------|----------|
| | Zmax | θ | Zmax | θ |
| D7S501 | 0.54 | 0.24 | 0.72 | 0.20 |
| D7S486 | 3.59 | 0.10 | 3.62 | 0.10 |
| D7S522 | 2.04 | 0.00 | 2.09 | 0.00 |
| D7S480 | 7.42 | 0.00 | 7.53 | 0.00 |
| D7S490 | 3.43 | 0.09 | 4.85 | 0.05 |
| D7S686 | 5.69 | 0.00 | 6.00 | 0.00 |
| D7S514 | 7.13 | 0.00 | 7.23 | 0.00 |
| D7S504 | 2.68 | 0.07 | 4.57 | 0.00 |
| D7S530 | 4.29 | 0.01 | 6.69 | 0.05 |

Table 2.2 The order and distances of microsatellite markers used in this study on chromosome 7q. This data is taken from the Marshfield genetic linkage map (Marshfield Center for Medical Genetics homepage, 1999).

| Marker | Sex Averaged Kosambi cM |
|---------|-------------------------|
| D7S490 | 127.82 |
| D7S648 | 128.41 |
| D7S2471 | 128.99 |
| D7S686 | 129.58 |
| D7S1874 | 129.58 |
| D7S635 | 130.17 |
| D7S514 | 130.17 |
| D7S680 | 130.76 |
| D7S504 | 130.76 |
| D7S530 | 134.55 |
| D7S461 | 135.73 |

2.3.2 Elucidating the genomic structure of GRM8

Dr. Steve Scherer and colleagues in the hospital for Sick Children, Toronto, used a full length mouse mGluR8 cDNA clone to screen a human chromosome 7 specific cosmid library and phage library. Several clones were identified as containing GRM8 sequence and fragments of these were subcloned into the plasmid vector BlueScript (pBS). A number of these genomic DNA plasmid clones spanning GRM8 were provided to us by Dr. Scherer, which enabled us to begin elucidating the structure of the gene.

Large scale plasmid purifications were performed on the pBS clones (some of the clones were purified by Dr. Fiona Mansergh). A series of forward primers were designed from the mouse cDNA sequence in areas known to be conserved in the metabotropic glutamate receptor family. These primers, along with pBS primers from areas of the vector flanking the insert, were used in automated sequencing reactions with the GRM8 clones. Each primer was used in a sequencing reaction with each GRM8 clone. A number of these reactions resulted in what was identifiable as GRM8 coding sequence. As many of the primers were designed within the coding regions of the gene, the sequence generated began within the exons and continued into intron

sequence. Subsequent use of reverse primers within the intron sequence allowed us to sequence back into the coding region and sequence each exon in its entirety. Alignment of this sequence with the mouse cDNA sequence allowed the determination of a number of exon boundaries; specifically those of the arbitrarily named exons B, C, D and E (Figure 2.7). The boundaries of exons A, H, I and J were determined by Scherer and colleagues. There still remained an as yet uncharacterized region of 330bp, between exons E and H (Figure 2.7). This region had proven difficult to clone for unknown reasons. Attempts to amplify PCR products from the region, indicated that there were probably two exons within this gap. Without clones spanning the region however, it was not possible to employ the methods used for other sections of the gene to pinpoint precisely the internal exon boundaries or to generate the flanking sequence necessary to sequence both exons in their entirety.

2.3.3 Mutation screening of GRM8 in family FA-84

Once most of the gene structure of the GRM8 gene had been elucidated, it was possible to begin screening the coding regions of the gene for a disease mutation. It was decided to use both single stranded conformational polymorphism electrophoresis (SSCP) analysis and direct sequencing in the screening of GRM8. SSCP would allow a relatively fast initial screening of the gene. As not all mutations are detectable in this manner however the absence of a disease mutation was subsequently confirmed by sequencing. It was decided to use direct sequencing for the purposes of mutation detection as the results from direct sequencing are more clear-cut than is the case with automated sequencing.

SSCP and sequencing were carried out on 2 affected members of family FA-84; individuals IV-5 and V-7, and 2 unaffected members; individuals IV-8 and III-3, simultaneously (see accompanying pedigree -Figure 2.3). This was in order to allow distinction between harmless polymorphisms and a disease mutation. Again, this was carried out together with Dr. Fiona Mansergh. Primer pairs (Appendix B.2) from intron sequence, flanking each of the characterised exons, were used to uniquely amplify each of the GRM8 exons. No conformational shifts were observed for any of the exons amplified from affected individuals. Following this, both strands of all exons were

sequenced using nested primers (Appendix B.2) also derived from intronic sequence. No mutations were found in any of the exons sequenced from any of the four samples.

2.3.4 Mutational screening of portion of GRM8 using illegitimately transcribed RNA

Primers within the coding region, but close to the exon boundaries, were used to screen a large portion of each of the two exons within the uncharacterized region of the gene. There still remained approximately 50bp which had not been screened however. The diagnostic utility of the existence of illegitimate RNA transcripts in blood was taken advantage of in this regard. RNA samples from two affected individuals of family FA-84, individual IV-5 and individual V-7, were isolated by Dr. Carmen Ayuso, Fundacion Jimenez Diaz, Madrid. RNA from non affected individuals, necessary for comparison of the cDNA sequence, was isolated from two random individuals of the Irish population (referred to as RNA 1 and RNA 2). The RNA extraction protocol yielded high quality RNA with an average concentration of 300ng/ μ l. An initial RT-PCR with a "house-keeping" gene, G3PDH, primers (Appendix B.3) was performed to ensure that all RNA samples were amenable to RT-PCR. The expected 452bp fragment was observed subsequent to agarose gel electrophoresis and therefore attempts to amplify GRM8 illegitimate transcripts were initiated.

Primers (Appendix B.4) were designed in the exons flanking the uncharacterized region of the gene in order to amplify the required stretch of coding sequence from peripheral blood RNA (Figure 2.8). The reverse primer A was used in the cDNA synthesis step. This primer was paired with the forward primer B in an initial PCR of 30 cycles which resulted in the generation of a 800bp fragment, undetectable by ethidium bromide staining of an agarose gel. Primers C and D were subsequently used in a nested PCR of 40 cycles. The primer pair C and D would be expected to give a product of 700 base pairs in size. Products of this size were obtained following nested PCR amplifications on the initial PCR samples amplified from RNA 1 and RNA V-7 (Figure 2.9). This amplification product was obtained from sample RNA 1 following reactions using 350ng RNA. However, a fragment of the correct size was only obtained with RNA V-7 when a substantially greater amount of RNA (3 μ g) was used in reactions. Reactions with RNAs 2 and IV-5 failed to give products.

In order to confirm that the PCR fragments had been amplified from the GRM8 gene, these were sequenced with primers C and D on the automated sequencer. The fact that the amplified product spans at least two intron sites eliminates the potential for DNA contamination, leaving no doubt that this was a genuine RT-PCR product.

Having confirmed that the amplification products were genuine RT-PCR products, primers (Appendix B.4) from sequence flanking the region remaining to be screened (C and D) and an internal primer (E) were used to screen this segment in its entirety. This was carried out in both the affected and unaffected individual, using direct sequencing. Although this method did not allow the precise location of the internal exon boundaries to be determined, it enabled the sequencing of the hitherto unscreened portion of GRM8 and in doing so eliminated the need to establish the splice sites. No sequence variations in the coding sequence of GRM8 were identified in affected individuals indicating that GRM8 is unlikely to be involved in the etiology of the RP10 retinopathy.

2.3.5 Screening of GRM8 in family CVRP4

The possibility that the disease in family CVRP4, reported by Millan *et al.* (1995) to show linkage to 7q, was caused by a different mutation or even a different gene to that in family FA-84 led us to screen GRM8 in this family also. Haplotype comparisons had indicated that the two Spanish families were not related meaning that this scenario was a possibility (Millan *et al.*, 1995). Each of the 8 exons for which flanking sequence was available was sequenced in two affected individuals (II-2 and III-13) and two unaffected individuals (III-7 and III-16) of this family (Figure 2.10).

As with family FA-84 no mutations were found within the coding sequence of this family. RT-PCR on illegitimate transcripts was not undertaken in this family as fresh blood samples were not readily available and there was a degree of uncertainty regarding the Millan *et al.* linkage results. Hence the region of the gene for which no intron sequence has been generated has not as yet been analysed in this family.

2.3.6 Screening of DGK τ in family FA-84

The location of the DGK τ gene on chromosome 7q and the involvement of a DGK gene in a retinal degeneration of the fruit fly made the DGK τ gene an exciting candidate for the RP10 gene. Using a radiation hybrid panel the DGK τ gene was mapped in the proximity of the 7q marker D7S512 (Prof. Steve Daiger, personal communication, 1997). If this mapping is precise, this is in fact slightly distal to the disease interval as defined by linkage. The mapping technique used to place the gene has its limitations however, and as it had not been mapped using a more precise means at the time of the present study, it was decided to adopt DGK τ as a candidate for the RP10 gene. Since this study the fluorescent *in situ* hybridization has been used to map the gene to 7q32.3-33.

Prof. Steve Prescott and colleagues, in the Huntsman Cancer Institute, Utah, embarked on a project to elucidate the structure of the gene. It is a large gene, with >3kb of coding sequence, and possesses 34 exons. The sequence of the DGK τ exons along with flanking intron sequence was kindly made available to us by them. SSCP analysis was the method of choice used to screen each of the exons initially. Although this method does not guarantee complete mutation detection it allows a rapid screening of a gene which, given the number of DGK τ exons, seemed appropriate. Primers (Appendix B.5) were designed in the intron sequences to give PCR products of a size suitable for SSCP analysis i.e. 200-400bp. 25 of the 34 DGK τ exons were screened in this manner. Each exon was screened in three affected members (IV-5, IV-7 and V-7) and three unaffected members (IV-8, IV-10 and IV-4) of the Spanish adRP pedigree, FA-84, under at least two different electrophoresis conditions. Exons 9, 13, 14 and 15 were also screened by direct sequencing. Exons 13 and 14 were specifically chosen for sequencing as they code for the ATP binding site of the DGK τ protein. It is a mutation in this site in the *Drosophila* DGK2 gene which brings about the *rdgA* phenotype (Ding *et al.*, 1998).

The SSCP screening revealed a sequence change in a single unaffected individual in exon four and in an unaffected individual in exon 7. It also identified a variant in the sequence of exon 12 in a single affected individual. Of greater significance however, the SSCPE screening of exon 32 revealed a common sequence variant present in the family in intron 31 (Figure 2.11). Sequencing of the exon 32 PCR

fragments in a number of the family revealed the existence of two alleles, differing from each other by a single base, in the intron sequence flanking the exon (Figure 2.12).

Allele 1 corresponds to an A at this base position and allele 2, to a G at this position.

Three shift patterns were observed on the SSCP gel and were determined to correspond to each of the homozygous states and the heterozygous state at this locus.

This two-allele polymorphism was adopted as a genetic marker and typed through the DNA of 44 members of the adRP Spanish pedigree, FA-84. Allele types for all individuals were assigned according to their shift pattern on an SSCP gel. One of the two alleles at this locus creates an *EcoRI* restriction enzyme site and the allele typing was confirmed by digestion of exon 32 PCR fragments with *EcoRI*, in all 44 individuals (Figure 2.13). Allele 1 segregates with the disease in the main branch of the family whereas allele 2 segregates with the disease in the other branches of the pedigree (Figure 2.14). The lod scores at this locus were calculated, with respect to the adRP gene on 7q, and a maximum lod score of 0.72 at $\theta = 0.2$. A lod score of -4.94 at $\theta = 0.001$ indicates that the disease gene is not likely to lie within 100kb of this polymorphic locus thereby, essentially excluding the region in which the *DGK1* gene lies. Another single recombinational event was detected in individual V-14. He has been diagnosed as unaffected but he carries the affected allele at this marker.

The relatively weak lod scores obtained with this marker give a strong indication that the *DGK1* gene does not map sufficiently near the disease locus to be RP10. In fact they indicate that the adRP disease gene is likely to lie distal to *DGK1*. This DGK marker has also been typed in DNA from members of the American adRP pedigree, UTAD045, which also shows linkage to this region of 7q (McGuire *et al.*, 1995b). A number of individuals are also recombinant for the marker in this family, strengthening the evidence that the *DGK1* gene is not RP10. The linkage data obtained from this polymorphic marker indicates that *DGK1* is significantly excluded as RP10.

2.4 CONCLUSION

A number of changes during the time which had elapsed since the original linkage study, which localized an adRP gene to chromosome 7q, necessitated a re-evaluation of the data defining the disease interval. This re-evaluation did not allow the interval to be narrowed but in fact widened it slightly. Two genes mapping to the region, GMR8 and DGK₁, were screened for the RP10 mutation. In the case of GRM8 the structure of the gene had to be determined firstly. This was carried out in conjunction with Dr. Steve Scherer in The Hospital for Sick Children in Toronto. The coding sequence of GRM8 was screened in its entirety in family FA-84 using both SSCP and direct sequencing. This involved screening a portion of the gene in the form of cDNA, transcribed from illegitimate RNA transcripts. All but two of the GRM8 exons were also screened in their entirety in family CVRP4. No disease causing mutations were identified in GRM8.

25 of the 34 DGK₁ exons were also screened for the RP10 mutation using SSCP and, occasionally, direct sequencing. No disease causing mutations were identified in these exons and the gene was finally excluded as the RP10 gene by adopting an intragenic polymorphism as a marker which revealed recombinants in the family. The exclusion of both GRM8 and DGK₁ as the RP10 gene means it will be necessary to search for other candidate genes on 7q.

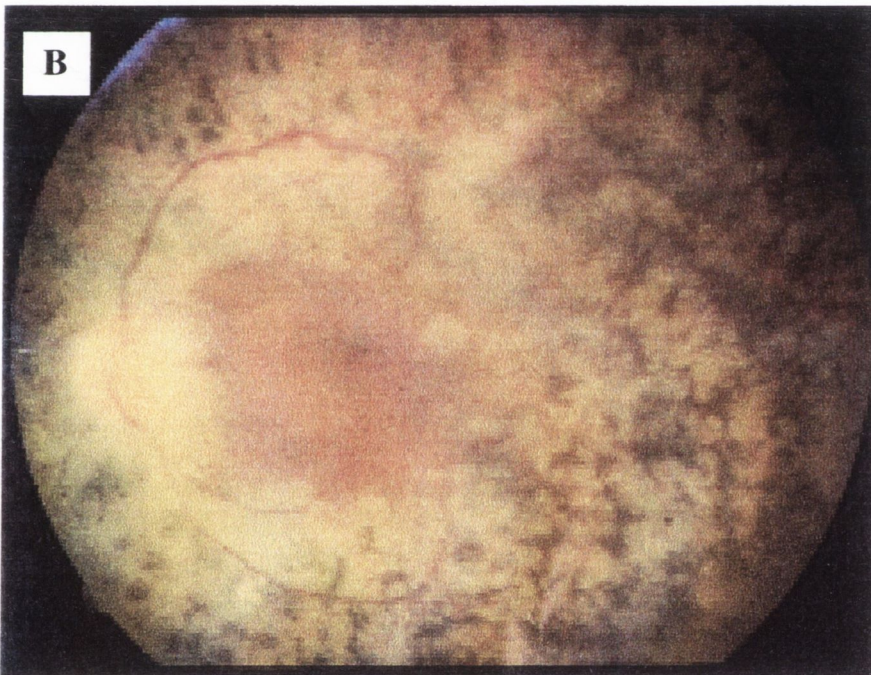
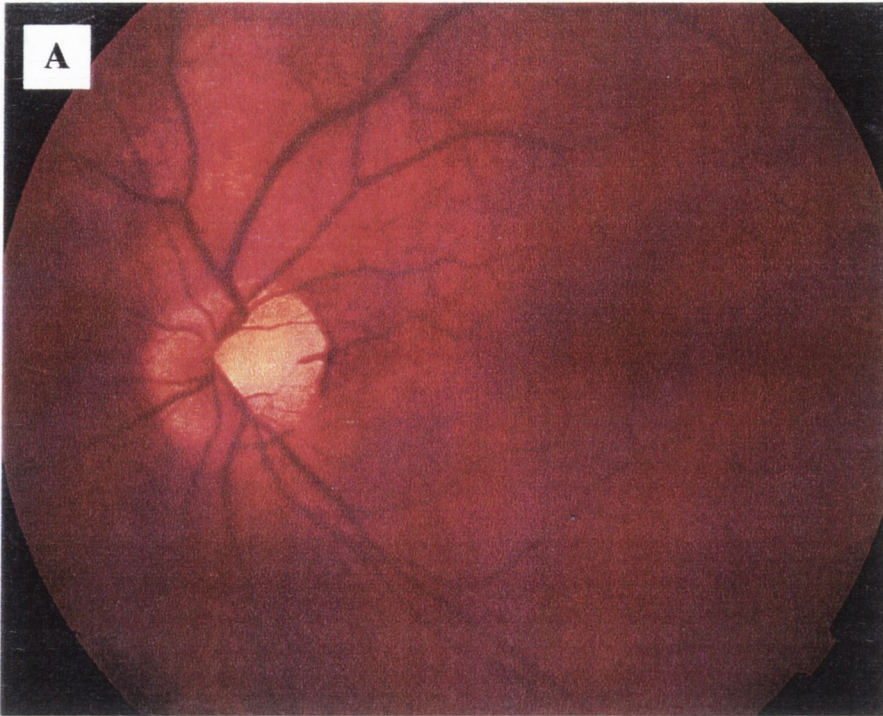


Figure 2.1 Fundus photographs of a normal and an FA-84 RP retina. (A) The retina of a healthy individual. (B) the retina of an FA-84 individual showing some of the typical clinical features of the disease; bone spicule pigmentation, atrophy of the blood vessels and a pallor of the optic disc.

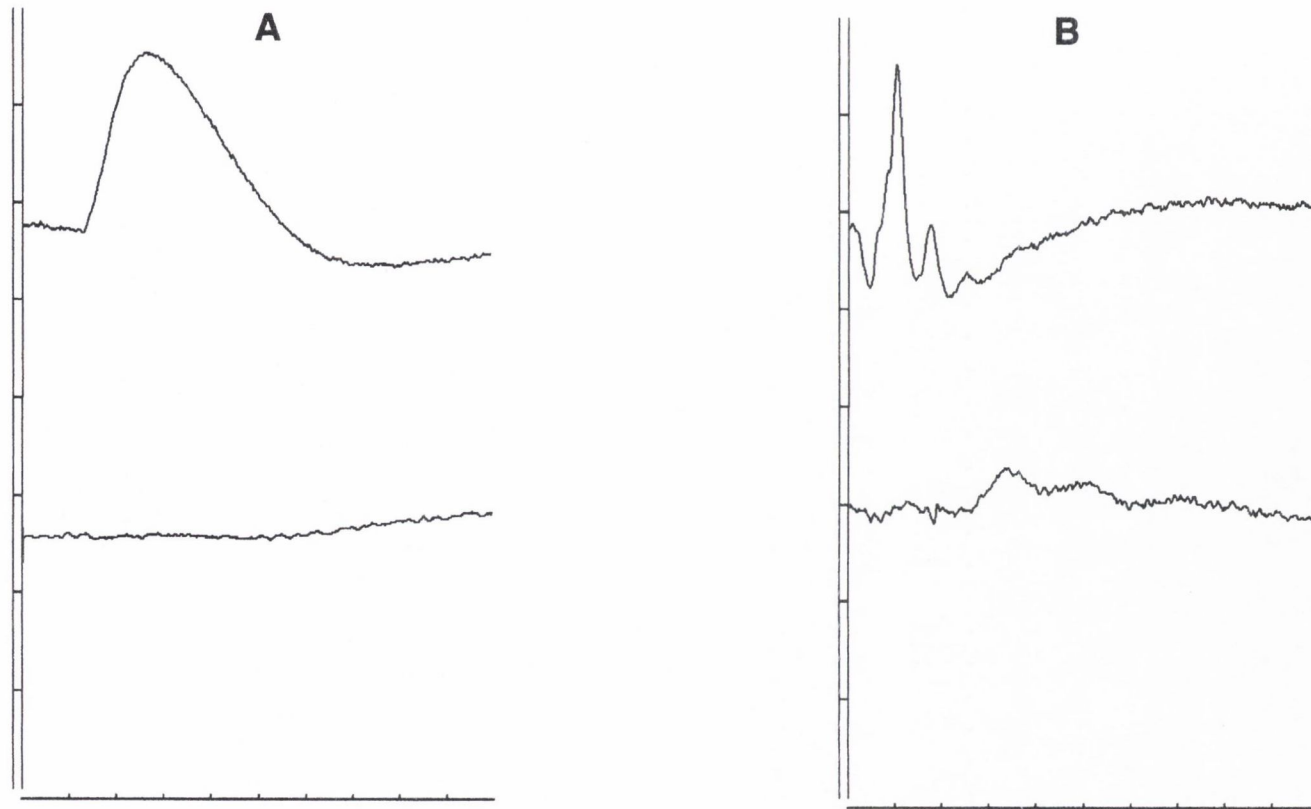


Figure 2.2 Electretinogram responses from healthy and RP individuals. (A) ERG tracings from dark adapted individuals. The top tracing represents a normal individual and the bottom shows a a nonrecordable response from an RP patient. (B) ERG responses from light adapted individuals showing cone isolated tracings. The top tracing represents a normal individual while the bottom tracing shows a very delayed and reduced amplitude reading from an RP patient.

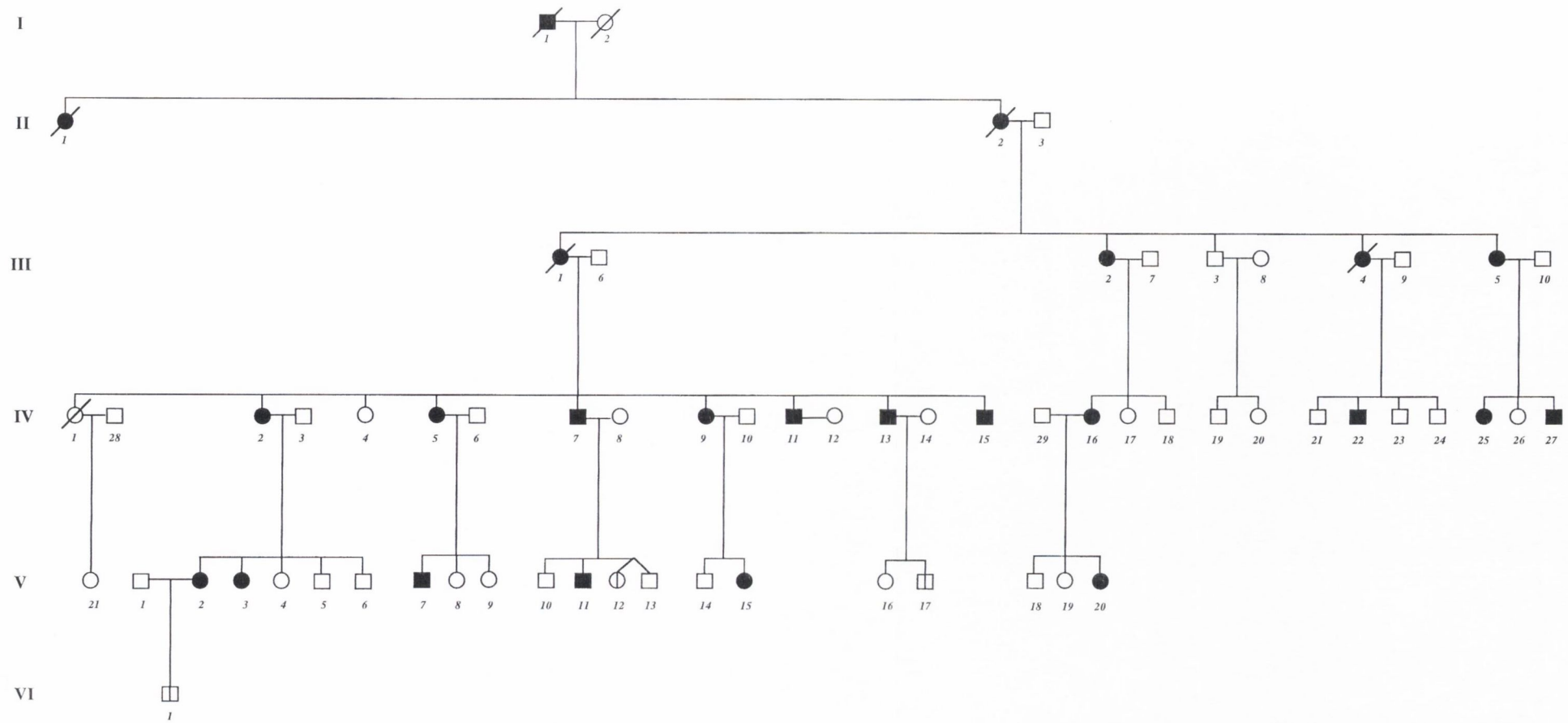


Figure 2.3 Family FA-84 pedigree. Individuals whose diagnosis status is uncertain are denoted by a vertical line in the middle of a square or circle.

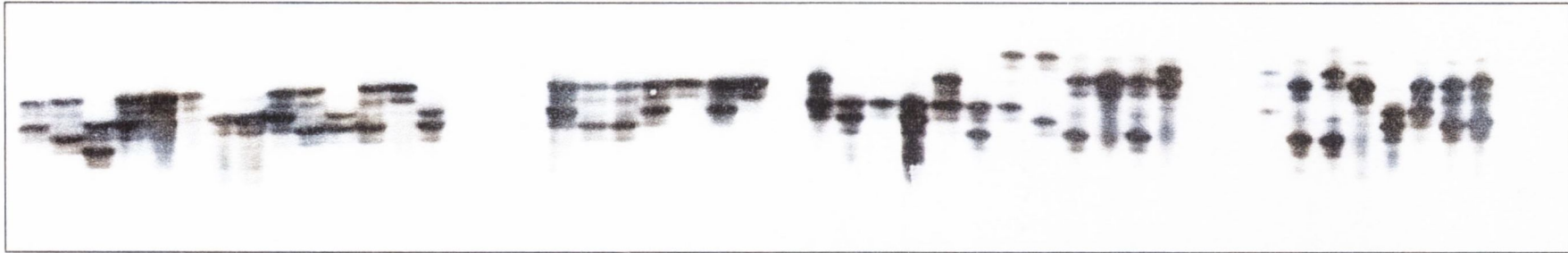


Figure 2.4 Representative gel of microsatellite D7S530 typed through members of family FA-84. D7S530 had previously been determined to flank the RP10 interval on chromosome 7q. No new recombinants were identified in the family.



Figure 2.5 Representative gel of microsatellite D7S686 typed through members of family FA-84. D7S686 had previously been determined to flank the RP10 interval on chromosome 7q. No new recombinants were identified in the family.

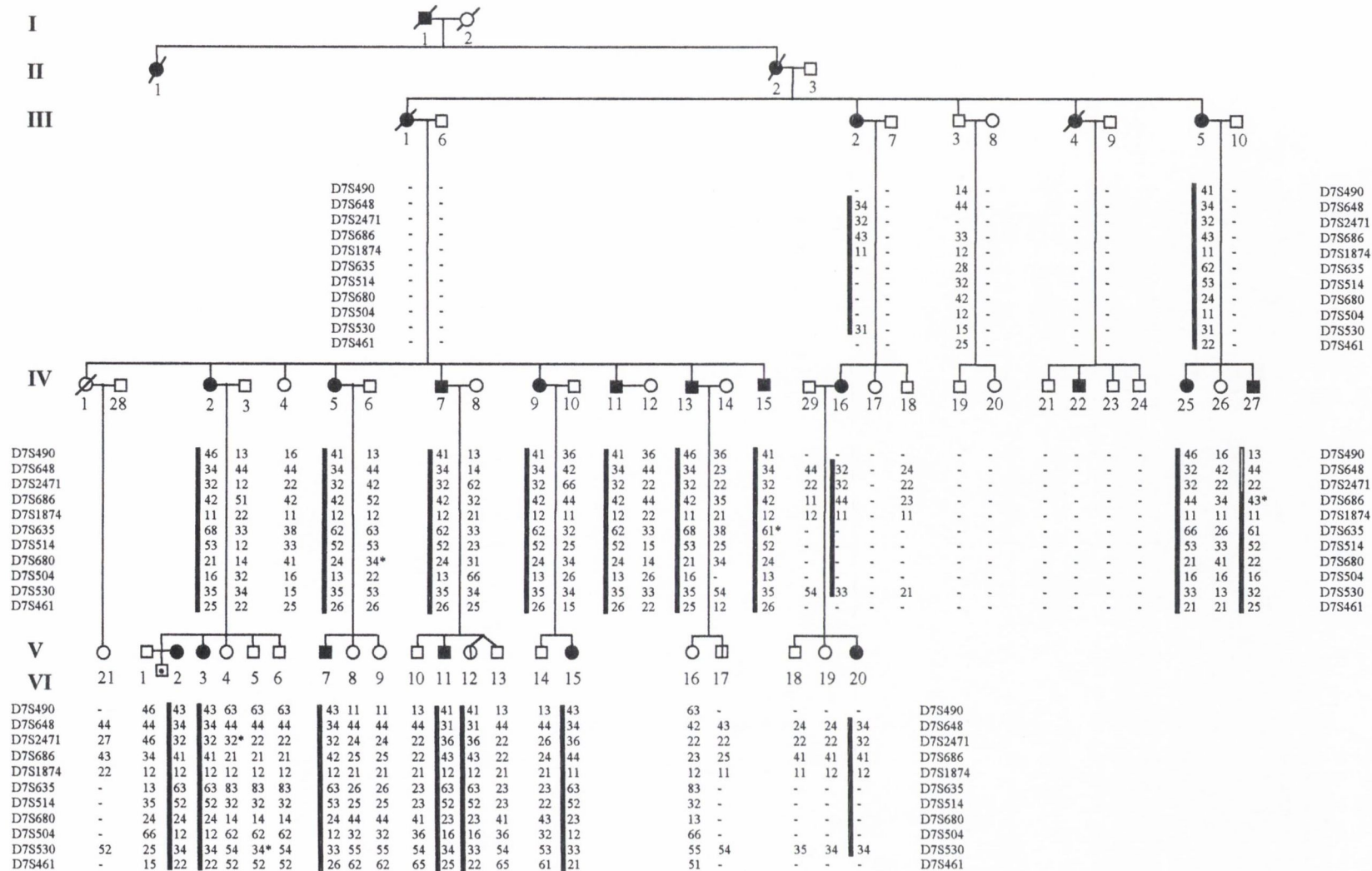


Figure 2.6 Haplotype analysis of family FA-84 across the RP10 interval on chromosome 7q. The alleles for markers across the interval are listed below members of the family for whom DNA was available. Black bars represent the affected haplotype. White bars represent an unaffected haplotype following a recombination event. An asterisks indicates a possible mistyping. Individual IV-27 possesses the unaffected haplotype above D7S686 making D7S2471 the proximal flanking marker.

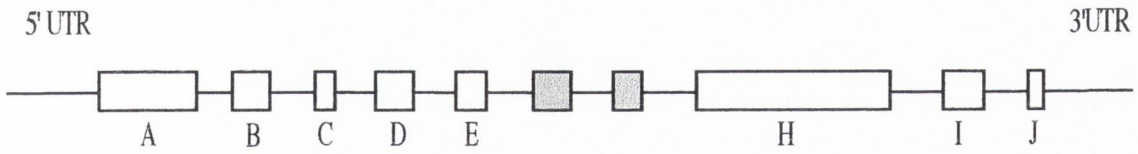


Figure 2.7 Schematic diagram of the structure of the GRM8 gene. The exons are represented by boxes. The shaded boxes indicate those exons for which the structure has not been fully elucidated. The entire coding sequence of the gene spans 2724bp

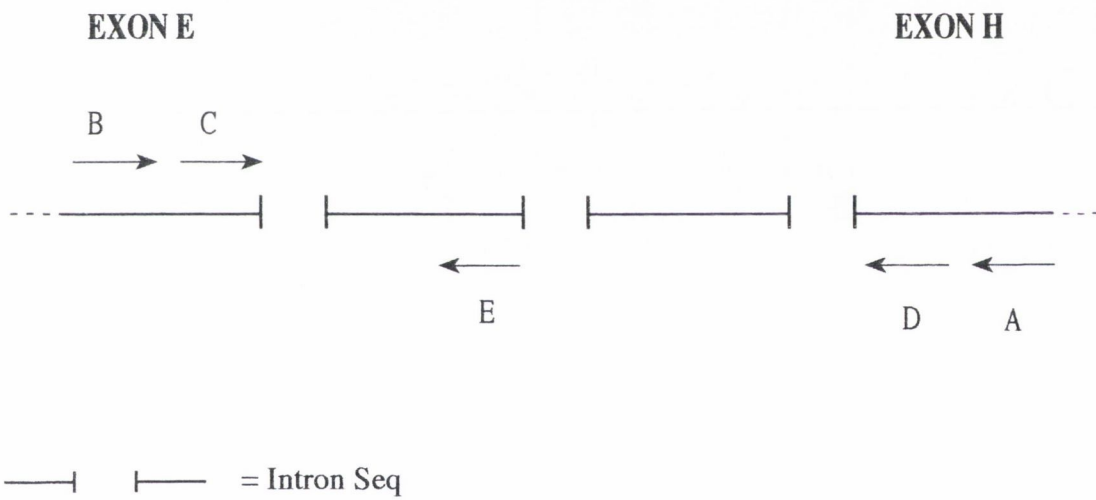


Figure 2.8 Schematic representation of primers used in RT-PCR of illegitimate GRM8 transcripts.

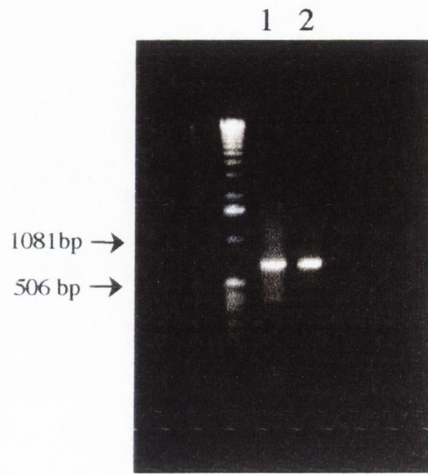


Figure 2.9 Amplification products following RT-PCR on GRM8 illegitimate transcripts. Lane 1, 5 μ l of PCR product amplified from RNA 1; lane 2, 2.5 μ l of PCR product amplified from RNA V-7.

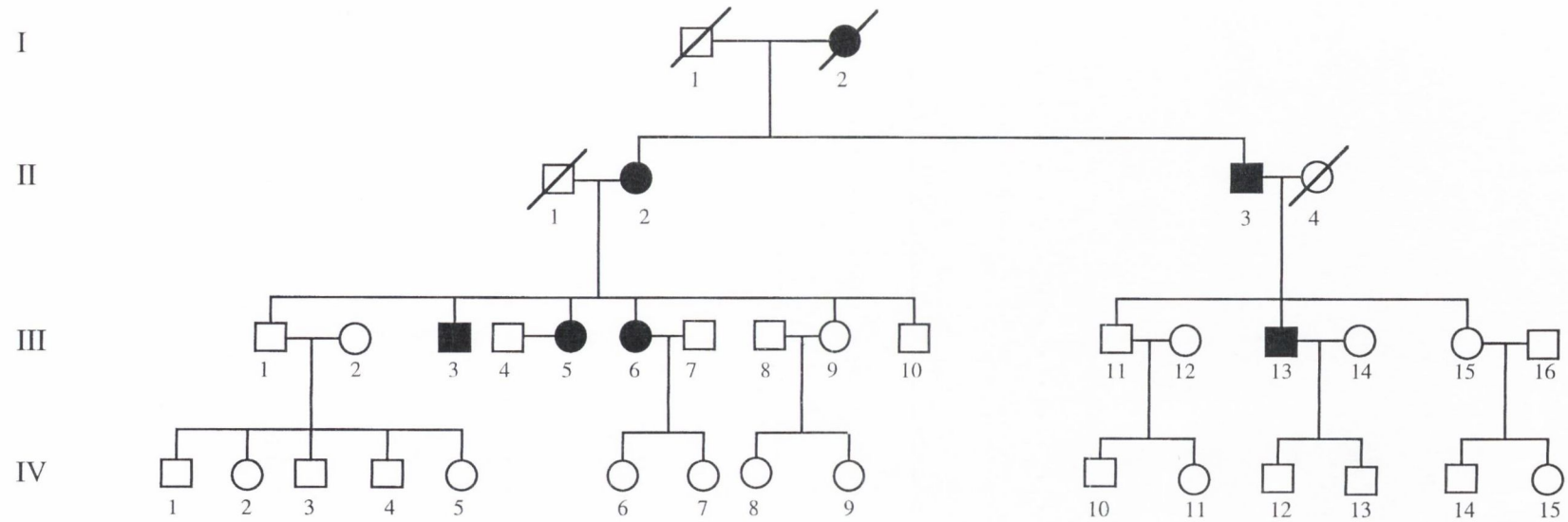


Figure 2.10 Family CVRP4 pedigree

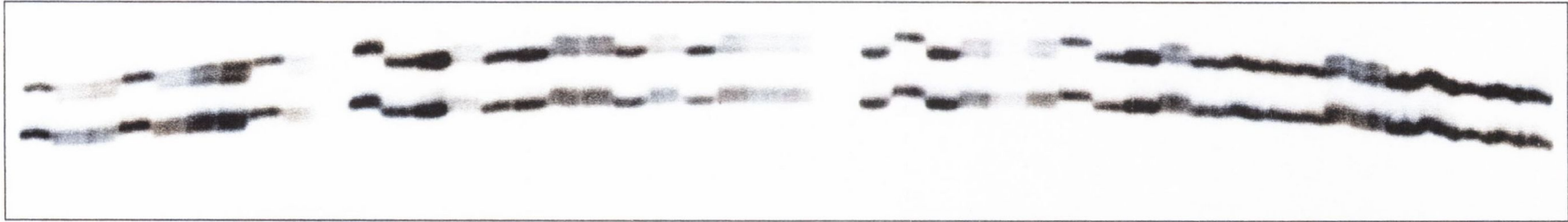


Figure 2.11 Typing of an intragenic intron 31 DGK ι polymorphism using SSCP analysis. The SSCP analysis was performed on PCR-amplified DNA spanning the polymorphism from members of family FA-84. The two alleles can be distinguished on the gel with individuals being either homozygous for allele 1, homozygous for allele 2 or heterozygous.

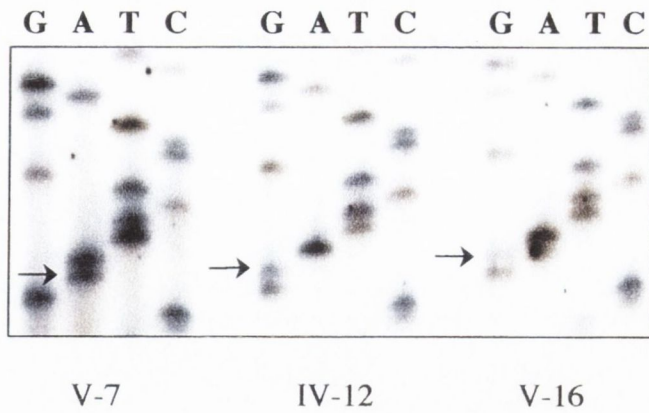


Figure 2.12 sequence analysis of the DGK ι intron 31 polymorphism identified by SSCP. The three different genotypes present in family FA-84 are shown. Individual V-7 is homozygous A at the base position indicated by the arrow. Individual IV-12 is homozygous G at while individual V-16 is heterozygous at this position. An A at this position corresponds to allele 1 and a G to allele 2.

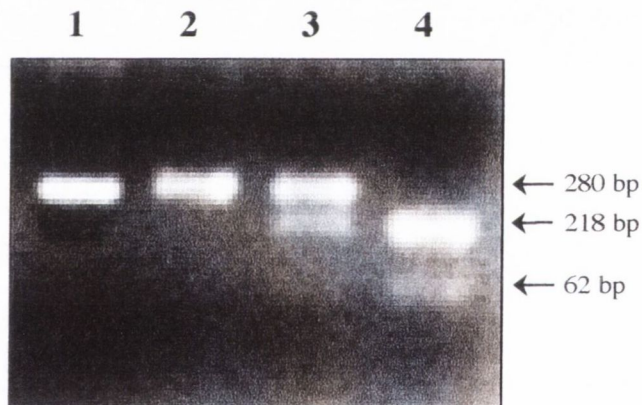


Figure 2.13 *EcoRI* digest of PCR products spanning the DGK ι intron 31 polymorphism. Digestion of the 280 bp PCR products yields fragments of 62 bp and 218 bp in allele 1 while allele 2 remains uncut. The gel shows the three different genotypes present in family FA-84. Lane 1, uncut PCR product; lane 2, digested PCR product amplified from individual IV-14 with the genotype 2,2; lane 3, digested PCR product amplified from individual IV-15 with the genotype 1,2; digested PCR product amplified from individual III-3 with the genotype 1,1.

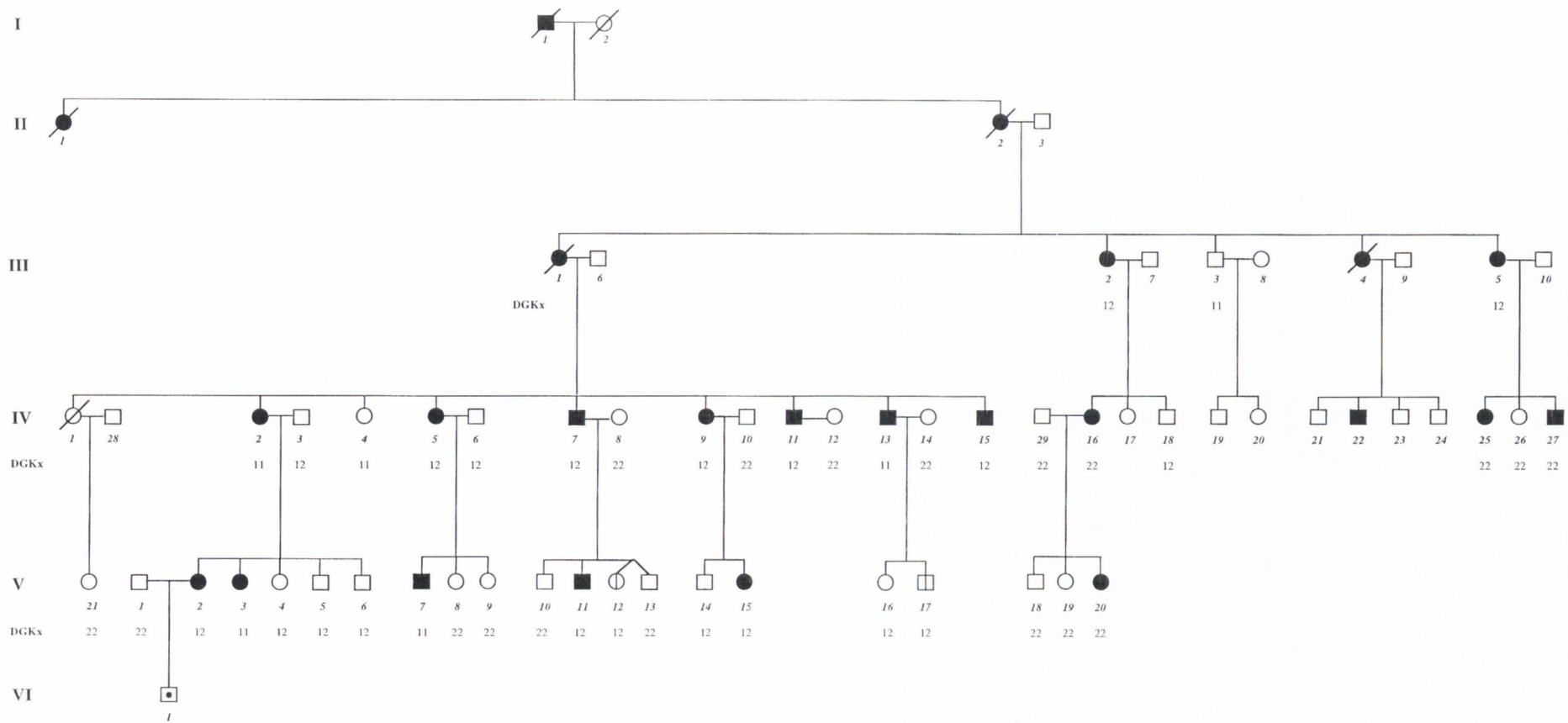


Figure 2.14 Genotyping of the DGKx intron 31 polymorphism in family FA-84. Allele 1 segregates with the disease in the largest branch of the pedigree, except in the case of the recombinant individual, V-14, who is unaffected. Allele 2 segregates with the disease in the smaller branches of the pedigree. These results exclude DGKx as RP10.

CHAPTER 3

METHODS TO IDENTIFY CANDIDATES FOR THE RP10 GENE

3.1 INTRODUCTION

3.1.1 Introduction

With the exclusion of all known genes mapping to the RP10 disease interval as defined by linkage (as outlined in chapter 2), it became necessary to begin a search for novel genes in order to identify the disease gene. The aim of the present research was to isolate and functionally characterize the 7q adRP gene. The use of standard approaches in this task would first necessitate the generation of contiguous clones containing the RP10 disease interval. This would entail a large scale physical mapping exercise and would be a considerable undertaking, particularly in light of the fact that the RP10 interval spans 5cM. Given that our collaborators in the U.S., Professor Daiger and colleagues, had previously constructed a YAC contig spanning the disease interval (McGuire *et al.*, 1996b), it was felt that to duplicate this work would be superfluous. A variety of approaches have been adopted therefore, in the search for candidate genes involving the use of long-range PCR, expressed sequence tags (ESTs), the rhodopsin knockout mouse, and *in situ* hybridization. A discussion of each of these is given below and the results from each method presented.

3.1.2 Long-range PCR

Long-range PCR is a relatively new branch of PCR technology which, through the modification of PCR conditions, allows effective amplification of longer targets than is generally possible with regular PCR conditions. Amplification of products up to 22kb from human genomic DNA and 42kb phage lambda DNA have been reported (Cheng *et al.*, 1994b). Key criteria for the success of long-range PCR are the maintenance of template integrity and the optimization of the specificity of amplification (Barnes, 1994; Cheng *et al.*, 1994a & Cheng *et al.*, 1994b). This is achieved to a large extent through the use of a two-polymerase system, with both processive polymerase activity and 3' to 5' exonuclease activity, to remove mismatches. Modified PCR buffers and thermal cycling profiles are also employed (Cheng *et al.*, 1994a). It was intended to harness the

potential of this technique in a system to generate contiguous PCR products spanning the RP10 interval.

3.1.3 ESTs

The major goal of the human genome project is to complete the sequencing of all 3 billion base pairs in the human genome. Only 3% of the genome actually encodes protein however, and it is this 3% of sequence which is of most interest to biologists (Benson and Rap, 1996). Because of this and the relatively long wait till the sequence of the entire genome is available, large scale expressed sequence tag (EST) sequencing has been undertaken in the last number of years. ESTs are short, single pass DNA sequence reads from the ends of cDNA molecules. They are randomly sequenced from cDNA libraries and therefore are representative of gene sequences. They are frequently derived from directional cloned, oligo(dt)-primed mRNA (Boguski and Schuler, 1995). In order to select a single representative stretch of sequence from a gene, they are generally derived from 3' UTRs. The reasons for selecting 3' UTRs are firstly, they almost never contain introns and secondly, they are less well conserved than coding regions and therefore are better for the purpose of distinguishing between members of paralogous gene family members (Boguski and Schuler, 1995).

Large sequencing groups such as the Washington University genome sequencing center, under contract with Merck & Co (Hillier *et al.*, 1996), and The Institute for Genomic Research (TIGR) began generating human EST data on a massive scale a number of years ago and presently generate up to 10,000 sequences a week from cDNA libraries of various human tissues (Marra *et al.*, 1998). These ESTs are submitted to databases such as the division of GenBank known as dbEST and are, therefore, publicly accessible. The number of human ESTs in dbEST as of July 1999 is 1,505,046.

With the generation of large amounts of human gene information an international consortium was established to map gene based sequences, using 2 radiation hybrid panels and a yeast artificial chromosome (YAC) library (Schuler *et al.*, 1996). This has enabled the generation of a human transcript map, known as GeneMap, which includes more than 30,000 clusters of sequences, each of which represents a human gene (Deloukas *et al.*, 1998). With an estimated 60,000 - 80,000 genes in the

human genome it appears that up to one half of these genes may be represented in some form in this transcript map.

This human transcript map is publicly available on the internet (Deloukas *et al.*, 1998). Mapped ESTs are becoming immensely important in the positional candidate approach to the identification of human disease genes. The website allows the identification of cDNA markers on the basis of map location and provides links to sequence data and information on the libraries from which a particular EST was sequenced. The markers are mapped relative to approximately 700 well spaced microsatellite markers which is useful for the purpose of retrieving an inventory of genes within linkage-based disease intervals (Schuler *et al.*, 1996). These features make the human transcript map an invaluable resource for disease gene hunters. It is of interest that 82% of the genes currently known to be involved in human disease are represented by one or more ESTs in Genbank (Benson and Rap, 1996).

One of the problems when mapping ESTs is the high degree of redundancy in the sequence data, as well as overlap with sequences of functionally cloned genes (Boguski and Schuler, 1995). In an undertaking known as the UniGene project these problems have been tackled with much success (Boguski and Schuler, 1995; Schuler *et al.*, 1996). In the Unigene project all ESTs are first screened for contaminating sequences such as mitochondrial, ribosomal or vector sequences and also for repetitive elements and low-complexity sequence (UniGene build procedure, 1999). A single gene may be represented by many ESTs which correspond to different regions of the gene or alternatively spliced transcripts. The EST sequences are therefore then screened against functionally cloned gene sequences in GenBank and against each other. Those sequences which share statistically significant similarity are grouped together in a process known as clustering. Subsets of sequences derived from the same gene are in this way grouped together in a gene oriented cluster (Benson and Rap, 1996). Clustering uses only the 3' reads of an EST but knowledge of common clone identifiers allow the corresponding 5' sequence of a cDNA sequence to be added (Boguski and Schuler, 1995). A UniGene cluster number is given for all the cDNA markers in GeneMap '99, where available.

ESTs have been adopted as tools in a number of other areas of molecular biology also. The availability of EST sequences in the databases has proved particularly beneficial in allowing the identification of novel human genes. The large volumes of gene based sequence being generated allows investigators to search for the human

homologues of genes previously identified in model organisms. Many human genes have been identified in this manner, such as a human telomerase catalytic subunit (Nakamura *et al.*, 1997) and a human homologue of the *Drosophila* TOLL protein (Medzhitov *et al.*, 1997). ESTs have also been adopted in the generation of physical maps and in the identification of alternative gene splice sites (Marra *et al.*, 1998).

While mapped ESTs are a tremendous resource, the data they provide is limited in the information it holds and may be flawed. ESTs are generated from single-pass unedited sequence and are, therefore, subject to errors. The accuracy rate is at best 97% (Hillier *et al.*, 1996). However, it is possible to view the trace data of a sequence read in order to choose high quality sequence when designing experiments. Not all clones from which the ESTs are generated will have both 5' and 3' reads and no attempt to generate contigs of sequences from a particular gene is made (UniGene system, 1999). In addition, ESTs are subject to expression bias. Genes transcribed at a high level are likely to be over-represented in the EST libraries while those that are expressed at a very low level may not be represented at all (Marra *et al.*, 1998). Methods to "normalize" cDNA libraries in order to reduce the number of clones derived from abundant transcripts have been devised (Bonaldo *et al.*, 1996). Subtractive hybridization techniques to remove redundant clones from the libraries have also been developed (Bonaldo *et al.*, 1996). Such methods do not eliminate redundancy completely however (Hillier *et al.*, 1996; Marra *et al.*, 1998). Another potential problem in using ESTs as candidates for human disease is their potential mis-mapping to chromosomal locations. It is estimated that 99% of ESTs are mapped to the correct chromosome and that of these, 95% are mapped with relatively high precision to the correct location on the chromosome (Schuler *et al.*, 1996). These limitations however, are the small price to be paid for the availability of such immense amounts of valuable data on the location and expression of human genes.

3.1.4 The rhodopsin knockout mouse

The generation of a rhodopsin knockout mouse has been of great benefit to the study of retinopathies. This mouse was generated following a targeted insertion into exon II of the rhodopsin gene (Humphries *et al.*, 1997). In Rho^{-/-} mice the absence of rhodopsin disrupts the outer segment structure and the photoreceptors possess no outer segments.

In Rho-/+ the outer segments are present but they are shorter than those of wildtype mice and appear disorganized. There is an evident decline with age in the number of photoreceptors in Rho-/- mice. At 24 days of age the Rho-/- mice show 8-10 rows of photoreceptor nuclei in the outer nuclear layer compared to 10-12 rows in the wildtype mice. By three months of age the outer nuclear layer is reduced to single cell thickness. By this stage therefore, the degeneration of the photoreceptors is essentially complete. Immunocytochemistry, using an anti-opsin antibody, fails to detect the presence of opsin. The absence of the photoreceptors is also reflected by the completely extinguished ERG responses in Rho-/- mice (Humphries *et al.*, 1997).

This mouse is enormously beneficial in the study of the pattern and mode of photoreceptor degeneration, in providing a model for development of therapeutic strategies to RP and in experiments to observe the expression of other genes on a rhodopsin null background. It may also, as demonstrated in the results section, be of use in learning more of the expression pattern of retinally expressed genes.

3.1.5 *In situ* hybridization on tissue sections

In situ hybridization (ISH) is a sensitive and widely applicable technique for the detection of nucleic acids in morphologically preserved tissues, chromosomes or cells. The technique was developed from Southern and Northern blotting techniques which involve hybridizations to membrane bound nucleic acids (Chevalier *et al.*, 1997). In contrast to hybridizations to membrane bound nucleic acids however, ISH not only allows the detection of a particular sequence but also its precise location within cells or tissues.

RNA-ISH on tissue sections allows the study of the particular expression pattern of a gene of interest, thereby providing insight into its role in the tissue. ISH has a number of advantages over immunocytochemistry, including the fact that it does not require the availability of an antibody to the protein of interest and that it targets the exact site of RNA expression rather than the site of the protein location.

RNA-ISH to tissue sections is a multi-step process which is generally carried out over a period of a few days. The variations in the protocols used by different researchers are endless but generally involve a number of key steps. These steps include, fixation, embedding and sectioning of the tissue, various treatments of the

tissue sections prior to hybridization, hybridization with a specific probe and subsequent detection of the probe. Critical aspects of the procedure are briefly discussed below.

A. Tissue preparation.

The two most common methods to prepare tissue for ISH involve either paraffin embedding or freezing of the tissue. In both cases fixation is a crucial step in the procedure in order to preserve the morphology of the tissue and to retain the cellular RNA. It is necessary to optimize the method of fixation for individual tissue types in order to achieve a balance between preservation of tissue morphology and the accessibility of the target sequences to the probe and immunochemicals (Dirks *et al.*, 1993). Stronger fixation gives better preservation of tissue morphology but the increased cross-linking reduces the accessibility of the target sequence (Wilkinson, 1994). Commonly used are the cross-linking fixatives formalin, (para)formaldehyde and glutaraldehyde (Dirks, 1996). It is important to fix the tissue as soon as possible post enucleation in order to help prevent the action of nucleases on the cellular RNA. Following fixation, the tissue is embedded either in a paraffin wax block or in cryoprotective medium and rapidly frozen. Freezing the tissue also allows for the possibility of fixation after sectioning which can be advantageous, as length of fixation required is much shorter and it probably allows for better penetration of the probe (Wilkinson, 1994). Preservation of tissue morphology tends to be poorer however, in frozen sections (Chevalier *et al.*, 1997).

Paraffin sections of 4 to 8 μM are cut from the tissue on a microtome, or frozen sections of 6 to 12 μM on a cryostat. Thinner sections allow for better resolution of the signal while thicker sections give a stronger signal.

B. Glass Slides

The choice of slides in ISH with tissue sections is an important factor in the success of the experiment. Slides must be coated in a substance which helps in the adherence of the sections to the glass throughout the course of the protocol and prevents the probe sticking to the glass and causing background signal (Sirinathsinghji, 1993). Different coating agents are recommended, including poly-l-lysine, gelatin, APES and glucose (Wilkinson 1992).

C. Tissue treatments

Many protocols recommend various treatments of the tissue prior to hybridization in order to increase the accessibility of the target RNA following the use of cross-linking fixatives (Dirks, 1996). Proteases, organic solvents and detergents are all employed for this purpose. Proteinase K is regularly used as a protein denaturant to hydrolyze the cross linked proteins surrounding the target sequence (Grunewald-Janho, 1996). Over treatment of the tissue with protein denaturants can compromise cellular morphology however, so the time length of such steps have to be optimized (Wilkinson, 1992). Preparations are also often treated with HCl. The precise mechanism of the acid is unclear but it may cause extractions of proteins and partial hydrolysis of the target sequences, resulting in better signal (Grunewald-Janho, 1996). Treatment with detergents such as triton may also be carried out and may aid extraction of lipid membrane components (Grunewald-Janho, 1996).

D. Probes

Different types of nucleic acid probes are used to detect RNA transcripts on tissue sections. Single stranded DNA, oligonucleotide and RNA probes have all been used with success. Each type of probe has both advantages and disadvantages and it is necessary to consider carefully the optimal probe for a particular experiment. Oligonucleotides have the advantage of being easily and quickly synthesized. They are generally stable and their small size means that they can penetrate the tissue section easily (Dirks, 1996). Once they have formed a hybrid however, it is only relatively stable due to its low melting temperature (Dirks, 1996). Their small size also means relatively few incorporated labeled nucleotides per molecule and hence a relatively weak signal. Therefore, they may not be suitable for rarer transcripts. Single stranded DNA probes are sometimes used but they have the inherent problem of having the same thermal stability as the target sequences and therefore, may allow renaturation of the target DNA (Grunewald-Janho, 1996). The most sensitive probes for RNA-ISH are RNA probes. Although they are larger in size than oligonucleotides and therefore, the target RNA may be less accessible to them, they have more incorporated label per molecule of probe and hence result in a strong signal following hybridization. RNA probes are generally reverse transcribed from cloned PCR products, although it is possible to reverse transcribe them directly from PCR products with promoters on the ends of the primers. They are relatively unstable and care must be taken to prevent their

degradation, but once they have formed a hybrid it is extremely stable (Cox *et al.*, 1984).

E. Hybridization

The hybridization and post-hybridization washing conditions are critical to ISH hybridization experiments in order to achieve specific results with a particular probe. For a particular ISH experiment the concentration of the probe, the hybridization temperature and the time-length of hybridization all have to be optimized. The melting temperature of the hybrid, formed by the probe and the target sequence, depends to a large extent on the nature of the probe. RNA-RNA hybrids are more stable than RNA-DNA hybrids (Wilkinson, 1992). Longer probes and probes with higher G+C contents also form more stable hybrids (Wilkinson, 1992). The nature of the hybridization buffer also effects the stability of the hybrid. For example, the addition of formamide to the buffer increase stability and therefore allows the use of lower hybridization temperatures.

Post-hybridization washes are carried out to remove probe which has bound to unspecific sequences. The aim of these washes is to achieve a stringency which will remove non specifically bound probe without the loss of specific signal.

F. Label

There are many different labels available for the detection of hybridized nucleic acid probes. Such labels are generally incorporated into the probe during its synthesis or added to the terminal ends of the probe post synthesis. It is an essential criteria of these labels that they are small enough so as to avoid steric hindrances between the probe and its target nucleic acid. They must also be easily detectable either directly or indirectly (Chevalier *et al.*, 1997)

Initial *in situ* hybridization studies used radioactively labeled probes (Gall and Pardue, 1969; John, 1969). Such probes give a strong and specific signal and consequently are sometimes still used (Dirks, 1996). Safety concerns, together with their poor resolution qualities however, has meant that they have generally been replaced by non-radioactive alternatives. Haptens, such as digoxigenin (DIG) and biotin or fluorochromes, such as fluorescein and rhodamine are now commonly used. DIG is a compound derived from the foxglove plant, digitalis. Because it is a compound unique to the foxglove, problems with unspecific binding of its antibody are

generally avoided, which is not the case with biotinylated probes (Chevalier *et al.*, 1997). Fluorochromes have the advantage of being directly detectable, providing the investigator has access to a fluorescent microscope. Because of the availability of fluorochromes with different excitation and emission spectrums it means that they can, if necessary, be used to detect more than one target nucleic acid simultaneously. They are relatively low in sensitivity however (Chevalier *et al.*, 1997).

G. Detection

Labeled probes may either be detected directly, as is the case with radioactively or fluorescently labeled probes, or indirectly as is the case with digoxigenin (DIG) or biotin labeled probes. Direct detection of a probe can be desirable as the ISH process is considerably shorter and there is no background staining introduced by immunochemicals (Dirks *et al.*, 1993). Indirect detection, on the other hand, has the advantage that the signal may be amplified by the secondary detection step and is therefore, better for low copy number target nucleic acids (Siadat-Pajouh *et al.*, 1994). The secondary detection step involves an antibody conjugated to either a reporter molecule, as is the case with DIG, or a binding protein, as is the case with biotin. The reporter molecule may be an enzyme, such as alkaline phosphatase, in which case the bound probe is visualized following addition of an alkaline phosphatase, insoluble, colour substrate. A slight variation on this method of detection is the addition of a fluorescent alkaline phosphatase substrate.

H. Controls

A number of controls are recommended during *in situ* hybridization experiments in order to distinguish a true signal from non-specific artifacts. Hybridization with a sense probe which is the equivalent of the antisense probe, is generally carried out and should not result in a signal. The sense probe makes a suitable control as it is the same length and has the same G+C content as the antisense probe and therefore has similar hybridization properties as the antisense probe (Braissant and Wahli, 1994).

An RNase A step prior to hybridization, to digest all endogenous RNA, is often used (Grunewald-Janho, 1996). This should abolish all signal if the probe is specifically binding to RNA transcripts. An RNase A step post hybridization will digest all single stranded RNA while leaving RNA hybrids intact and hence, if the signal is true it should remain unchanged. Co-localization of the signal with

immunocytochemistry is another good control but not always a possibility due to the different conditions required for each. Unfortunately the results from ISH are not always clear cut. For example, researchers regularly find that they get hybridization of the sense probe (Dr. Catherine Winchester, personal communication, 1998). In this case the RNase experiments may also be carried out with the sense probe and a "picture" of the reliability of the result built up.

3.1.6 Study aim

The aim of the present study therefore, was to apply the methods discussed above to the identification of candidate disease genes in the RP interval on 7q31.3. The first approach taken involved the use of long-range PCR in an attempt to amplify large stretches of sequence across the disease interval and in this way generate a contig in the form of PCR fragments. The availability of a human transcript map is central to the other methods which were adopted. These methods involved RT-PCR on RNA extracted from normal and knockout rhodopsin mice and ISH on tissue sections. The aim of these methods was to learn more of the expression pattern of ESTs mapping within the disease interval and in this way to prioritize particular ESTs as candidates for the adRP gene.

3.2 MATERIALS AND METHODS

All reagents were purchased from BDH unless otherwise stated

For all RNA protocols H₂O and solutions were pretreated with DEPC. All glassware was made RNase free by baking at 180°C for at least 8 hours or treating with RNase away (Molecular Bio Products). Sterile plastic-ware was presumed to be RNase free.

3.2.1 Phage library titration

100ml of LB broth (Appendix A.2), supplemented with 0.2% maltose and 10mM MgSO₄ was inoculated from a glycerol stock of the host strain, XL1 - Blue MRA (Stratagene). The culture was incubated at 37°C overnight, with shaking. 100ml of fresh LB broth was inoculated with this overnight culture and incubated at 37°C until the cells reached an OD₆₀₀ of 0.5. The culture was divided in two and the cells harvested by centrifugation at 2,000 rpm for 10 minutes. The pellets were gently re-suspended in 15ml 10mM MgSO₄ and then diluted to an OD₆₀₀ of 0.5. 5µl of the λ DASH II library stock was added to 95µl SM buffer (Appendix A.2) and 10-fold serial dilutions were made of this stock in SM buffer to 10⁻⁹. 200µl of the host cell suspension was added to each of the dilutions and the mixture incubated at 37°C for 15 minutes with shaking. 3ml of NZY top agar (Appendix A.2) was added to each dilution and the mixtures immediately plated on NZY agar plates (Appendix A.2). These plates were inverted and incubated overnight at 37°C. The phage plaques were then counted and the number of plaque forming units (pfu's) per µl of each of the dilutions determined.

3.2.2 Phage library amplification

It was determined from the phage library titration that 23µl of the 10⁻² dilution of phage stock should contain 50,830 pfu's. The preparation of the host strain was carried out as above and appropriate dilutions of the phage library stock carried out in order to have 23µl of the 10⁻² dilution for each of 20 NZY plates. This would give a total of approximately one million pfu's. 600µl of cells was added to each of the 23µl and the

plating carried out as before except on larger plates of 15cm diameter. The plates were incubated overnight at 37°C. Each plate was then overlaid with 9ml of SM buffer. The plates were sealed with parafilm (American National Can) and left at room temperature for 5 hours. The bacteriophage suspension was then removed from each of the plates using a syringe and mixing needle. 1/50 the volume of chloroform was added to each stock and they were then stored at 4°C.

3.2.3 Phage DNA extraction

The extraction of the phage library DNA was performed using a λ DNA purification kit (Stratagene). Each of the 20 phage stocks were aliquoted into smaller volumes in 1.5ml eppendorph tubes and residual cell debris removed by centrifugation at 13,200 rpm for 10 minutes. An approximate volume of 1ml was taken from each tube and added to a fresh tube. 1 μ l of Dnase 1 was added to each tube at a final concentration of 20 μ g/ml. The tubes were left at room temperature for 15 minutes and then centrifuged at 13,200 rpm for 5 minutes. Approximately 1ml of supernatant was carefully removed from each tube and placed in a fresh tube. 500 μ l of DEAE slurry was added to each and the tubes left at room temperature for 10 minutes, with mixing by hand carried out every 2 minutes. The tubes were centrifuged at 13,200 rpm for 1 minute and the supernatants placed in fresh tubes. 40 μ l of 0.5M EDTA , 4 μ l of 2mg/ml RNase A and 1.4 μ l of 50mg/ml pronase stock solution was added to each tube and all samples incubated at 37°C for 15 minutes. 30 μ l of 5% CTBA stock solution was added to each tube and all samples incubated at 65°C for 3 minutes. 1.5 μ l of carrier glycogen was added to each tube and the samples incubated on ice for 5 minutes. The samples were then centrifuged at 13,200 rpm for 10 minutes and the supernatants discarded. Pellets were gently re-suspended in 200 μ l of 1.2M NaCl. 500 μ l of 100% ethanol was added to each tube, the DNA pellet harvested at 13,200 rpm for 10 minutes and washed twice in 70% ethanol. The pellets were air dried and re-suspended in sterile H₂O.

3.2.4 Long-range PCR amplification

Long-range PCR amplifications were performed using the Gene Amp XL PCR kit (Perkin Elmer). DNA and Mg²⁺ concentrations were varied for individual reactions and annealing temperature varied with the primers used. Amplification was performed on a DNA Engine PTC-200 (MJ Research). Standard thermal cycling conditions were as follows:

94°C for 1min: 1 cycle

94°C for 30s, 66°C for 10min: 16 cycles

94°C for 30s, 66°C for 10min (15sec increments/cycle): 19 cycles

72°C for 10min: 1 cycle

3.2.5 Reverse transcriptase - PCR (RT-PCR)

The reverse transcription mix consisted of 6µl 5x RT buffer (BoehringerMannheim), 10mM DTT (BoehringerMannheim), 100µM of each dNTP (BoehringerMannheim), 1µl random primers Pd(N)6 (BoehringerMannheim), 24U of RNase inhibitor (Promega) and 400U M-MLV RT (BoehringerMannheim). DNased RNA samples in a volume of 15µl was added to 14.1µl of this reaction mix. The reaction was incubated at 37°C for 2 hours and terminated by heating to 65°C for 10 minutes using a heated lid to prevent evaporation.

3.2.6 Preparation of the template DNA for ISH riboprobe

A PCR product was used as the template DNA. A T7 promoter was attached to the reverse primer (Appendix B.9) to be used in the PCR, in order to allow reverse transcription of an antisense probe. A T3 promoter was attached to the forward primer (Appendix B.9) to allow transcription of the equivalent sense probe. The template DNA was extracted with phenol/chloroform and then precipitated with absolute ethanol and

3M sodium acetate. It was then washed in 70% ethanol and re-suspended in DEPC-H₂O.

3.2.7 Transcription of riboprobe from template DNA

500ng -1mg of DNA was incubated with transcription mix consisting of 4µl 5x transcription buffer (BoehringerMannheim), 2µl 100mM DTT (Gibco-BRL), 2µl 10mM dNTPs (ATP, GTP, CTP, 6.5mM UTP and 3.5mM DIG-UTP) (BoehringerMannheim), 0.5µl RNasin Ribonuclease Inhibitor (Promega), 2µl RNA polymerase (BoehringerMannheim) and DEPC-H₂O to final volume of 20µl, at 37°C for four hours. The riboprobe was precipitated with absolute ethanol and 3M sodium acetate (DEPC) at -70°C, washed with 70% ethanol, vacuum dried and re-suspended in 40µl DEPC-H₂O.

3.2.8 Dot blot to test labeling of riboprobe

The BoehringerMannheim DIG Wash and Block buffer set was used for all solutions. Riboprobe production was first checked on an agarose gel and the concentration estimated. A DIG-labeled riboprobe (BoehringerMannheim) of known concentration was carried along through the dot blot to help get a more accurate estimate of concentrations. Starting with the riboprobe at a concentration on 1ng/µl, 10 fold serial dilutions were carried out in DEPC-H₂O to give dilutions of 100pg/µl, 10pg/µl, 1pg/µl, 0.1pg/µl and 0.01pg/µl. A small piece of hybond -N+ membrane (Amersham) was gridded and 1µl of dilutions 10pg/µl to 0.1pg/µl spotted on. This was allowed to dry briefly and then the RNA was UV cross linked for 12 seconds. The membrane was washed briefly in washing buffer in a 50ml universal, the washing buffer was discarded and the membrane incubated in blocking solution for 30 minutes with shaking, at room temperature. 1µl of anti-DIG antibody, AP-coupled (BoehringerMannheim), was diluted in 5mls of blocking solution and the membrane incubated in this solution for 30 minutes with shaking at room temperature. The antibody solution was discarded and two 15 minute washes in washing buffer carried out. The membrane was washed in

detection buffer for 2 minutes. 45µl NBT solution (BoehringerMannheim) and 35µl BCIP solution (BoehringerMannheim) was added to 10mls of detection buffer and the membrane incubated in this detection solution until the colour developed sufficiently (30 minutes to 16 hours). The reaction was stopped by washing with dH₂O.

3.2.9 Coating slides for ISH

Pre-washed glass slides (Chance Propper Ltd.) were placed in slide racks and washed in 1% Triton X-100 (Sigma) for 10 minutes with shaking. They were then rinsed in cold running water for 10 minutes, shaken in acetone for 10 minutes and then shaken in 2% 3-aminopropyl-triethoxysilane (APES) (Sigma)/acetone for 10 minutes. They were given a final rinse in cold running water for 10 minutes and then air dried overnight or on a heated block. Coated slides were stored in a box at room temperature.

3.2.10 Tissue Preparation for cryosections

To minimize the possibility of RNA degradation, RNase free instruments were used for enucleation of the eyes wherever possible. The unfixated eyes were embedded in the tissue freezing medium OCT compound as soon as possible post-enucleation and snap frozen in liquid nitrogen. They were stored at -70°C until ready to section. The tissue block was attached to the cryostat chuck with OCT compound and the temperature allowed to equilibrate before cryo-sectioning. Sections of 8-12µm were cut and thaw mounted on APES coated slides. The slides were labeled with details of tissue, riboprobe, concentration of riboprobe etc. The ISH protocol was proceeded with immediately after sectioning.

3.2.11 *In situ* hybridization protocol for cryosections

A. Slides with cryosections were placed in a slide rack and immersed in a dish containing 4% paraformaldehyde. Fixation was carried out for 10-30 minutes with shaking.

B. Two 15 minute washes with shaking in PBS (Appendix A.6) containing 0.1% active DEPC (Sigma) were carried out.

C. The sections were allowed to equilibrate in 5x SSC (Appendix A.6) for 15 minutes.

D. Taking a few slides at a time, to prevent the sections drying out, the excess liquid was drained off and the area around the sections dried. The slides were laid flat in a moist box and covered with pre-hybridization solution (Appendix A.6). They were incubated at 58°C for 2 hours without coverslips.

E. The DIG-labeled riboprobe was diluted to the required concentration (e.g. 400ng/ml) in the buffer used for pre-hybridization. It was heated to 90°C for 2-3 minutes to denature any secondary structures and then placed on ice immediately. A range of dilutions were carried out with all new riboprobes.

F. Coverslips (Chance Proper Ltd.) were wiped with ethanol to remove any dust or dirt.

G. The area around the sections was dried. 20-50µl (depending on the size of the tissue section) of the diluted riboprobe was pipetted onto a coverslip and the slide placed on top, taking care to prevent the formation of air bubbles. The slides were laid flat in a moist box and heated at 70°C for 2 minutes. Hybridization was preformed overnight at 42°C -58°C in the moist box.

H. The sections were transferred to a slide rack and washed in 2x SSC at room temperature for 10 minutes with shaking in order to remove the coverslips.

I. The sections were washed for a further 20 minutes in 2x SSC, at room temperature following the removal of the coverslips

J. The sections were washed in 2x SSC for 1 hour at 65°C, followed by 1 hour in 0.1x SSC at 65°C.

- K.** The sections were allowed to equilibrate in DIG 1 buffer (Appendix A.6) for 5 minutes at room temperature, with shaking.
- L.** The anti-DIG, AP-coupled, antibody was diluted (1:4000) in antibody blocking solution (Appendix A.6). The slides were laid flat in a moist box and the sections covered with antibody solution. They were incubated at room temperature for 2 hours.
- M.** Two washes in DIG 1 buffer for 15 minutes were carried out with shaking in order to remove residual antibody.
- N.** The sections were allowed to equilibrate in DIG 2 buffer (Appendix A.6) for 5 minutes with shaking.
- O.** The slides were laid flat in a moist box and the sections covered with detection solution (Appendix A.6). They were incubated at room temperature and the progress of the colour reaction checked microscopically every 30 minutes (without removing the solution). If the reaction was slow it was left to proceed overnight. In this case, to prevent background staining, the concentrated solution was drained off and the sections covered with a 1:9 dilution of detection solution. The sections were left in the moist box overnight at room temperature. The reaction is light sensitive so the box was covered with tin foil.
- P.** The section were immersed in water to stop the reaction.
- Q.** The mounting medium, glycerol gelatin (Sigma), was melted in a microwave and then kept molten in a beaker of hot water. The area around the sections was dried, 20-50µl of the mounting medium placed onto a coverslip and then the slide placed on top taking care to prevent the formation of bubbles.
- R.** Once the mounting medium was dry, the sections were studied using a Zeiss Axioplan 2 microscope.

3.2.12 *In situ* hybridisation protocol for paraffin embedded sections

This protocol has been used for tissues fixed with either formalin or glutaraldehyde that have subsequently been embedded in paraffin wax. Sections were cut at 3-8mm and collected on APES coated slides. Prior to analysis the sections were stored at room temperature in a dust free environment. Paraffin embedding and sectioning were carried out by Rod Ferrick in the Pathology Department in Glasgow University and Colma Barnes in the Pathology laboratory at the Eye and Ear Hospital, Dublin.

A. The sections were de-waxed by immersion in xylene for 10 minutes, followed by three washes in 100% ethanol for 1-2 minutes each.

B. The sections were washed in PBS (Appendix A.6) for 5 minutes, with shaking.

C. The sections were immersed in 0.2M HCl (Sigma) for 15 minutes, with shaking.

D. The sections were rinsed in PBS and then transferred to 0.3% Triton X-100 (Sigma) for 15 minutes, with shaking.

E. The sections were washed for 10 minutes in PBS. Taking a few slides at a time so that the sections did not dry out, the excess liquid was drained off and the area around the sections dried. The slides were laid flat in a moist box and the sections covered with 100µg/ml - 300µg/ml proteinase K (Sigma) in PBS. They were incubated at 37°C for 20-30 minutes without coverslips (the concentration of the proteinase K solution and the time length of incubation depend on the method of fixation used and have to be optimized for individual batches of sections).

F. The sections were rinsed briefly in PBS and transferred to 2% paraformaldehyde for 5 minutes at room temperature, with shaking.

G. An RNase prehybridization step was performed here, if required. The slides were laid flat in a moist box and covered with RNase A (Sigma) solution at 100µg/ml. They were incubated at 37°C for 10 minutes after which time the sections were rinsed three times in PBS. This step was carried out in a different area and with different glassware to the other steps.

H. The sections were washed for 10 minutes in PBS, laid flat in a moist box and covered with pre-hybridization solution (Appendix A.6). They were incubated at 37°C for 2 hours without coverslips.

I. The DIG-labelled riboprobe was diluted to the required concentration (e.g. 400ng/ml) in the hybridization buffer (Appendix A.6). It was heated to 90°C for 2-3 minutes to denature any secondary structures and then placed immediately on ice. A range of dilutions were carried out with all new riboprobes.

J. The area around the sections was dried. 20-50µl (depending on the size of the tissue section) of the diluted riboprobe was pipetted onto a coverslip and the slide placed on top, taking care to prevent the formation of air bubbles. The slides were laid flat in a moist box and heated at 70°C for 2 minutes. Hybridization was performed overnight at 42°C -58°C in the moist box.

K. The sections were transferred to a slide rack and washed in 2x SSC (Appendix A.6) at room temperature for 10 minutes with shaking, in order to remove the coverslips.

L. The sections were washed for a further 20 minutes in 2x SSC, at room temperature, following the removal of the coverslips.

M. The sections were washed in 0.1xSSC for 10 minutes at room temperature, followed by 0.1xSSC in a waterbath at 50°C for 30 minutes and finally 0.1xSSC at room temperature for 10 minutes.

N. The sections were allowed to equilibrate in DIG 1 buffer (Appendix A.6) for 5 minutes at room temperature, with shaking.

O. An RNase post-hybridization step was performed here, if required. The slides were laid flat in a moist box and covered with RNase A solution at 100µg/ml. They were incubated at 37°C for 10 minutes after which time the sections were rinsed three times in DIG 1 buffer. This step was carried out in a different area and with different glassware to the other steps.

P. The anti-DIG Ab was diluted (1:2000) in antibody blocking solution (Appendix A.6). The slides were laid flat in a moist box and the sections covered with antibody solution. They were incubated at room temperature for 2 hours.

Q. In order to remove residual antibody two washes in DIG 1 buffer, for 15 minutes, were carried out, with shaking.

R. The sections were allowed to equilibrate in DIG 2 buffer (Appendix A.6) for 5 minutes with shaking.

S. The slides were laid flat in a moist box and the sections covered with detection solution (Appendix A.6). They were incubated at room temperature and the progress of the colour reaction checked microscopically every 30 minutes (without removing solution). If the reaction was slow it was left to proceed overnight. In this case, to prevent background staining, the concentrated solution was drained off and the sections covered with a 1:9 dilution of detection solution. They were left in the moist box overnight at room temperature. The reaction is light sensitive so the box was covered with tin foil.

T. The section were immersed in water to stop the reaction.

U. The mounting medium, glycerol gelatin, was melted in a microwave and then kept molten in a beaker of hot water. The area around the sections was dried. 20-50µl of the mounting medium was placed onto a coverslip and then the slide placed on top, taking care to prevent the formation of bubbles.

V. Once the mounting medium was dry the sections were studied using a Zeiss Axioplan 2 microscope.

3.3 RESULTS AND DISCUSSION

3.3.1 A novel method involving long-range PCR in an attempt to isolate RP10

This study involved the use of long-range PCR in an attempt to amplify contiguous PCR products spanning the RP10 interval on 7q. Long-range PCR appears to be more successful when used to amplify cloned DNA than when used with genomic DNA. For this reason genomic libraries, with which success had been achieved by various groups (Cheng *et al.*, 1994b; Barnes, 1994), were employed. A phage library was chosen as the relatively small inserts, which range in size from 9 - 23kb, would be more amenable to long-range PCR amplification than the larger inserts of cosmid or YAC libraries. This library was a human, total genomic DNA library obtained from human umbilical endothelial cells. It was calculated that 1 million plaque forming units (pfu) should be a sufficient number to ensure that every sequence in the genome was present at least once. In an attempt to minimize the possibility of multiple amplification products, the titrated library was fractionated into 20 pools of 50,000 pfu.

Three of the microsatellite markers within the 7q adRP disease interval D7S680, D7S648 and D7S686, which show no recombination with the disease locus in both families (FA-84 and UTAD045), were adopted as sequence tagged sites (STSs). They were used, by means of a PCR based assay, to identify those fractions of the library which contained clones from this region of the genome. The primers specific for microsatellite marker D7S680 (Appendix B.6) were used in this project for the PCR amplifications. Library fractionations and phage DNA extractions were also performed by Fiona Mansergh, who subsequently carried out PCR reactions using marker D7S648 primers and Denis Allman, using marker D7S686. Genethon microsatellite primers, D7S680f and D7S680r (Appendix B.6), were used in standard PCR reactions on DNA extracted from each of the 20 pools.

Following amplification and agarose gel electrophoresis a visible amplification product of the expected 125bp was apparent in 12 of the 20 stocks (Figure 3.1). Having identified those stocks which contained clones with DNA inserts from the RP10 interval on 7q, primers designed from the sequence flanking the microsatellite (D7S680) were paired with primers derived from the lambda DASH II arms (Appendix B.6) and used in long-range PCR reactions on these stocks. Using this approach, it was predicted that it

would be possible to generate a series of contiguous PCR products across the entire disease interval, which could be used in the direct sequencing of the interval or in gene detection methods, with the aim of identifying the RP10 gene.

While it was possible to use the long-range PCR technique to successfully amplify the control DNA supplied with the kit, it proved impossible to achieve discreet and reproducible amplification products from any of the 12 stocks used in the reactions. The variation of parameters, including annealing temperature, Mg^{2+} ion concentration, primer concentration etc., unfortunately failed to achieve the desired result and further efforts in this area were deemed to be futile. Perhaps refinements to the long-range PCR technique will allow the use of such an approach in physical mapping studies in the future. In the meantime it was necessary to devise other ways to identify candidate genes within the RP10 interval.

3.3.2 Expressed sequence tags (ESTs) mapping to the RP10 disease interval

Following exclusion of potential RP candidates mapping to the 7q adRP interval there were no other known genes in the region fitting the criteria for the RP10 gene. Because of this it was decided to take advantage of the developments in the mapping of human ESTs, in the search for candidate RP genes. The latest human transcript map, GeneMap '99, can be accessed via a user-friendly world wide web site (Deloukas, 1998). Knowledge of the Genthon markers spanning a disease interval allows the retrieval of a partial inventory of genes from that interval.

All the GeneMap markers have been mapped using either or both of two radiation hybrid panels: the Genebridge4 panel (GB4) and the Stanford G3 panel. These panels possess different properties, with the GB4 panel providing long-range map continuity and the G3 panel providing higher map resolution. The microsatellite markers which are used as anchor points in the human transcript map have been mapped using both panels and give results consistent with each other and with the Génethon human genetic map. In some cases where a gene marker has been mapped using both RH panels, discrepancies in map position are encountered. Such discrepancies are indicated by asterisks and the marker is placed at different positions in the two panels.

The markers flanking the 7q disease interval have been identified as D7S2471 and D7S530. The marker D7S2471 is not used as a reference maker in GeneMap '99

but the marker D7S686, which is 0.6cM distal to D7S2471, is. When D7S686 and D7S530 were input into GeneMap '99 as flanking markers a total list of 73 genes or ESTs, which have been mapped to this interval, was retrieved. 14 of these were placed on G3 map and 59 on the GB4 map. Six markers were mapped to the interval using both panels however, so the total number of gene markers mapping to the interval is 67. Another 15 markers are part of the same UniGene cluster as other markers within the interval and therefore the number of unique genes listed for this interval is 52. A further six markers were mapped in both panels but were only placed in the D7S686 – D7S530 interval in one of the panels. At present, it is not possible to tell which of the map positions given to these markers is the correct one.

For each marker on the human transcript map information is available, through the use of hypertext links, on how it was mapped, its UniGene cluster number (if available), a list of results from e-PCR of GenBank (the primers for the marker are compared to all sequences in the database and those that give hits are listed) and sometimes on protein similarities identified using blast programs.

It was decided to initially prioritize genes on the basis of the cDNA libraries from which they had been identified. As all the adRP genes identified to date are expressed exclusively in the retina it was decided therefore to concentrate on those ESTs identified only from retinal sources (Molday, 1998; Liu *et al.*, 1996, Freund *et al.*, 1997; Sullivan *et al.*, 1999). It appears in fact that all genes which have been implicated in all forms of RP to date are in fact retina specific (Dryja and Li, 1995; Molday, 1998; Daiger *et al.*, 1999). The only exception to this is the RPGR gene which is expressed ubiquitously (Meindl *et al.*, 1996). Data available, through UniGene or sequence data base links, on which human tissue the original transcripts were isolated from, allowed the determination of ESTs which were identified from retinal specific libraries.

Two ESTs, which have been arbitrarily named EST 34 and EST 38, have been identified which are of particular interest to us (Table 3.1). EST 34 maps to the disease interval in both the G3 and GB4 RH panels. EST 38 maps within the critical interval in the G3 map but in the GB4 map it maps to the interval below (D7S530-D7S509). At present it is not possible to tell which of these map positions is the correct one, so for now it is considered a candidate gene. Both of these genes have been identified only from retinal libraries. A third EST, EST 35, is also of interest, but to a lesser extent (Table 3.1). It maps to the critical disease interval and is expressed in retina. As well as being expressed in retina however it is also expressed in ovary tumors and testes. It is

less likely therefore to be the RP gene but the fact that expression in tumor cells probably does not always reflect normal expression patterns and that only one of the number of clones in its UniGene cluster is derived from testis, it was decided to adopt EST 35 as a candidate gene also. This EST has not been mapped in the G3 RH panel, but maps to the critical interval in the GB4 panel.

Table 3.1 Details of the ESTs mapping to the 7q critical disease interval which have been identified as candidates for the RP10 gene.

| EST | EST 34 | EST 35 | EST 38 |
|--|-------------------------|---|--------------------------------------|
| Markers | SHGC-31135 WI-31135 | SGC31025 | SGC30795 SHGC-30795 |
| G3 Map Interval | D7S686-D7S530 | — | D7S686-D7S530 |
| GB4 Map Interval | D7S686-D7S530 | D7S686-D7S530 | D7S530-D7S509 |
| Genetic Position | 131.7-136.4 cM | 131.7-136.4 cM | 136.4-145.8 cM |
| UniGene Cluster | — | Hs.40507 | Hs.32718 |
| CDNA source | Soares retina N2b4HR | Soares retina N2b4HR Soares ovary tumor NbHOT Soares testis NHT | Soares retina N2b4HR |
| I.M.A.G.E. clones of transcript | 222130 | 742135 222188 361191 362906 1737951 222188 362882 | 380322 275543 190975 363228 |

I.M.A.G.E.: Integrated Molecular Analysis of Genomes and their Expression.

As D7S2471, not D7S686, has been defined as a flanking marker, markers from the next GeneMap reference interval up were also looked at. This interval stretches from

D7S655 to D7S686, a distance of 5.2cM. ESTs mapping to this interval within 1cM of D7S686 were looked at but none were identified from retinal libraries.

Having identified ESTs of interest it was decided to devise methods to learn more of the expression patterns of the genes rather than carrying out time consuming methods to generate more sequence for these genes for which very little is known about. Initially these methods involved initially the rhodopsin knockout mouse and subsequently, *in situ* hybridization on tissue sections.

3.3.3 A novel method to determine whether candidate genes are rod photoreceptor specific

The majority of the genes so far implicated in RP are photoreceptor specific: rhodopsin, peripherin/RDS, PDEA, PDEB, CNCG1, ROM1, ABCR, CRX and the gene of unknown function on 8q (Molday, 1998; Dryja and Li, 1995, Sullivan *et al.*, 1999). It was decided therefore that knowledge of whether or not an EST of interest was expressed specifically in the photoreceptors would give further insight into its potential role in adRP. A novel method was designed to determine whether or not candidate genes are specific for the photoreceptors within the retina.

The ability to distinguish genes expressed in the photoreceptors from those expressed in other retinal cell types is made possible by the availability of the rhodopsin knockout mouse. The disruption of the rhodopsin gene induces a retinopathy in Rho^{-/-} animals, leading to the death of the photoreceptors occurring over a period of 3 months. Following this period, histological studies indicate that there are no photoreceptors remaining in the retinas of these mice (Humphries *et al.*, 1997). Likewise, it follows that photoreceptor-specific RNA transcripts are absent at this stage of the induced retinopathy. While levels of transcript from other retinal cells might be affected by the absence of rods, the remaining retinal layers are remarkably intact.

Therefore, it might be possible to test whether a gene is photoreceptor specific or not, by attempting to amplify transcript using RT-PCR on RNA extracted from Rho^{-/-} mice prior to and post photoreceptor cell death. If a transcript is photoreceptor cell specific, a positive signal, in the form of a PCR product, should be obtained from samples extracted before the death of these cells. After photoreceptor cell death however, the positive signal would be expected to be very much reduced in amplitude or

completely eliminated. Alternatively, if a protein is expressed in other retinal cell types, a positive signal should be detected from samples extracted both before and after rod photoreceptor death. This concept would apply to all mouse models of retinopathies.

The feasibility of this experiment has been tested using PCR primers (Appendix B.7) specific for a gene known to be expressed specifically in rod cells: the cGMP-gated channel and another gene known to be expressed in other cell layers of the retina (including the inner nuclear layer and the ganglion cell layer): mGluR8 (Duvoisin *et al.*, 1995). RNA was extracted from a Rho^{+/+} mouse at 5 months, a Rho^{-/-} mouse at 1 month and a Rho^{-/-} mouse at four months by Marian Humphries. RT-PCR, using both cGMP and mGluR8 specific primers (Appendix B.6), was performed on all 3 samples. A positive signal for mGluR8 transcript was apparent on an agarose gel in all 3 RNA samples. For the cGMP-gated channel transcript, positive signals were obtained with both Rho^{+/+} RNA and Rho^{-/-} RNA from the one month old animal. For the RNA from the Rho^{-/-} animal at four months however, a positive signal was essentially eliminated (Figure 3.2). This experiment was repeated using different animals of the same ages (with the exception of the Rho^{+/+} mouse which was four months old) and the same results were obtained.

3.3.4 Testing 7q ESTs for rod photoreceptor specificity

Having proven the feasibility of this experiment, we wished to test the three 7q ESTs, EST 34, EST 35 and EST 38, for photoreceptor specificity. As primers designed from mouse sequence were previously used in the sequencing of human genomic GRM8 clones (chapter 2), we chose to attempt this experiment with the human EST primers in the hope that they would amplify the homologous genes in mouse.

Primer sequences (Appendix B.8) were obtained from the sequence data bases and used in PCR reactions with both human and mouse DNA. However, while all three primer pairs successfully amplified human genomic DNA, they failed to amplify mouse DNA. Three more sets of primers (Appendix B.8) were designed in different regions of the sequence available in the databases, but these primers, while successfully amplifying human DNA, once again failed to amplify mouse DNA. This lack of success obviously results from sequence variation between mouse and human genomes. Significantly,

ESTs are often chosen from the 3' untranslated region of genes where the sequence is least conserved (Boguski *et al.*, 1993).

It appears therefore, that in order to test whether genes are photoreceptor specific, it will be necessary to have sequence information from the mouse homologue of the gene in question. This poses a problem as, while mouse EST mapping projects are also underway, there is as yet little correlation between mouse and human projects. Thus, while it was possible to retrieve EST information specifically for the RP10 disease interval, it has proven difficult to correlate a specific human EST with an homologous EST in mouse.

The rapid progress in EST mapping projects may make this task increasingly feasible over the next few years. In the meantime however, it will probably be necessary, when encountering an EST of particular interest in the search for the RP10 gene, to use human EST sequence to probe mouse cDNA libraries in order to retrieve sufficient mouse sequence to allow the design of primers for RT-PCR. As this approach will necessarily entail a considerable amount of work, it would be impractical to test each of the ESTs of interest mapping to the RP10 region for photoreceptor specificity. Because of this, *in situ* hybridization on tissue sections was adopted as the method to characterize the expression pattern of the retinal specific ESTs

3.3.5 Development of the ISH technique on tissue sections

Eye tissue sections were required in order to carry out the ISH experiments to localize the expression of the 7q ESTs at the cellular level. Since the EST primers had been found not to amplify mouse DNA, it was decided that mouse sections would not be appropriate for the experiment and that human eye sections would be required. In order to develop the technique however, mouse eye sections were used initially with mouse specific RNA probes.

DIG-labeled RNA was chosen as the probe for these experiments. Riboprobes were chosen due to their sensitivity and to the stability of the hybrids they form post-hybridization. DIG was selected as a label as problems with unspecific binding of its antibody are generally not detected. Mouse specific probes for two photoreceptor specific genes, rhodopsin and peripherin/RDS, were designed. The rhodopsin probe was designed in exon 1 of the gene, 27 bp after the start of translation and is 224 bp in

length. The peripherin/RDS probe is 182 bp, beginning 53 bp before the ATG start site of the gene. Sense and antisense DIG labeled probes were generated from PCR templates as detailed in the methods section. These probes were made by Sophia Millington-Ward. Labeling of the riboprobes was tested by dot blotting using anti-DIG antibody. The inclusion of a DIG labeled riboprobe of known concentration also allowed estimation of probe concentrations.

The ISH technique was developed using both paraffin and cryo sections. Paraffin embedded rat eyes were initially unavailable and therefore paraffin rat sections were kindly provided by Dr. Catherine Winchester, University of Glasgow. These rat sections had been fixed in glutaraldehyde. The probe concentrations used ranged from 0.3ng/ μ l to 5ng/ μ l. Hybridization was performed at 55°C overnight.

Specific labeling was detected with the rhodopsin antisense probe in the inner segments of the photoreceptor cells (Figure 3.4). The most intense signal following detection of the probe with an anti-DIG antibody was obtained at a probe concentration of 0.3ng/ μ l. Notably the colour staining at this concentration was consistently more intense than found with higher concentrations of riboprobe. Unspecific staining in the inner segment, inner nuclear and ganglion layers of the retina was detected with the rhodopsin sense probe (Figure 3.5). An RNase A pre-hybridization step performed on the sections eliminated all signal from both the anti-sense and sense experiments. This indicated that the sense probe was binding to RNA transcripts in the retina. Following an RNase A post-hybridization step the unspecific staining with the sense probe was eliminated however, indicating it was not forming specific hybrids with RNAs in the sections. A post-hybridization RNase A step on sections with hybridized anti-sense probe did not eliminate the signal in the inner segment layer confirming that the antisense probe was forming specific hybrids (Figure 3. 5).

The hybridization results with the peripherin/RDS probe on paraffin rat eye sections did not result in such specific results. Staining was seen in the inner segment, inner and outer nuclear and ganglion layers of the retina with this probe. As the paraffin rat eye sections were limited further hybridizations to attempt to optimize conditions for this probe were not carried out.

The ISH technique was also developed using mouse eye cryo-sections (see Figure 3.3 for a cross section of a normal mouse retina). Hybridization of rhodopsin anti-sense probe to cryo-sections also gave specific staining in the inner segments of the photoreceptors. Staining with the peripherin/RDS probe was more specific than in

paraffin sections and seemed to be concentrated, as with rhodopsin, in the inner segment layer but with a very light background staining in all other retinal layers (Figure 3.4). As the rhodopsin anti-sense probe was an appropriate positive control however, no further hybridizations with the peripherin/RDS probe were carried out.

Having optimized the technique using the rhodopsin probe on both paraffin and cryo sections, a human rhodopsin probe, designed in the equivalent region of the human gene as the mouse gene, was generated. During the course of these experiments a transgenic mouse carrying a human rhodopsin transgene on a knockout rhodopsin background was generated (McNally *et al.*, 1999). Eyes from these animals were cryo-sectioned and used to optimize conditions for ISH of the human rhodopsin probe. The optimal concentration for this probe was found to be 0.3ng/ μ l and specific staining in the inner segment photoreceptor layer of the retina was once again obtained.

3.3.6 ISH on human eye sections

Having developed and optimized the ISH technique on mouse tissue sections, the application of the technique to the investigation of the expression of the 7q retinal ESTs was initiated. Probes were designed for the three ESTs of interest, EST 34, 35 and 38, which were subsequently made by Sophia Millington-Ward. All the EST probes were designed in the short stretches of sequence which the ESTs consist of and hence are probably designed in the 3' UTRs of the genes from which they are derived. The probes for ESTs 34, 35 and 38 are 239, 280 and 178 bp, respectively. A second probe for EST 35 of 320 bp long was also generated.

Unfortunately, the ascertainment of well preserved human eye sections has proven very difficult. The first human eye sections to be used in ISH were taken from a trauma eye which was removed, fixed in formalin, paraffin embedded and sectioned at the Royal Victoria Eye and Ear Hospital, Dublin. The morphological preservation of the eye was poor and there remained only a small portion of retina (Figure 3.6). A mouse eye was included in each ISH trial and these positive controls continued to show specific staining in the inner photoreceptor segments. Despite many repeated attempts and varied conditions however, no positive signal was obtained for any of the human probes on the human eye sections, including the human rhodopsin probe. The varied conditions included changes in hybridization conditions and probe concentrations.

Strong treatments with proteinases were also performed on these sections, in case the failure to achieve a signal was due to over-fixation of the eye, but did not result in a signal. Given the poor morphology of the sections it is possible the trauma to the eye resulted in the cessation of RNA transcription or the rapid loss of RNA transcripts following transcription. Alternatively, the time length between enucleation of the eye and fixation may have been too long and resulted in degradation of transcripts.

Following this, a tiny portion of unfixed retina from another human eye was obtained in tissue freezing medium from the Royal Victoria Hospital. This portion of retina was also from a trauma eye although the morphology in this case was superior to the first eye. ISH was performed on cryosections taken from this embedded tissue. Once again however, no positive signal was obtained despite the variation of parameters. The reasons for this are once again unclear but may also be due to the trauma to the eye or a delayed time period between enucleation and freezing.

Two post mortem eyes were also obtained from the Central Florida Lions Eye Bank. These eyes were fixed in formalin and subsequently embedded and sectioned at the Royal Victoria Hospital. The morphological preservation of these eyes were excellent (Figure 3.6). The time delay between death and preservation was 15 hours and 20 minutes however, and no positive signal was obtained with these eyes. This was presumably due to RNA degradation.

At the time of writing, an alternative source of human retinal material has become available from Dr. Brian Clarke. In situ hybridisation using the human rhodopsin probe gives a positive signal in the photoreceptor cells of the retina in these sections (Figure 3.7). Experiments using probes for the three ESTs of interest are currently in progress.

3.4 CONCLUSION

The objectives of this project were, and continue to be, the prioritization of candidate genes for the adRP gene on chromosome 7q. Initial attempts to generate large amounts of sequence across the RP10 disease interval, through the use of long-range PCR, proved unsuccessful. As this method was designed for the purpose of identifying coding sequence in the interval however, it could in fact be considered outdated, given the advances in EST sequencing. The large amount of EST data available has allowed the identification of a number of candidate genes for the RP10 gene on the basis of chromosomal location and tissue expression. As each EST usually contains only a small portion of the coding sequence of a gene, retrieving and deciphering the entire sequence of each gene would necessarily entail a considerable amount of work. Because of this, it is necessary to further prioritize each of the candidate ESTs. Given that a large majority of the RP genes identified to date are expressed exclusively in the photoreceptors of the retina, it was decided to choose photoreceptor specific expression as a criterion for selecting those candidates to be screened in affected family members. The first experiment designed to determine whether or not a particular EST is expressed exclusively in the photoreceptors involved the use of the rhodopsin knockout mouse. This experiment was unsuccessful however, due to the fact that it proved impossible to amplify mouse DNA with the human EST primers. The second method devised to achieve this end involved ISH on eye sections. This method was developed successfully using rodent eye sections but has not been successful to date in investigating the expression pattern of ESTs due to the poor quality of human eye sections obtained. This project is ongoing however.

Following the identification of a candidate gene, based on the map position of its sequence tag and its pattern of expression within the retina, it will be necessary to determine its genomic structure in order that screening of coding regions may be carried out in affected individuals. At the TIGR website, tentative human consensus sequences (THCs) are available (TIGR human gene index, 1999). These are assemblies of human ESTs which are created by assembling available EST sequences into longer stretches of contiguous sequence. This site may provide a valuable first step in the retrieval of sequence for an EST of interest. The THCs are "virtual transcripts" and therefore there are not clones available for them. The clones for the underlying ESTs are available however, and may be purchased from a number of sources, including the American

Type Culture Collection (ATCC) (ATCC homepage, 1999). Mapping of these clones to contigs spanning the disease interval should allow the subsequent elucidation of the genomic structure of the gene of interest.

If all three retina specific ESTs are excluded as candidates it will be necessary to adopt other ESTs mapping to the interval as candidates. As one of the genes which causes X-linked RP, the RPGR gene, is also expressed in other tissues of the body, those ESTs which were identified from cDNA libraries from several tissues, including retina, will be characterised for their expression patterns. It may also be necessary to consider that a number of retinal proteins are also expressed in the pineal gland in the brain (Yamaki *et al.* 1990). ESTs in this region which were identified from brain libraries, may also be considered therefore.

It is almost certain that even with the use of normalized cDNA libraries, genes expressed at low levels are not as yet represented in the human EST collection and therefore, it is possible that the RP10 gene is not yet represented in the human transcript map. New ESTs are continuously being generated however, and it cannot be long before this gene is identified in the form of an expressed sequence tag. If we fail to identify a candidate gene in this manner, a new approach in the search for the RP10 gene may have to be taken. This may involve the use of YAC contigs spanning the disease interval which have been generated by other research groups (McGuire, 1996b). Alternatively, methods involving the direct analysis of the 7q sequence data, presently being generated by the human genome project, could be adopted (Bouffard *et al.*, 1997).

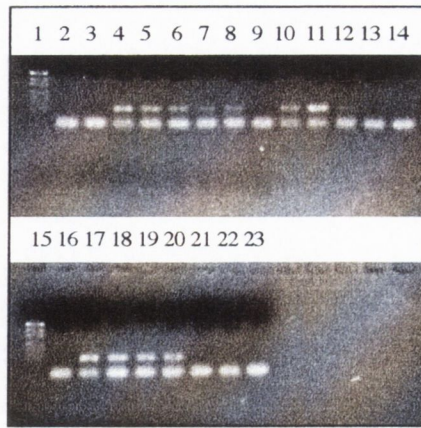


Figure 3.1 PCR analysis of 20 fractions of a human total genomic library using marker D7S680 primers. The presence of a 125 bp fragment following amplification indicated stocks containing clones from the RP10 region on chromosome 7q. Lanes 1 and 13, *Puc19/MspI*; lanes 2-14 and 16-20, PCR products from library fractions 1-20; lane 23, H₂O PCR control.

Note: the smaller fragment apparent in all PCR samples is due to excess primer.

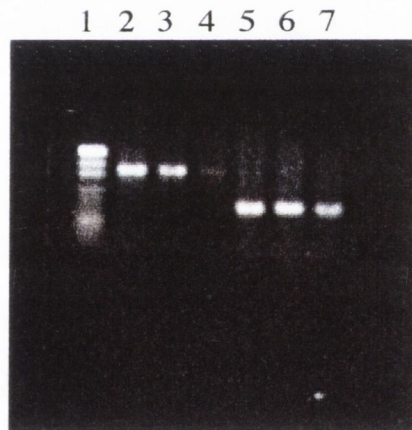


Figure 3.2 RT-PCR on RNA extracted from *Rho*^{+/+} mice and *Rho*^{-/-} mice using cGMP and mGluR8 primers. Lane 1, *Puc19/MspI*; lane 2, *Rho*^{+/+} RNA amplified with cGMP primers; lane 3, *Rho*^{-/-} RNA from a 1 month old mouse amplified with cGMP primers; lane 4, *Rho*^{-/-} RNA from a 4 month old mouse amplified with cGMP primers; lane 5, *Rho*^{+/+} RNA amplified with mGluR8 primers; lane 6, *Rho*^{-/-} RNA from a 1 month old mouse amplified with mGluR8 primers; lane 7, *Rho*^{-/-} RNA from a 4 month old mouse amplified with mGluR8 primers.

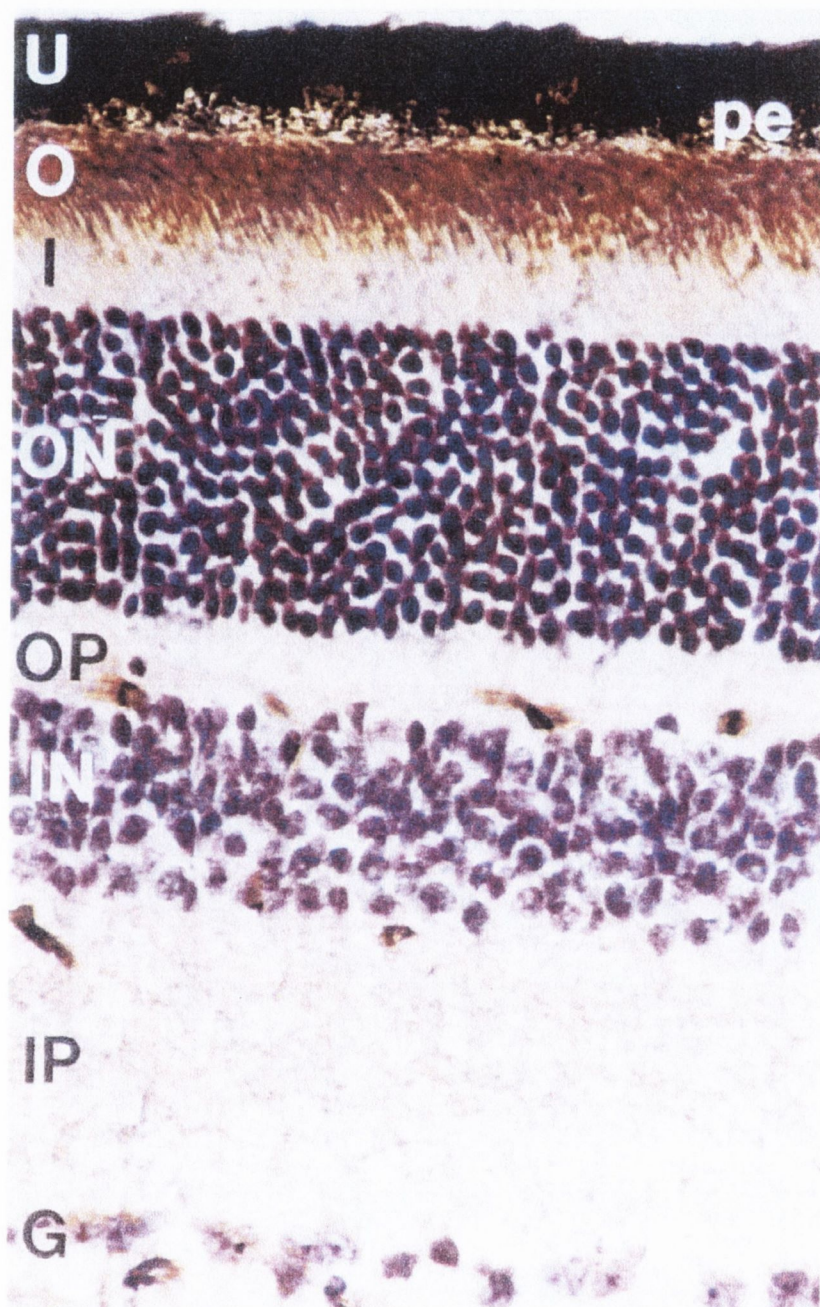


Figure 3.3 A cross section of a normal mouse retina, stained with haematoxylin and eosin. (PE) retinal pigment epithelium, (O) photoreceptor outer segment layer, (I) photoreceptor inner segment layer, (ON) outer nuclear layer, (OP) outer plexiform layer, (IN) inner nuclear layer, (IP) inner plexiform layer, (G) ganglion cell layer.

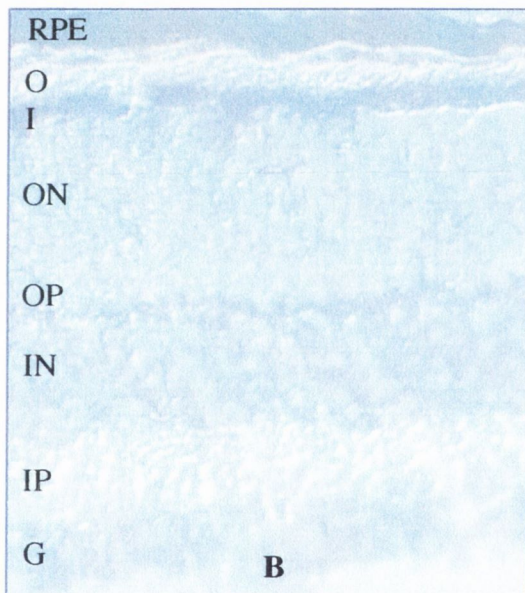
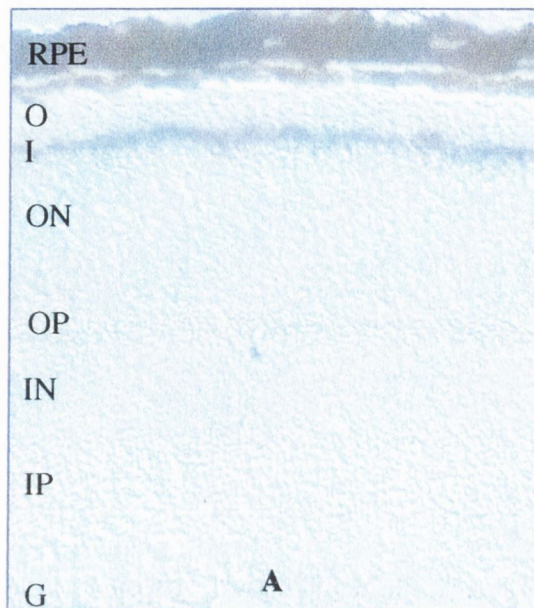


Figure 3.4 *In situ* hybridizations on mouse retinal cryosections with rhodopsin and peripherin/rds probes. (A) Hybridization with mouse rhodopsin antisense probe. The purple staining indicates hybridization to the photoreceptor inner segment layer. (B) Hybridization with mouse peripherin/rds antisense probe. A light non-specific staining of all layers of the retina is apparent but a more intense staining in the photoreceptor inner segment layer can be seen. 200X magnification

(RPE) retinal pigment epithelium (O) Outer segment layer, (I) inner segment layer, (ON) outer nuclear layer, (OP) outer plexiform layer, (IN) inner nuclear layer, (IP) inner plexiform layer, (G) ganglion cell layer.

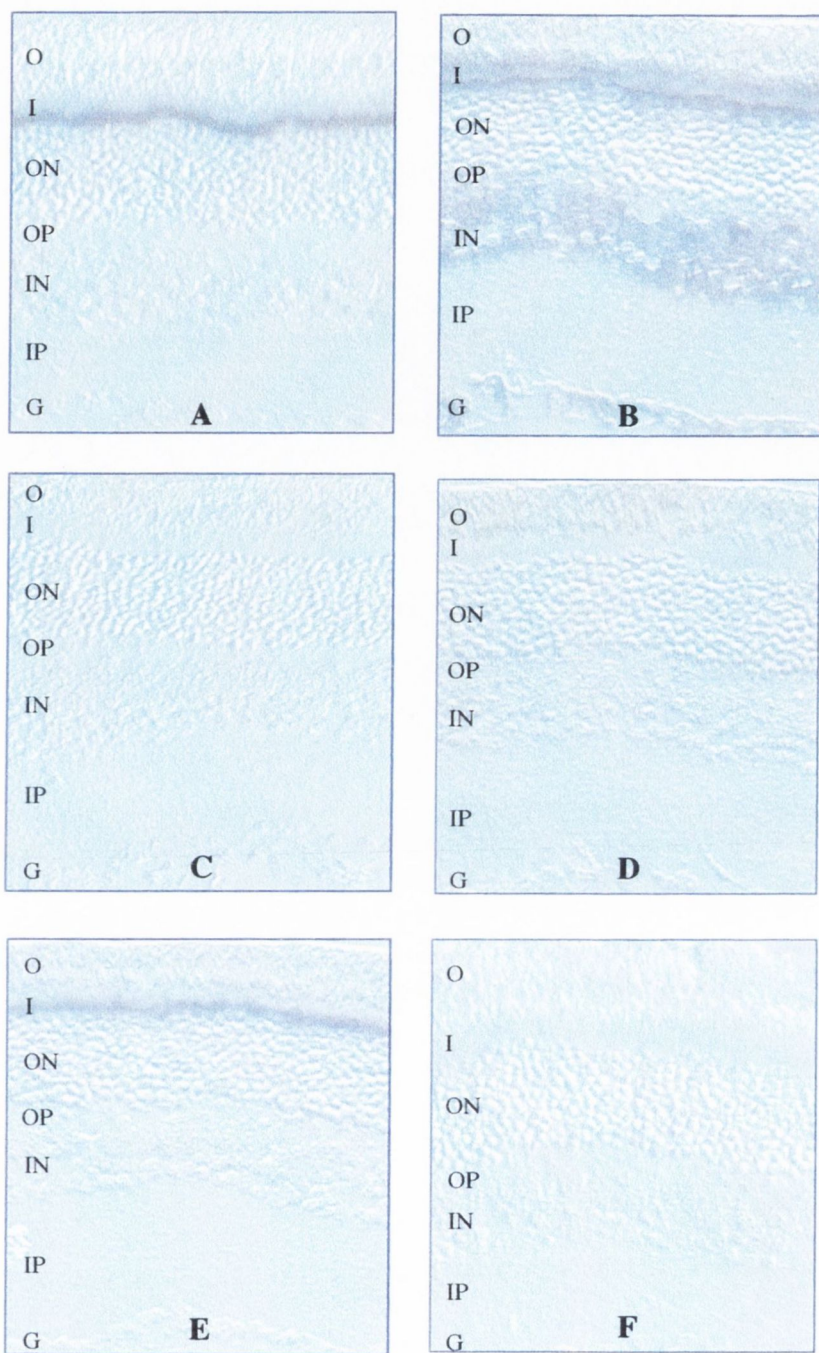


Figure 3.5 Mouse rhodopsin antisense probe hybridised to a rat eye section shown alongside controls. The sections were taken from a paraffin embedded eye and the RPE has become detached in all. All probes are at a concentration of 0.3ng/ μ l. (A) antisense probe. (B) sense probe. (C) antisense probe with a prehybridisation RNase A step. (D) sense probe with a prehybridisation RNase A step. (E) antisense probe with a posthybridisation RNase A step. (F) sense probe with a posthybridisation RNase A step. 200X Magnification.

(O) Outer segment layer, (I) inner segment layer, (ON) outer nuclear layer, (OP) outer plaxiform layer, (IN) inner nuclear layer, (IP) inner plexiform layer, (G) ganglion cell layer.

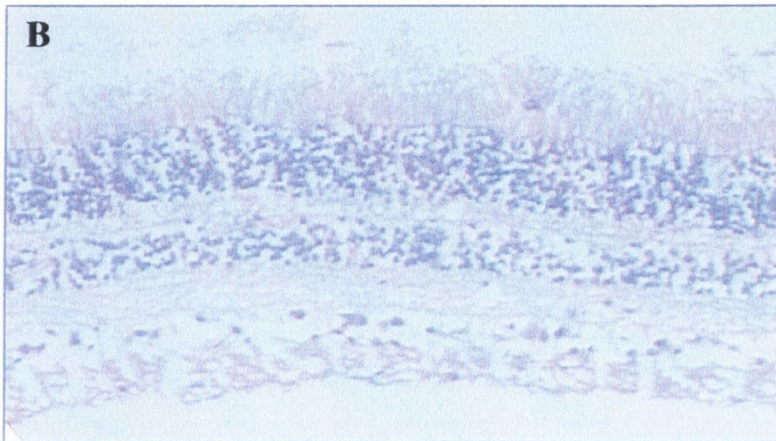
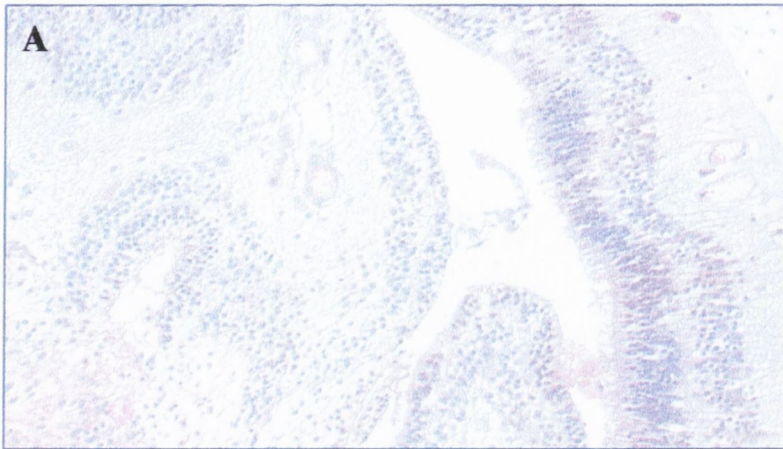


Figure 3.6 Histological features of human retinal sections used in *in situ* hybridizations. Both sections have undergone haematoxylin and eosin staining. (A) Section taken from a paraffin embedded eye donated by the Royal Victoria Eye and Ear hospital. Trauma to the eye resulted in retinal detachment and visible disruption to overall morphology. (B) Section taken from a paraffin embedded donor eye supplied by the Central Florida Lions Eye Bank. As is apparent the morphological preservation of this eye was reasonably good. 200X Magnification.

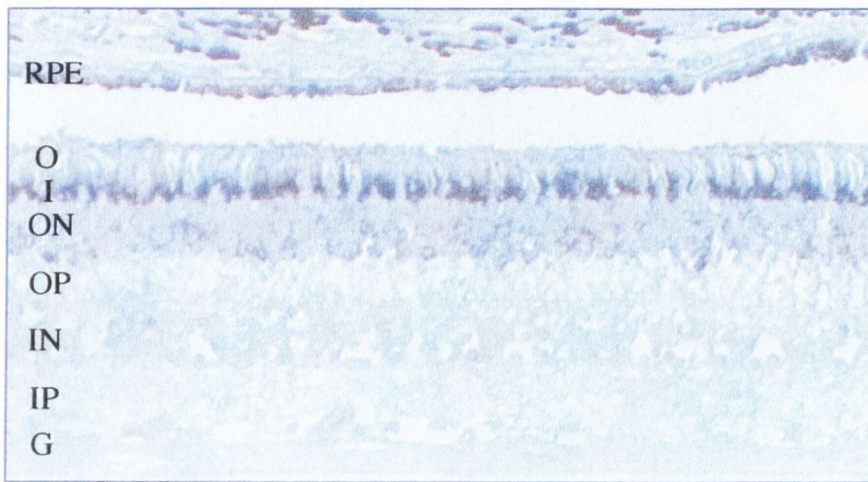


Figure 3.7 *In situ* hybridization on a human retinal paraffin section with a rhodopsin probe. The purple staining indicates hybridization to the photoreceptors with the staining concentrated in the inner segment layer. The RPE has become detached from the rest of the retina. 200X magnification

(RPE) retinal pigment epithelium (O) Outer segment layer, (I) inner segment layer, (ON) outer nuclear layer, (OP) outer plexiform layer, (IN) inner nuclear layer, (IP) inner plexiform layer, (G) ganglion cell layer.

CHAPTER 4

THE IDENTIFICATION OF A NOVEL ASP380ALA MUTATION IN THE MYOCILIN GENE IN A FAMILY WITH JUVENILE ONSET PRIMARY OPEN ANGLE GLAUCOMA

4.1 INTRODUCTION

4.1.1 Introduction

The term glaucoma describes a clinically and genetically heterogeneous group of diseases that result in optic neuropathy and progressive loss of visual fields. A gene for juvenile onset primary open-angle glaucoma (JOAG) has recently been mapped to 1q21-31. Mutations in the trabecular meshwork-induced glucocorticoid response gene (TIGR, also known as myocilin or the GLC1A locus) have been found to cause both juvenile and later-onset primary open-angle glaucoma. Family TCD-POAG1 is a Spanish kindred which segregates JOAG in an autosomal dominant fashion. This family have previously been found to be linked to the GLC1A locus on chromosome 1q. The aim of this study was to screen the coding regions of the myocilin gene for a disease causing mutation in family TCD-POAG1.

A background to the clinical features of glaucoma, along with a detailed discussion on the genetic loci involved in the causation of glaucoma are presented. A discussion of the myocilin gene and the reports to date implicating it in glaucoma are provided. In the results section, the identification of a pathologic mutation in the myocilin gene in family TCD-POAG1 is reported.

4.1.2 Glaucoma

The term glaucoma encompasses a heterogeneous group of optic neuropathies, which bring about loss of visual field and which, if left untreated, can lead to total blindness. Glaucoma has been subdivided into various categories, depending on factors such as the shape of the irido-corneal angle, whether or not the glaucoma is primary or secondary in nature and the age of onset of the disease. The different forms of glaucoma, however, generally have a number of underlying clinical features in common. Patients usually experience a painless progression of the disease, leading to loss of the visual field and show a characteristic abnormal appearance of the optic nerve head, due to atrophy of the retinal ganglion cells. Ocular hypertension, defined by intraocular pressures (IOPS) being consistently > 21 mm Hg in both eyes, is considered a risk factor for glaucoma

and is frequently observed in affected individuals. This is widely believed to be due to impaired aqueous humour outflow from the anterior chamber of the eye and is implicated in the damage to the optic neurons.

The three traditionally recognised major categories of the disease are based on the classification of the disease as open angle, closed angle or congenital. Open angle glaucoma, called such because of the open irido-corneal angle in the anterior chamber of the eye, is the most common of these and is estimated to affect approximately half of the 70 million people affected with glaucoma world-wide (Quigley, 1996). Closed angle glaucoma is more rare and usually a result of anatomical abnormalities. Congenital glaucoma is a pediatric form of the disease which is generally apparent in the first year of life but may manifest itself up to the age of 3 years (Sarfarazi, 1997). It is also known as buphthalmos, meaning ox eye, because of the appearance of the eye due to the increased IOPs which are due to the maldevelopment of the trabecular meshwork .

There are a number of developmental anomalies of which glaucoma is one of the symptoms. These anomalies generally show high penetrance but with variable expressivity. Iridogoniodysgenesis anomaly (IDGA) is an autosomal dominant disorder which presents with iris hypoplasia, goniodysgenesis and juvenile onset glaucoma. IDG syndrome (IGDS) is similar but also manifests somatic abnormalities, including dental and jaw anomalies. Reiger syndrome is another autosomal dominant disorder which is characterised by anomalies of the anterior chamber of the eye, which results in glaucoma in >50% of cases and a variety of other symptoms including dental hypoplasia and, in some cases, umbilical abnormalities. Glaucoma is also a feature of the pigment dispersion syndrome (Anderson *et al.*, 1997) and has been shown to co-segregate with nail patella syndrome (McIntosh *et al.*, 1987).

4.1.3 Primary open-angle glaucoma

The most frequently observed form of glaucoma, primary open-angle glaucoma (POAG) affects approximately 2% of the caucasian population over the age of forty-five (Raymond, 1997; Stone *et al.*, 1997). Characteristics of POAG include atrophy of the optic nerve as a result of degeneration of the retinal ganglion cells, resulting in the loss of visual field and a continual progression of symptoms. Losses in visual field are often

preceded and accompanied by elevated intraocular pressures; however, the trabecular meshwork is usually normal in appearance (Raymond, 1997; Sarfarazi, 1997). Medical treatment of the disease varies from patient to patient. For some, the administration of eyedrops is sufficient to keep the disease in check while others require surgery to relieve intraocular pressures.

POAG varies in its age of onset and has been classified into the late onset form, generally termed chronic open angle glaucoma (COAG), and the less frequently observed juvenile onset form (JOAG). The disease is generally classified as juvenile if the age of onset is before the age of 40 and chronic if onset is after 40 (Wiggs *et al.*, 1996). However, given that the age of onset varies in POAG families that carry the same causative mutation, this classification is somewhat arbitrary (Morrissette *et al.*, 1995; Dubois *et al.*, 1997). Also, the painless nature of the disease means that patients often remain unaware that they are affected for many years which further complicates this classification.

JOAG is inherited in an autosomal dominant fashion with high penetrance (Harris, 1995). The late age of onset means that the segregation pattern of COAG is not so clear but it is probably inherited in an autosomal dominant fashion with reduced penetrance (Stoilova *et al.*, 1996; Wirtz *et al.*, 1997). The symptoms in JOAG are generally more severe than those exhibited in COAG and patients frequently show substantial visual impairment. In general, early onset cases present with higher IOPs than later onset cases and interventive surgery is often required. In a study on five JOAG families linked to 1q, the average of the initially recorded intraocular pressures of the 23 affected individuals was 38.5 mm Hg. 83% of these patients needed surgery to prevent loss of vision (Wiggs *et al.*, 1995).

4.1.4 Genetic loci implicated in glaucoma

Genetic factors play a substantial role in the etiology of glaucoma; first degree relatives of patients with POAG have a much higher chance of developing glaucoma than other members of the population (Wolfs *et al.*, 1998). Families that show a hereditary predisposition to glaucoma, have been of immense value in the elucidation of the molecular pathology of this disease. Many large scale mapping projects have been carried out of late, in the hope of identifying genes involved in the causation of

glaucoma. Recently, several loci have been implicated in the aetiology of various forms of the disease.

It is important to note that more recently, the different forms of glaucoma are often referred to by the names of the loci they have been linked to. GLC 1, 2 and 3 refer to the open angle, closed angle and congenital subtypes of the disease respectively. The letters A, B, C, etc. refer to the loci a particular subtype has been linked to in order of identification of the loci (Raymond, 1997).

A locus for adult onset POAG on 2cen-q13 was described in 1996 and designated GLC1B (Stoilova *et al.*, 1996). Six families were found to show tight linkage to markers in an 11.2cM interval in this region of chromosome 2. Affected patients from these families showed similar clinical characteristics including moderate IOPs, onset of the disease in the late 40's and good responses to medical treatment. It has been suggested that this locus may be responsible for many cases of moderate tension COAG (Sarfarazi, 1997).

A second locus for COAG (GLC1C) has been identified at 3q21-24 in an American family segregating the disease (Wirtz *et al.*, 1997). The subjects in this family presented with moderate to high IOPs. More recently third, fourth and fifth loci for the adult onset form of the disease have been reported. The third locus (GLC1D) maps to a 6.3 cM region on 8q23 (Trifan *et al.*, 1998). The phenotype in the pedigree used in this study is variable but the IOPs were generally moderately elevated. The fourth locus (GLC1E) maps to 10p15-p14. This was localized in a large British family segregating normal tension open angle glaucoma. The fifth locus (GLC1F) has been mapped to 7q35-36 (Wirtz *et al.*, 1998). With five loci identified in the etiology of COAG to date it is clear that this form of the disease shows considerable genetic heterogeneity.

Congenital glaucoma is generally inherited in an autosomal recessive fashion. In a large study carried out on 17 families with primary congenital glaucoma, a locus for this subtype of glaucoma, known as GLC3A, was mapped to 2p21 (Sarfarazi *et al.*, 1995). This locus was refined to a 2.5 cM interval and the linkage was confirmed in other families of different ethnic backgrounds, suggesting that this was a major locus for the disease (Bejjani *et al.*, 1996). Mutations in the cytochrome P4501B1 gene have since been found to be responsible for cases of the disease that map to 2p21 (Stoilova *et al.*, 1997). This gene is expressed in many tissue types in the eye along with many non-ocular tissues.

Six out of the 17 families studied by Sarafarazi *et al.* (1995) did not show linkage to 2p21, thereby providing evidence that the disease is genetically heterogeneous. A second locus for the disease has been pinpointed on 1p36 (Akarsu *et al.*, 1996). Other families did not link to either the 2p or 1p loci and hence there must be at least one other locus for the condition.

There has been some success also in the mapping of some of the developmental anomalies of which glaucoma is a feature. Reigers syndrome has been shown to be caused by mutations in the REIG gene on 4q25, which encodes a homeobox transcription factor, solurshin (Semina *et al.*, 1996). A second locus for Reiger syndrome has also been localised to 13q14 (Phillips *et al.*, 1996). Interestingly, the REIG gene has also been shown to harbour mutations in patients with IDGS (Alward *et al.*, 1998). The involvement of a forkhead/winged helix gene on 6p25, FKHL7 which is also a transcription factor, has been proven in a spectrum of anomalies which involve the anterior chamber of the eye and are frequently associated with glaucoma. These disorders are IDGA, Reiger anomaly, Axenfield anomaly and iris hypoplasia (Nishimura *et al.*, 1998). It is possible that there is a second gene involved in anterior eye segment disorders on 6p25 as no mutations were identified in FKHL7 in two families with IDGA which are linked to the region (Mears *et al.*, 1998).

4.1.5 The GLC1A locus

Many studies have concentrated on the juvenile onset form of open angle glaucoma. The early age at which this disease can be diagnosed, together with the autosomal dominant pattern of inheritance, makes pedigrees segregating it amenable to linkage analysis. Linkage analysis in a large American family with autosomal dominant JOAG resulted in the identification of the first locus for the condition (named GLC1A) to a 23 cM interval on 1q21-31 (Johnson *et al.*, 1993; Sheffield *et al.*, 1993). The highest lod score was given by the marker D1S212 with a Z max of 6.5 at theta = 0. This linkage was subsequently confirmed in another large family also segregating JOAG and phenotypically similar to the original family (Richards *et al.*, 1994). Many reports of other families linked to 1q followed the initial linkage, which reduced the disease interval and indicated that the 1q locus plays a significant role in the juvenile onset form of open angle glaucoma (Wiggs *et al.* 1994; Meyer *et al.*, 1994; Graff *et al.*, 1995).

The GLC1A critical interval on 1q21-31 was narrowed to <5Mb following further analysis of the pedigree used in the original linkage study, along with another large JOAG pedigree (Sunden *et al.*, 1996). This study involved the construction of a YAC contig across the region in order to refine the mapping of the interval towards the identification of the disease gene. The generation of another contig spanning the region and the identification of recombinant haplotypes allowed the disease interval to be further refined to a 2.8 Mb interval at the cytogenetic 1q24 G-band (Belmouden *et al.*, 1997). This group excluded a number of genes which map to the region.

A large study on a multigenerational French Canadian family, segregating autosomal dominant POAG was carried out by Morissette *et al.* (1995). Among those 40 individuals carrying the disease haplotype were individuals showing a juvenile onset of the disease and also a smaller number who had not been diagnosed till after 40 years of age and hence were considered to have COAG. This observation led Morissette *et al.* to conclude that the GCL1A gene on 1q was responsible for both juvenile onset and adult onset POAG. Another unrelated POAG family linked to 1q, showing similarly variable ages of onset was also subsequently reported (Meyer *et al.*, 1996). It has been suggested however that the later onset of the disease in this family may be as a result of variable expressivity of the GLC1A gene and that the GLC1A gene will not necessarily prove to be responsible for a significant proportion of adult onset POAG cases (Wiggs *et al.*, 1996).

4.1.6 The TIGR/myocilin gene

Following the exclusion of a number of genes, the TIGR gene (Trabecular Meshwork Inducible Glucocorticoid Response protein), which maps to the critical disease interval on 1q, was found to harbour mutations in patients with POAG (Stone *et al.*, 1997). TIGR was initially isolated from a human trabecular meshwork cDNA library isolated from human trabecular meshwork cell cultures that had been exposed to dexamethasone (Polansky *et al.*, 1997). Given that the administration of glucocorticoids such as dexamethasone had previously been found to raise intraocular pressure (IOP), TIGR was a plausible candidate for a disease in which patients often display obstructed aqueous humor outflow and elevated intraocular pressures (Polansky *et al.*, 1997). This protein is expressed in the trabecular meshwork, ciliary body and sclera of the eye

(Adam *et al.*, 1997). It has also been shown to be expressed in various non-ocular tissues including the heart, skeletal muscle, the cilia of the neuroepithelium and the cochlea (Kubota *et al.*, 1997). Its high level of expression in the ciliary body, which is responsible for the production of aqueous humour and the trabecular meshwork cells, the site of resorption of aqueous humour, is consistent with the widely held belief that the obstruction of aqueous humour by the TIGR protein is responsible for the increased IOPs observed in patients (Adam *et al.*, 1997).

The TIGR gene has been shown to be identical to an independently identified myosin like protein named myocilin (Kubota *et al.*, 1997; Adam *et al.*, 1997). Myocilin was identified from a retina-specific cDNA library and was found to be expressed in the inter-connecting cilia of photoreceptor cells. (Note: Prior usage of the acronym TIGR led to the suggestion that the gene be referred to as myocilin and/or GLC1A. Henceforth the gene is referred to as myocilin in this text).

Myocilin is encoded by a gene with three exons and two introns and is 504 amino acids in length (Polansky *et al.*, 1997). Putative structural features include various specific promoter motifs thought to be involved in the control of expression, a signal sequence for secretion, putative sites thought to be involved in cell-cell and glycoprotein interactions, an N-terminus hydrophobic region, a myosin-like domain, a leucine zipper probably involved in homodimerization, and a C-terminal olfactomedin-like domain (Polansky *et al.*, 1997).

4.1.7 The involvement of myocilin in POAG

The first screening of the myocilin gene identified POAG patients harbouring tyr430his, gly357val and glu361stop mutations. Subsequent research has resulted in the identification of a large number of additional mutations in families with both JOAG and COAG, suggesting that the gene plays a significant role in the etiology of all forms of POAG (Adam *et al.*, 1997; Fingert *et al.*, 1997; Stoilova *et al.*, 1997; Mansergh *et al.*, 1998; Michels-Rautenstrauss, 1998; Richards *et al.*, 1998). In a particularly interesting case, one branch of a family segregating POAG had a number of individuals homozygote for a lys423glu TIGR mutation (Raymond *et al.*, 1997). These homozygotes did not develop the disease while their heterozygote siblings did. The authors postulated that this "protective effect" was due to a dominant negative mutation

which results in defective heteromultimeric proteins but functional homomultimeric proteins.

Significantly, all of the myocilin mutations reported to date are confined to exon III of the myocilin gene and many are clustered in predicted functional motifs in the olfactomedin-like domain (Roza FW *et al.*, 1998). It has been suggested that mutations in this region may interfere with the metabolism or uptake of the myocilin protein which could lead to its accumulation and hence obstruction of the flow of aqueous humour (Sarfarazi, 1997).

4.1.8 Family TCD-POAG1

TCD-POAG1 is a large multi-generational Spanish family, segregating autosomal dominant JOAG (Figure 4.1). They show the typical features of JOAG with IOPs often above 30mM Hg and sometimes over 40mM Hg. Medically uncontrolled, raised intraocular pressures and continuing loss of visual field have necessitated drainage operations in many of the patients, usually within the third and fourth decades. Linkage analysis carried out in this family by Dr. Fiona Mansergh had previously revealed that this family was linked to the GLC1A locus on chromosome 1 (Mansergh, 1997). The microsatellite marker D1S242 had given a maximum lod score of 5.478 at 0% recombination. Multi-point analysis gave a Z_{max} of just over 6 in the interval flanked by the markers D1S2658 and D1S2659.

4.1.9 The aim of the study

The aim of this study was to identify the disease causing mutation in family TCD-POAG1. Reports of the involvement of the myocilin gene in the aetiology of glaucoma prompted the screening of this gene for mutations within the family. A novel Asp380Ala base change within the myocilin gene is reported here along with evidence that it is causative of the disease in family TCD-POAG1.

4.2 MATERIALS AND METHODS

PCR, SSCP, automated and direct sequencing were carried out according to the methods detailed in Chapter 1. For primer sequences see Appendix B.10.

4.2.1 Patient diagnosis

TCD-POAG1 is a large multi-generational pedigree segregating JOAG (Figure 4.1). All family members from whom DNA samples were available were clinically assessed by Dr. Carmen Ayuso at the Fundacion Jimenez Diaz in Madrid, Spain. Initial diagnosis of affected individuals was made, in most case, on the basis of raised IOPs, which were often above 30mm Hg and sometimes above 40mM Hg (the upper limit of normal IOP is 21mm Hg). Clinical assessment consisted of best corrected near and distance visual acuity and perimetry using either a Goldmann bowl perimeter or an automated perimeter, special attention being directed to any possible nasal step or Bjerrum area defects. Intraocular pressures were measured using Goldmann applanation tonometry. This was followed by detailed fundoscopic examination, with particular attention being paid to the condition of the optic disks, including assessment of the cup to disk ratio, disk asymmetry, displacement of disk blood vessels, the health of the neuroretinal rim and any evidence of localized nerve fibre bundle atrophy. In all individuals, the drainage angle was assessed using a Goldmann triple mirror. Angle structures were identified, the width of the angle through 360 degrees was assessed and any potential cause for secondary glaucoma was sought.

4.2.2 DNA extraction

Extraction of DNA from pelleted blood lymphocytes was carried out using standard methods by Dr. Carmen Ayuso and Dr. Paul Kenna (Mansergh, 1997).

4.2.3 PCR digestion

An aliquot of each PCR product was digested with 20 units of *Sly I* (NE Biolabs) at 37°C overnight with the buffer supplied by the manufacturers. Samples were analysed on 2.5% ethidium bromide stained agarose gels.

4.3 RESULTS AND DISCUSSION

4.3.1 Screening of the myocilin gene in family TCD-POAG1

Family TCD-POAG1 had previously been found to show linkage to the GLC1A locus on chromosome 1. The reported involvement of the myocilin gene, which maps to this region of chromosome 1, in the etiology of glaucoma prompted the screening of the coding regions of the gene in members of this family. Four individuals from the family were selected for screening of the myocilin gene. Individuals IV-5 and IV-13 are both affected with JOAG. Individual V-12 is a family member who has been diagnosed as unaffected and individual IV-4 is an unaffected spouse of a family member. Direct sequencing of exon 3 of the myocilin gene using primers (Appendix B.10) designed in the intron sequence flanking the exon, revealed an A to C transition in codon 380 (Figure 4.3). This base change results in the substitution of an alanine for an aspartic acid and was not present in the unaffected individuals. The reverse strand was also sequenced in all four individuals and the base change was once again apparent only in affected individuals.

4.3.2 Screening of all family members and control individuals for the Asp380Ala mutation

The substitution created a *Sty I* restriction site which permitted rapid screening of all 32 individuals of the family for whom DNA was available (Figure 4.4). This confirmed that the mutation segregated with the JOAG phenotype. 60 CEPH individuals were used as controls and screened for the Asp380Ala mutation using the *Sty I* assay. This restriction site was not present in any of the 60 control individuals i.e. 120 chromosomes. Therefore these data suggest that the Asp380Ala amino acid change is causative of JOAG in this pedigree.

4.3.3 Anomalies in diagnostic status

The inheritance of JOAG has previously been described as autosomal dominant with reduced penetrance (Raymond, 1997 & Sarfarazi, 1997). There are no cases within this pedigree of persons who have inherited the disease mutation and who do not have glaucoma. However, four family members were initially diagnosed as affected and have since been found not to carry the Asp380Ala mutation. These individuals were screened for the mutation using both direct sequencing and the *Sty 1* assay. Subject V-30 was diagnosed with high IOP and glaucomatous field changes at 18 and has been operated on to control the progression of disease. However, she has subsequently been found to have closed angle glaucoma (Carmen Ayuso, personal communication). Subject V-8 was diagnosed as affected on the basis of mild visual field defects; however, her IOP was normal. Subject V-19 was diagnosed as affected on the basis of high IOP and asymmetric cupping of the optic disks. Subject IV-10 was diagnosed at the age of 47 (later than is usual for the rest of the family) with high IOP and diffuse reduction of sensitivity in the visual fields. With the exception of V-30, (whose glaucoma is of a demonstrably different cause to that which runs through the rest of the family), the remaining three anomalous individuals have mild symptoms of glaucoma and were therefore classified as "unknown" for the purposes of linkage analysis. Given that younger members of the family are considered as being at very high risk of developing glaucoma, intense medical scrutiny could have resulted in the misdiagnosis of some of these people as affected on marginal grounds. Alternatively, these people could be affected with POAG of a different cause to that which is a result of the Asp380Ala mutation. Later onset POAG affects approximately 2% of the over 45's in Caucasian populations (Raymond, 1997). Given the mildness and later onset of symptoms observed in IV-10, V-8 and V-19, it is entirely possible that they represent phenocopies of the more severe form of POAG noted in family members that do carry the Asp380Ala amino acid change.

4.3.4 The effects of the Asp380Ala mutation at the molecular level

The fact that this substitution results in the replacement of an acidic and hydrophilic amino acid by a neutral and hydrophobic one is further evidence that the Asp380Ala

mutation may disrupt the secondary structure of myocilin to pathogenic effect. Further evidence to this effect involves comparisons between myocilin and three related proteins from the bullfrog, rat and *C. elegans*; OLF, NORP and F11C3.2. This amino acid sequence alignment shows that the aspartic acid residue at position 380 of myocilin is conserved in all four proteins (Adam *et al.*, 1997).

Other mutations in myocilin have been implicated in both JOAG and adult onset POAG (Stone *et al.*, 1997; Adam *et al.*, 1997; Fingert *et al.*, 1997; Stoilova *et al.*, 1997; Mansergh *et al.*, 1998; Michels-Rautenstrauss, 1998; Richards *et al.*, 1998). So far, these appear to be confined to exon 3 as is the present mutation. Exon 3 encodes the olfactomedin-like C-terminal domain. Homozygotes with a Lys423Glu mutation in myocilin have been shown to be phenotypically normal (Raymond *et al.*, 1997). Given that myocilin is thought to form homodimers *in vivo*, (Sarfarazi *et al.*, 1997; Raymond *et al.*, 1997; Polansky *et al.*, 1997) a mechanism of homo-allelic complementation was proposed in which homodimeric normal or mutant protein molecules were functional, while heterodimers were not (Raymond *et al.*, 1997). Perhaps most of the exon 3 myocilin mutations act by introducing an asymmetry to heterodimeric molecules that disrupts their normal function. It will be interesting to see if these findings are repeated with any of the other myocilin mutations.

Myocilin has been found to be implicated in a substantial proportion of JOAG and a smaller portion of COAG cases. The clustering of all pathogenic mutations identified to date in the third exon of the gene may simplify the screening of at risk individuals. This would aid early diagnosis of patients with the disease with the result that IOPs can be controlled and damage to the optic neurons minimised.

4.4 CONCLUSION

Family TCD-POAG1 had previously been shown to be linked to 1q21-31 and following reports of the involvement of the myocilin gene in cases of glaucoma mapping to this interval, the coding regions of the gene were screened in this family. This study presents evidence that the Asp380Ala amino acid change is causative of JOAG in Family TCD-POAG1. This amino acid change is only present in family members with JOAG and is not present in unaffected family members. In addition, the Asp380Ala mutation is not present in 60 controls from the general population. Further understanding of the biochemistry and functions of myocilin will hopefully lead to the development of improved medication for glaucoma and possibly to the identification of further genes involved in its pathogenesis.

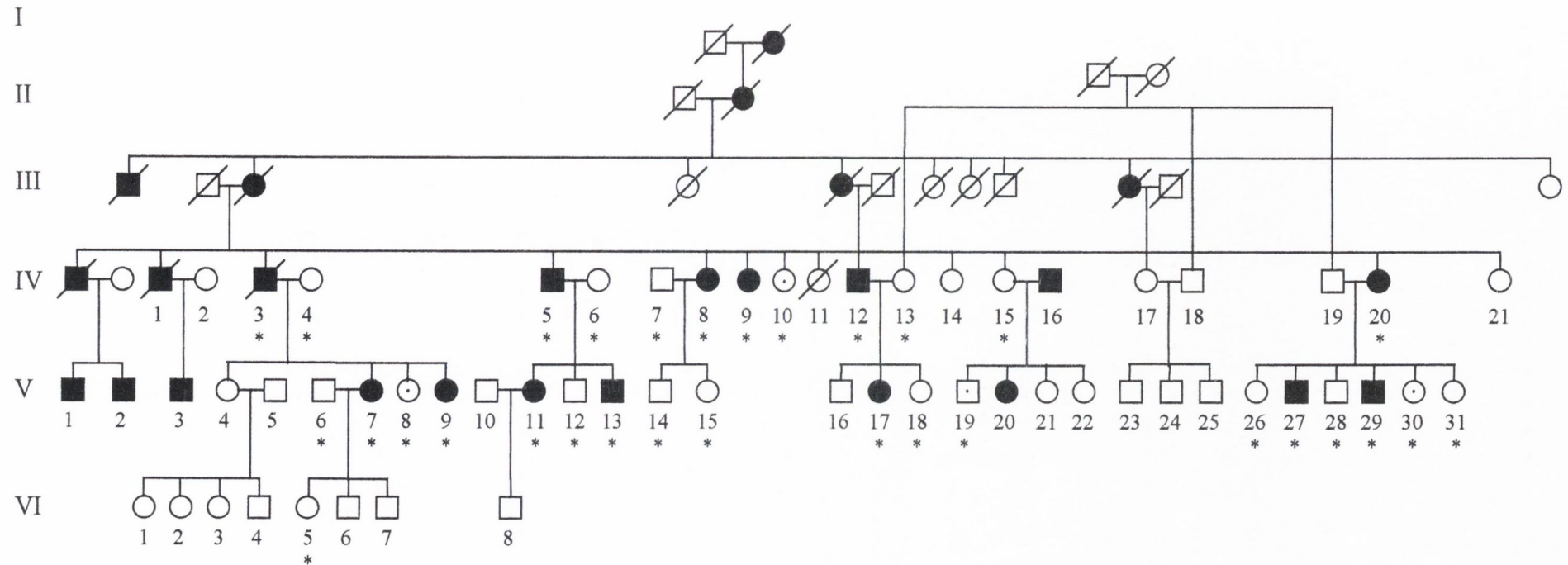


Figure 4.1 Family TCD-POAG1 pedigree. Subjects used in analysis are marked with asterisk. Those whose diagnostic status was uncertain are marked with a small dot in the middle of the circle or square.

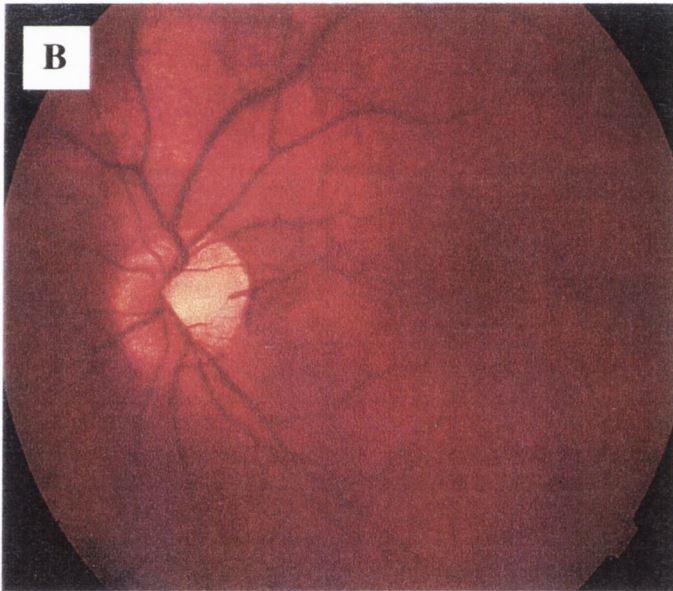
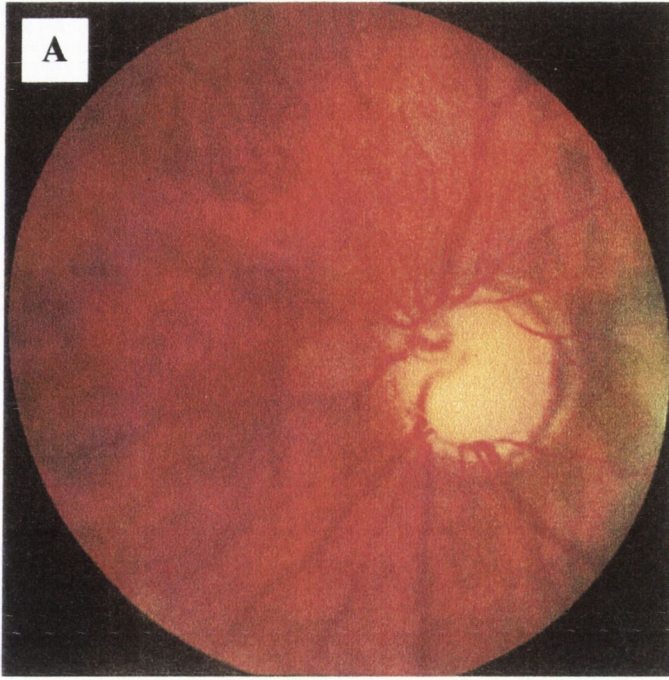


Figure 4.2 Fundus photograph of a TCD-POAG1 individual (A) shown alongside the retina of a healthy individual (B). Note the pallor and cupping of the optic disc in the glaucoma retina and the resulting displacement of the blood vessels (they disappear into the optic disc).

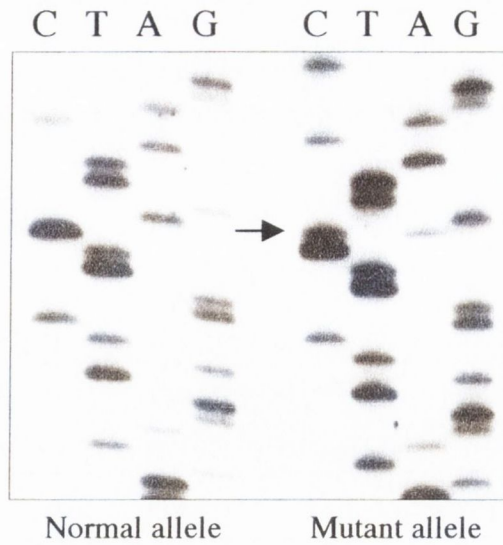


Figure 4.3 Partial nucleotide sequence from a genomic PCR amplification product of exon 3 of the myocilin gene showing a heterozygous C to A substitution. Reverse sequence for both normal and affected subjects is shown.



Figure 4.4 *Sty I* digestion of genomic 197bp PCR amplification product of exon 3 of the myocilin gene. The gel shows a small family group within TCD-POAG1 with two affected subjects, IV-12 and V-17 and two unaffected subjects, IV-13 and V-18. Digestion of the disease allele yields fragments of 143 bp and 54 bp in length while the unaffected allele remains uncut. Lane 1 contains the molecular weight marker Puc 19 cut with *MspI*. Note: the 54 bp fragment is difficult to visualise.

CHAPTER 5

RETINITIS PIGMENTOSA AND PROGRESSIVE SENSORINEURAL HEARING LOSS CAUSED BY A C12258A MUTATION IN THE MITOCHONDRIAL MTTS2 GENE.

5.1 INTRODUCTION

5.1.1 Introduction

Usher syndrome refers to a group of diseases which involve both progressive RP and sensorineural deafness. Family ZMK are a large Irish kindred segregating a disease very similar to Usher syndrome. Previous linkage studies tentatively identified a putative disease locus on chromosome 9q. Subsequent data however, excluded this locus and no other significant linkages were identified within the genome. Because of this and also because of similarities between the disease segregating in this family and documented mitochondrial disorders, the possibility of mitochondrial inheritance was considered. The aim of this study therefore, was to screen the mitochondria for a disease-causing mutation and upon identification of a sequence variant, to confirm its pathogenicity. A number of Usher syndrome patients were also screened for this mutation.

A clinical description of Usher syndrome and the background to the long-running study to identify the ZMK disease gene are presented. An overview of the mitochondrion and its role in disease, particularly diseases involving RP and/or sensorineural deafness, is also given. In the results section the identification of a mitochondrial mutation in family ZMK is reported. The significance of this mutation is discussed at length and its absence in 19 Usher syndrome patients reported.

5.1.2 Usher syndrome

Usher syndrome refers to a heterogeneous group of disorders that manifest sensory impairments of both the inner ear and retina. It is the most frequent cause of deaf-blindness in humans and believed to affect 4.4 people per 100,000 in the United States (Boughman *et al.*, 1983). Usher syndrome, which was named after the British ophthalmologist Charles Usher, is inherited in an autosomal recessive fashion. It is characterized by progressive RP along with varying severities of congenital sensorineural deafness and frequently, vestibular deformities. The disease is clinically heterogeneous and has been divided into three subtypes on the basis of severity and

onset of symptoms, the presence or absence of balance defects and whether the hearing loss is congenital or progressive.

Type I Usher syndrome is the most common and most severe of the subtypes. Hearing loss is congenital and severe to profound. Vestibular function is lacking and the onset of progressive RP is prepubertal. This form of the disease is frequent in the Acadian population of Louisiana (Boughman *et al.*, 1983). Type II Usher syndrome shows congenital deafness, which is moderate to severe with normal vestibular function. Onset of RP is generally during adolescence or early adulthood. Type III is the rarest of the subtypes and shows progressive deafness. The onset of retinal degeneration occurs at puberty or later. Cases of type III Usher syndrome are particularly frequent in the Finnish population (Sankila *et al.*, 1995).

Usher syndrome is not only clinically heterogeneous but also genetically heterogeneous. The first Usher locus to be identified was one for Usher syndrome type I (USH1) on 14q (Kaplan *et al.*, 1992c). Further loci for this form of the disease have since been identified on 11p (Kimberling *et al.*, 1992), 11q (Smith *et al.*, 1992), 10q (Wayne *et al.*, 1996) and 21q21 (Chaib *et al.*, 1997).

The gene on chromosome 11q13.5 (designated USH1B) has been identified as myosin VIIA (Weil *et al.*, 1995). This is an unconventional myosin, which is expressed in tissues involved in Usher syndrome including the cochlear and vestibular neuroepithelia, the retinal photoreceptors and the RPE (Weil *et al.*, 1996). The unconventional myosins are motor molecules. They have structurally conserved heads which use actin-activated ATPase activity to move along actin filaments. Their tails are highly divergent and bind to different macromolecules which they then move relative to the actin filaments (Weil *et al.*, 1995). Within the inner ear the myosin VIIA protein is located in the hair cell kinocilium (Liu *et al.*, 1997). In the photoreceptors myosin VIIA is believed to play a key role in the transportation of molecules between the inner and outer segments of the cell (Liu *et al.*, 1997). Defective cilia between the inner and outer segments of the photoreceptors have in fact been observed in some USH1B patients (Weil *et al.*, 1995)

Loci for the type II subtype of the disease have been localized to 1q14 (Kimberling *et al.*, 1990) and 5q (Kimberling, personal communication). The gene on chromosome 1q14 has been identified as a member of the nuclear receptor superfamily and is termed the USH2A gene (Eudy *et al.*, 1998). A locus for Usher syndrome type III has also been identified and maps to chromosome 3q21-25 (Sankila *et al.*, 1995).

5.1.3 Family ZMK

Family ZMK is a previously described, large Irish pedigree segregating progressive RP along with progressive sensorineural deafness (Kumar-Singh *et al.*, 1993b; Kenna *et al.*, 1997) (Figure 5.1). The symptoms of the disease in this family are similar to type III Usher syndrome. Unlike Usher Syndrome type III, however, the pattern of inheritance of the disease is not consistent with autosomal recessive transmission. Upon observation of the family pedigree it could appear that the inheritance pattern is autosomal dominant. The conclusion that the disease is transmitted in an X-linked dominant pattern could also be arrived upon the observation that there are no recorded cases of male to male transmission in the pedigree. This is unlikely however as it is a rare phenomenon and the lack of male to male transmission is to a large part due to the fact that the men in the family have not had children. Significant exclusion of the X chromosome using microsatellite markers also discounted this possibility (Kenna *et al.*, 1997) The pattern of transmission of the disease through the generations is also consistent with maternal inheritance (i.e. mitochondrial inheritance).

This family makes an unusual case as the symptoms and age of onset of the disease is extremely variable from individual to individual (Kenna *et al.*, 1997). Certain family members have perfect hearing while others are profoundly deaf. There is a similar range of visual capabilities in the family with some individuals suffering only from mild night vision problems late in life while others are legally blind by the age of 20 (Kenna *et al.*, 1997). Even in small family groups within the larger pedigree the age of onset and the severity of the symptoms are often not consistent between the various affected individuals.

Most individuals become aware of mild symptoms in their thirties which become progressively worse with age (Kenna *et al.*, 1997). The reduced amplitude of rod and cone photoreceptor responses recorded by electroretinograms (ERGs) however, reveal the onset of retinal degeneration before this. Generally the ERG responses are completely extinguished by the sixth decade (Kumar-Singh, *et al.*, 1993b). Fundoscopy reveals the classic RP symptoms in affected individuals, with bone spicule pigmentary deposits, waxy pallor of the optic disc and attenuation of blood vessels being apparent (Kenna *et al.*, 1997). Audiometric analysis of certain patients reveals moderate to severe sensorineural deafness with impairment being particular evident at middle range frequencies. There is also evidence of recruitment, which is a physical discomfort and

distortion and as a result of loud noises and evidence of persistent tinnitus (Kenna *et al.*, 1997). In addition to the problems of sight and hearing two members of the family are also mentally impaired.

5.1.4 The search for the ZMK disease gene

In an attempt to identify the disease causing mutation in this pedigree, linkage studies were performed on DNAs from 29 family members and 5 unaffected individuals married to members of the family. Loci previously shown to be involved in Usher syndrome, RP and some in sensorineural deafness were firstly excluded (Kumar-Singh *et al.*, 1993a; 1993b). Following this a genome wide screen for the mutation was carried out (Kenna *et al.*, 1997). This extensive study excluded 90-95% of the genome and led to the identification of a putative linkage on the distal end of chromosome 9q (Kenna *et al.*, 1997; Mansergh *et al.*, 1999). Lod scores of marginally greater than 3 were obtained with markers D9S118, D9S121 and ASS. None of the available markers mapped at zero recombination in respect to the disease gene however and since then there has been various evidence to suggest that this is not a true linkage (Mansergh *et al.*, 1999; Mansergh, 1997). The critical markers on 9q had not been mapped in relation to Genethon markers at the time of the first indication of linkage. This was carried out and revealed that they were interspersed with the markers which showed lower lod scores and recombinations with respect to the disease locus (Mansergh *et al.*, 1999). Having mapped all markers in relation to each other, multipoint analyses were carried out and these results excluded the disease gene from this region of the genome (Mansergh *et al.*, 1999).

Haplotype analysis also excluded the region as the affected individuals do not all carry the same haplotype across the area (Mansergh *et al.*, 1999). Also, the disease status of one affected individual has since changed from unaffected to affected. Individual III-5, who was originally classified as unaffected, has since been shown to have an affected granddaughter (Professor Carr, New York, personal communication). Individual III-5, while appearing unimpaired into her 70's, was bed ridden and therefore unable to undergo ERG and audiometry studies. Such studies may have revealed signs of the disease but alternatively she may be a case of reduced penetrance of the disease. Exclusion of III-5 from the linkage analysis reduces the lod scores to just less than 3,

which is considered the significance threshold for linkage (Mansergh, 1997). Linkage analysis using the 9q markers was subsequently performed with affected individuals only and again excluded the region (Mansergh, 1997).

With the exclusion of 9q it became necessary to rethink the possibilities for the location of the ZMK disease gene. There were a number of small gaps in the genome which had not been excluded but it was deemed unlikely that the mutation would reside in any of these, given the low lod scores in the surrounding regions (Mansergh, 1997). There also remained the possibility that the gene was located in a number of regions, which had shown slightly positive lod scores. These regions had been further analyzed and excluded (Mansergh, 1997). If reduced penetrance was playing a role in the expression of the disease however (as the case of III-5 indicated possible), these exclusions may have been erroneous. This possibility was largely precluded by performing the linkage analysis using affected individuals only (Mansergh, 1997). The possibility of a large-scale chromosomal abnormality was also abolished following high resolution karyotyping (Kenna *et al.*, 1997).

Another possibility for the location of the gene also existed - the mitochondrion. A number of features of the disease in this family were indicative of cytoplasmic inheritance of the disease. These included the fact that all females who have had children have passed the disease on to the next generation, the nature of the hearing problems (which are similar to those found in a number of mitochondrial disorders) and the abnormally high mitochondrial count observed in muscle tissue following a biopsy from one of the ZMK family (see results and discussion).

5.1.5 The mitochondria

The mitochondria are organelles that are present in large numbers in the cell cytosol and fulfill most of the cell's energy requirements. There is much evidence to indicate that they are descendants of a eubacterial ancestor, closely related to the alpha-proteobacteria, which formed an endosymbiotic relationship with an ancestor of extant eukaryotes. Recent data, derived from sequencing of protist mitochondrial genomes, suggests that the mitochondrion had a monophyletic origin and possibly originated at a time close in evolutionary history to the arrival of the nuclear component of eukaryotic cells (Gray *et al.*, 1999). The human mitochondrion still retains vestiges of its bacterial

ancestors. It has retained an inner and an outer cell membrane, circular genome and mitochondrial specific transcriptional and translational machinery.

The mitochondria generate the cells energy requirements by a process of oxidative phosphorylation (OXPHOS). The protein complexes responsible for OXPHOS are located in the inner cell membrane of the mitochondria. These include components of the electron transport chain (ETC), the ATP synthase and the adenine nucleotide translocator (ANT). The ETC is composed of a total of 90 different proteins which are the subunits of the five ETC enzyme complexes (complexes I-V), (Sudbery, 1998). Electrons, generated from hydrogen following the oxidation of carbohydrates and fats, are passed along the series of complexes of the ETC and ultimately transferred to molecular oxygen to give H₂O. Energy is released from this transfer of electrons and used to pump protons out of the mitochondrial inner membrane. This results in an electrochemical gradient that is harnessed to enable the ATP synthase to synthesize the cells energy carrier, adenosine 5'-triphosphate (ATP). This ATP is then transported to the cytosol by the ANT, where it is exchanged for a molecule of adenosine 5'-diphosphate (ADP), (Wallace, 1999 and Saraste, 1999).

There are hundreds of mitochondria per cell and within each of these several copies of the mitochondrial genome (Wallace, 1999). The human mitochondrial genome is 16569 base pairs in length (Wallace *et al.*, 1995). It has retained 16 genes encoding proteins of the OXPHOS pathway, 12S and 16S mitochondrial ribosomal RNAs (rRNAs) and 22 tRNA genes which are sufficient for the translation of all mitochondrial codons (Gray, 1999). The other essential proteins for mitochondrial function are encoded by the nuclear genome where it is believed they were transferred to from the ancestral mitochondrial genome (Schatz, 1996). There are very few redundant bases in mitochondrial DNA (mtDNA). There are no introns or leader and trailer sequences in-between coding regions and there are genes encoded on both of the DNA strands (Weaver and Hedrick, 1981). There is an asymmetric distribution of G's and C's on each of the strands which gives rise to what are termed the heavy and light strands. RNA transcription proceeds around the mitochondrial genome in both directions from the control region (Wallace *et al.*, 1995).

5.1.6 Mitochondrial mutations

Defects in the mitochondria play a role in a wide variety of degenerative diseases. Mitochondrial DNA abnormalities can be classified as either base substitutions or DNA rearrangements. If the mutation is within one of the 13 protein coding genes it will result in a specific defect in the OXPHOS pathway, whereas mutations within one or more of the RNA genes will have a global effect on mitochondrial protein synthesis. The end result in both cases is a reduction in the efficiency of energy production (Wallace, 1999). A mutation in a nuclear gene, the protein of which is required for mitochondrial function will have a similar effect (Wallace, 1999).

Mitochondrial mutations affecting the OXPHOS pathway may simply cause a reduction in energy output or alternatively they may bring about pathogenic effects by preventing the detoxification of reactive oxygen species (ROS). A blockage in OXPHOS can result in a build-up of ROS which can cause oxidative damage within the cell and are mutagenic to cellular DNA (Sudbery, 1998). The mitochondria have also been shown to play a key role in the induction of apoptosis and defects in the functions of the mitochondria can activate the apoptosis control factors and initiate cell death. All these factors interact to bring about the disease pathology (Wallace, 1999).

Mitochondrial DNA is strictly maternally inherited. The mitochondria are transmitted to the offspring via the cytoplasm of the oocyte at fertilization. The sperm mitochondria, of which there are a much smaller number, appear to be selectively eliminated (DiMauro *et al.*, 1998). It would therefore be expected that if a mother has a mitochondrial disease it would be expressed by all of her progeny. The inheritance of mitochondrial diseases is complicated however, by a phenomenon known as heteroplasmy. If a mutation occurs in a particular mitochondrion, while it may be replicated, it will only be present in a subset of the mitochondria of the cell. The cell is therefore said to be heteroplasmic, containing a mixture of mutant and wildtype DNAs. During cell division the daughter cells will acquire a random ratio of wildtype to mutant mtDNAs. A particular cell lineage can drift therefore, to either all mutant or all wildtype mtDNAs (homoplasmy). This trend is known as replicative segregation (Wallace, 1999).

Replicative segregation also occurs during oogenesis with the result that different offspring will inherit varying amounts of mutant mtDNAs. Large variances in heteroplasmy have been recorded over single generations, an effect that has been

postulated to be due to a reduction in the number of mitochondria in the oocyte. This would result in a population bottleneck that could reduce the genetic diversity of the mitochondria (Grossman *et al.*, 1990). The effect of heteroplasmy on a particular individual is therefore such that they inherit a random sample of mutant mtDNAs from their mother and over their lifetime the mutant population may drift to heteroplasmy or homoplasmy in a particular tissue type.

As the number of mutant mtDNAs within a particular cell type increase, the efficiency of the energy generating OXPHOS pathway declines. At some point the energy capacity of the cell falls below the bioenergetic threshold, which is the minimum energy level required by the cell to function in a normal manner, and at this point the disease symptoms are manifested (Shoffner and Wallace, 1995). The particular expression pattern of a mitochondrial disease is not only influenced by the severity of the mutation and the degree of heteroplasmy but also by the fact that different tissues have different energy requirements and therefore will be affected to a greater or lesser extent by a reduction in energy outputs. The human tissue with the highest energy demands is neural tissue, followed by muscle, renal, endocrine and liver tissue, in decreasing order (Shoffner *et al.*, 1990).

Another factor, which has influence on the expression of a mitochondrial disease, is age. Mitochondrial diseases often show delayed onset and a progressive course. There is evidence to indicate that this is due to the accumulation of somatic mitochondrial mutations over time which act in concert with the predisposing mutation (Melov *et al.*, 1997). These somatic mutations are hypothesised to be caused by oxidative damage by ROS from the ETC and not only play a role in disease pathology but also in the aging process (Wallace, 1999).

The interplay of the above-mentioned influences on the phenotypic expression of a mitochondrial disease, help to explain the large variations in expressivity within pedigrees segregating a mitochondrial disease. It also means that particular mutations often give different phenotypes and different mutations can also result in similar diseases.

5.1.7 Mitochondrial diseases involving RP and/or sensorineural deafness

There are many previously reported mitochondrial diseases that have either or both sensorineural deafness and retinopathies as a feature. One such disease is Leber hereditary optic neuropathy (LHON), characterised by mid-life central vision loss, which is acute or subacute and leads to central scotoma and blindness. LHON may or may not be associated with a variety of other clinical features which include neurological problems, cardiac abnormalities and dystonia (Sudbery, 1998). To date at least 18 mutations, all in the genes encoding the complexes of the OXPHOS pathway have been shown to be involved in the causation of LHON (Wallace *et al.*, 1995). These mutations either act autonomously or interact with each other to bring about the disease (Wallace *et al.*, 1995). LHON mutations have been divided into primary mutations and secondary mutations. Primary mutations, if present, are likely to bring about blindness and secondary mutations generally act in concert with a primary mutation and are thought to increase the likelihood of clinical expression of the disease (Wallace *et al.*, 1995). The three primary mutations most frequently recorded are MTDN4*LHON11778A, MTDN1*LHON3460A and MTDN6*LHON14484A, all of which cause amino acid changes in the NADH dehydrogenase genes (Riordan and Harding, 1995). These 3 mutations are believed to be involved in at least 90% of all LHON cases (Brown *et al.*, 1997). The other primary mutation, the MTND6*LDYT14459A mutation, causes the most severe clinical manifestations but is less frequently encountered (Jun *et al.*, 1994 and Shoffner *et al.*, 1995).

LHON is a particularly complex disease in terms of its expressivity. As previously mentioned, secondary mutations are thought to predispose towards expression of the disease. The possibility that the presence of specific LHON mutations on a mitochondrial haplotype J predisposes to higher penetrance and more severe symptoms has also been suggested (Torrioni *et al.*, 1997). Various environmental factors including smoking (Cullom *et al.*, 1993) have also been postulated to have an influence on the expression of the disease. Another point of interest is the evidence that indicates that there is a male bias in Caucasian expression of the disease (Newman *et al.*, 1991). The reason for this remains elusive although there has been a single report of the involvement of an X-linked recessive allele (Bu and Rotter, 1991).

Neuropathy, ataxia and retinitis pigmentosa (NARP) have been associated with a T-G transversion at mitochondrial position 8993 in another gene of the OXPHOS pathway,

the mitochondrial ATPase 6 gene (Holt *et al.*, 1990). This gene encodes a key component of the mitochondrial proton channel and a defect in it may interfere with proton translocation across the membrane (Trounce *et al.*, 1994). There is a definite correlation, with this mutation, between the severity of clinical symptoms and the level of mutant mitochondria the patient possesses. Children who inherit very high levels of this mutation develop a severe and often lethal disease associated with basal ganglion degeneration, known as Leigh syndrome (Tatuch *et al.*, 1992).

A large and complex array of symptoms are observed in diseases caused by mutations in the mitochondrial protein synthesis genes. Many feature sensorineural deafness along with other defects of the central nervous system, including stroke-like episodes, epilepsy and progressive dementia. Mitochondrial myopathy with ragged-red fibres (mitochondrial encephalomyopathy) is also frequently observed, as well as cardiomyopathy, lactic acidosis and diabetes mellitus (Wallace, 1999).

A homoplasmic mutation in the mitochondrial 12s rRNA gene, MTRNR1*DEAF1555G, has been associated with both non-syndromic and aminoglycoside induced deafness (Prezant *et al.*, 1993). The aminoglycosides are antibiotics that are used in medicine to target the bacterial ribosome. The evolutionary relationship between bacteria and the human mitochondrion can explain the fact that a one base pair difference in the sequence of the mitochondrial rRNA gene can make it a target for the antibiotic which results in irreversible hearing loss (Prezant *et al.*, 1993). A nuclear involvement in the non-syndromic form of the disease has also been predicted (Guan *et al.*, 1996).

The MTTTL1*MELAS3243G mutation, in one of the tRNA leu genes, gives rise to mitochondrial encephalomyopathy, lactic acidosis and stroke-like episodes (MELAS) when inherited at a high percentage of overall mtDNA (Goto *et al.*, 1990). When inherited at a lower percentage however, it causes non-insulin dependant diabetes mellitus (NIDDM) which is frequently associated with deafness (van den Ouweland *et al.*, 1992). A pigmentary retinal degeneration has also been reported in association with this mutation (Schulz *et al.*, 1993). Another of the heterogeneous spectrum of diseases caused by mutations in this tRNA leu gene includes encephalomyopathy, pigmentary retinopathy, dementia, hypoparathyroidism and diabetes mellitus as symptoms. This is caused by a T-C mutation at position 3252 (Morten *et al.*, 1993).

An A to G nucleotide transition at position 7445, in the mitochondrial serine gene, MTTS1, gives rise to a progressive, maternally inherited form of sensorineural

hearing loss (Reid *et al.*, 1994). Hearing loss can also result from a heteroplasmic insertion, resulting in an extra cytosine, at position 7472 of the MTTT1 gene. The clinical severity of the disease correlates with the degree of heteroplasmy. Along with deafness, the symptoms observed in patients with this mutation include ataxia and myoclonus (Tiranti *et al.*, 1995).

A number of mutations within the mitochondrial tRNA lys gene (MTTK) have been documented which give a variety of phenotypes including myoclonic epilepsy and ragged-red fibre syndrome (MERRF) (Shoffner *et al.*, 1990), cardiomyopathy with deafness (Santorelli *et al.*, 1996) and diabetes mellitus-deafness syndrome (Kameoka *et al.*, 1998). Within this group is perhaps the best studied of all the mitochondrial tRNA mutants. This is the MTTK*MERRF8344 mutation (Shoffner *et al.*, 1990).

Pathogenic rearrangements of the mitochondrial DNA generally result in one of four interrelated phenotypes: Kearns-Sayre syndrome (KSS), Pearson marrow/pancreas syndrome, maternally inherited diabetes and deafness and chronic progressive external ophthalmoplegia (CPEO), (Wallace *et al.*, 1999). It has been suggested that the four diseases represent a continuum of phenotypic expression, with the symptoms expressed depending on the severity of the DNA rearrangement and the tissue distribution of the mutant mitochondria (Wallace *et al.*, 1996). CPEO and KSS are multi-system disorders characterised by mitochondrial myopathy, ophthalmoplegia (paralysis of the eye muscles) and ptosis (Wallace *et al.*, 1995). Of the two, KSS is more severe and may also present with a number of other disorders, including pigmentary degeneration of the retina and hearing loss. Pearson's syndrome is another multi-system disorder with a childhood onset. Its symptoms include bone marrow failure, pancytopenia and neuromuscular problems. Pearsons patients often die young (Smith *et al.*, 1995).

As discussed previously, most of the genes required for mitochondrial function are in fact coded for by the nuclear genome and the gene products subsequently transported to the mitochondria (Schatz, 1996). Mutations in nuclear DNA can therefore give rise to disorders with symptoms similar to those caused by mutations in the mitochondrial genome. Such diseases however, are inherited in a mendelian fashion (Wallace, 1999). Mutations in a number of different nuclear genes give rise to Leigh's syndrome. These genes include the flavoprotein sub-unit of OXPHOS complex II (Bourgeron *et al.*, 1995) and the NDUF8 N-2 Fe-S center protein of complex I (Loeffen *et al.*, 1998). A mutation in the mitochondrial adenosine triphosphatase has been shown to cause autosomal dominant spastic paraplegia (Casari *et al.*, 1998). An autosomal

recessive disease, Friedreich's ataxia, results from a mutation in the gene that is responsible for transportation of iron out of the mitochondria, frataxin (Rotig *et al.*, 1997). These are but a few examples of the many diseases caused by mutations in nuclear genes that bring about diseases due to mitochondrial defects.

5.1.8 The aim of the study

The comparisons between documented mitochondrial diseases and the disease segregating in family ZMK, together with the fact that no genomic locus had been linked to the disease in this family, led us to consider the possibility of a mitochondrial mutation. The aim of this study therefore, was to screen the mitochondrial genome for a disease-causing mutation in family members. Upon the identification of a variant in the mitochondrial DNA the aim became to decipher whether or not this base change was causative of the disease in family ZMK. The possible role of this mitochondrial DNA change in Usher syndrome was also investigated.

5.2 MATERIALS AND METHODS

PCR, SSCP, automated and direct sequencing were carried out according to the methods detailed in Chapter 1. For primer sequences see appendices 8.11, 8.12 and 8.13.

5.2.1 Patient Clinical assessment

Patients were clinically assessed in detail by Dr. Paul Kenna in the Royal Victoria Eye and Ear Hospital in Dublin. Informed consent was obtained from all individuals participating in this study. Among the many tests carried out was Ganzfeld electroretinography, which was used to record the rod and cone photoreceptors responses of all patients. Pure tone audiometry was also performed on some individuals in the kindred (Kenna *et al.*, 1997). DNA extractions were performed on whole blood donated by 29 clinically assessed family members and five unaffected spouses, using standard methods (Mansergh, 1997). A quadriceps femoris muscle biopsy was taken from individual IV-22. Half of this was used for analysis by light and electron microscopy by Ms. Anne Mynes and Dr. Michael Farrell at St. James' Hospital, Dublin and the DNA was extracted from the other half by Dr. Fiona Mansergh (Mansergh, 1997). Four family members, IV-22, V-4, V-5 and V-6 underwent electrocardiography and electromyography in St. James' Hospital and the Adelaide Hospital, respectively (Mansergh, 1997).

5.3 RESULTS AND DISCUSSION

5.3.1 Evidence implicating the mitochondria in the disease in family ZMK

As previously discussed, a genome wide search had been undertaken in an attempt to identify a location for the disease gene in this family, within the nuclear genome. This resulted in the identification of a putative linkage on 9q which was subsequently revealed to be questionable. The failure to identify a nuclear locus for the disease gene, together with a number of features of the disease within this family, led to speculation that the disease was mitochondrial.

The possibility that the disease was due to a mitochondrial DNA defect had been initially disregarded due to the fact that the family was of the opinion that the disease had been transmitted through the pedigree by individual 1-1, a male who died at the turn of the century (see accompanying pedigree - Figure 5.1) (Mansergh *et al.*, 1999). Older members of the family recall that his wife, individual 1-2, did not appear to have sight or hearing difficulties, despite the fact that she lived into her eighties. Further investigation reveals however, that there is no clear recollection of the disease status of 1-1. It is therefore a possibility that 1-2 was the progenitor and that, as in the case of III-5, she was an example of reduced penetrance or alternatively, only had mild symptoms. If this is so, then the disease is transmitted purely through the maternal line, as is the case in mitochondrial disorders. None of the men included in the study have had offspring however, so this evidence alone was not enough to merit a screening of the mitochondrial genome for the disease mutation.

Sensorineural deafness and retinal degeneration are the most frequently observed symptoms of the disease in family ZMK. Mitochondrial dysfunction often leads to such symptoms due to the high energy demands of neural tissue (Shapira, 1998). The complaints by affected individuals of family ZMK of persistent tinnitus and marked recruitment have also been previously recorded in association with mitochondrial disease (Kimberling W, personal communication).

Muscle tissue is another of the tissue types most affected by the reduction in energy output resulting from mitochondrial mutations (diMauro *et al.*, 1998). Four of the affected individuals (IV-22, V-4, V-5 and V-6) underwent electrocardiogram assessment and all were revealed to have right axis cardiac deviations. One individual

also showed signs of global hypertrophy. A single quadriceps femoris muscle biopsy, taken from individual IV-22, was analysed by electron microscopy and revealed an abnormally high number of mitochondria within the cells of the muscle tissue. Excessive mitochondrial proliferation has been shown to occur in skeletal muscle tissue due to respiratory dysfunction caused by mitochondrial mutations (diMauro *et al.*, 1998). Electromyography carried out on the same individual also showed abnormalities which was consistent with a mild myopathy.

There are large variations, both in the symptoms and the levels of expression of the disease between the individuals of this pedigree. Such variations are frequently seen in families suffering from a mitochondrial disease due to the effects of heteroplasmy and replicative segregation (Wallace, 1999).

5.3.2 Sequencing the mitochondria

With the various evidence to indicate that the disease was possibly mitochondrial, a project was embarked upon to sequence the entire mitochondrial genome, in search for a family specific mutation. The DNA of four family members was used in the mutation screening. DNA extracted from blood was used from individuals IV-18, IV-23, and V-14 and DNA extracted from half the muscle biopsy by Dr. Fiona Mansergh was used from individual IV-22. Individual IV-23 is married into the family and was used as an unaffected control. Individual IV-18 is only mildly affected with hearing problems. Individual V-14 is one of the most severely affected of the pedigree with profound deafness and complete loss of sight. Individual IV-22 is also quite severely affected both by blindness and loss of hearing. The DNA extracted from muscle in this case was used in the mutation screening as the degree of heteroplasmy in mitochondrial diseases, regularly varies between muscle and blood. As clinical symptoms are only observable in muscle tissues, it was felt that muscle may show a higher percentage of a mitochondrial mutation, should it exist.

The sequencing of the mitochondria was carried out in conjunction with Dr. Fiona Mansergh and Sophia Millington-Ward and revealed a number of variations from the consensus sequence (Table 5.1). Most of these were previously reported polymorphisms. Four however, were previously unreported base changes. One of these was not within the coding region of the genome. Of the three within coding regions,

two resulted only in silent substitutions. The third was located within the second tRNA serine gene (MTTS2) by Dr. Fiona Mansergh and its potential as a disease causing mutation was investigated. This base change within the MTTS2 gene was at position 12258 and resulted in the substitution of a C for an A (Figure 5.3). The mitochondrial genome was sequenced in its entirety to ensure that there were no other variants which could potentially be disease causing mutations.

Table 5.1 Sequence variations found in family ZMK members.

Note: The disease-causing mutation in the serine tRNA gene is highlighted in bold. Additional sequence variations were found both in ‘married-in’ members of family ZMK and across all four individuals sequenced including the unaffected control individual (data not presented). Many of the variations from the consensus sequence presented below are either previously reported sequence variations, indicated with *, or do not alter encoded amino acids.

| Position | Consensus | ZMK | Gene | Amino Acid |
|--------------|-----------|----------|--------------|------------|
| 533* | A | G | Control | - |
| 6776* | T | C | MTCO1 | H-H |
| 11953 | C | T | MTND4 | L-L |
| 12258 | C | A | MTTS2 | - |
| 13404 | T | C | MTND5 | I-I |
| 14272* | C | G | MTND6 | F-L |
| 14569* | G | A | MTND6 | P-P |
| 14766* | A | G | MYCYB | I-T |
| 16239* | C | G | Control | - |
| 16519* | T | C | Control | - |
| 16569 | T | C | Control | - |

5.3.3 Evidence of the pathogenicity of the C12258A mutation

The gene was sequenced in all members of the family and the C12258A substitution was evident in blood from almost all individuals. The gene was also sequenced in the reverse in the four individuals used in the large-scale screening and the mutation was

also apparent on this strand of the DNA. Observation of the sequencing gels revealed clearly that this sequence variant was heteroplasmic. This was of significance as neutral polymorphisms are generally found only in the homoplasmic state (Silvestri *et al.*, 1994b). Screening of the tRNA gene in 270 normal individuals was carried out by Dr. Sophie Kiang, using automated sequencing. None had the substitution despite all being of the same ethnic background as family ZMK. Further evidence of the pathogenicity of this base change was acquired from a multiple sequence alignment of the MTT2 gene from different species, carried out by Dr. Andrew Lloyd (Table 5.2). This showed a conservation of the cytosine at this position in 12 out of 12 organisms including in evolutionarily distant species such as the frog, vulture and platypus. These results amounted to convincing evidence that the disease in this family is caused by the C12258A mutation.

Table 5.2 CLUSTAL W (1.7) multiple sequence alignment of the MTT2 gene in various species. The sequence named MTT2 (mutation) refers to the variant found in family ZMK. Position 12258 is indicated with bold typeface. Note the conservation of the normal C base in all species included in the alignment.

| Species | Sequence |
|-----------------|---|
| MTT2 (mutation) | CAAGAACTGC-T-AACT-CATGCCCCATGTCTAAC-AA-CATGG A TTT-CTC |
| Human | CAAGAACTGC-T-AACT-CATGCCCCATGTCTAAC-AA-CATGG C TTT-CTC |
| Chimpanzee | TAAGAACTGC-T-AATT-CATATCCCCATGCCTAAC-AA-CATGG C TTT-CTC |
| Gibbon | CAAGAACTGC-T-AACT-CACTATCCCATGTATAAC-AA-CATGG C TTT-CTC |
| Mouse | CAAGAACTGC-T-AATT-CATGCTTCCATGTTTAAA-AA-CATGG C TTT-CTT |
| Rhinoceros | CAAGAACTGC-T-AACT-CATGCCCCATATTTAAC-AA-TATGG C TTT-CTC |
| Cat | CAAGAACTGC-T-AATT-CATGCCTCCACGTATAAAA-AA-CGTGG C TTT-TTC |
| Seal | CAAGAACTGC-T-AACT-CATGCCCCACGTATAAAA-AA-CGTGG C TTT-TTC |
| Horse | CAAGAACTGC-T-AATT-CATGCCCCATGTCCAAC-AAACATGG C TCT-CTC |
| Donkey | CAAGAACTGCCT-AATT-CATGCTTCCGCGTCTGAC-AAACACGG C TCT-CTC |
| Opossum | CAAGAACTGC-T-AATT-CATGAACCCATATTTAAC-AA-TATGG C TTT-CTC |
| Platypus | TAAGAACTGC-T-AATC-CTTAACTTCATGCCTAAC-CA-CATG A CTCTACTT |
| Vulture | CAGGAACTGC-T-AACT-CTTG C ATCTGAGTCTAAA-AC-CTCAG C CC-CCTT |
| Frog | TAAGAACTGC-T-AATTACTTACG-CTGTG-TTCAT T C--CACGG C TTG-TTC |
| | * |

5.3.4 Analysis of levels of heteroplasmy of the C12258A mutation and correlation with disease symptoms

As previously discussed, the severity of symptoms of a mitochondrial disease can in some cases be correlated with the degree of heteroplasmy (Hamman *et al.*, 1993). A number of methods were used to analyse levels of heteroplasmy in blood from family members. DNA from blood of all family members was sequenced across the mutation and the relative intensities of the bands representing both the normal C nucleotide and the mutant A nucleotide, on the sequencing gel, estimated. A PCR product spanning the mutation was also amplified from all individuals and the product run on SSCP gels (Figure 5.4). The PCR products with the mutation shifted relative to those with the consensus sequence. This allowed relative intensities to be again estimated by eye (Table 5.3). The estimations of the ratio of wildtype mitochondria to mutant mitochondria were comparable in both methods.

These results, while not fully quantitative, clearly showed that there was no correlation between the levels of heteroplasmy in blood and the severity of symptoms. In both methods DNA isolated from muscle tissue from individual IV-22 was included. This allowed a comparison of levels of heteroplasmy between blood and muscle mitochondria from the same individual. Both the sequencing gels and the SSCP gels revealed that while there were approximately equal proportions of mutant and normal mitochondrial DNA in blood, in muscle tissue the level of mutant DNA was almost homoplasmic.

Another method to estimate the levels of heteroplasmy was also used by Sophia Millington-Ward. PCR products spanning the mutation, amplified from blood from individuals IV-22, IV-18 and V-14 and also from muscle in individual IV-22 were generated. These products were subsequently cloned into the cloning vector, pCDNA3. Forty clones from each of the four groups were chosen and sequenced on the automated sequencer in order to reveal how many clones in each possessed the mutant sequence. These results did not reveal a strong correlation between percentage mutant DNA and severity of symptoms either. They did confirm however, a large discrepancy between levels of mutant DNA in blood and muscle of the same individual.

Of all the family members for whom DNAs were available, the mutation was undetectable in blood, from both sequence and SSCP gels, for only two; individual III-3 and individual III-5. Individual III-3 has not been medically examined but family

members believe her to be in possession of all faculties. There are no medical records available for her offspring either so it is not clear whether or not she passed on the mutation. Individual III-V is also believed by family members to be without symptoms of the disease but once again, has not been medically examined. While DNA from her progeny were not available for inclusion in this study, there has been a report of an affected grandchild (Professor Carr. New York, personal communication).

There are a number of possibilities as to why the mutation is not detectable in sequence from blood in individual III-V and yet was apparently present in her germ cells. It may be that the effects of replicative segregation resulted in individual III-5 possessing a large number of mutant mitochondria in her germ cells and less in the cells of other tissues. The effect of a mitochondrial population bottleneck within the oocyte has been shown to result in large variances in heteroplasmy occurring over single generations (Grossman *et al.*, 1990). Another possibility as to why the mutation is undetectable in blood in individual III-5, is that it may have been selectively eliminated from blood cells. It has been shown that cells that are energetically normal have a growth advantage over those possessing large numbers of energy inefficient mitochondria (Siregar *et al.*, 1998). Blood cells are continuously being regenerated and therefore it is possible that over time, the subset of cells with a high load of less efficient, mutant mitochondria would be diluted out of the overall mitochondrial population. It is interesting to note that for the three oldest members of the pedigree for which DNA is available, (III-3, III-5 and III-9) the mutation is either not detectable in blood or present only in a minute quantity, as in the case of III-9.

There are a number of family members for whom the mutant band was detectable on gels but have not manifested symptoms of the disease. These are individuals IV-18, IV-20, V-1, V-3, V-16, V-10 and V-12. Notably many of these family members are young and may yet manifest symptoms. Given that it has been shown however that there is no correlation between levels of heteroplasmy in blood and severity of symptoms, the fact that the mutation is detectable in blood does not indicate that these individuals will definitely develop the disease.

Table 5.3 Estimated levels of heteroplasmy of the C12258A mutation for members of family ZMK (estimated by eye). A is the mutated variant, C is the normal base. Tissue refers to the type of tissue from which DNA was extracted. Unaffected members of the family have been referred to as asymptomatic, given that some individuals are still young and that there is evidence for a widely variable age of onset and penetrance in the pedigree. Similar results were obtained with SSCPE analysis (Figure 5.4).

| Individual | Ratio A:C | Tissue | Status |
|------------|-----------|--------|--------------|
| III-3 | 0:100 | Blood | Asymptomatic |
| III-5 | 0:100 | Blood | Asymptomatic |
| III-9 | 5:95 | Blood | Unclear |
| IV-14 | 50:50 | Blood | Affected |
| IV-15 | 30:70 | Blood | Affected |
| IV-16 | 40:60 | Blood | Affected |
| IV-17 | 0:100 | Blood | Married-In |
| V-1 | 80:20 | Blood | Asymptomatic |
| V-2 | 95:5 | Blood | Affected |
| V-3 | 40:60 | Blood | Asymptomatic |
| IV-18 | 60:40 | Blood | Asymptomatic |
| IV-20 | 40:60 | Blood | Asymptomatic |
| IV-22 | 50:50 | Blood | Affected |
| IV-22 | 95:5 | Muscle | Affected |
| IV-23 | 0:100 | Blood | Married-In |
| V-4 | 80:20 | Blood | Affected |
| V-5 | 80:20 | Blood | Affected |
| V-6 | 80:20 | Blood | Affected |
| IV-24 | 50:50 | Blood | Affected |
| IV-27 | 30:70 | Blood | Affected |
| IV-28 | 50:50 | Blood | Affected |
| IV-32 | 10:90 | Blood | Affected |
| IV-33 | 0:100 | Blood | Married-In |
| V-16 | 20:80 | Blood | Asymptomatic |
| IV-34 | 50:50 | Blood | Affected |
| IV-35 | 0:100 | Blood | Married-In |
| V-17 | 80:20 | Blood | Affected |
| IV-38 | 40:60 | Blood | Affected |
| IV-39 | 0:100 | Blood | Married-In |
| V-8 | 50:50 | Blood | Affected |
| V-10 | 40:60 | Blood | Asymptomatic |
| V-12 | 40:60 | Blood | Asymptomatic |
| V-14 | 60:40 | Blood | Affected |
| IV-40 | 20:80 | Blood | Affected |
| IV-41 | 50:50 | Blood | Affected |

5.3.5 Influences on the expression of the disease in family ZMK

The particular symptoms exhibited by different individuals of family ZMK are likely to be due to an interplay between the percentage of mutant DNA inherited by a particular individual, the amount of mutant DNA present in the different tissues of that individual and the distinct energy requirements of the different tissues. The mutation in this family primarily affects the retina and cochlea with milder symptoms observable in muscle in some individuals. While the levels of heteroplasmy in blood do not correlate with phenotypic expression of the disease in this family, it is possible that levels of heteroplasmy in neural tissues do.

Random genetic drift during development, together with selective elimination of mitochondria during aging can result in different quantities of mutant mitochondrial DNA in different tissues of the body (Wallace, 1999 and Siregar *et al.*, 1998). While selective elimination can reduce the number of mutant mitochondria in dividing tissues, such a reduction cannot occur in non-dividing tissue such as neural or muscular tissues. One could speculate that the high percentage of mutant DNA in muscle, a post mitotic tissue, from individual IV-22, might reflect the level of mutant DNA in the retinas and cochleas of affected individuals.

It has been shown that small amounts of wildtype DNA can give the cell protection from mitochondria defective in the OXPHOS pathway. In fact, the energy capacity of the cell may not fall below the bioenergetic threshold in some cases, until the percentage of mutant mitochondria is 90-95% (DiMauro *et al.*, 1998). The threshold of neural tissue is lower than for other tissue however (Shoffner *et al.*, 1990), which is another factor that may influence the particular expression of the disease in this family. The mental deficiencies, exhibited by 2 of the family members, are perhaps the outcome of an even higher mutational load in neural tissue.

Another potential influence on expression of the disease within family ZMK, is the effect of differences in nuclear DNA background. Various studies have shown that nuclear background can have an effect on expression of a disease (Torrioni *et al.*, 1997, Hao *et al.*, 1999). However, over 400 nuclear markers have been typed through the family however in the genome wide search for a disease locus (Mansergh, 1997), with no undisputed linkages identified, which makes this scenario unlikely.

5.3.6 Effects of the C12258A mutation at the molecular level

Without further studies it is not possible to predict how this mutation brings about the disease etiology at the molecular level but it is interesting to speculate on its effects. The C12258A mutation is located within the amino acid acceptor arm of the serine tRNA. Such a change in a widely conserved base may result in a change in the secondary structure of the tRNA resulting in a change in its base pairing ability. This may cause a reduction in efficiency of the amino-acylation of the tRNA or in its ability to interact with the ribosome and translation factors or cause it to be degraded more quickly.

A MERRF causing mutation in the tRNA-lys gene (MTTK) has been shown to cause a decrease of 50-60% in the level of charged lysine tRNAs in mutant cells (Enriquez *et al.*, 1995). This is due to both a reduction in amount of tRNA-lys and a reduction in aminoacylation efficiency. The diminished levels of charged tRNA-lys are believed to bring about premature termination of translation at or near lysine codons resulting in an overall impairment of protein synthesis (Enriquez *et al.*, 1995). This mutation is not located in the amino-acid acceptor arm however, but the TΨC loop and no other mitochondrial tRNA mutations have been shown to result in premature termination of translation to date (Chomyn, 1998).

The deafness-associated mutation at position 7445 in the tRNA-ser (UCN) gene is also located at a highly conserved position in the amino-acid acceptor stem. It has been shown to cause a reduction in the steady state levels of the tRNA, reducing them by 60-75% (Guan *et al.*, 1998). Rather than this bringing about a termination in translation however, it appears instead to cause a transient pause in it (Chomyn 1998). It may also interfere with processing of polycistronic mRNA produced from transcription of the mitochondrial heavy strand (Guan *et al.*, 1998). The 3243 mutation in the tRNA leucine gene also causes a reduction in tRNA levels within the mitochondria (Chomyn *et al.*, 1997).

At this stage it is not possible to tell how the C12258A mutation affects mitochondrial translation. The tRNA-ser AGU/C codon does not comprise a large portion of the entire number of codons in any of the mitochondrial protein coding genes (Table 5.4). It would not be expected therefore to affect any of the proteins of the OXPHOS pathway significantly more than others. In fact the relative numbers of the

serine AGU/C codons in coding regions of the mitochondrial genome are small with only 49 serine AGU/C codons in comparison to the 204 tRNA-ser UCN codons.

Table 5. 4 The number and percentage of the tRNA serine AGU/C codons within each of the protein coding genes of the mitochondrion. Adapted from MITOMAP, 1999.

| Protein | No. of ser AGU/C | % ser AGU/C |
|----------------|-----------------------------|--------------------|
| MtATP6 | 3 | 1.3 |
| MtATP8 | 0 | 0.0 |
| MtND1 | 3 | 0.9 |
| MtND2 | 5 | 1.4 |
| MtND3 | 1 | 0.9 |
| MtND4 | 10 | 2.2 |
| MtND4L | 0 | 0.0 |
| MtND5 | 13 | 2.2 |
| MtND6 | 5 | 2.9 |
| MtCO1 | 4 | 0.8 |
| MtCO2 | 1 | 0.4 |
| MtCytB | 4 | 1.1 |

Whatever the molecular mechanism involved however, the mutation more than likely results in an overall reduction in efficiency of energy production. As previously mentioned, neural tissues are the first to be affected by a decrease in the levels of available ATP. Photoreceptors have particularly high energy requirements which is reflected by the large number of mitochondria they possess (Travis, 1998). Defects of the OXPHOS pathway also result in a build up of reactive oxygen species which can cause damage to the cell (Sudbery, 1998). Such defects can also lead to the initiation of apoptosis (Wallace, 1999). It is of interest to note that in all retinopathies studied to date the photoreceptors die by means of apoptosis (Travis, 1998).

5.3.7 The identification of the C12258A mutation in a second family

Since the identification of this mutation it has also been identified in two members of an English family (Lynn *et al.*, 1998). It appears that this family is in fact related, through the maternal line, to family ZMK. The mitochondrial haplotype is the same in both families confirming that the mutation has not arisen independently in this family (Lynn *et al.*, 1998). Interestingly however, the clinical symptoms of the disease in this family are considerably different to those seen in family ZMK. This family suffer from cerebellar ataxia, cataracts, diabetes and deafness (Lynn *et al.*, 1998). No members of family ZMK have been identified with cerebellar ataxia. Cataracts frequently occur in RP patients and a number of the ZMK family have reported with them. Medical examination of the English patients may reveal sub-clinical symptoms of RP. Two of the older members of family ZMK have been diagnosed with diabetes. Given the large size of the family however, this is very possibly due to causes other than the C12258A mutation. The significantly different spectrum of symptoms observed in the English branch of the family to those observed in family ZMK provide another example of the complexity of phenotypic expression associated with mitochondrial disease.

5.3.8 Screening of Usher syndrome patients for the C12258A mutation

The involvement of this mutation in a disease that encompasses classic RP as a symptom may have implications for other retinopathies and in particular Usher syndrome type III that so closely resembles the disease in this family. Eight loci involved in Usher syndrome have been identified to date, all in the nuclear genome. There are additional families that do not map to any of these loci which suggests further genetic heterogeneity of the syndrome.

Nineteen Usher DNAs were screened for the C12258A mutation. These DNAs were acquired from Bill Kimberling's lab having been carefully chosen from a large stock of Usher DNA samples. Families showing clear-cut Mendelian inheritance were excluded from the study. There were no large families within the stock which showed segregation patterns consistent with mitochondrial inheritance. All DNAs received were from small family groups segregating Usher syndrome, for which the mode of inheritance could not be defined or from isolated cases of the disease. Most of these

patients are described as having atypical Usher syndrome and the clinical data for many of them are limited (Table 5.5).

Automated sequencing of the *MTTS2* gene had previously been proven to give very clear sequence and so automated sequencing was chosen as the method of screening in this case. The entire gene was sequenced in all cases. A DNA sample that was almost homoplasmic for the mutation and one that was heteroplasmic, from family ZMK, were sequenced as controls to ensure that the mutation was clearly identifiable. These samples confirmed that the mutation was readily detectable (Figure 5.5). A G to A transversion was identified at base 12236 in the affected individual from family 10. This is a silent change however and has been previously reported as a polymorphism. None of the 19 samples showed the C12258A mutation.

Despite none of these Usher samples possessing the C12258A mutation, the analysis of further DNA samples may still reveal that it plays a role in other cases of deaf-blindness. The gathering of more Usher DNAs is presently in progress. It may also be worthwhile to screen the *MTTS2* gene in cases of sporadic retinal degeneration or sensorineural deafness occurring on their own.

Table 5.5 Summary of known clinical symptoms of Usher syndrome patients screened for the C12258A mutation.

| Family number | No. affected individuals | Clinical Symptoms |
|----------------------|---------------------------------|--|
| 1 | 2 | RP early but stabilized. HL rapidly progressive |
| 2 | 1 | Optic disc pallor and atrophy of RPE. Mental retardation. Facial dymorphism |
| 3 | 1 | Atypical Usher syndrome |
| 4 | 1 | Atypical Usher syndrome resembling type II. Severe HL |
| 5 | 2 | Atypical Usher syndrome |
| 6 | 1 | Atypical Usher syndrome with cerebellar ataxia and pyramidalism |
| 7 | 2 | Atypical Usher syndrome. Individ. 1. has severe RP, skin & teeth problems. Individ. 2. has mild RP & progressive HL. |
| 8 | 1 | Atypical Usher syndrome |
| 9 | 3 | Atypical Usher syndrome |
| 10 | 1 | Atypical Usher syndrome |
| 11 | 1 | Atypical Usher syndrome. Other siblings reported deaf |
| 12 | 1 | Atypical Usher syndrome |
| 13 | 1 | Atypical Usher syndrome |
| 14 | 1 | Atypical Usher syndrome. Mild retardation |

HL: hearing loss

Individ: individual

5.4 CONCLUSION

This study reports the identification of a disease causing mutation in family ZMK, which segregates a disease similar to Usher syndrome. The C12258A mutation was identified following the sequencing of the entire mitochondrial genome. Evidence of heteroplasmy of the mutation in affected members of the family, its absence in 270 normal controls and the conservation of the C residue in 12 species, provide convincing evidence that the disease in family ZMK is caused by this mutation. Analysis of the levels of heteroplasmy among individuals of the family indicate that there is no correlation between these levels in blood and the severity of the disease.

Given the similarity of the symptoms in this family to those of Usher syndrome, 19 Usher syndrome patients were screened for the C12258A mutation. These patients were chosen for screening as they do not show clear-cut mendelian inheritance. None however, were found to possess the mutation.

The identification of the C12258A mutation in a pedigree segregating a disease very similar to Usher syndrome furthers the understanding of the role of the mitochondria in human disease. A pathogenic mutation in this tRNA gene had not been previously identified. Its identification may lead other investigators to screen this gene in patients with similar diseases. It is hoped that in the long term the identification of the disease mutation will lead to development of therapies for family ZMK and other families suffering from similar diseases.

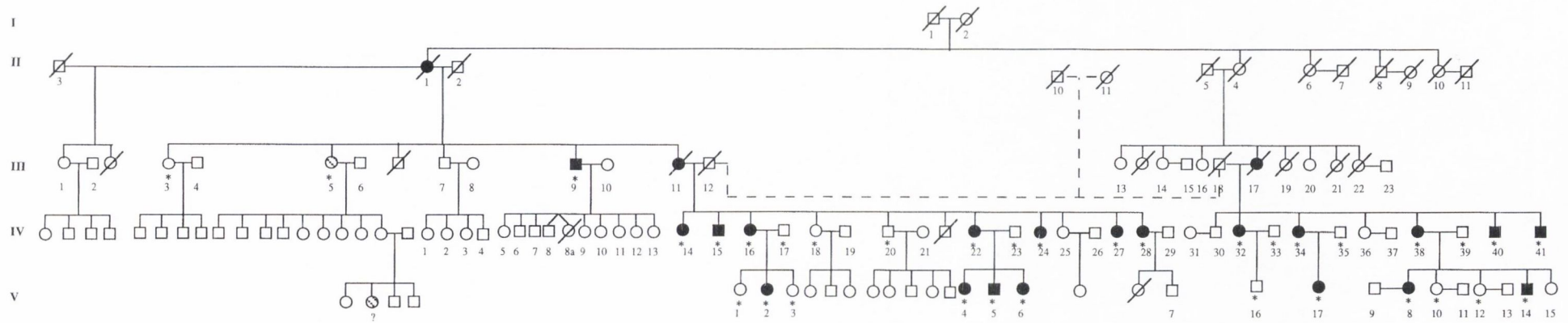


Figure 5.1 Family ZMK pedigree. Individuals marked with an asterisk are those for whom full diagnostic information has been obtained and DNA samples exist. Shaded squares or circles indicate individuals who have been examined clinically but whose diagnosis is uncertain. The shaded individual marked with a question mark is the affected granddaughter of the apparently unaffected individual III-5.

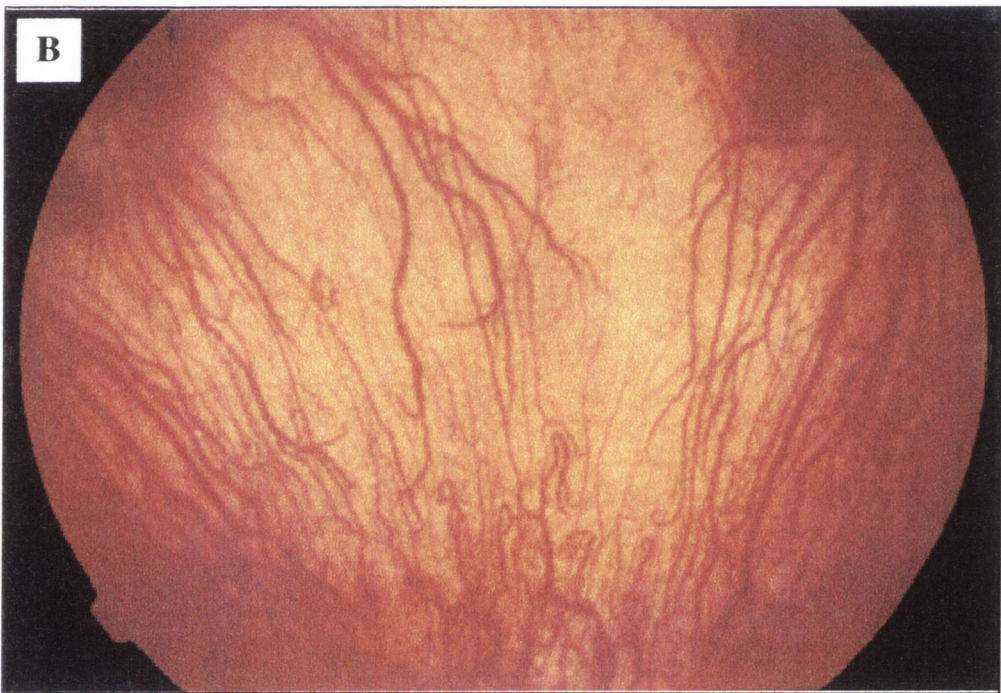
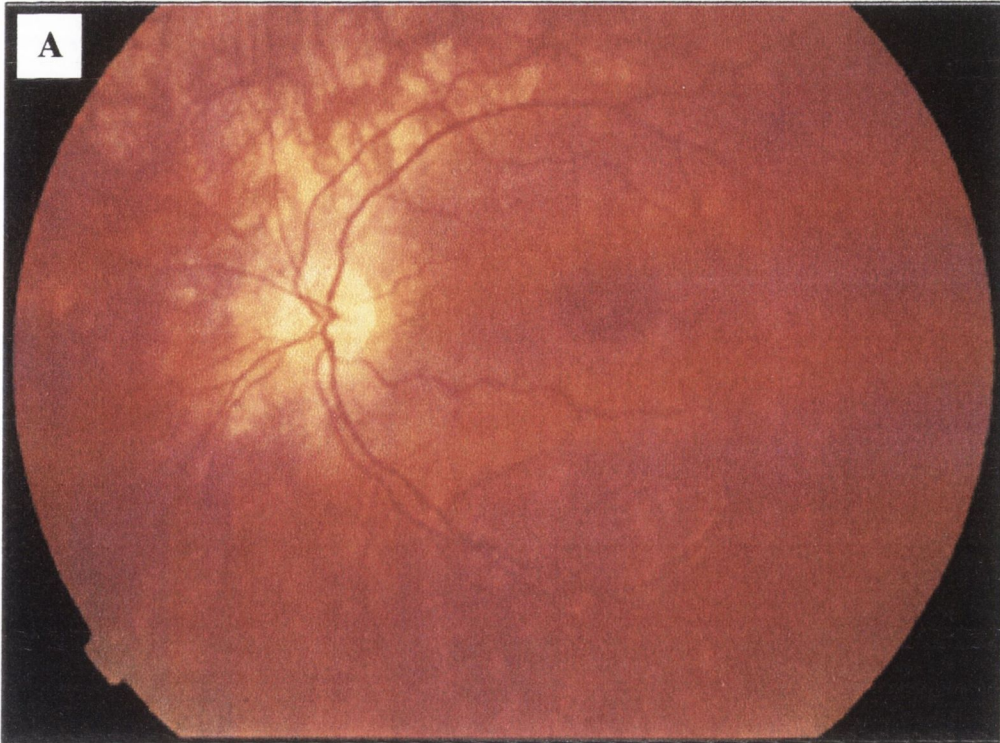


Figure 5.2 Fundus photographs from affected ZMK individuals. (A) a mildly affected individual exhibiting the early stages of RP. A thinning of the retina and a mild attenuation of the blood vessels is apparent. (B) a more seriously affected individual. The thinning of the retina is so extreme that the choroidal blood vessels can be seen.

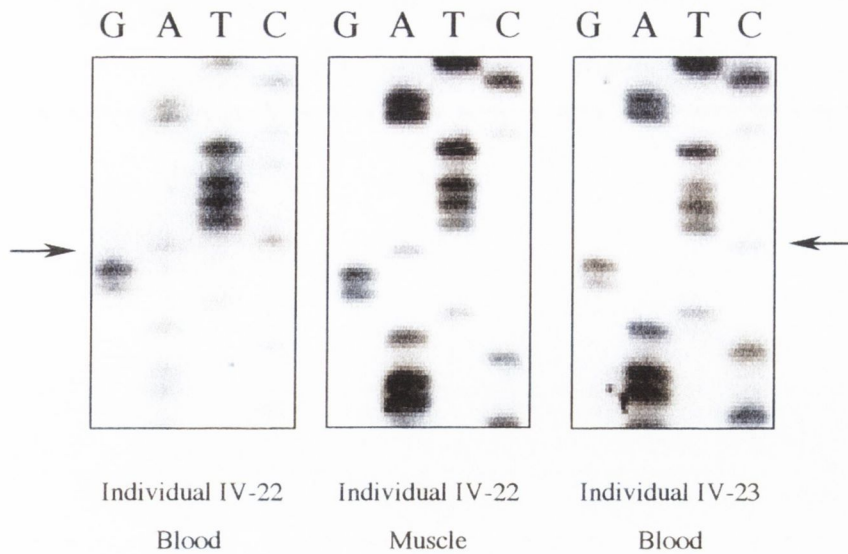


Figure 5.3 Mitochondrial sequence analysis of family ZMK individuals showing the C12258A mutation. Sequence analysis of mitochondrial DNA samples from blood lymphocytes and muscle from affected individual IV-22 and from blood lymphocytes from unaffected control IV-23 is shown. The C to A mutation at position 12258 is present in both blood (in a heteroplasmic state) and muscle (in a homoplasmic state) in individual IV-22. It is absent in the unaffected control.

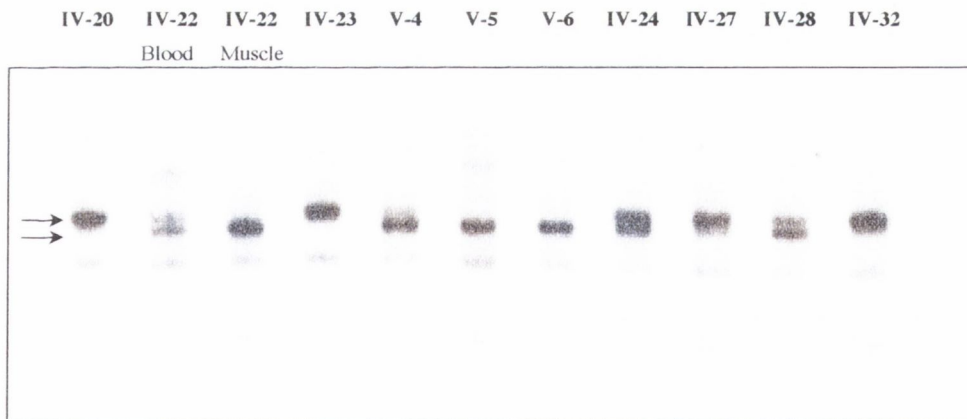


Figure 5.4 SSCP analysis using PCR products spanning the C12258A mutation from members of family ZMK. The wild-type (upper band) and mutant (lower band) mitochondrial DNA fragments can be distinguished. Both conformations of mitochondrial DNA are present in most affected individuals (e.g., individuals IV-22, V-4 and V-24). However, some affected individuals have mitochondrial DNA that is mostly mutant. It is noteworthy that the wild-type:mutant DNA ratio in blood and muscle tissue varies significantly in individual IV-22. The data indicate that there is no clearly evident correlation between the wild-type:mutant mitochondrial DNA ratio in blood and disease severity.

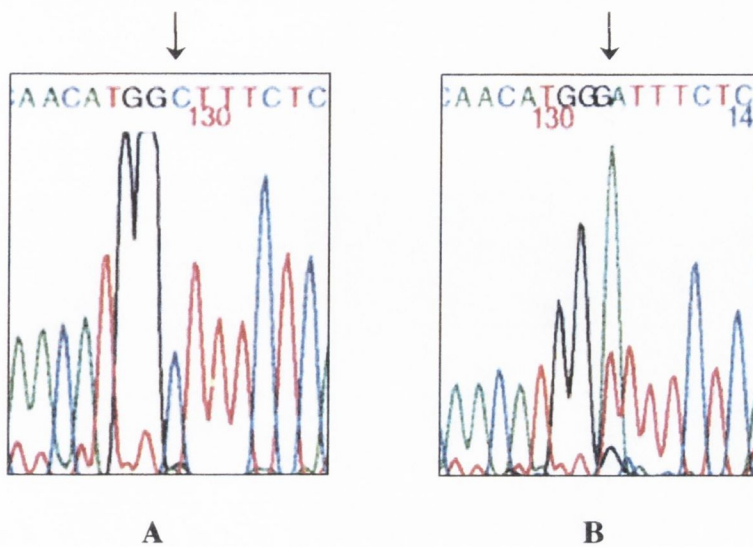


Figure 5.5 Automated sequence analysis of mitochondrial samples from an Usher syndrome patient, shown alongside an affected ZMK individual. (A) sequence analysis of blood lymphocytes from the Usher syndrome patient from Usher family 4 and (B) the affected ZMK individual V-14. The Usher family 4 individual possesses the consensus C at position 12258 of the mitochondrial sequence (indicated by an arrow). ZMK individual V-14 possesses the mutant A at this position. Notably, while direct sequencing clearly indicated that the mutation was heteroplasmic in individual V-14, the consensus C is not detectable in the automated sequence.

CHAPTER 6

**INVESTIGATIONS INTO THE ETIOLOGY OF AMD IN THE
IRISH POPULATION**

6.1 INTRODUCTION

6.1.1 Introduction

Age-related macular degeneration (AMD) is a prevalent, visually debilitating disease of the elderly which appears to be on the increase. It is a multi-factorial disease and, despite its prevalence, relatively little is known of its cause. Recently a member of the ABC transporter family of genes, the ABCR gene, has been implicated in its etiology. The first aim of this study therefore was to carry out a preliminary investigation into the possible role of the ABCR gene in AMD sufferers of the Irish population.

Sunlight is one of the reported risk factors for AMD, due to the damaging effects of its high-energy blue light which may bring about apoptosis of the photoreceptor cells. Recently, the RPE65 gene, previously implicated in a number of retinal degenerations, has been shown to be involved in a protective effect against light induced apoptosis in a strain of albino mice. The second aim of this study was therefore, to determine whether the RPE65 gene plays a role in the susceptibility to the damaging sunlight rays in humans, with a view to potential implications in the case of AMD sufferers.

A review of the macular degenerations is presented in this chapter. The role of the ABCR gene in diseases of the retina, including AMD, is discussed, along with knowledge to date of the function of its protein. The broad role of apoptosis in retinal degenerations is also detailed and recent studies indicating the role of the RPE65 gene in both a protective effect from light-induced apoptosis and in a number of retinal degenerations are outlined. Finally, results from the screening of two ABCR exons in AMD patients and the screening of the RPE65 gene in 244 individuals, for the substitution predicted to bring about the discussed protective effect in mice, are presented.

6.1.2 The macular degenerations

The macular degenerations are a complex set of disorders which are a leading cause of visual impairment world wide. Stargardt disease (STGD) is the most frequently observed, hereditary autosomal recessive form of macular dystrophy (Lewis *et al.*,

1999). It is characterised by onset of symptoms in childhood or early adulthood with central vision loss, accompanied by progressive bilateral atrophy of the macular retina and RPE. Orange-yellow flecks, distributed around the macula and mid-peripheral retina are frequently observed. Histologically, an accumulation of lipofuscin-like material, which is comprised of a mixture of lipid, protein and frequently pigment, is apparent in the RPE. Another autosomal recessive disorder, fundus flavimaculatus (FFM), shows very similar clinical manifestations to STGD. Its age of onset is generally later however, and its symptoms are slower in progression. Despite these differences, recent linkage studies have revealed that STGD and FFM are allelic (Kaplan *et al.*, 1993; Gerber *et al.*, 1995). Another of the macular degenerations, AMD, is a visually debilitating disease of the elderly. It is a prevalent disease and shares many of the clinical features of STGD and FFM.

6.1.3 Age related macular dystrophy

AMD is the leading cause of visual impairment in the elderly, estimated to affect nearly 30% of those over 75 years of age in the United States (Klein R *et al.*, 1993). It is clinically sub-divided into dry and wet forms of the disease with 80% of patients having the dry form of the disease (Allikmets *et al.*, 1997b). There are a number of hallmarks of the dry form of AMD including the accumulation of drusen (cellular debris) within and under the RPE. Uneven pigmentation and atrophy of the RPE are also classic manifestations of the disease (Figure - fundus photo). Approximately 20% of patients manifest the wet or exudative form of the disease (Allikmets *et al.*, 1997b). This is more destructive than the dry form of the disease and is responsible for approximately 90% of AMD patients that have been recorded as legally blind (Hyman *et al.*, 1983). In this form of the disease the retinal pigment epithelium may become detached from the retina. This can be accompanied by choroidal neovascularisation which results in the formation of scar tissue on the retina and hence the creation of blind spots. There are no effective medical therapies available for the treatment of dry AMD at present. In contrast, a variety of therapies including laser photocoagulation, low dose radiation and drugs which work to decrease neovascularisation are employed in the treatment of the wet form of the disease. These treatments are relatively ineffective for the majority of sufferers however (Walsh, 1997).

6.1.4 Risk factors for AMD

AMD is a multifactorial disease with both genetic and environmental factors having an influence on the expression of the disease. The involvement of a genetic component has been observed in twins with the concordance of the disease in monozygotic twins being significantly higher than in dizygotic twins (Klein ML *et al.*, 1994; Meyers *et al.*, 1995). Other evidence to indicate that AMD has a familial component is the higher prevalence of the disease in first degree relatives of patients with AMD than in first degree relatives of control subjects (Seddon *et al.*, 1997; Silvestri *et al.*, 1994a).

There are also many documented non-genetic risk factors associated with AMD of which age is the most significant (Hirvela *et al.*, 1996). Even with longer life spans being taken into consideration, the incidence of AMD appears to on the increase in developing countries (Evans & Wormald, 1996). This increase must therefore be due to the influence of environmental factors. Many risk factors have been proposed including smoking, cardiovascular abnormalities, high body mass index, hyperopia, light coloured irises, abnormal skin sensitivity to sun and lens opacities (Chaine *et al.*, 1998; Mitchell *et al.*, 1998; Walsh, 1997; Delcourt *et al.*, 1998).

Of particular interest is the widely held theory that sunlight exposure can lead to a higher risk of AMD (Cruickshanks *et al.*, 1993; Darzins *et al.*, 1997; Mitchell *et al.*, 1998; Taylor *et al.*, 1990). Exposure to sunlight can lead to photochemical damage of the cells in the retina by the high-energy blue light. This is linked to light coloured irises being a risk factor for the disease as they may permit greater blue light damage than dark iris colour (Mitchell *et al.*, 1998). Abnormal skin sensitivity to sunlight may reflect less ability of the pigmented regions of the eye to absorb the harmful rays (Mitchell *et al.*, 1998; Walsh *et al.*, 1997). Individuals with low density macular pigment may be at risk, also due to lower levels of protection from visible light (Landrum *et al.*, 1997).

None of the above risk factors, including sunlight, have been shown to independently result in the development of AMD (West *et al.*, 1989). It appears that expression of the disease requires the interaction of genetic factors, age and various environmental risk factors. There remains much to be elucidated however, in the etiology of the disease.

6.1.5 The involvement of ABCR in STGD

In 1997 the involvement of an ABC transporter gene in recessive STGD was reported (Allikmets *et al.*, 1997a). Linkage studies had previously resulted in the identification of a locus for STGD at 1p13-p21 (Kaplan *et al.*, 1993; Hoyng *et al.*, 1996). Subsequent to this Allikmets *et al.* (1997a), during the course of a large scale study to map members of the ATP-binding cassette (ABC) superfamily, identified an ABC gene which mapped to this region of chromosome 1. Among the ABC superfamily are transmembrane proteins involved in the energy dependant transportation of various products across membranes. Defects in such proteins have previously been shown to result in a variety of disease phenotypes including cystic fibrosis (Riordan *et al.*, 1989), adrenoleukodystrophy (Mosser *et al.*, 1993) and zellweger syndrome (Shimozawa *et al.*, 1992).

The ABC gene on chromosome 1p was initially identified from libraries of retinal ESTs and has since been shown to be expressed specifically in retinal tissue (Allikmets *et al.*, 1997a). It is hence referred to as the retina-specific ABC transporter (ABCR). The ABCR gene has an open reading frame of 6,705bp and spans approximately 100kb across the 1p22.2-1p22.3 region with a total of 51 exons (Allikmets *et al.*, 1998). Its protein product possesses two transmembrane domains and two ATP-binding domains which is typical of the ABC transporter family (Allikmets *et al.*, 1997a).

Mutation screening of the ABCR gene was carried out in 48 STGD families, previously shown to be linked to chromosome 1p (Allikmets *et al.*, 1997a). The initial screening of the gene was performed on 21 of the 51 ABCR exons and revealed the presence of 19 sequence alterations in STGD patients that were not present in at least 40 normal control individuals. These sequence alterations were shown to segregate with the disease phenotypes in the families they were identified in and hence were presumed to be causative of the disease. They consisted mainly of missense mutations, although some frameshift mutations were also identified. Among the groups screened in this study there were both homozygote and compound heterozygote families (Allikmets *et al.*, 1997a).

Other studies involving the screening of the ABCR gene in STGD patients have confirmed the involvement of the gene in the disease (Nasonkin *et al.*, 1998; Rozet *et al.*, 1998; Maugeri *et al.*, 1999). Nineteen novel mutations were identified in STGD

patients of Western European origin (Maugeri *et al.*, 1999). One of these, the 2588G-C transversion, which either results in the deletion of a glycine or its substitution for an alanine, was present in 37.5% of patients examined. It was found to be in linkage disequilibrium with a rare polymorphism at position 2828 and this therefore suggested a founder effect. It appears however, to have only a mild effect and to only bring about the disease when found in combination with another more severe ABCR mutation. Its apparent high frequency in the population (1 in every 35 Western Europeans) would support this theory (Maugeri *et al.*, 1999).

A large scale study in which all the exons of the ABCR gene were screened for disease mutations in 150 families with STGD revealed that most of the mutations associated with the disease are missense mutations and that they occur in equal frequency in both conserved and non-conserved regions of the gene (Lewis *et al.*, 1999). The combined analysis of genotype and phenotype in these families revealed that mutations in the amino terminal one-third of the protein appear to be associated with earlier onset of the disease than those residing in the rest of the protein. It is suggested that, as is the case with some mutations of the CFTR gene, these mutations represent misfolding alleles or result in altered processing of the protein (Lewis *et al.*, 1999)

6.1.6 The involvement of ABCR in RP and CORD

Since the original reports of the involvement of the ABCR gene in the etiology of STGD, it has also been found to be mutated in a number of other degenerative diseases of the retina. A homozygous 1bp deletion in exon 13 has been found to cause recessive RP in a consanguineous family (Martinez-Mir *et al.*, 1998). This deletion causes a frameshift in the protein coding sequence and the patients would be expected to have no functional ABCR protein. The complete lack of functional protein may result in the degeneration of the rod cells which would result in the RP phenotype. The distinctly different phenotype resulting from this mutation in contrast to those mutations previously mentioned, may be due to the fact that in all of the STGD patients characterised to date at least one of the ABCR proteins would be expected to have retained at least partial function. The rod cells in these cases may remain partially active but lead to the accumulation of lipofuscin-like material (Martinez-Mir *et al.*, 1998).

A combination of two null ABCR alleles has also been shown to result in an RP phenotype in a second consanguineous family (Cremers *et al.*, 1997). The mutation in this case is an intron 30 splice site mutation. It is also found in a compound heterozygous state within the same family together with another splice site mutation in intron 40, and in this case it gives rise to cone-rod dystrophy (CORD). The less severe phenotype resulting from the compound heterozygous state would imply that the intron 40 mutation gives rise to an at least partially functional splice site (Cremers *et al.*, 1997).

6.1.7 The involvement of ABCR in AMD

The similarities between STGD and AMD, including the atrophy of the RPE and the accumulation of drusen, have also led to the screening of the ABCR gene in patients with AMD. All exons of the ABCR gene and their intron junctions were screened for sequence alterations in 167 unrelated AMD patients (Allikmets *et al.*, 1997b). 98 unrelated STGD patients and 220 racially matched, normal controls were screened for all sequence alterations identified in the AMD population. Thirteen different variants were identified in this study which were postulated to be AMD-associated as they were identified only in the AMD samples or that they were identified significantly more frequently in the AMD samples than in the control population.

These alterations were identified in over 16% of the AMD population and are comprised mostly of missense mutations, two deletions and one splice donor site change. The alterations were scattered throughout the coding sequence of the gene although there was an apparent clustering of variants towards the 3' end of the coding sequence. Notably, there did not appear to be any correlation between particular mutations and specific symptoms of the disease. Six of the alterations postulated to be AMD-associated were also identified in STGD patients leading the authors to speculate that ABCR mutations which may lead to STGD in the homozygous or compound heterozygous state might increase susceptibility to AMD in the heterozygous state (Allikmets *et al.*, 1997b). AMD-associated mutations may result in aberrant proteins that accumulate over time and in combination with the interaction of other risk factors bring about macular degeneration in the elderly (Allikmets *et al.*, 1997b).

6.1.8 Speculation on the role of ABCR in AMD

The report of a correlation between a sequence variation in the ABCR gene and AMD by Allikmets *et al* (1997b) has generated a considerable amount of controversy. The fact that many of the alterations which have been proposed as AMD-associated alterations have only been found in one individual, have not been shown to segregate with the disease and have an unknown effect on the structure and function of the protein has led to speculation regarding their role in AMD (Dryja *et al.*, 1998). It has been pointed out that AMD patients in the study by Allikmets and colleagues do not show a significantly higher frequency of variations than controls and that as the gene was not screened in its entirety for the control group, that there may be more such non randomly distributed sequence anomalies in the controls (Dryja *et al.*, 1998; Klaver *et al.*, 1998).

Allikmets *et al.*, while acknowledging certain flaws in their study, have countered criticisms of their conclusions and maintain that the ABCR gene does play a role in AMD (Dean *et al.*, 1998). The fact that three of the variants identified in AMD patients are likely to produce null or severely impaired proteins and that six of the variants have also been identified in STGD patients, indicate to them that these alterations are likely to be pathogenic (Dean *et al.*, 1998). Since the original study they have identified a grandparent suffering from AMD who has transmitted the ABCR mutation to two sets of grandchildren who have developed STGD, due to the presence of an ABCR mutation on the other chromosome. They also report 25 additional pedigrees in which both STGD and AMD are segregating. These observations are taken as further evidence of the link between AMD and STGD (Dean *et al.*, 1998).

Subsequent studies have added to the debate on the role of the ABCR gene in the etiology of AMD. One such study involved the screening of the ABCR gene in 215 STGD patients and 182 AMD patients along with 96 ethnically matched controls (Stone *et al.*, 1998). While there was a significantly higher number of non-conservative variants identified in STGD patients compared with controls, the same did not hold true for the AMD patients. Also, the 18 identified variants predicted to result in truncation of the protein before the ATP-binding domain were found only in STGD subjects (Stone *et al.*, 1998). Other studies have given evidence to support the hypothesis that variants in the ABCR gene may be AMD related with specific ABCR variants being

identified in both STGD and AMD patients within the same family (Rozet *et al.*, 1999; Shroyer *et al.*, 1999).

The role of the ABCR gene in the etiology of AMD remains to be elucidated. If further evidence emerges suggesting that ABCR mutations in the carrier state may predispose to AMD, then it will also become necessary to establish which of the alterations, including STGD mutations, predispose to AMD and what effect these mutations have on the protein.

6.1.9 The ABCR protein and disease etiology

The ABCR gene is closely related to the mouse genes *Abc1* and *Abc2* (Luciani *et al.*, 1994) and to the human ABCC gene on chromosome 16p13.3 (Klugbauer & Hoffman, 1996; Allikmets *et al.*, 1995; 1996). The mouse homologue of ABCR maps to the distal end of chromosome 3, a region syntenic with human chromosome 1p13-p21 (Allikmets *et al.*, 1997a). These proteins are grouped together into the ABC1 family within the ABC superfamily. A yeast ortholog has not been identified for the members of this subfamily and therefore it appears that these proteins evolved to perform functions specific to multicellular organisms (Michaelis & Berkower, 1995).

The ABCR protein has been shown to reside in the outer segments of the rod photoreceptors but is absent from cone photoreceptors (Allikmets *et al.*, 1997a; Sun & Nathans, 1997). Confocal microscopy studies have revealed that it is specifically located in the discs within the rod outer segments, although it remains unclear whether or not there is a small amount of the protein present in the plasma membrane (Sun & Nathans, 1997). These in-depth studies of the ABCR protein have revealed it to be identical to two independently identified proteins, the bovine glycoprotein, ROS1.2 and another bovine outer segment membrane protein, the rim glycoprotein (Sun & Nathans, 1997).

The location of ABCR indicates that it is a defect in the rod outer segment which leads to the STGD and AMD phenotypes. The roles played by other members of the ABC transporter family suggest that the ABCR protein is involved in the transportation of an essential molecule or ion either within the outer segment or possibly across the plasma membrane of the photoreceptors. Histopathological studies of STGD eyes reveal the accumulation of a lipofuscin-like material within the cells of the RPE (Sun & Nathans, 1997). The morphology of the photoreceptors is also abnormal in appearance

(Birnbach *et al.*, 1994). It is possible that the build-up of lipofuscin is due to the ingestion of abnormal photoreceptor cells by the RPE (Sun & Nathans, 1997). The molecule for which the ABCR protein is responsible for transporting has not yet been identified. It has been suggested that it may be a lipid, a lipid component such as vitamin E or a retinoid (Allikmets *et al.*, 1997a). Failure to successfully transport any of these components between the RPE and the photoreceptors may alternatively be the cause of the accumulation of lipofuscin (Allikmets *et al.*, 1997a). However, given the localization of the ABCR protein to the discs of the rod cells, it seems more likely that it is involved in the intracellular transport of small molecules, perhaps between the lumen and cystolic faces of the outer segment disc membrane (Sun & Nathans, 1997). It may be involved in the transport of retinoids within the rod cell in this manner. Retinoids, in particular retinal, have in fact been shown to stimulate purified ABCR *in vitro*, suggesting that they are indeed the substrates for the ABCR protein (Sun *et al.*, 1999). It has been shown that much of the lipofuscin that occurs in the normal aging eye is comprised of N-retinyl-N-retinylethanolamine which is postulated to be due to reaction of retinal and phosphatidylethanolamine (Eldred & Lasky, 1993). It is possible that the lipofuscin deposits present in the RPE of STGD patients are of similar constitution and are as a result of defective transportation of retinoids within the outer segments (Sun & Nathans, 1997).

Given that the manifestation of the disease appears to result from cone dysfunction it is of some curiosity that the ABCR gene is expressed only in the rod and not in the cone photoreceptors. The compromised ability of the cones to function however, is presumed to be due to dysfunction of the RPE which is in turn caused by the primary defect in the rod cells (Allikmets *et al.*, 1997a).

6.1.10 The role of apoptosis in photoreceptor cell death

It has been previously mentioned that sunlight is considered a risk factor for the onset of AMD. It is of interest therefore, that animals that have been exposed to bright light for prolonged periods of time have been shown to undergo photoreceptor cell death (Noell *et al.*, 1966; Alber *et al.*, 1996). Apoptosis has been determined as the method of cell death in these studies (Alber *et al.*, 1996; Hafezi *et al.*, 1997). Apoptosis is a fundamental, genetically regulated form of cell death which involves individual cells

and is not accompanied by inflammation, as in the case of necrotic cell death. Apoptotic cells undergo cytoplasmic and nuclear condensation and subsequent fragmentation into apoptotic bodies. These apoptotic bodies are then phagocytosed by neighboring cells often without the apparent involvement of macrophages. Internucleosomal fragmentation of nuclear DNA allows apoptosis to be distinguished experimentally from other forms of cell death at the molecular level.

Apoptosis plays an essential role in life, required in both development and in tissue homeostasis. It has in fact been shown to play a role in the developing retina as the various neuronal layers undergo differentiation (Young, 1984; Penfold and Provis, 1986; Ilshner and Waring, 1992). As well as light, a large range of stimuli can induce apoptosis in the retina including underlying genetic mutations (Chang *et al.*, 1993; Portera-Cailliau *et al.*, 1994), toxic exposure to lead (Fox *et al.*, 1997) and various other agents (Nakajima *et al.*, 1996). These stimuli compromise the structure and function of the photoreceptor cells in different ways but all lead to the death of the cells by a final common pathway of apoptosis.

In the last number of years apoptosis has been shown to be the mode of cell death, which leads to eventual blindness, in a number of retinal degenerations of rodents. These include the naturally occurring retinopathy models, the retinal degeneration (rd) and retinal degeneration slow (rds) mice (Portera-Cailliau *et al.*, 1994) and the Royal College of Surgeons (RCS) Rats (Tso *et al.*, 1994). Mice carrying mutant rhodopsin transgenes and a rhodopsin knockout mouse also show apoptotic photoreceptor cell death (Portera-Cailliau *et al.*, 1994; Hobson *et al.*, In press). The first direct evidence for the involvement of apoptosis in degeneration of the human retina was provided by the postmortem analysis of an RP patient carrying a Thr-17-Met mutation in the rhodopsin gene. This retina showed cells clearly undergoing apoptosis at the boundary of dying and preserved photoreceptor cells (Li *et al.*, 1994).

6.1.11 Light-induced apoptosis

In the case of prolonged exposure to light it has been shown that cells of the RPE also die by apoptosis, as do the photoreceptors. The response of the retina suggests that it is possibly the visual pigments and phototransduction which mediate the apoptotic response (Reme *et al.*, 1995; Hafezi *et al.*, 1997). It may be induced as a result of

oxidative stress due to the reactive oxygen species generated during over-exposure to light (Hafezi *et al.*, 1997; Dillon, 1991). These observations suggest that cells of the retina have an intrinsic ability to undergo apoptosis which is normally inhibited by various factors, such as neurotrophic factors, but may be induced by various genetic and/or external agents (Portera-Cailliau *et al.*, 1994).

For people with an inherited retinal degeneration, exposure to light may exacerbate the genetically mediated apoptotic photoreceptor cell death. Rearing transgenic VVP mice that carry three point mutations within the opsin gene, in the dark has been shown to retard the process of retinal degeneration (Naash *et al.*, 1996). There do not appear to have been studies, as of yet, on the nature of cell death in AMD but it appears likely that, as is the case with any of the retinal degenerations analysed to date, the cells of the macula are undergoing apoptosis in the case of AMD also. It is not inconceivable therefore that sunlight is an apparent risk factor for AMD because it accelerates the rate of apoptotic photoreceptor cell death.

6.1.12 The role of the RPE65 gene in a protective effect against light-induced apoptosis

Very recently, a sequence variant in the Rpe65 gene of the albino strain of mice C57BL/6J-c2J has been shown to give a protective effect against light-induced apoptosis of the retinal photoreceptors (Danciger *et al.*, 1998; Danciger *et al.*, 1999 and Dr. Michael Danciger, personal communication, 1999). These mice were observed to undergo significantly less photoreceptor degeneration following exposure to constant light than another inbred strain of albino mice, BALB/c, and all other albino strains tested (Danciger *et al.*, 1998). This was presumed to be due to the effect of differences in genetic background and a search for the underlying genes was undertaken (Danciger *et al.*, 1998; Danciger *et al.*, 1999). 194 progeny mice from a (c2J x BALB/c)F1 x c2J backcross were quantified for photoreceptor degeneration, measured by thickness of the retinal outer nuclear layer, following constant exposure to light for two weeks. Using microsatellite markers from the Whitehead mouse genetic database linkage analysis was performed on DNA extracted from these mice. Quantitative trait locus (QTL) analysis was used to identify genes playing a role in the light damage protection. Two QTLs of significance were identified by this analysis. One of these, on

mouse chromosome 3 (with a lod score of 19.1) has been calculated to account for approximately 50% of the protective effect and another on chromosome 14 (with a lod score of 3.3) which has been estimated to be responsible for approximately 10% of the protective effect (Danciger *et al.*, 1999). The responsible gene on chromosome 3 was subsequently identified as the Rpe65 gene (Danciger, personal communication). A C to A transversion in exon 13 of the gene results in the substitution of a leucine for a methionine at amino acid 450.

6.1.13 The RPE65 protein

RPE65 is a microsomal protein which is specifically and abundantly expressed in the RPE (Hamel *et al.*, 1993). It is a 61-kD protein and is developmentally regulated (Nicoletti *et al.*, 1995). The gene has been mapped to human chromosome 1p31 and spans approximately 20 kb of genomic sequence possessing 14 exons (Hamel *et al.*, 1994; Nicoletti *et al.*, 1995). Its abundance in the RPE, its specificity of expression, its developmental regulation and its evolutionary conservation between different species suggested to investigators that this was a protein with an important role in the RPE.

A role in the metabolism of vitamin A was suggested by the biochemical association of the protein with both the retinal binding protein (RBP) and 11-*cis*-retinol dehydrogenase (Bavik *et al.*, 1992; Simon *et al.*, 1995). It was initially proposed as the RPE retinal binding protein (RBP) receptor (Bavik *et al.*, 1992). More recently however, studies on Rpe65-deficient mice have indicated that Rpe65 is essential for the production of 11-*cis*-retinal, the chromophore of rhodopsin (Redmond *et al.*, 1998). This was inferred by the fact that Rpe65 *-/-* mice show normal levels of opsin apoprotein in the rod outer segments but lack functional rhodopsin. These mice also show an over-accumulation of all-*trans*-retinal esters in the RPE. Rpe65 is therefore believed to play a role in the isomerization of the all-*trans*-retinal esters to 11-*cis*-retinal (Redmond *et al.*, 1998). However, its precise role in this isomerization is as yet unclear.

6.1.14 The role of RPE65 in retinal dystrophies

Recently, mutations within the RPE65 gene have been shown to cause certain early onset, severe retinal dystrophies (Marlhens *et al.*, 1997; Gu *et al.*, 1997; Morimura *et al.*, 1998). These retinal dystrophies are often termed autosomal recessive childhood-onset severe retinal dystrophy (arCSR) and include Leber congenital amaurosis (LCA) and early onset RP. The diseases are similar in their manifestation with both rods and cones affected simultaneously, attenuation of retinal blood vessels, variable retinal pigmentation in older patients and reduced or extinguished ERGs (Morimura *et al.*, 1998). RP patients show good central vision through the first decade of life however, while LCA patients are blind from birth or lose their vision within a few months of birth (Morimura *et al.*, 1998).

A number of patients have been identified with either compound heterozygous or homozygous mutations within the RPE65 sequence (Marlhens *et al.*, 1997; Gu *et al.*, 1997; Morimura *et al.*, 1998). Mutations within RPE65 have been estimated to be responsible for approximately 2% of cases of recessive RP and approximately 16% of LCA cases (Morimura *et al.*, 1998).

6.1.15 The aim of the study

The aims of this study were two-fold. Firstly, the initial stages of screening of the ABCR gene in AMD individuals from the Irish population was undertaken in order to begin to determine whether the gene plays a role in AMD among the Irish population. Given the controversy surrounding the involvement of the ABCR gene in AMD such a study is of particular interest.

Secondly, a screening of codon 450 of the RPE65 gene was undertaken in both AMD and control individuals. It is not clear how the substitution of a methionine for a leucine at position 450 of the mouse Rpe65 gene results in a protective effect against light induced apoptosis. Given that a number of studies have suggested sunlight as a risk factor for AMD however, it is interesting to speculate that differences in genetic background in humans, and in particular at this position of the RPE65 gene, may result in individuals being more or less susceptible to the damaging effects of light on the retina. Modifier loci, which have an influence on the severity of the phenotype, have

been identified in a number of human diseases including adenomatous polyposis (Tomlinson *et al.*, 1996), enteropancreatic malignancy (Burgess *et al.*, 1998) and polycystic kidney disease (Upadhy *et al.*, 1999). Such modifier loci are often identified through studies on mouse models (Houlston and Tomlinson, 1998; Rozmahel *et al.*, 1996). Therefore, the screening the RPE65 codon 450, in both AMD patients and controls, was carried out in order to determine if this site is polymorphic in humans and to determine if it may potentially play a role as a modifier locus in the human disease AMD.

6.2 MATERIALS AND METHODS

PCR, SSCP, automated and direct sequencing were carried out according to the methods detailed in Chapter 1. For primer sequences see appendices 8.14 and 8.15.

6.2.1 Patient Clinical assessment and DNA extraction

AMD Patients were clinically assessed in detail by Dr. David Mooney in the Royal Victoria Eye and Ear Hospital in Dublin. The minimum criteria for diagnosis of dry AMD were slow deterioration of central and fine vision, drusen formation (indicated by the presence of white spots on the retina) and pigment-epithelium atrophy. The criteria for characterisation of wet AMD were sudden onset of distorted vision, serous retinal detachment and subretinal hemorrhage.

DNA was extracted from lymphocytes using standard methods involving SDS lysis, proteinase K digestion and phenol extraction by Dr. Paul Kenna.

6.2.2 Control DNAs

The control DNAs were obtained from bloods provided by the Pelican House Blood Bank. The DNA was extracted, once again using standard methods, by Dr. Lesley Mynett Johnson

6.3.3 PCR digestion of RPE65 PCRs

A 25µl aliquot of each RPE65 PCR product was digested with 20 units of *Alu I* (New England Biolabs) at 37°C overnight with the buffer supplied by the manufacturers. Samples were analysed on 2.5% ethidium bromide stained agarose gels.

6.3 RESULTS AND DISCUSSION

6.3.1 Screening of the ABCR gene in AMD patients

Reports of the involvement of the ABCR gene in the etiology of AMD led us to begin the screening of the gene in 44 Irish AMD patients. Exons 47 and 48 of the ABCR gene were screened for variants using SSCP analysis (time constraints prevented screening of other exons of the gene). Primers (Appendix B.14) which amplified both the exons and their corresponding intron junctions were used. A shift in the exon 48 PCR fragment was identified on the SSCP gel in individual AMD 6. Both strands of this PCR product were sequenced and revealed that the shift was due to a G to A transition at position 2177 of the coding sequence (Figure 6.1). This is a missense mutation which results in the substitution of an aspartic acid for an asparagine.

Individual AMD 6 has been diagnosed with the more severe wet form of AMD. In 1993, at the age of 79 years of age he was examined due to a floating dot complaint. At that time his visual acuity was reported as being 20/20 and both maculas were described as normal. The following year the visual acuity in his right eye had deteriorated to the level of counting fingers and visual acuity of 6/18 was reported in his left eye. This rapid loss of vision, particularly in one eye at a time, is characteristic of wet AMD. Inspection of the right fovea revealed a slightly elevated, oval-shaped, white lesion on the macula. The macula of the left eye displayed a roundish pigmented area below the fovea. Vessel ingrowth under the RPE and retina caused hemorrhaging, leading to the pigmented appearance of the macula (Figure 6.2). The patient was not eligible to laser photocoagulation treatment, as is the case with 95% of individuals with wet type AMD, as the neovascular membrane was in the region over the highly sensitive fovea. A positive family history in both his parents and grandparents was reported by the patient.

This variant, Asp²¹⁷⁷ → Asn²¹⁷⁷ (D2177N), has been previously reported and proposed as an AMD-associated variant (Allikmets *et al.*, 1997b). Out of 167 AMD patients screened by Allikmets *et al.* (1997b), this sequence change was present in seven individuals. Although it was also identified in 1 of 220 control individuals they report that this is a significant difference by Fishers exact test (P = 0.023). Despite the controversy regarding whether or not many of the variants reported by Allikmets and

colleagues are AMD associated, there seems to be general agreement that this particular variant is found significantly more frequently in AMD patients than in controls (Klaver *et al.*, 1998; Dryja *et al.*, 1998). As Allikmets *et al.* (1997b) did not use aged match controls in their study the possibility that this unaffected individual will develop AMD later in life must also be considered. The high frequency of AMD, affecting as many as 30% of the population over the age of 75, makes this realistic possibility (Klein *et al.*, 1992). The D2177N alteration was not identified in any of the 98 STGD patients screened for ABCR variants (Allikmets *et al.*, 1997b).

Although 33 of the 167 AMD patients screened were diagnosed as having wet AMD, an ABCR alteration was found in only one (Allikmets *et al.*, 1997b). The authors do not specify which of the variants identified this variant is, although it does not appear to be the D2177N variant. They go on to speculate that given that only a single variant was identified in a wet AMD case that the ABCR gene may not play a role in this form of the disease. The identification of the D2177N alteration in a wet AMD patient from the Irish population is evidence that there may in fact be a correlation between the ABCR gene and wet AMD. If this variant is truly AMD associated then an AMD phenotype in this patient is not surprising. The exudative nature of the disease in this case however is surprising. Perhaps other genetic or environmental risk factors cause the same alterations in this gene to manifest different symptoms of the macula. If this mutation is confirmed by subsequent studies to be pathogenic, a more in-depth knowledge of the ABCR protein is required before it can be determined how the same mutation may result in distinctly different phenotypes.

Until many more genetic studies of the ABCR gene in patients with macular degenerations are carried out and the function of its protein is more fully understood, it is not possible to determine whether the D2177N alteration is AMD-associated or not. Ideally the screening of Irish controls for this variation should be carried out but time constraints did not permit this in the present study. The identification of a possible link between the ABCR gene and AMD is the first major breakthrough toward the understanding of the complex multifactorial disease. The identification of the D2177N variant in an Irish AMD patient lends further evidence to the hypothesis that the ABCR gene plays a role in the etiology of the visually debilitating disease of the elderly, AMD.

6.3.2 Results of screening human RPE65 gene.

The observation by Dansiger *et al.*, (1998, 1999, personal communication) that a methionine at codon 450 of the mouse Rpe65 gene, confers a considerable degree of protection against light-induced apoptosis in c2J mice led us to consider the potential role of the RPE65 gene in a disease of the retina for which sunlight is a risk factor, AMD. The c2J mice possess an A at position 1347 of the coding sequence, instead of the consensus C which results in a substitution of a leucine for a methionine in the RPE65 protein.

Without knowing more of the structure and properties of the RPE65 protein it is difficult to speculate how this change of a single amino acid may result in such a degree of protection from apoptosis of the photoreceptors, induced by prolonged exposure to light. Regardless of the precise mechanism of its inhibition of apoptosis however, the fact that the substitution of an amino acid at this position has such a considerable effect in these mice provoked us to determine whether or not this site is polymorphic in humans. We also compared the sequence of this codon in AMD patients and normal individuals in order to see if a change at this position may act as a modifier locus, playing a role in the response of different individuals to sunlight over the course of a lifetime.

The mouse sequence was not available in order to determine that codon 450 in the mouse sequence was homologous to codon 450 in the human sequence. The sequences of the RPE65 genes for rat, dog, salamander and chicken were available however, allowing a multiple sequence alignment of the RPE65 genes from these species to be carried out together with the human sequence. This sequence alignment revealed that there was a leucine at codon 450 in all species aligned and that the sequence of exon 13 was highly conserved (Figure 6.3). This suggests that the amino acid at position 450 of the human protein probably has the same location and function within the protein as the leucine at position 450 within the mouse protein.

The consensus sequence across this codon was determined to create an *Alu I* restriction site. Another *Alu I* restriction site only 9 base pairs away within the exon however, complicated the use of *Alu I* in an assay to determine whether the sequence at this position encoded the consensus leucine or not. Given the small distance between the enzyme recognition sites it would be difficult to determine whether the enzyme was cutting one or both sites. For this reason a forward primer (Appendix B.15) was

designed, with an incorporated mismatch, in order to eliminate the *Alu I* site nine base pairs from the site of interest (Figure 6.5). The PCR product amplified across this region was sequenced on the automated sequencer to confirm that the mismatch in the forward primer had eliminated this *Alu I* site. The forward primer was designed to span 40 base pairs in order that the fragment would be visible on a gel subsequent to digestion.

200, unrelated, control individuals from the Irish population (i.e. 400 chromosomes) and 44 AMD patients from the Irish population were screened for the presence or absence of a leucine at position 450 of the RPE65 gene. All samples digested to completion indicating that all possess the consensus leucine. It appears therefore that this site is probably not polymorphic in humans (Figure 6.4).

This result may indicate that the RPE65 gene plays no role in the response of different individuals to the damaging effects of light on the retina and hence does not play a role in the development of AMD. As the full results from the linkage studies on the c2J mice are not available to us, it could be speculated that it is not the methionine at position 450 of the RPE65 gene that is conferring the protective effect from light induced apoptosis but another variant within the gene or another gene in linkage disequilibrium with this locus. It is possible that there may be another site within the human protein which influences the response to light damage and hence it may be of interest to look at the entire human gene.

6.4 CONCLUSION

The screening of two exons of the ABCR gene was carried out in 44 AMD patients. Since initial reports of the involvement of the ABCR gene in STGD a number of studies have been carried out to determine whether the gene also plays a role in the etiology of AMD (Allikmets *et al.*, 1997b; Stone *et al.*, 1998; Rozet *et al.*, 1999). There have been reports providing evidence both for (Allikmets *et al.*, 1997b) and against (Stone *et al.*, 1998) its involvement and therefore it is important that many AMD patients are screened for ABCR alterations, in order that a clearer picture of its role in the disease can be arrived at. Unfortunately, time constraints permitted the screening of only two exons of the gene (exons 47 and 48) in 44 AMD sufferers of the Irish population. The screening of exon 48 revealed a variant (D2177N) which had previously been reported as an AMD- associated variant (Allikmets *et al.*, 1997b). It is of particular interest that it was identified in a patient with wet AMD as it appears that this alteration has previously been associated with only dry AMD (Allikmets *et al.*, 1997b). The identification of this variant in the Irish AMD population provides further evidence that this alteration may be associated with AMD.

The screening of codon 450 of the RPE65 gene indicated that this site is probably not polymorphic in humans. It appears therefore that this site is unlikely to be involved in the susceptibility of different individuals to the damaging effects of sunlight on the retina. Despite the negative result, this study was nevertheless an important one to carry out in striving to understand the factors which predispose to macular degeneration of the elderly and also in attempting to learn more of the nature of apoptosis of the photoreceptor cells of the retina.

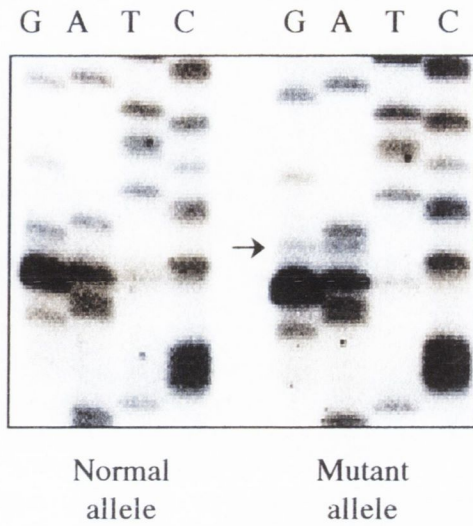


Figure 6.1 Sequence analysis of the ABCR gene of an Irish AMD patient; individual AMD 6. A G to A transition at position 2177 of the coding sequence is indicated by the arrow. Sequence from another AMD patient who does not possess this mutation is shown alongside.

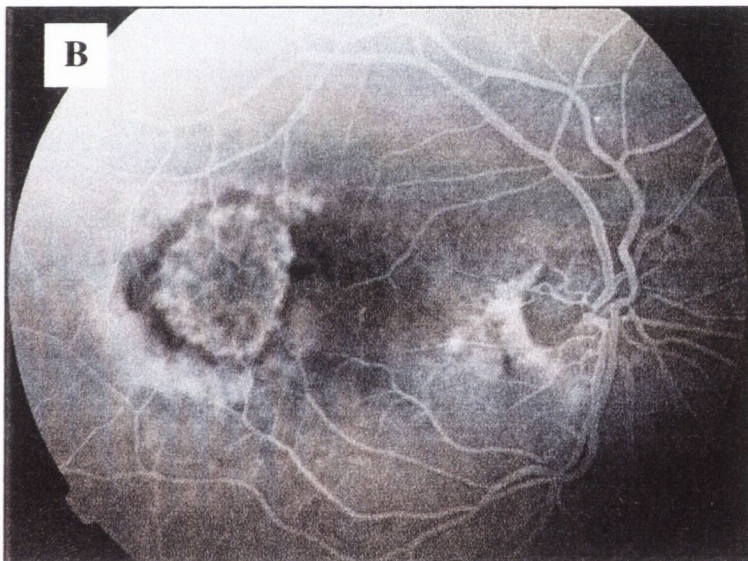


Figure 6.2 Fluorescein angiogram of AMD individual 6 shown alongside fluorescein angiogram of normal individual. (A) A normal retina. Note the avascular zone in the centre of the macula. (B) Angiogram of individual AMD 6 showing a clearly visible sub-retinal neovascular membrane just temporal to the centre of the macula. Its proximity to the fovea unfortunately rendered it unsuitable for laser photo-coagulation treatment.

↓

| | |
|------------|---|
| Human | TCACTTTGTTCCAGATAGGCTCTGTAAGCTGAAATGTCAAAACTAAAGAAACTTGGGTTTG |
| Dog | TCACTTCGTTCCGGACAGGCTCTGCAAGCTGAACGTCAAGACTAAAGAAACGTGGGTATG |
| Rat | TCACTTTGTTCCAGACAAGTTGTGTAAGCTGAAATGTCAAAACTAAAGAAATCTGGATGTG |
| Salamander | TCACTTTGTCCCAGACCGGCTTTCCAAGTTGAAATGTGAAAACAAAGGAGACCTGGGTGTG |
| Chicken | TCACTTTGTTCCAGACAGGCTTTGCAAGCTGAAATGTTAAAACAAAGGAGACCTGGGTGTG |

***** *

Figure 6.3 Multiple sequence of exon 13 of the RPE65 gene in five different species including human. Codon 450 of the gene is highlighted with a box and encodes a leucine in all species. This alignment indicated that the human leucine at position 450 was likely to correspond to the leucine at position 450 of the mouse protein.

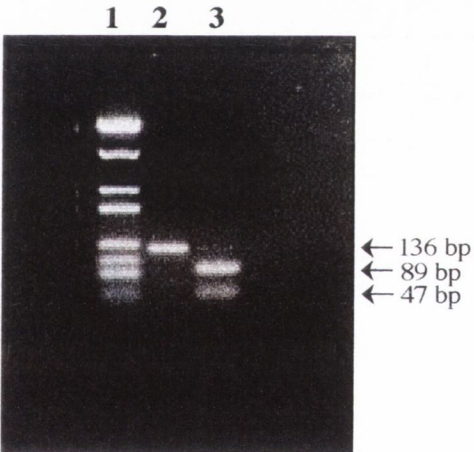
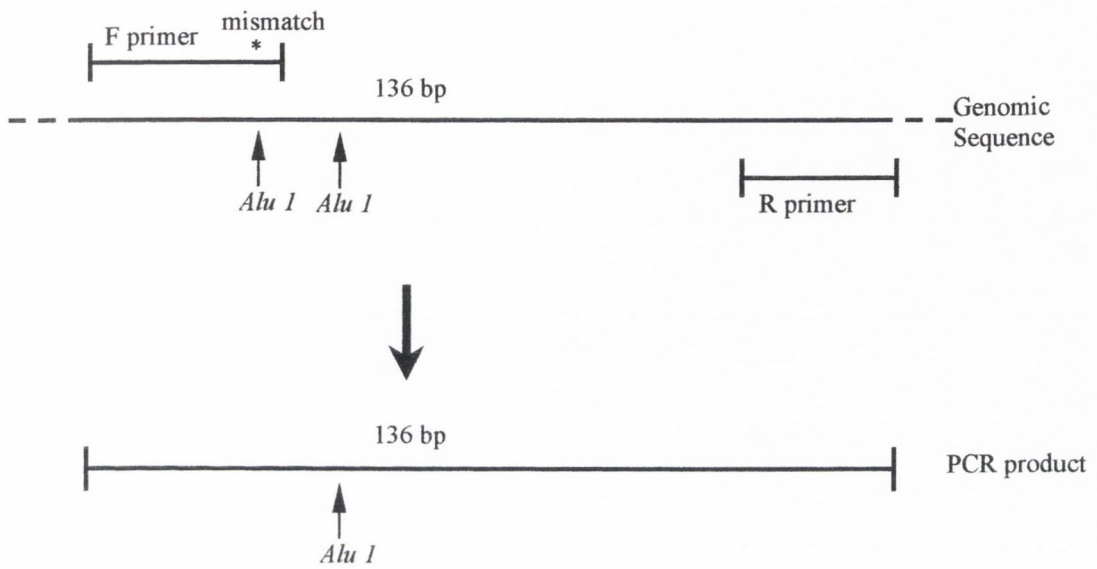


Figure 6.4 *Alu I* digest of the RPE65 exon 13 PCR product. *Alu I* cuts the consensus sequence indicating the absence of methionine at amino acid position 450 of the gene. Lane 1, molecular weight marker Puc 18/*Sau 3A*; lane 2, uncut PCR product; lane 3, digested PCR product with the concensus leucine at position 450.

STEP 1: PCR



STEP 2: ALU I DIGEST OF PCR PRODUCT



Figure 6.5 Schematic representation of assay to determine the presence or absence of a leucine to methionine substitution at amino acid position 450 of the RPE65 gene.

REFERENCES

- Abler AS, Chang CJ, Ful J, Tso MO, Lam TT (1996) Photic injury triggers apoptosis of photoreceptor cells. *Res Commun Mol Pathol Pharmacol* **92**:177-89
- Adam MF, Belmouden A, Binisti P, Brezin AP, Valtot F, Bechetoille A, Dascotte JC, *et al* (1997) Recurrent mutations in a single exon encoding the evolutionarily conserved olfactomedin-homology domain of TIGR in familial open-angle glaucoma. *Hum Mol Genet* **6**:2091-7
- Akarsu AN, Turacli ME, Aktan SG, Barsoum-Homsy M, Chevrette L, Sayli BS, Sarfarazi M (1996) A second locus (GLC3B) for primary congenital glaucoma (Buphthalmos) maps to the 1p36 region. *Hum Mol Genet* **5**:1199-203
- al-Jandal N, Farrar GJ, Kiang AS, Humphries MM, Bannon N, Findlay JB, Humphries P, *et al* (1999) A novel mutation within the rhodopsin gene (Thr-94-Ile) causing autosomal dominant congenital stationary night blindness. *Hum Mutat* **13**:75-81
- al-Maghtheh M, Inglehearn CF, Keen TJ, Evans K, Moore AT, Jay M, Bird AC, *et al* (1994) Identification of a sixth locus for autosomal dominant retinitis pigmentosa on chromosome 19. *Hum Mol Genet* **3**:351-4
- Aldred MA, Dry KL, Knight-Jones EB, Hardwick LJ, Teague PW, Lester DH, Brown J, *et al* (1994) Genetic analysis of a kindred with X-linked mental handicap and retinitis pigmentosa. *Am J Hum Genet* **55**:916-22
- Allikmets R, Gerrard B, Glavac D, Ravnik-Glavac M, Jenkins NA, Gilbert DJ, Copeland NG, *et al* (1995) Characterization and mapping of three new mammalian ATP-binding transporter genes from an EST database. *Mamm Genome* **6**:114-7

Allikmets R, Gerrard B, Hutchinson A, Dean M (1996) Characterization of the human ABC superfamily: isolation and mapping of 21 new genes using the expressed sequence tags database. *Hum Mol Genet* **5**:1649-55

Allikmets R, Shroyer NF, Singh N, Seddon JM, Lewis RA, Bernstein PS, Peiffer A, et al (1997a) Mutation of the Stargardt disease gene (ABCR) in age-related macular degeneration [see comments]. *Science* **277**:1805-7

Allikmets R, Singh N, Sun H, Shroyer NF, Hutchinson A, Chidambaram A, Gerrard B, et al (1997b) A photoreceptor cell-specific ATP-binding transporter gene (ABCR) is mutated in recessive Stargardt macular dystrophy [see comments]. *Nat Genet* **15**:236-46

Allikmets R, Wasserman WW, Hutchinson A, Smallwood P, Nathans J, Rogan PK, Schneider TD, et al (1998) Organization of the ABCR gene: analysis of promoter and splice junction sequences. *Gene* **215**:111-22

Alward WL, Semina EV, Kalenak JW, Heon E, Sheth BP, Stone EM, Murray JC (1998) Autosomal dominant iris hypoplasia is caused by a mutation in the Rieger syndrome (RIEG/PITX2) gene. *Am J Ophthalmol* **125**:98-100

Andersen JS, Pralea AM, DelBono EA, Haines JL, Gorin MB, Schuman JS, Mattox CG, et al (1997) A gene responsible for the pigment dispersion syndrome maps to chromosome 7q35-q36 [see comments]. *Arch Ophthalmol* **115**:384-8

ATCC homepage (1999) [Internet] 4-10-1999. Available from:
<http://www.atcc.org/forms/tigr-atcc_order.html> [Accessed 8th October 1999]

Attwood J, Bryant S (1988) A computer program to make linkage analysis with LIPED and LINKAGE easier to perform and less prone to input errors. *Ann Hum Genet* **52**:259

Banerjee P, Kleyn PW, Knowles JA, Lewis CA, Ross BM, Parano E, Kovats SG, et al (1998) TULP1 mutation in two extended Dominican kindreds with autosomal recessive retinitis pigmentosa. *Nat Genet* **18**:177-9

Bardien S, Ebenezer N, Greenberg J, Inglehearn CF, Bartmann L, Goliath R, Beighton P, et al (1995) An eighth locus for autosomal dominant retinitis pigmentosa is linked to chromosome 17q. *Hum Mol Genet* **4**:1459-62

Barnes WM (1994) PCR amplification of up to 35-kb DNA with high fidelity and high yield from lambda bacteriophage templates. *Proc Natl Acad Sci U S A* **91**:2216-20

Bascom RA, Manara S, Collins L, Molday RS, Kalnins VI, McInnes RR (1992) Cloning of the cDNA for a novel photoreceptor membrane protein (rom-1) identifies a disk rim protein family implicated in human retinopathies. *Neuron* **8**:1171-84

Bascom RA, Schappert K, McInnes RR (1993) Cloning of the human and murine ROM1 genes: genomic organization and sequence conservation. *Hum Mol Genet* **2**:385-91

Bavik CO, Busch C, Eriksson U (1992) Characterization of a plasma retinol-binding protein membrane receptor expressed in the retinal pigment epithelium. *J Biol Chem* **267**:23035-42

Bayes M, Martinez-Mir A, Valverde D, del Rio E, Vilageliu L, Grinberg D, Balcells S, et al (1996) Autosomal recessive retinitis pigmentosa in Spain: evaluation of four genes and two loci involved in the disease. *Clin Genet* **50**:380-7

Bayes M, Goldaracena B, Martinez-Mir A, Iragui-Madoz MI, Solans T, Chivelet P, Bussaglia E, et al (1998) A new autosomal recessive retinitis pigmentosa locus maps on chromosome 2q31-q33. *J Med Genet* **35**:141-5

Beales PL, Warner AM, Hitman GA, Thakker R, Flinter FA (1997) Bardet-Biedl syndrome: a molecular and phenotypic study of 18 families. *J Med Genet* **34**:92-8

Benson D, Rapp B (1996) UniGene Collection. In: *NCBI news* [Internet] August 1996. Available from: < <http://www.ncbi.nlm.nih.gov/Web/Newsltr/aug96.html> > [accessed July 8th 1999]

Bessant DA, Payne AM, Mitton KP, Wang QL, Swain PK, Plant C, Bird AC, et al (1999) A mutation in NRL is associated with autosomal dominant retinitis pigmentosa [letter]. *Nat Genet* **21**:355-6

Bhattacharya SS, Wright AF, Clayton JF, Price WH, Phillips CI, McKeown CM, Jay M, et al (1984) Close genetic linkage between X-linked retinitis pigmentosa and a restriction fragment length polymorphism identified by recombinant DNA probe L1.28. *Nature* **309**:253-5

Bird AC (1995) Retinal photoreceptor dystrophies LI. Edward Jackson Memorial Lecture [see comments]. *Am J Ophthalmol* **119**:543-62

Birnbach CD, Jarvelainen M, Possin DE, Milam AH (1994) Histopathology and immunocytochemistry of the neurosensory retina in fundus flavimaculatus. *Ophthalmology* **101**:1211-9

Boguski MS, Schuler GD (1995) ESTablishing a human transcript map [news]. *Nat Genet* **10**:369-71

Bonaldo MF, Lennon G, Soares MB (1996) Normalization and subtraction: two approaches to facilitate gene discovery. *Genome Res* **6**:791-806

Bouffard GG, Idol JR, Braden VV, Iyer LM, Cunningham AF, Weintraub LA, Touchman JW, et al (1997) A physical map of human chromosome 7: an integrated YAC contig map with average STS spacing of 79 kb. *Genome Res* **7**:673-92

Boughman JA, Vernon M, Shaver KA (1983) Usher syndrome: definition and estimate of prevalence from two high- risk populations. *J Chronic Dis* **36**:595-603

Bourgeron T, Rustin P, Chretien D, Birch-Machin M, Bourgeois M, Viegas-Pequignot E, Munnich A, et al (1995) Mutation of a nuclear succinate dehydrogenase gene results in mitochondrial respiratory chain deficiency. *Nat Genet* **11**:144-9

Braissant O, Walter W (1998) A simplified *in situ* hybridization protocol using non-radioactively labeled probes to detect abundant and rare mRNAs on tissue sections. Boehringer Mannheim Biochemica. Vol. 1, pp 10-16

Braley AE (1966) Dystrophy of the macula. *Am J Ophthalmol* **61**:1-24

Brown MD, Sun F, Wallace DC (1997) Clustering of Caucasian Leber hereditary optic neuropathy patients containing the 11778 or 14484 mutations on an mtDNA lineage. *Am J Hum Genet* **60**:381-7

Bryant SP (1997) Software for genetic linkage analysis. In: Boultwood J (ed) *Methods in molecular biology*. Humana Press Inc., Totowa, pp 261-277

Bu XD, Rotter JI (1991) X chromosome-linked and mitochondrial gene control of Leber hereditary optic neuropathy: evidence from segregation analysis for dependence on X chromosome inactivation. *Proc Natl Acad Sci U S A* **88**:8198-202

Bunting M, Tang W, Zimmerman GA, McIntyre TM, Prescott SM (1996) Molecular cloning and characterization of a novel human diacylglycerol kinase zeta. *J Biol Chem* **271**:10230-6

Burgess JR, Greenaway TM, Parameswaran V, Challis DR, David R, Shepherd JJ (1998) Enteropancreatic malignancy associated with multiple endocrine neoplasia type 1: risk factors and pathogenesis. *Cancer* **83**:428-34

Casari G, De Fusco M, Ciarmatori S, Zeviani M, Mora M, Fernandez P, De Michele G, et al (1998) Spastic paraplegia and OXPHOS impairment caused by mutations in paraplegin, a nuclear-encoded mitochondrial metalloprotease. *Cell* **93**:973-83

Caskey CT, Kruh GD (1979) The HPRT locus. *Cell* **16**:1-9

Chaib H, Kaplan J, Gerber S, Vincent C, Ayadi H, Slim R, Munnich A, et al (1997) A newly identified locus for Usher syndrome type I, USH1E, maps to chromosome 21q21. *Hum Mol Genet* **6**:27-31

- Chaine G, Hullo A, Sahel J, Soubrane G, Espinasse-Berrod MA, Schutz D, Bourguignon C, et al (1998) Case-control study of the risk factors for age related macular degeneration. France-DMLA Study Group. *Br J Ophthalmol* **82**:996-1002
- Chang GQ, Hao Y, Wong F (1993) Apoptosis: final common pathway of photoreceptor death in rd, rds, and rhodopsin mutant mice. *Neuron* **11**:595-605
- Chelly J, Concordet JP, Kaplan JC, Kahn A (1989) Illegitimate transcription: transcription of any gene in any cell type. *Proc Natl Acad Sci U S A* **86**:2617-21
- Chelly J, Gilgenkrantz H, Hugnot JP, Hamard G, Lambert M, Recan D, Akli S, et al (1991) Illegitimate transcription. Application to the analysis of truncated transcripts of the dystrophin gene in nonmuscle cultured cells from Duchenne and Becker patients. *J Clin Invest* **88**:1161-6
- Cheng S, Chang SY, Gravitt P, Respass R (1994a) Long PCR. *Nature* **369**:684-5
- Cheng S, Fockler C, Barnes WM, Higuchi R (1994b) Effective amplification of long targets from cloned inserts and human genomic DNA. *Proc Natl Acad Sci U S A* **91**:5695-9
- Chevalier J, Yi J, Michel O, Tang XM (1997) Biotin and digoxigenin as labels for light and electron microscopy in situ hybridization probes: where do we stand? *J Histochem Cytochem* **45**:481-91
- Chomyn A (1998) The myoclonic epilepsy and ragged-red fiber mutation provides new insights into human mitochondrial function and genetics. *Am J Hum Genet* **62**:745-51
- Cideciyan AV, Jacobson SG (1994) Image analysis of the tapetal-like reflex in carriers of X-linked retinitis pigmentosa. *Invest Ophthalmol Vis Sci* **35**:3812-24
- Collins A, Frezal J, Teague J, Morton NE (1996) A metric map of humans: 23,500 loci in 850 bands. *PNAS* **93**:14771-14775

Connell GJ, Molday RS (1990) Molecular cloning, primary structure, and orientation of the vertebrate photoreceptor cell protein peripherin in the rod outer segment disk membrane. *Biochemistry* **29**:4691-8

Cotton RG (1996) Detection of unknown mutations in DNA: a catch-22 [editorial; comment]. *Am J Hum Genet* **59**:289-91

Cox KH, DeLeon DV, Angerer LM, Angerer RC (1984) Detection of mRNAs in sea urchin embryos by in situ hybridization using asymmetric RNA probes. *Dev Biol* **101**:485-502

Cremers FP, van de Pol DJ, van Driel M, den Hollander AI, van Haren FJ, Knoers NV, Tijmes N, et al (1998) Autosomal recessive retinitis pigmentosa and cone-rod dystrophy caused by splice site mutations in the Stargardt's disease gene ABCR. *Hum Mol Genet* **7**:355-62

Cruickshanks KJ, Klein R, Klein BE (1993) Sunlight and age-related macular degeneration. The Beaver Dam Eye Study. *Arch Ophthalmol* **111**:514-8

Daiger SP, McGuire RE, Sullivan LS, Sohocki MM, Blanton SH, Humphries P, Green ED, et al (1997) Progress in positional cloning of RP10 (7q31-3), RP1 (8q11-q21) and VMD2 (8q24). In: LaVail MM, Hollyfield JG, Anderson RE (eds) *Degenerative retinal diseases*. Plenum Press, New York, pp 277-290

Daiger SP, Sullivan, LS, Rossiter, BJB (1999) RetNet; retinal information network [Internet] 6-5-1999. Available from: <<http://www.sph.uth.tmc.edu/Retnet/home.htm>> [Accessed 10th September 1999]

Danciger M, Rickabaugh T, Matthes MT, Yasumura D, Kumar N, LaVail MM, Farber DB (1998) Identification of a QTL on mouse chromosome 3 that influences the severity of light-induced damage of the retina. *Am J Hum Gen* **63** (4; supplement): abstract number 1653

Danciger M, Rickabaugh T, Matthes MT, Yasumura D, LaVail MM, Farber DB (1999) Quantitative trait loci in the mouse influences the severity of light damage. Invest Ophthalmol Vis Sci 40(4): S595 abstract number 3121

Darzins P, Mitchell P, Heller RF (1997) Sun exposure and age-related macular degeneration. An Australian case- control study. *Ophthalmology* **104**:770-6

Das SR, Bhardwaj N, Kjeldbye H, Gouras P (1992) Muller cells of chicken retina synthesize 11-cis-retinol. *Biochem J* **285**:907-13

Delcourt C, Diaz JL, Ponton-Sanchez A, Papoz L (1998) Smoking and age-related macular degeneration. The POLA Study. Pathologies Oculaires Liees a l'Age. *Arch Ophthalmol* **116**:1031-5

Deloukas P, Schuler GD, Gyapay G, Beasley EM, Soderlund C, Rodriguez-Tome P, Hui L, et al (1998) A physical map of 30,000 human genes. *Science* **282**:744-6

Dib C, Faure S, Fizames C, Samson D, Drouot N, Vignal A, Millasseau P, et al (1996) A comprehensive genetic map of the human genome based on 5,264 microsatellites [see comments]. *Nature* **380**:152-4

Dillon J (1991) The photophysics and photobiology of the eye. *J Photochem Photobiol B* **10**:23-40

DiMauro S, Bonilla E, Davidson M, Hirano M, Schon EA (1998) Mitochondria in neuromuscular disorders. *Biochim Biophys Acta* **1366**:199-210

Ding L, Traer E, McIntyre TM, Zimmerman GA, Prescott SM (1998) The cloning and characterization of a novel human diacylglycerol kinase, DGKiota. *J Biol Chem* **273**:32746-52

Dirks RW, van de Rijke FM, Fujishita S, van der Ploeg M, Raap AK (1993) Methodologies for specific intron and exon RNA localization in cultured cells by haptenized and fluorochromized probes. *J Cell Sci* **104**:1187-97

Dirks RW (1996) RNA molecules lighting up under the microscope. *Histochem Cell Biol* **106**:151-66

Dizhoor AM, Hurley JB (1999) Regulation of photoreceptor membrane guanylyl cyclases by guanylyl cyclase activator proteins. *Methods* **19**:521-31

Djamgoz MBA, Archer SN, Vallegra S (1995) Neurobiology and clinical aspects of the outer retina. Chapman and Hall, London

Dowling JE (1987) The retina; an approachable part of the brain. The Belknap Press of Harvard University Press, Cambridge, Massachusetts and London

Dryja TP, McGee TL, Reichel E, Hahn LB, Cowley GS, Yandell DW, Sandberg MA, et al (1990) A point mutation of the rhodopsin gene in one form of retinitis pigmentosa. *Nature* **343**:364-6

Dryja TP, Berson EL, Rao VR, Oprian DD (1993) Heterozygous missense mutation in the rhodopsin gene as a cause of congenital stationary night blindness. *Nat Genet* **4**:280-3

Dryja TP, Li T (1995) Molecular genetics of retinitis pigmentosa. *Hum Mol Genet* **4**:1739-43

Dryja TP, Finn JT, Peng YW, McGee TL, Berson EL, Yau KW (1995) Mutations in the gene encoding the alpha subunit of the rod cGMP-gated channel in autosomal recessive retinitis pigmentosa. *Proc Natl Acad Sci U S A* **92**:10177-81

Dryja TP, Hahn LB, Reboul T, Arnaud B (1996) Missense mutation in the gene encoding the alpha subunit of rod transducin in the Nougaret form of congenital stationary night blindness. *Nat Genet* **13**:358-60

Dryja TP, Hahn LB, Kajiwara K, Berson EL (1997) Dominant and digenic mutations in the peripherin/RDS and ROM1 genes in retinitis pigmentosa. *Invest Ophthalmol Vis Sci* **38**:1972-82

Dubois S, Morissette J, Winstall E, Hladky E, Falardeau P, Bergeron J, Cote G, et al (1997) Important phenotypic variability of the Lys 423Glu mutation in the TIGR gene within a huge GLC1A-linked glaucoma family. *Am J Hum Genet* **61**(4; supplement): abstract number 1939

Duvoisin RM, Zhang C, Ramonell K (1995) A novel metabotropic glutamate receptor expressed in the retina and olfactory bulb. *J Neurosci* **15**:3075-83

Ehrlich G, Viegas-Pequignot E, Ginzberg D, Sindel L, Soreq H, Zakut H (1992) Mapping the human acetylcholinesterase gene to chromosome 7q22 by fluorescent in situ hybridization coupled with selective PCR amplification from a somatic hybrid cell panel and chromosome-sorted DNA libraries. *Genomics* **13**:1192-7

Eldred GE, Lasky MR (1993) Retinal age pigments generated by self-assembling lysosomotropic detergents [see comments]. *Nature* **361**:724-6

Eudy JD, Yao S, Weston MD, Ma-Edmonds M, Talmadge CB, Cheng JJ, Kimberling WJ, et al (1998) Isolation of a gene encoding a novel member of the nuclear receptor superfamily from the critical region of Usher syndrome type IIa at 1q41. *Genomics* **50**:382-4

Evans J, Wormald R (1996) Is the incidence of registrable age-related macular degeneration increasing? [see comments]. *Br J Ophthalmol* **80**:9-14

Farrar GJ, Kenna P, Jordan SA, Kumar-Singh R, Humphries MM, Sharp EM, Sheils DM, et al (1991) A three-base-pair deletion in the peripherin-RDS gene in one form of retinitis pigmentosa. *Nature* **354**:478-80

Fishman GA, Stone EM, Alexander KR, Gilbert LD, Derlacki DJ, Butler NS (1997) Serine-27-phenylalanine mutation within the peripherin/RDS gene in a family with cone dystrophy. *Ophthalmology* **104**:299-306

Fitzgibbon J, Appukuttan B, Gayther S, Wells D, Delhanty J, Hunt DM (1994) Localisation of the human blue cone pigment gene to chromosome band 7q31.3-32. *Hum Genet* **93**:79-80

Fox DA, Campbell ML, Blocker YS (1997) Functional alterations and apoptotic cell death in the retina following developmental or adult lead exposure. *Neurotoxicology* **18**:645-64

Freund CL, Gregory-Evans CY, Furukawa T, Papaioannou M, Looser J, Ploder L, Bellingham J, et al (1997) Cone-rod dystrophy due to mutations in a novel photoreceptor-specific homeobox gene (CRX) essential for maintenance of the photoreceptor. *Cell* **91**:543-53

Fu K, Hartlen R, Johns T, Genge A, Karpati G, Shoubridge EA (1996) A novel heteroplasmic tRNA^{Leu}(CUN) mtDNA point mutation in a sporadic patient with mitochondrial encephalomyopathy segregates rapidly in skeletal muscle and suggests an approach to therapy. *Hum Mol Genet* **5**:1835-40

Fuchs S, Nakazawa M, Maw M, Tamai M, Oguchi Y, Gal A (1995) A homozygous 1-base pair deletion in the arrestin gene is a frequent cause of Oguchi disease in Japanese. *Nat Genet* **10**:360-2

Furukawa T, Morrow EM, Cepko CL (1997) Crx, a novel otx-like homeobox gene, shows photoreceptor-specific expression and regulates photoreceptor differentiation. *Cell* **91**:531-41

Gal A, Orth U, Baehr W, Schwinger E, Rosenberg T (1994) Heterozygous missense mutation in the rod cGMP phosphodiesterase beta- subunit gene in autosomal dominant stationary night blindness. *Nat Genet* **7**:551

Gall JG, Pardue ML (1969) Formation and detection of RNA-DNA hybrid molecules in cytological preparations. *Proc Natl Acad Sci U S A* **63**:378-83

Gerber S, Rozet JM, Bonneau D, Souied E, Camuzat A, Dufier JL, Amalric P, et al (1995) A gene for late-onset fundus flavimaculatus with macular dystrophy maps to chromosome 1p13. *Am J Hum Genet* **56**:396-9

Getman DK, Eubanks JH, Camp S, Evans GA, Taylor P (1992) The human gene encoding acetylcholinesterase is located on the long arm of chromosome 7. *Am J Hum Genet* **51**:170-7

Gieser L, Fujita R, Goring HH, Ott J, Hoffman DR, Cideciyan AV, Birch DG, et al (1998) A novel locus (RP24) for X-linked retinitis pigmentosa maps to Xq26-27. *Am J Hum Genet* **63**:1439-47

Goldberg AF, Molday RS (1996a) Subunit composition of the peripherin/rds-rom-1 disk rim complex from rod photoreceptors: hydrodynamic evidence for a tetrameric quaternary structure. *Biochemistry* **35**:6144-9

Goldberg AF, Molday RS (1996b) Defective subunit assembly underlies a digenic form of retinitis pigmentosa linked to mutations in peripherin/rds and rom-1. *Proc Natl Acad Sci U S A* **93**:13726-30

Goto Y, Nonaka I, Horai S (1990) A mutation in the tRNA(Leu)(UUR) gene associated with the MELAS subgroup of mitochondrial encephalomyopathies [see comments]. *Nature* **348**:651-3

Goto K, Kondo H (1993) Molecular cloning and expression of a 90-kDa diacylglycerol kinase that predominantly localizes in neurons. *Proc Natl Acad Sci U S A* **90**:7598-602

Graff C, Urbak SF, Jerndal T, Wadelius C (1995) Confirmation of linkage to 1q21-31 in a Danish autosomal dominant juvenile-onset glaucoma family and evidence of genetic heterogeneity. *Hum Genet* **96**:285-9

Gray MW, Burger G, Lang BF (1999) Mitochondrial evolution. *Science* **283**:1476-81

Green ED, Olson MV (1990) Chromosomal region of the cystic fibrosis gene in yeast artificial chromosomes: a model for human genome mapping. *Science* **250**:94-8

Green ED, Braden VV, Fulton RS, Lim R, Ueltzen MS, Peluso DC, Mohr-Tidwell RM, et al (1995) A human chromosome 7 yeast artificial chromosome (YAC) resource: construction, characterization, and screening. *Genomics* **25**:170-83

Greenberg J, Goliath R, Beighton P, Ramesar R (1994) A new locus for autosomal dominant retinitis pigmentosa on the short arm of chromosome 17. *Hum Mol Genet* **3**:915-8

Grossman LI (1990) Mitochondrial DNA in sickness and in health. *Am J Hum Genet* **46**:415-7

Grunewald-Janho S, Keesey J, Leous M, van Miltenburg R, Schroeder C (1996) Nonradioactive *in situ* hybridization application manual. Boehringer Mannheim GmbH, Germany

Gu SM, Thompson DA, Srikumari CR, Lorenz B, Finckh U, Nicoletti A, Murthy KR, et al (1997) Mutations in RPE65 cause autosomal recessive childhood-onset severe retinal dystrophy. *Nat Genet* **17**:194-7

Gu S, Kumaramanickavel G, Srikumari CR, Denton MJ, Gal A (1999) Autosomal recessive retinitis pigmentosa locus RP28 maps between D2S1337 and D2S286 on chromosome 2p11-p15 in an Indian family [In Process Citation]. *J Med Genet* **36**:705-7

Guan MX, Fischel-Ghodsian N, Attardi G (1996) Biochemical evidence for nuclear gene involvement in phenotype of non-syndromic deafness associated with mitochondrial 12S rRNA mutation. *Hum Mol Genet* **5**:963-71

Guan MX, Enriquez JA, Fischel-Ghodsian N, Puranam RS, Lin CP, Maw MA, Attardi G (1998) The deafness-associated mitochondrial DNA mutation at position 7445, which affects tRNA^{Ser}(UCN) precursor processing, has long-range effects on NADH dehydrogenase subunit ND6 gene expression. *Mol Cell Biol* **18**:5868-79

Guillonneau X, Piriev NI, Danciger M, Kozak CA, Cideciyan AV, Jacobson SG, Farber DB (1999) A nonsense mutation in a novel gene is associated with retinitis pigmentosa in a family linked to the RP1 locus. *Hum Mol Genet* **8**:1541-6

Hafezi F, Marti A, Munz K, Reme CE (1997) Light-induced apoptosis: differential timing in the retina and pigment epithelium. *Exp Eye Res* **64**:963-70

Hagstrom SA, North MA, Nishina PL, Berson EL, Dryja TP (1998) Recessive mutations in the gene encoding the tubby-like protein TULP1 in patients with retinitis pigmentosa. *Nat Genet* **18**:174-6

Hammans SR, Sweeney MG, Brockington M, Lennox GG, Lawton NF, Kennedy CR, Morgan-Hughes JA, et al (1993) The mitochondrial DNA transfer RNA(Lys)A-->G(8344) mutation and the syndrome of myoclonic epilepsy with ragged red fibres (MERRF). Relationship of clinical phenotype to proportion of mutant mitochondrial DNA. *Brain* **116**:617-32

Hao H, Morrison LE, Moraes CT (1999) Suppression of a mitochondrial tRNA gene mutation phenotype associated with changes in the nuclear background. *Hum Mol Genet* **8**:1117-24

Harris D (1965) The inheritance of glaucoma a - pedigree of familial glaucoma. *Am J Ophthalmol* **60**:91-95

He L, Campbell ML, Srivastava D, Blocker YS, Harris JR, Swaroop A, Fox DA (1998) Spatial and temporal expression of AP-1 responsive rod photoreceptor genes and bZIP transcription factors during development of the rat retina. *Mol Vis* **4**:32

Heckenlively J (1988) Retinitis Pigmentosa. JB Lipencott Company, Philadelphia
Heon E, Sheth BP, Kalenak JW, Sunden SL, Streb LM, Taylor CM, Alward WL, et al (1995) Linkage of autosomal dominant iris hypoplasia to the region of the Rieger syndrome locus (4q25). *Hum Mol Genet* **4**:1435-9

Hillier LD, Lennon G, Becker M, Bonaldo MF, Chiapelli B, Chissoe S, Dietrich N, et al (1996) Generation and analysis of 280,000 human expressed sequence tags. *Genome Res* **6**:807-28

Hirvela H, Luukinen H, Laara E, Sc L, Laatikainen L (1996) Risk factors of age-related maculopathy in a population 70 years of age or older. *Ophthalmology* **103**:871-7

Hobsen AH, Donovan M, Humphries MM, Carmody R, Tuohy G, Cotter T, Farrar J, et al. Apoptotic photoreceptor death in the rhodopsin knockout mouse in the presence and absence of c-fos. In press.

Holt IJ, Harding AE, Petty RK, Morgan-Hughes JA (1990) A new mitochondrial disease associated with mitochondrial DNA heteroplasmy. *Am J Hum Genet* **46**:428-33

Holub BJ, Kuksis A (1978) Metabolism of molecular species of diacylglycerophospholipids. *Adv Lipid Res* **16**:1-125

Horrigan S, Westbrook C (1997) Construction and use of YAC contigs in disease regions. In: Boultonwood J (ed) *Methods in molecular biology*. Humana Press Inc., Totowa, pp 123-136

Hotta Y, Benzer S (1970) Genetic dissection of the *Drosophila* nervous system by means of mosaics. *Proc Natl Acad Sci U S A* **67**:1156-63

Houlston RS, Tomlinson IP (1998) Modifier genes in humans: strategies for identification. *Eur J Hum Genet* **6**:80-8

Howell N (1994) Mitochondrial gene mutations and human diseases: a prolegomenon [editorial]. *Am J Hum Genet* **55**:219-24

Hoyng CB, Poppelaars F, van de Pol TJ, Kremer H, Pinckers AJ, Deutman AF, Cremers FP (1996) Genetic fine mapping of the gene for recessive Stargardt disease. *Hum Genet* **98**:500-4

Huang SH, Pittler SJ, Huang X, Oliveira L, Berson EL, Dryja TP (1995) Autosomal recessive retinitis pigmentosa caused by mutations in the alpha subunit of rod cGMP phosphodiesterase. *Nat Genet* **11**:468-71

Humphries P, Farrar GJ, Kenna P, McWilliam P (1990) Retinitis pigmentosa: genetic mapping in X-linked and autosomal forms of the disease. *Clin Genet* **38**:1-13

Humphries P, Kenna P, Farrar GJ (1992) On the molecular genetics of retinitis pigmentosa. *Science* **256**:804-8

Humphries MM, Rancourt D, Farrar GJ, Kenna P, Hazel M, Bush RA, Sieving PA, et al (1997) Retinopathy induced in mice by targeted disruption of the rhodopsin gene [see comments]. *Nat Genet* **15**:216-9

Hyman LG, Lilienfeld AM, Ferris FLd, Fine SL (1983) Senile macular degeneration: a case-control study. *Am J Epidemiol* **118**:213-27

Ilschner SU, Waring P (1992) Fragmentation of DNA in the retina of chicken embryos coincides with retinal ganglion cell death. *Biochem Biophys Res Commun* **183**:1056-61

Inglehearn CF, Hardcastle AJ (1996) Nomenclature for inherited diseases of the retina [letter; comment]. *Am J Hum Genet* **58**:433-5

Inglehearn CF, Tarttelin EE, Plant C, Peacock RE, al-Magthteh M, Vithana E, Bird AC, et al (1998) A linkage survey of 20 dominant retinitis pigmentosa families: frequencies of the nine known loci and evidence for further heterogeneity. *J Med Genet* **35**:1-5

Ioannou PA, Amemiya CT, Garnes J, Kroisel PM, Shizuya H, Chen C, Batzer MA, et al (1994) A new bacteriophage P1-derived vector for the propagation of large human DNA fragments. *Nat Genet* **6**:84-9

Jansen HG, Sanyal S (1984) Development and degeneration of retina in rds mutant mice: electron microscopy. *J Comp Neurol* **224**:71-84

Jenuth JP, Peterson AC, Fu K, Shoubridge EA (1996) Random genetic drift in the female germline explains the rapid segregation of mammalian mitochondrial DNA [see comments]. *Nat Genet* **14**:146-51

John HA, Birnstiel ML, Jones KW (1969) RNA-DNA hybrids at the cytological level. *Nature* **223**:582-7

Johnson AT, Drack AV, Kwitek AE, Cannon RL, Stone EM, Alward WL (1993) Clinical features and linkage analysis of a family with autosomal dominant juvenile glaucoma. *Ophthalmology* **100**:524-9

Jordan SA, Farrar GJ, Kenna P, Humphries MM, Sheils DM, Kumar-Singh R, Sharp EM, et al (1993) Localization of an autosomal dominant retinitis pigmentosa gene to chromosome 7q [comment]. *Nat Genet* **4**:54-8

Jordan T, Ebenezer N, Manners R, McGill J, Bhattacharya S (1997) Familial glaucoma iridogoniodysplasia maps to a 6p25 region implicated in primary congenital glaucoma and iridogoniodysgenesis anomaly. *Am J Hum Genet* **61**:882-8

Jun AS, Brown MD, Wallace DC (1994) A mitochondrial DNA mutation at nucleotide pair 14459 of the NADH dehydrogenase subunit 6 gene associated with maternally inherited Leber hereditary optic neuropathy and dystonia. *Proc Natl Acad Sci U S A* **91**:6206-10

Junqueira LC, Carneiro J, Kelley RO (1995) Basic histology. Prentice-Hall International, Inc., London

Kai M, Sakane F, Imai S, Wada I, Kanoh H (1994) Molecular cloning of a diacylglycerol kinase isozyme predominantly expressed in human retina with a truncated and inactive enzyme expression in most other human cells. *J Biol Chem* **269**:18492-8

Kajiwara K, Hahn LB, Mukai S, Travis GH, Berson EL, Dryja TP (1991) Mutations in the human retinal degeneration slow gene in autosomal dominant retinitis pigmentosa. *Nature* **354**:480-3

Kajiwara K, Berson EL, Dryja TP (1994) Digenic retinitis pigmentosa due to mutations at the unlinked peripherin/RDS and ROM1 loci. *Science* **264**:1604-8

Kameoka K, Isotani H, Tanaka K, Azukari K, Fujimura Y, Shiota Y, Sasaki E, et al (1998) Novel mitochondrial DNA mutation in tRNA(Lys) (8296A-->G) associated with diabetes. *Biochem Biophys Res Commun* **245**:523-7

Kanoh H, Yamada K, Sakane F (1990) Diacylglycerol kinase: a key modulator of signal transduction? *Trends Biochem Sci* **15**:47-50

Kaplan J, Pelet A, Martin C, Delrieu O, Ayme S, Bonneau D, Briard ML, et al (1992a) Phenotype-genotype correlations in X linked retinitis pigmentosa. *J Med Genet* **29**:615-23

Kaplan JC, Kahn A, Chelly J (1992b) Illegitimate transcription: its use in the study of inherited disease. *Hum Mutat* **1**:357-60

Kaplan J, Gerber S, Bonneau D, Rozet JM, Delrieu O, Briard ML, Dollfus H, et al (1992c) A gene for Usher syndrome type I (USH1A) maps to chromosome 14q. *Genomics* **14**:979-87

Kaplan J, Gerber S, Larget-Piet D, Rozet JM, Dollfus H, Dufier JL, Odent S, et al (1993) A gene for Stargardt's disease (fundus flavimaculatus) maps to the short arm of chromosome 1 [published erratum appears in *Nat Genet* 1994 Feb;**6**(2):214]. *Nat Genet* **5**:308-11

Keen TJ, Inglehearn CF, Lester DH, Bashir R, Jay M, Bird AC, Jay B, et al (1991) Autosomal dominant retinitis pigmentosa: four new mutations in rhodopsin, one of them in the retinal attachment site. *Genomics* **11**:199-205

Khaliq S, Hameed A, Ismail M, Mehdi SQ, Bessant DA, Payne AM, Bhattacharya SS (1999) Refinement of the locus for autosomal recessive Retinitis pigmentosa (RP25) linked to chromosome 6q in a family of Pakistani origin. [letter]. *Am J Hum Genet* **65**:571-4

Kikkawa U, Kishimoto A, Nishizuka Y (1989) The protein kinase C family: heterogeneity and its implications. *Annu Rev Biochem* **58**:31-44

Kimberling WJ, Weston MD, Moller C, Davenport SL, Shugart YY, Priluck IA, Martini A, et al (1990) Localization of Usher syndrome type II to chromosome 1q. *Genomics* **7**:245-9

King MC (1997) Leaving Kansas ... finding genes in 1997 [news]. *Nat Genet* **15**:8-10

Kinoshita A, Ohishi H, Nomura S, Shigemoto R, Nakanishi S, Mizuno N (1996) Presynaptic localization of a metabotropic glutamate receptor, mGluR4a, in the cerebellar cortex: a light and electron microscope study in the rat. *Neurosci Lett* **207**:199-202

Kirschner R, Rosenberg T, Schultz-Heienbrok R, Lenzner S, Feil S, Roepman R, Cremers FP, et al (1999) RPGR transcription studies in mouse and human tissues reveal a retina-specific isoform that is disrupted in a patient with X-linked retinitis pigmentosa. *Hum Mol Genet* **8**:1571-8

Klauck TM, Xu X, Mousseau B, Jaken S (1996) Cloning and characterization of a glucocorticoid-induced diacylglycerol kinase. *J Biol Chem* **271**:19781-8

Klein R, Klein BE, Linton KL (1992) Prevalence of age-related maculopathy. The Beaver Dam Eye Study. *Ophthalmology* **99**:933-43

Klein ML, Mauldin WM, Stoumbos VD (1994) Heredity and age-related macular degeneration. Observations in monozygotic twins. *Arch Ophthalmol* **112**:932-7

Klugbauer N, Hofmann F (1996) Primary structure of a novel ABC transporter with a chromosomal localization on the band encoding the multidrug resistance-associated protein. *FEBS Lett* **391**:61-5

Knauss TC, Jaffer FE, Abboud HE (1990) Phosphatidic acid modulates DNA synthesis, phospholipase C, and platelet-derived growth factor mRNAs in cultured mesangial cells. Role of protein kinase C. *J Biol Chem* **265**:14457-63

Kniazeva MF, Chiang MF, Cutting GR, Zack DJ, Han M, Zhang K (1999) Clinical and genetic studies of an autosomal dominant cone-rod dystrophy with features of Stargardt disease [see comments]. *Ophthalmic Genet* **20**:71-81

Kogelnik AM, Lott MT, Brown MD, Navathe SB, Wallace DC (1996) MITOMAP: a human mitochondrial genome database. *Nucleic Acids Res* **24**:177-9

Koulen P, Kuhn R, Wassle H, Brandstatter JH (1999) Modulation of the intracellular calcium concentration in photoreceptor terminals by a presynaptic metabotropic glutamate receptor. *Proc Natl Acad Sci U S A* **96**:9909-14

Krill AE, Deutman AF, Fishman M (1973) The cone degenerations. *Doc Ophthalmol* **35**:1-80

Krizman DB (1997) Gene isolation by exon trapping. In: Boulton J (ed) *Methods in molecular biology*. Humana Press Inc., Totowa, pp 167-183

Kubota R, Noda S, Wang Y, Minoshima S, Asakawa S, Kudoh J, Mashima Y, et al (1997) A novel myosin-like protein (myocilin) expressed in the connecting cilium of the photoreceptor: molecular cloning, tissue expression, and chromosomal mapping. *Genomics* **41**:360-9

Landrum JT, Bone RA, Joa H, Kilburn MD, Moore LL, Sprague KE (1997) A one year study of the macular pigment: the effect of 140 days of a lutein supplement. *Exp Eye Res* **65**:57-62

Larsen F, Gundersen G, Lopez R, Prydz H (1992) CpG islands as gene markers in the human genome. *Genomics* **13**:1095-107

Leighton DA (1976) Survey of the first-degree relatives of glaucoma patients. *Trans Ophthalmol Soc U K* **96**:28-32

Lewis RA, Shroyer NF, Singh N, Allikmets R, Hutchinson A, Li Y, Lupski JR, et al (1999) Genotype/Phenotype analysis of a photoreceptor-specific ATP-binding cassette transporter gene, ABCR, in Stargardt disease. *Am J Hum Genet* **64**:422-34

Li ZY, Jacobson SG, Milam AH (1994) Autosomal dominant retinitis pigmentosa caused by the threonine-17- methionine rhodopsin mutation: retinal histopathology and immunocytochemistry. *Exp Eye Res* **58**:397-408

Linari M, Ueffing M, Manson F, Wright A, Meitinger T, Becker J (1999) The retinitis pigmentosa GTPase regulator, RPGR, interacts with the delta subunit of rod cyclic GMP phosphodiesterase. *Proc Natl Acad Sci U S A* **96**:1315-20

Liu Q, Ji X, Breitman ML, Hitchcock PF, Swaroop A (1996) Expression of the bZIP transcription factor gene Nrl in the developing nervous system. *Oncogene* **12**:207-11

Liu X, Vansant G, Udovichenko IP, Wolfrum U, Williams DS (1997) Myosin VIIa, the product of the Usher 1B syndrome gene, is concentrated in the connecting cilia of photoreceptor cells. *Cell Motil Cytoskeleton* **37**:240-52

Loeffen JL, Triepels RH, van den Heuvel LP, Schuelke M, Buskens CA, Smeets RJ, Trijbels JM, et al (1998) cDNA of eight nuclear encoded subunits of NADH:ubiquinone oxidoreductase: human complex I cDNA characterization completed. *Biochem Biophys Res Commun* **253**:415-22

Luciani MF, Denizot F, Savary S, Mattei MG, Chimini G (1994) Cloning of two novel ABC transporters mapping on human chromosome 9. *Genomics* **21**:150-9

Lyness AL, Ernst W, Quinlan MP, Clover GM, Arden GB, Carter RM, Bird AC, et al (1985) A clinical, psychophysical, and electroretinographic survey of patients with autosomal dominant retinitis pigmentosa. *Br J Ophthalmol* **69**:326-39

Lynn S, Wardell T, Johnson MA, Chinnery PF, Daly ME, Walker M, Turnbull DM (1998) Mitochondrial diabetes: investigation and identification of a novel mutation. *Diabetes* **47**:1800-2

Mainzer F, Saldino RM, Ozonoff MB, Minagi H (1970) Familial nephropathy associated with retinitis pigmentosa, cerebellar ataxia and skeletal abnormalities. *Am J Med* **49**:556-62

Maniatis T, Fritsh EF, Sambrook J (1992) Molecular cloning; a laboratory manual. Cold Spring Harbour Laboratory, New York

Mansergh FC (1997) On the molecular genetics of inherited retinopathies and glaucoma. PhD thesis, University of Dublin, Trinity College

Mansergh FC, Kenna PF, Ayuso C, Kiang A-S, Humphries P, Farrar GJ (1997) Two novel mutations in the TIGR gene in primary open angle glaucoma. *Am J Hum Genet* **61**(4; supplement): abstract number 101

Mansergh FC, Kenna PF, Ayuso C, Kiang AS, Humphries P, Farrar GJ (1998) Novel mutations in the TIGR gene in early and late onset open angle glaucoma. *Hum Mutat* **11**:244-51

Mansergh FC, Millington-Ward S, Kennan A, Kiang AS, Humphries M, Farrar GJ, Humphries P, et al (1999) Retinitis Pigmentosa and Progressive Sensorineural Hearing Loss Caused by a C12258A Mutation in the Mitochondrial MTTS2 Gene. *Am J Hum Genet* **64**:971-985

Margulis L (1981) Symbiosis in cell evolution. Freeman, San Francisco

Mariotti C, Tiranti V, Carrara F, Dallapiccola B, DiDonato S, Zeviani M (1994) Defective respiratory capacity and mitochondrial protein synthesis in transformant cybrids harboring the tRNA(Leu(UUR)) mutation associated with maternally inherited myopathy and cardiomyopathy. *J Clin Invest* **93**:1102-7

Marlhens F, Bareil C, Griffoin JM, Zrenner E, Amalric P, Eliaou C, Liu SY, et al (1997) Mutations in RPE65 cause Leber's congenital amaurosis [letter]. *Nat Genet* **17**:139-41

Marra MA, Hillier L, Waterston RH (1998) Expressed sequence tags--ESTablishing bridges between genomes. *Trends Genet* **14**:4-7

Marshfield Center for Medical Genetics homepage (1999) [Internet] 23-9-1999.

Available from: < <http://www.marshmed.org/genetics> > [Accessed 27th September 1999]

Martinez-Mir A, Paloma E, Allikmets R, Ayuso C, del Rio T, Dean M, Vilageliu L, et al (1998) Retinitis pigmentosa caused by a homozygous mutation in the Stargardt disease gene ABCR [letter; comment]. *Nat Genet* **18**:11-2

Masai I, Okazaki A, Hosoya T, Hotta Y (1993) Drosophila retinal degeneration A gene encodes an eye-specific diacylglycerol kinase with cysteine-rich zinc-finger motifs and ankyrin repeats. *Proc Natl Acad Sci U S A* **90**:11157-61

Masai I, Suzuki E, Yoon CS, Kohyama A, Hotta Y (1997) Immunolocalization of Drosophila eye-specific diacylglycerol kinase, rdgA, which is essential for the maintenance of the photoreceptor. *J Neurobiol* **32**:695-706

Massof RW, Finkelstein D (1981) Two forms of autosomal dominant primary retinitis pigmentosa. *Doc Ophthalmol* **51**:289-346

Matsumoto E, Hirosawa K, Takagawa K, Hotta Y (1988) Structure of reticular cells in a Drosophila melanogaster visual mutant, rdgA, at early stages of degeneration. *Cell Tissue Res* **252**:293-300

Maugeri A, van Driel MA, van de Pol DJ, Klevering BJ, van Haren FJ, Tijmes N, Bergen AA, et al (1999) The 2588G-->C Mutation in the ABCR Gene Is a Mild Frequent Founder Mutation in the Western European Population and Allows the Classification of ABCR Mutations in Patients with Stargardt Disease. *Am J Hum Genet* **64**:1024-1035

Maw MA, Kennedy B, Knight A, Bridges R, Roth KE, Mani EJ, Mukkadan JK, et al (1997) Mutation of the gene encoding cellular retinaldehyde-binding protein in autosomal recessive retinitis pigmentosa. *Nat Genet* **17**:198-200

McGuire RE, Sullivan LS, Blanton SH, Church MW, Heckenlively JR, Daiger SP (1995a) X-linked dominant cone-rod degeneration: linkage mapping of a new locus for retinitis pigmentosa (RP 15) to Xp22.13-p22.11 [see comments]. *Am J Hum Genet* **57**:87-94

McGuire RE, Gannon AM, Sullivan LS, Rodriguez JA, Daiger SP (1995b) Evidence for a major gene (RP10) for autosomal dominant retinitis pigmentosa on chromosome 7q: linkage mapping in a second, unrelated family. *Hum Genet* **95**:71-4

McGuire RE, Jordan SA, Braden VV, Bouffard GG, Humphries P, Green ED, Daiger SP (1996a) Mapping the RP10 locus for autosomal dominant retinitis pigmentosa on 7q: refined genetic positioning and localization within a well-defined YAC contig. *Genome Res* **6**:255-66

McGuire RE. (1996b) The story of RP10: a positional cloning approach to the identification of an autosomal dominant Retinitis Pigmentosa gene. Ph.D thesis, University of Texas, Health Science Center, Houston

McIntosh I, Lichter PR, Clough MV, Roig CM, Wong D., Scott C, Downs C., Stringham H, et al (1987) Glaucoma and nail-patella syndrome (NPS) cosegregate: One gene or two? *Am J Hum Genet* **61**(4; supplement): abstract number 58

McLaughlin ME, Sandberg MA, Berson EL, Dryja TP (1993) Recessive mutations in the gene encoding the beta-subunit of rod phosphodiesterase in patients with retinitis pigmentosa. *Nat Genet* **4**:130-4

McNally N, Kenna P, Humphries MM, Hobson AH, Khan NW, Bush RA, Sieving PA, et al (1999) Structural and functional rescue of murine rod photoreceptors by human rhodopsin transgene. *Hum Mol Genet* **8**:1309-12

McWilliam P, Farrar GJ, Kenna P, Bradley DG, Humphries MM, Sharp EM, McConnell DJ, et al (1989) Autosomal dominant retinitis pigmentosa (ADRP): localization of an ADRP gene to the long arm of chromosome 3. *Genomics* **5**:619-22

Mears AJ, Mirzayans F, Gould DB, Pearce WG, Walter MA (1996) Autosomal dominant iridogoniodysgenesis anomaly maps to 6p25. *Am J Hum Genet* **59**:1321-7
Medzhitov R, Preston-Hurlburt P, Janeway CA, Jr. (1997) A human homologue of the Drosophila Toll protein signals activation of adaptive immunity [see comments]. *Nature* **388**:394-7

Meindl A, Dry K, Herrmann K, Manson F, Ciccodicola A, Edgar A, Carvalho MR, et al (1996) A gene (RPGR) with homology to the RCC1 guanine nucleotide exchange factor is mutated in X-linked retinitis pigmentosa (RP3). *Nat Genet* **13**:35-42

Melov S, Hinerfeld D, Esposito L, Wallace DC (1997) Multi-organ characterization of mitochondrial genomic rearrangements in ad libitum and caloric restricted mice show striking somatic mitochondrial DNA rearrangements with age. *Nucleic Acids Res* **25**:974-82

Meyer A, Valtot F, Bechetoille A, Rouland JF, Dascotte JC, Ferec C, Bach JF, et al (1994) [Linkage between juvenile glaucoma and chromosome 1q in 2 French families]. *C R Acad Sci III* **317**:565-70

Meyer A, Bechetoille A, Valtot F, Dupont de Dinechin S, Adam MF, Belmouden A, Brezin AP, et al (1996) Age-dependent penetrance and mapping of the locus for juvenile and early-onset open-angle glaucoma on chromosome 1q (GLC1A) in a French family. *Hum Genet* **98**:567-71

Meyers SM, Greene T, Gutman FA (1995) A twin study of age-related macular degeneration. *Am J Ophthalmol* **120**:757-66

Michaelis S, Berkower C (1995) Sequence comparison of yeast ATP binding cassette (ABC) proteins. *Protein Kinesis - the dynamics of protein trafficking and stability*. Vol. LX: *Cold Spring Harbour symposium on quantitative biology*. Cold Spring Harbour Laboratory Press, New York

Michels-Rautenstrauss K, Mardin CY, Budde WM, Liehr T, Timmerman V, Van Broekhoven C, et al (1997) Autosomal dominant juvenile open angle glaucoma (GLC1A): fine mapping of the TIGR gene to 1q24.3-25.2 and identification of a novel mutation in a German family. *Am J Hum Genet* **61**(4; supplement): abstract number 1992

Millan JM, Martinez F, Vilela C, Beneyto M, Prieto F, Najera C (1995) An autosomal dominant retinitis pigmentosa family with close linkage to D7S480 on 7q. *Hum Genet* **96**:216-8

Mitchell P, Smith W, Wang JJ (1998) Iris color, skin sun sensitivity, and age-related maculopathy. The Blue Mountains Eye Study. *Ophthalmology* **105**:1359-63

Mohamed Z, Bell C, Hammer HM, Converse CA, Esakowitz L, Haites NE (1996) Linkage of a medium sized Scottish autosomal dominant retinitis pigmentosa family to chromosome 7q. *J Med Genet* **33**:714-5

Molday RS (1998) Photoreceptor membrane proteins, phototransduction, and retinal degenerative diseases. The Friedenwald Lecture. *Invest Ophthalmol Vis Sci* **39**:2491-513

- Morimura H, Fishman GA, Grover SA, Fulton AB, Berson EL, Dryja TP (1998) Mutations in the RPE65 gene in patients with autosomal recessive retinitis pigmentosa or leber congenital amaurosis. *Proc Natl Acad Sci U S A* **95**:3088-93
- Morissette J, Cote G, Anctil JL, Plante M, Amyot M, Heon E, Trope GE, et al (1995) A common gene for juvenile and adult-onset primary open-angle glaucomas confined on chromosome 1q [see comments]. *Am J Hum Genet* **56**:1431-42
- Morissette J, Falardeau P, Dubois S, Bergeron J, Vonck., Cote G, Anctil J-L, et al (1997) A common gene for developmental and familial open angle glaucomas confined on chromosome 6p25. *Am J Hum Genet* **61**(4; supplement): abstract number 1670.
- Morten KJ, Cooper JM, Brown GK, Lake BD, Pike D, Poulton J (1993) A new point mutation associated with mitochondrial encephalomyopathy. *Hum Mol Genet* **2**:2081-7
- Mosewich RK, Donat JR, DiMauro S, Ciafaloni E, Shanske S, Erasmus M, George D (1993) The syndrome of mitochondrial encephalomyopathy, lactic acidosis, and strokelike episodes presenting without stroke. *Arch Neurol* **50**:275-8
- Mosser J, Douar AM, Sarde CO, Kioschis P, Feil R, Moser H, Poustka AM, et al (1993) Putative X-linked adrenoleukodystrophy gene shares unexpected homology with ABC transporters [see comments]. *Nature* **361**:726-30
- Murray JC, Bennett SR, Kwitek AE, Small KW, Schinzel A, Alward WL, Weber JL, et al (1992) Linkage of Rieger syndrome to the region of the epidermal growth factor gene on chromosome 4. *Nat Genet* **2**:46-9
- Musarella MA, Anson-Cartwright L, Leal SM, Gilbert LD, Worton RG, Fishman GA, Ott J (1990) Multipoint linkage analysis and heterogeneity testing in 20 X-linked retinitis pigmentosa families. *Genomics* **8**:286-96
- Naash ML, Peachey NS, Li ZY, Gryczan CC, Goto Y, Blanks J, Milam AH, et al (1996) Light-induced acceleration of photoreceptor degeneration in transgenic mice expressing mutant rhodopsin. *Invest Ophthalmol Vis Sci* **37**:775-82

Nakajima M, Yuge K, Senzaki H, Shikata N, Miki H, Uyama M, Tsubura A (1996) Photoreceptor apoptosis induced by a single systemic administration of N-methyl-N-nitrosourea in the rat retina. *Am J Pathol* **148**:631-41

Nakamura M, Nakano S, Goto Y, Ozawa M, Nagahama Y, Fukuyama H, Akiguchi I, et al (1995) A novel point mutation in the mitochondrial tRNA(Ser(UCN)) gene detected in a family with MERRF/MELAS overlap syndrome. *Biochem Biophys Res Commun* **214**:86-93

Nakamura TM, Morin GB, Chapman KB, Weinrich SL, Andrews WH, Lingner J, Harley CB, et al (1997) Telomerase catalytic subunit homologs from fission yeast and human [see comments]. *Science* **277**:955-9

Nakase H, Moraes CT, Rizzuto R, Lombes A, DiMauro S, Schon EA (1990) Transcription and translation of deleted mitochondrial genomes in Kearns-Sayre syndrome: implications for pathogenesis. *Am J Hum Genet* **46**:418-27

Nasonkin I, Illing M, Koehler MR, Schmid M, Molday RS, Weber BH (1998) Mapping of the rod photoreceptor ABC transporter (ABCR) to 1p21-p22.1 and identification of novel mutations in Stargardt's disease. *Hum Genet* **102**:21-6

Nathans J, Maumenee IH, Zrenner E, Sadowski B, Sharpe LT, Lewis RA, Hansen E, et al (1993) Genetic heterogeneity among blue-cone monochromats. *Am J Hum Genet* **53**:987-1000

National Human Genome Research Institute (1999) Human chromosome 7 mapping and sequencing [Internet] 7-7-1999. Available from: < <http://genome.nhgri.nih.gov/>> [Accessed 20th August 1999]

Nawy S, Jahr CE (1990) Suppression by glutamate of cGMP-activated conductance in retinal bipolar cells. *Nature* **346**:269-71

Newell F (1982) *Ophthalmology; principles and concepts*. C. V. Mosby Company, Missouri

Newman NJ, Lott MT, Wallace DC (1991) The clinical characteristics of pedigrees of Leber's hereditary optic neuropathy with the 11778 mutation. *Am J Ophthalmol* **111**:750-62

Nichols BE, Drack AV, Vandeburgh K, Kimura AE, Sheffield VC, Stone EM (1993) A 2 base pair deletion in the RDS gene associated with butterfly-shaped pigment dystrophy of the fovea [published erratum appears in *Hum Mol Genet* 1993 Aug;2(8):1347]. *Hum Mol Genet* **2**:601-3

Nishimura DY, Patil S, Alward WLM, Stone EM, Sheffield VC (1995) Fine mapping of the chromosomal breakpoints in an individual with congenital glaucoma and a 6:13 translocation. *Invest Ophthalmol Vis Sci* **36**:2574

Noell WK, Walker VS, Kang BS, Berman S (1966) Retinal damage by light in rats. *Invest Ophthalmol* **5**:450-73

Nomura A, Shigemoto R, Nakamura Y, Okamoto N, Mizuno N, Nakanishi S (1994) Developmentally regulated postsynaptic localization of a metabotropic glutamate receptor in rat rod bipolar cells. *Cell* **77**:361-9

Nussbaum RL, Lewis RA, Lesko JG, Ferrell R (1985) Mapping X-linked ophthalmic diseases: II. Linkage relationship of X-linked retinitis pigmentosa to X chromosomal short arm markers. *Hum Genet* **70**:45-50

Ohlemiller KK, Hughes RM, Mosinger-Ogilvie J, Speck JD, Grosfeld DH, Silverman MS (1995) Cochlear and retinal degeneration in the tubby mouse. *Neuroreport* **6**:845-9

Ott J, Bhattacharya S, Chen JD, Denton MJ, Donald J, Dubay C, Farrar GJ, et al (1990) Localizing multiple X chromosome-linked retinitis pigmentosa loci using multilocus homogeneity tests. *Proc Natl Acad Sci U S A* **87**:701-4

Ott J (1991) Analysis of human genetic linkage. John Hopkins University Press, Baltimore

Palczewski K, Saari JC (1997) Activation and inactivation steps in the visual transduction pathway. *Curr Opin Neurobiol* **7**:500-4

Payne AM, Downes SM, Bessant DA, Taylor R, Holder GE, Warren MJ, Bird AC, et al (1998) A mutation in guanylate cyclase activator 1A (GUCA1A) in an autosomal dominant cone dystrophy pedigree mapping to a new locus on chromosome 6p21.1. *Hum Mol Genet* **7**:273-7

Pearlman JT, Flood TP, Seiff SR (1976) Retinitis pigmentosa without pigment. *Am J Ophthalmol* **81**:417-9

Penfold PL, Provis JM (1986) Cell death in the development of the human retina: phagocytosis of pyknotic and apoptotic bodies by retinal cells. *Graefes Arch Clin Exp Ophthalmol* **224**:549-53

Perrault I, Rozet JM, Calvas P, Gerber S, Camuzat A, Dollfus H, Chatelin S, et al (1996) Retinal-specific guanylate cyclase gene mutations in Leber's congenital amaurosis. *Nat Genet* **14**:461-4

Phillips JC, del Bono EA, Haines JL, Pralea AM, Cohen JS, Greff LJ, Wiggs JL (1996) A second locus for Rieger syndrome maps to chromosome 13q14. *Am J Hum Genet* **59**:613-9

Pin JP, Duvoisin R (1995) The metabotropic glutamate receptors: structure and functions. *Neuropharmacology* **34**:1-26

Polansky JR, Fauss DJ, Chen P, Chen H, Lutjen-Drecoll E, Johnson D, Kurtz RM, et al (1997) Cellular pharmacology and molecular biology of the trabecular meshwork inducible glucocorticoid response gene product. *Ophthalmologica* **211**:126-39

Portera-Cailliau C, Sung CH, Nathans J, Adler R (1994) Apoptotic photoreceptor cell death in mouse models of retinitis pigmentosa. *Proc Natl Acad Sci U S A* **91**:974-8

Prezant TR, Agopian JV, Bohlman MC, Bu X, Oztas S, Qiu WQ, Arnos KS, et al (1993) Mitochondrial ribosomal RNA mutation associated with both antibiotic- induced and non-syndromic deafness. *Nat Genet* **4**:289-94

Quigley HA (1996) Number of people with glaucoma worldwide [see comments]. *Br J Ophthalmol* **80**:389-93

Rao VR, Cohen GB, Oprian DD (1994) Rhodopsin mutation G90D and a molecular mechanism for congenital night blindness. *Nature* **367**:639-42

Raymond V (1997) Molecular genetics of the glaucomas: mapping of the first five "GLC" loci [editorial; comment]. *Am J Hum Genet* **60**:272-7

Redmond TM, Yu S, Lee E, Bok D, Hamasaki D, Chen N, Goletz P, et al (1998) Rpe65 is necessary for production of 11-cis-vitamin A in the retinal visual cycle. *Nat Genet* **20**:344-51

Reid FM, Vernham GA, Jacobs HT (1994) A novel mitochondrial point mutation in a maternal pedigree with sensorineural deafness. *Hum Mutat* **3**:243-7

Reme CE, Weller M, Szczesny P, Munz K, Hafezi F, Reinboth JJ, Clausen M (1995) Light-induced apoptosis in the rat retina *in vivo*: morphological features, threshold and time course. In: Anderson RE, LaVail MM, Hollyfield JG (eds) *Retinal degeneration*. Plenum Press, New York and London, pp 19-25

- Richards JE, Lichter PR, Boehnke M, Uro JL, Torrez D, Wong D, Johnson AT (1994) Mapping of a gene for autosomal dominant juvenile-onset open-angle glaucoma to chromosome 1q. *Am J Hum Genet* **54**:62-70
- Riordan JR, Rommens JM, Kerem B, Alon N, Rozmahel R, Grzelczak Z, Zielenski J, et al (1989) Identification of the cystic fibrosis gene: cloning and characterization of complementary DNA [published erratum appears in Science 1989 Sep 29;245(4925):1437]. *Science* **245**:1066-73
- Riordan-Eva P, Harding AE (1995) Leber's hereditary optic neuropathy: the clinical relevance of different mitochondrial DNA mutations. *J Med Genet* **32**:81-7
- Roberts RG, Barby TF, Manners E, Bobrow M, Bentley DR (1991) Direct detection of dystrophin gene rearrangements by analysis of dystrophin mRNA in peripheral blood lymphocytes. *Am J Hum Genet* **49**:298-310
- Rosenfeld PJ, Cowley GS, McGee TL, Sandberg MA, Berson EL, Dryja TP (1992) A null mutation in the rhodopsin gene causes rod photoreceptor dysfunction and autosomal recessive retinitis pigmentosa. *Nat Genet* **1**:209-13
- Rotig A, de Lonlay P, Chretien D, Foury F, Koenig M, Sidi D, Munnich A, et al (1997) Aconitase and mitochondrial iron-sulphur protein deficiency in Friedreich ataxia. *Nat Genet* **17**:215-7
- Rozet JM, Gerber S, Souied E, Perrault I, Chatelin S, Ghazi I, Leowski C, et al (1998) Spectrum of ABCR gene mutations in autosomal recessive macular dystrophies [published erratum appears in Eur J Hum Genet 1999 Jan;7(1):102]. *Eur J Hum Genet* **6**:291-5
- Rozet JM, Gerber S, Ducroq D, Ghazi I, Souied E, Kaplan J (1999) Extensive screening of the ABCR gene in a large panel of French patients affected with different retinal disorders. *Invest Ophthalmol vis sci* **40**(4): abstract number 4087

Rozmahel R, Wilschanski M, Matin A, Plyte S, Oliver M, Auerbach W, Moore A, et al (1996) Modulation of disease severity in cystic fibrosis transmembrane conductance regulator deficient mice by a secondary genetic factor [published erratum appears in *Nat Genet* 1996 May;13(1):129]. *Nat Genet* **12**:280-7

Ruiz A, Borrego S, Marcos I, Antinolo G (1998) A major locus for autosomal recessive retinitis pigmentosa on 6q, determined by homozygosity mapping of chromosomal regions that contain gamma-aminobutyric acid-receptor clusters. *Am J Hum Genet* **62**:1452-9

Sakane F, Yamada K, Kanoh H, Yokoyama C, Tanabe T (1990) Porcine diacylglycerol kinase sequence has zinc finger and E-F hand motifs. *Nature* **344**:345-8

Sakane F, Imai S, Kai M, Wada I, Kanoh H (1996) Molecular cloning of a novel diacylglycerol kinase isozyme with a pleckstrin homology domain and a C-terminal tail similar to those of the EPH family of protein-tyrosine kinases. *J Biol Chem* **271**:8394-401

Sankila EM, Pakarinen L, Kaariainen H, Aittomaki K, Karjalainen S, Sistonen P, de la Chapelle A (1995) Assignment of an Usher syndrome type III (USH3) gene to chromosome 3q. *Hum Mol Genet* **4**:93-8

Santorelli FM, Mak SC, El-Schahawi M, Casali C, Shanske S, Baram TZ, Madrid RE, et al (1996) Maternally inherited cardiomyopathy and hearing loss associated with a novel mutation in the mitochondrial tRNA(Lys) gene (G8363A). *Am J Hum Genet* **58**:933-9

Sarfarazi M, Akarsu AN, Hossain A, Turacli ME, Aktan SG, Barsoum-Homsy M, Chevrette L, et al (1995) Assignment of a locus (GLC3A) for primary congenital glaucoma (Buphthalmos) to 2p21 and evidence for genetic heterogeneity. *Genomics* **30**:171-7

Sarfarazi M (1997) Recent advances in molecular genetics of glaucomas. *Hum Mol Genet* **6**:1667-77

Sarfarazi M, Child A, Stoilova D, Brice G, Desai T, Trifan OC, Poinosawmy D, et al (1998) Localization of the fourth locus (GLC1E) for adult-onset primary open-angle glaucoma to the 10p15-p14 region. *Am J Hum Genet* **62**:641-52

Schapira AH (1998) Mitochondrial dysfunction in neurodegenerative disorders. *Biochim Biophys Acta* **1366**:225-33

Scherer SW, Feinstein DS, Oliveira L, Tsui LC, Pittler SJ (1996a) Gene structure and chromosome localization to 7q21.3 of the human rod photoreceptor transducin gamma-subunit gene (GNGT1). *Genomics* **35**:241-3

Scherer SW, Duvoisin RM, Kuhn R, Heng HH, Belloni E, Tsui LC (1996b) Localization of two metabotropic glutamate receptor genes, GRM3 and GRM8, to human chromosome 7q. *Genomics* **31**:230-3

Scherer SW, Soder S, Duvoisin RM, Huizenga JJ, Tsui LC (1997) The human metabotropic glutamate receptor 8 (GRM8) gene: a disproportionately large gene located at 7q31.3-q32.1. *Genomics* **44**:232-6

Schiller PH (1992) The ON and OFF channels of the visual system. *Trends Neurosci* **15**:86-92

Schuler GD, Boguski MS, Stewart EA, Stein LD, Gyapay G, Rice K, White RE, et al (1996) A gene map of the human genome. *Science* **274**:540-6

Schulz JB, Klockgether T, Dichgans J, Seibel P, Reichmann H (1993) Mitochondrial gene mutations and diabetes mellitus [letter; comment]. *Lancet* **341**:438-9

Schwahn U, Lenzner S, Dong J, Feil S, Hinzmann B, van Duijnhoven G, Kirschner R, et al (1998) Positional cloning of the gene for X-linked retinitis pigmentosa 2 [see comments]. *Nat Genet* **19**:327-32

- Seddon JM, Ajani UA, Mitchell BD (1997) Familial aggregation of age-related maculopathy [see comments]. *Am J Ophthalmol* **123**:199-206
- Semina EV, Reiter R, Leysens NJ, Alward WL, Small KW, Datson NA, Siegel-Bartelt J, et al (1996) Cloning and characterization of a novel bicoid-related homeobox transcription factor gene, RIEG, involved in Rieger syndrome. *Nat Genet* **14**:392-9
- Shastry BS (1994) Retinitis pigmentosa and related disorders: phenotypes of rhodopsin and peripherin/RDS mutations. *Am J Med Genet* **52**:467-74
- Sheffield VC, Stone EM, Alward WL, Drack AV, Johnson AT, Streb LM, Nichols BE (1993) Genetic linkage of familial open angle glaucoma to chromosome 1q21-q31. *Nat Genet* **4**:47-50
- Shimozawa N, Tsukamoto T, Suzuki Y, Orii T, Shirayoshi Y, Mori T, Fujiki Y (1992) A human gene responsible for Zellweger syndrome that affects peroxisome assembly. *Science* **255**:1132-4
- Shoffner JM, Lott MT, Lezza AM, Seibel P, Ballinger SW, Wallace DC (1990) Myoclonic epilepsy and ragged-red fiber disease (MERRF) is associated with a mitochondrial DNA tRNA(Lys) mutation. *Cell* **61**:931-7
- Shoffner JM, Wallace DC (1992) Mitochondrial genetics: principles and practice [editorial]. *Am J Hum Genet* **51**:1179-86
- Shoffner JM, Brown MD, Torroni A, Lott MT, Cabell MF, Mirra SS, Beal MF, et al (1993) Mitochondrial DNA variants observed in Alzheimer disease and Parkinson disease patients. *Genomics* **17**:171-84
- Shoffner JM, Brown MD, Stugard C, Jun AS, Pollock S, Haas RH, Kaufman A, et al (1995) Leber's hereditary optic neuropathy plus dystonia is caused by a mitochondrial DNA point mutation. *Ann Neurol* **38**:163-9

Shoffner JM, Wallace DC (1995) The metabolic and molecular basis of inherited disease. McGraw-Hill, New York

Shroyer NF, Lewis RA, Allikmets R, Singh N, Dean M, Leppert M, Lupski JR (1999) The rod photoreceptor ATP-binding cassette transporter gene, ABCR, and retinal disease: from monogenic to multifactorial. *Vision Res* **39**:2537-44

Shroyer NF, Lewis RA, Lupski JR (1999) Cosegregation of ABCR mutations in families which manifest Stargardt Disease and age-related macular degeneration. *Invest. Ophthalmol vis sci* **40**(4): abstract number 4090

Siadat-Pajouh M, Ayscue AH, Periasamy A, Herman B (1994) Introduction of a fast and sensitive fluorescent in situ hybridization method for single-copy detection of human papillomavirus (HPV) genome. *J Histochem Cytochem* **42**:1503-12

Silvestri G, Johnston PB, Hughes AE (1994a) Is genetic predisposition an important risk factor in age-related macular degeneration? *Eye* **8**:564-8

Silvestri G, Santorelli FM, Shanske S, Whitley CB, Schimmenti LA, Smith SA, DiMauro S (1994b) A new mtDNA mutation in the tRNA(Leu(UUR)) gene associated with maternally inherited cardiomyopathy. *Hum Mutat* **3**:37-43

Simon A, Hellman U, Wernstedt C, Eriksson U (1995) The retinal pigment epithelial-specific 11-cis retinol dehydrogenase belongs to the family of short chain alcohol dehydrogenases. *J Biol Chem* **270**:1107-12

Siregar NC, Jean-Francois MJ, Blok RB, Byrne E (1998) Genotypic and phenotypic changes in exhaustively grown cell lines from mitochondrial cytopathy patients. *Muscle Nerve* **21**:599-609

Sirinathsinghiji DJS, Dunnett SB (1993) Imaging gene expression in neural grafts. In: Sharif NA (ed) *Molecular imaging in neuroscience*. IRL Press at Oxford University Press, Oxford

- Skatchkov SN, Krusek J, Reichenbach A, Orkand RK (1999) Potassium buffering by Muller cells isolated from the center and periphery of the frog retina. *Glia* **27**:171-180
- Small KW (1998) North Carolina macular dystrophy: clinical features, genealogy, and genetic linkage analysis. *Trans Am Ophthalmol Soc* **96**:925-61
- Smith RJ, Lee EC, Kimberling WJ, Daiger SP, Pelias MZ, Keats BJ, Jay M, et al (1992) Localization of two genes for Usher syndrome type I to chromosome 11. *Genomics* **14**:995-1002
- Smith OP, Hann IM, Woodward CE, Brockington M (1995) Pearson's marrow/pancreas syndrome: haematological features associated with deletion and duplication of mitochondrial DNA. *Br J Haematol* **90**:469-72
- Snell RG (1996) The isolation of cDNAs by hybridization of YACs to cDNA libraries. *Methods Mol Biol* **54**:329-36
- Sohocki MM, Sullivan LS, Mintz-Hittner HA, Birch D, Heckenlively JR, Freund CL, McInnes RR, et al (1998) A range of clinical phenotypes associated with mutations in CRX, a photoreceptor transcription-factor gene. *Am J Hum Genet* **63**:1307-15
- Sokal I, Li N, Surgucheva I, Warren MJ, Payne AM, Bhattacharya SS, Baehr W, et al (1998) GCAP1 (Y99C) mutant is constitutively active in autosomal dominant cone dystrophy. *Mol Cell* **2**:129-33
- Stecher H, Gelb MH, Saari JC, Palczewski K (1999) Preferential release of 11-cis-retinol from retinal pigment epithelial cells in the presence of cellular retinaldehyde-binding protein. *J Biol Chem* **274**:8577-85
- Steinberg RH, Fisher SK, Anderson DH (1980) Disc morphogenesis in vertebrate photoreceptors. *J Comp Neurol* **190**:501-8

- Stoilov I, Akarsu AN, Sarfarazi M (1997) Identification of three different truncating mutations in cytochrome P4501B1 (CYP1B1) as the principal cause of primary congenital glaucoma (Buphthalmos) in families linked to the GLC3A locus on chromosome 2p21. *Hum Mol Genet* **6**:641-7
- Stoilova D, Child A, Trifan OC, Crick RP, Coakes RL, Sarfarazi M (1996) Localization of a locus (GLC1B) for adult-onset primary open angle glaucoma to the 2cen-q13 region. *Genomics* **36**:142-50
- Stoilova D, Child A, Brice G, Crick RP, Fleck BW, Sarfarazi M (1997) Identification of a new 'TIGR' mutation in a family with juvenile-onset primary open angle glaucoma. *Ophthalmic Genet* **18**:109-18
- Stone EM, Fingert JH, Alward WLM, Nguyen TD, Polansky JR, Sunden SLF, Nishimura D, et al (1997) Identification of a gene that causes primary open angle glaucoma [see comments]. *Science* **275**:668-70
- Stone EM, Webster AR, Vandenburg K, Streb LM, Hockey RR, Lotery AJ, Sheffield VC (1998) Allelic variation in ABCR associated with Stargardt disease but not age-related macular degeneration [letter]. *Nat Genet* **20**:328-9
- Sudbery P (1998) Genetics. Addison Wesley Longman, Singapore
- Sullivan LS, Daiger SP (1996) Inherited retinal degeneration: exceptional genetic and clinical heterogeneity. *Mol Med Today* **2**:380-6
- Sun H, Molday RS, Nathans J (1999) Retinal stimulates ATP hydrolysis by purified and reconstituted ABCR, the photoreceptor-specific ATP-binding cassette transporter responsible for Stargardt disease. *J Biol Chem* **274**:8269-81
- Sunden SL, Alward WL, Nichols BE, Rokhlina TR, Nystuen A, Stone EM, Sheffield VC (1996) Fine mapping of the autosomal dominant juvenile open angle glaucoma (GLC1A) region and evaluation of candidate genes. *Genome Res* **6**:862-9

Sung CH, Davenport CM, Nathans J (1993) Rhodopsin mutations responsible for autosomal dominant retinitis pigmentosa. Clustering of functional classes along the polypeptide chain. *J Biol Chem* **268**:26645-9

Swain PK, Chen S, Wang QL, Affatigato LM, Coats CL, Brady KD, Fishman GA, et al (1997) Mutations in the cone-rod homeobox gene are associated with the cone-rod dystrophy photoreceptor degeneration. *Neuron* **19**:1329-36

Sweeney MG, Bunday S, Brockington M, Poulton KR, Winer JB, Harding AE (1993) Mitochondrial myopathy associated with sudden death in young adults and a novel mutation in the mitochondrial DNA leucine transfer RNA(UUR) gene. *Q J Med* **86**:709-13

Tang W, Bunting M, Zimmerman GA, McIntyre TM, Prescott SM (1996) Molecular cloning of a novel human diacylglycerol kinase highly selective for arachidonate-containing substrates. *J Biol Chem* **271**:10237-41

Tatuch Y, Christodoulou J, Feigenbaum A, Clarke JT, Wherret J, Smith C, Rudd N, et al (1992) Heteroplasmic mtDNA mutation (T----G) at 8993 can cause Leigh disease when the percentage of abnormal mtDNA is high [see comments]. *Am J Hum Genet* **50**:852-8

Taylor HR, Munoz B, West S, Bressler NM, Bressler SB, Rosenthal FS (1990) Visible light and risk of age-related macular degeneration. *Trans Am Ophthalmol Soc* **88**:163-73; discussion 173-8

Taylor EW, Xu J, Wang E, Meyers DA (1997) Linkage analysis of genetic disorders. In: Boulton J (ed) *Methods in molecular biology*. Humana Press Inc., Totowa, pp 11-25

Terwilliger JD, Ott J (1994) Handbook of human genetic linkage. John Hopkins University Press, Baltimore

TIGR human gene index (1999) [Internet] 23-3-1999. Available from:
<<http://www.tigr.org/tdb/hgi/hgi.html>> [Accessed 20th July 1999]

Tiranti V, Chariot P, Carella F, Toscano A, Soliveri P, Girlanda P, Carrara F, et al (1995) Maternally inherited hearing loss, ataxia and myoclonus associated with a novel point mutation in mitochondrial tRNASer(UCN) gene. *Hum Mol Genet* **4**:1421-7

Tomlinson IP, Neale K, Talbot IC, Spigelman AD, Williams CB, Phillips RK, Bodmer WF (1996) A modifying locus for familial adenomatous polyposis may be present on chromosome 1p35-p36. *J Med Genet* **33**:268-73

Torrioni A, Petrozzi M, D'Urbano L, Sellitto D, Zeviani M, Carrara F, Carducci C, et al (1997) Haplotype and phylogenetic analyses suggest that one European-specific mtDNA background plays a role in the expression of Leber hereditary optic neuropathy by increasing the penetrance of the primary mutations 11778 and 14484. *Am J Hum Genet* **60**:1107-21

Travis GH, Brennan MB, Danielson PE, Kozak CA, Sutcliffe JG (1989) Identification of a photoreceptor-specific mRNA encoded by the gene responsible for retinal degeneration slow (rds). *Nature* **338**:70-3

Travis GH (1998) Mechanisms of cell death in the inherited retinal degenerations. *Am J Hum Genet* **62**:503-8

Trifan OC, Traboulsi EI, Stoilova D, Alozie I, Nguyen R, Raja S, Sarfarazi M (1998) A third locus (GLC1D) for adult-onset primary open-angle glaucoma maps to the 8q23 region. *Am J Ophthalmol* **126**:17-28

Trounce I, Neill S, Wallace DC (1994) Cytoplasmic transfer of the mtDNA nt 8993 T-->G (ATP6) point mutation associated with Leigh syndrome into mtDNA-less cells demonstrates cosegregation with a decrease in state III respiration and ADP/O ratio. *Proc Natl Acad Sci U S A* **91**:8334-8

Tso MO, Zhang C, Abler AS, Chang CJ, Wong F, Chang GQ, Lam TT (1994) Apoptosis leads to photoreceptor degeneration in inherited retinal dystrophy of RCS rats. *Invest Ophthalmol Vis Sci* **35**:2693-9

UniGene build procedure (1999) In: *NCBI homepage* [Internet] 28-6-1999. Available from: <<http://www.ncbi.nlm.nih.gov/UniGene/build.html>> [Accessed 1st September 1999]

UniGene System (1999) In: *NCBI homepage* [Internet] 17-9-1999. Available from: <<http://www.ncbi.nlm.nih.gov/UniGene/index.html>> [Accessed 1st September 1999]

Upadhy P, Churchill G, Birkenmeier EH, Barker JE, Frankel WN (1999) Genetic modifiers of polycystic kidney disease in intersubspecific KAT2J mutants. *Genomics* **58**:129-37

Valdes J, Tagle A (1997) Gene mapping goes from FISH to surfing the net. In: Boultonwood J (ed) *Methods in molecular biology*. Humana Press Inc., Totowa, pp 1-10

van den Ouweland JM, Lemkes HH, Ruitenbeek W, Sandkuijl LA, de Vijlder MF, Struyvenberg PA, van de Kamp JJ, et al (1992) Mutation in mitochondrial tRNA(Leu)(UUR) gene in a large pedigree with maternally transmitted type II diabetes mellitus and deafness. *Nat Genet* **1**:368-71

van Soest S, Ingeborgh van den Born L, Gal A, Farrar GJ, Bleeker-Wagemakers LM, Westerveld A, Humphries P, et al (1994) Assignment of a gene for autosomal recessive retinitis pigmentosa (RP12) to chromosome 1q31-q32.1 in an inbred and genetically heterogeneous disease population. *Genomics* **22**:499-504

van Soest S, Westerveld A, de Jong PT, Bleeker-Wagemakers EM, Bergen AA (1999) Retinitis pigmentosa: defined from a molecular point of view. *Surv Ophthalmol* **43**:321-34

Wald G (1968) The molecular basis of visual excitation. *Nature* **219**:800-7

Wallace DC, Lott MT, Shoffner JM, Ballinger S (1994) Mitochondrial DNA mutations in epilepsy and neurological disease. *Epilepsia* supplement **1**:S43-S50.

Wallace DC, Lott MT, Browne MD, Huoponen K, Torroni A (1995) Report of the committee on human mitochondrial DNA. In: Cuticchia AJ (ed) *Human gene mapping 1995: a compendium*. John Hopkins University Press, Baltimore, pp 910-954

Wallace DC, Browne MD, Lott MT (1996) Mitochondrial genetics. In: Rimoin DL, Connor JM, Pyeritz RE, Emery AEH (eds) *Emery and Rimoin's principles and practice of medical genetics*. Churchill Livingstone, London, pp 277-332

Wallace DC (1999) Mitochondrial diseases in man and mouse. *Science* **283**:1482-8

Walther C, Guenet JL, Simon D, Deutsch U, Jostes B, Goulding MD, Plachov D, et al (1991) Pax: a murine multigene family of paired box-containing genes. *Genomics* **11**:424-34

Wayne S, Der Kaloustian VM, Schloss M, Polomeno R, Scott DA, Hejtmancik JF, Sheffield VC, et al (1996) Localization of the Usher syndrome type ID gene (Ush1D) to chromosome 10. *Hum Mol Genet* **5**:1689-92

Weaver RF, Hedrick PW (1981) Genetics. Wm. C. Browne, Dubuque

Weber K, Wilson JN, Taylor L, Brierley E, Johnson MA, Turnbull DM, Bindoff LA (1997) A new mtDNA mutation showing accumulation with time and restriction to skeletal muscle. *Am J Hum Genet* **60**:373-80

Weil D, Blanchard S, Kaplan J, Guilford P, Gibson F, Walsh J, Mburu P, et al (1995) Defective myosin VIIA gene responsible for Usher syndrome type 1B. *Nature* **374**:60-1

Weil D, Levy G, Sahly I, Levi-Acobas F, Blanchard S, El-Amraoui A, Crozet F, et al (1996) Human myosin VIIA responsible for the Usher 1B syndrome: a predicted membrane-associated motor protein expressed in developing sensory epithelia. *Proc Natl Acad Sci U S A* **93**:3232-7

Weitz CJ, Miyake Y, Shinzato K, Montag E, Zrenner E, Went LN, Nathans J (1992) Human tritanopia associated with two amino acid substitutions in the blue-sensitive opsin. *Am J Hum Genet* **50**:498-507

Weleber RG, Carr RE, Murphey WH, Sheffield VC, Stone EM (1993) Phenotypic variation including retinitis pigmentosa, pattern dystrophy, and fundus flavimaculatus in a single family with a deletion of codon 153 or 154 of the peripherin/RDS gene. *Arch Ophthalmol* **111**:1531-42

Wells J, Wroblewski J, Keen J, Inglehearn C, Jubb C, Eckstein A, Jay M, et al (1993) Mutations in the human retinal degeneration slow (RDS) gene can cause either retinitis pigmentosa or macular dystrophy [see comments]. *Nat Genet* **3**:213-8

West SK, Rosenthal FS, Bressler NM, Bressler SB, Munoz B, Fine SL, Taylor HR (1989) Exposure to sunlight and other risk factors for age-related macular degeneration [see comments]. *Arch Ophthalmol* **107**:875-9

Wiggs JL, Haines JL, Paglinauan C, Fine A, Sporn C, Lou D (1994) Genetic linkage of autosomal dominant juvenile glaucoma to 1q21-q31 in three affected pedigrees. *Genomics* **21**:299-303

Wiggs JL, Allingham RR, Vollrath D, Jones K, Delapaz M, Reardon M, Del Bono EA, et al (1997) Frequency of mutations in TIGR in families with juvenile and adult onset primary open angle glaucoma. *Am J Hum Genet* **61**(4; supplement): abstract number 2054

Wilkinson DG (1992) The theory and practice of *in situ* hybridization. In: Wilkinson DG (ed) *In situ hybridization; a practical approach*. IRL Press at Oxford University Press, Oxford, pp 1-13

Wirtz MK, Samples JR, Kramer PL, Rust K, Topinka JR, Yount J, Koler RD, et al (1997) Mapping a gene for adult-onset primary open-angle glaucoma to chromosome 3q [see comments]. *Am J Hum Genet* **60**:296-304

Wolfs RC, Klaver CC, Ramrattan RS, van Duijn CM, Hofman A, de Jong PT (1998) Genetic risk of primary open-angle glaucoma. Population-based familial aggregation study. *Arch Ophthalmol* **116**:1640-5

Wright AF (1992) New insights into genetic eye disease. *Trends Genet* **8**:85-91

Wyllie AH, Kerr JF, Currie AR (1980) Cell death: the significance of apoptosis. *Int Rev Cytol* **68**:251-306

Xu S, Nakazawa M, Tamai M, Gal A (1995) Autosomal dominant retinitis pigmentosa locus on chromosome 19q in a Japanese family. *J Med Genet* **32**:915-6

Xu SY, Schwartz M, Rosenberg T, Gal A (1996) A ninth locus (RP18) for autosomal dominant retinitis pigmentosa maps in the pericentromeric region of chromosome 1. *Hum Mol Genet* **5**:1193-7

Yaffe MP (1999) The machinery of mitochondrial inheritance and behavior. *Science* **283**:1493-7

Yamamoto S, Sippel KC, Berson EL, Dryja TP (1997) Defects in the rhodopsin kinase gene in the Oguchi form of stationary night blindness [see comments]. *Nat Genet* **15**:175-8

Yan D, Swain PK, Breuer D, Tucker RM, Wu W, Fujita R, Rehemtulla A, et al (1998) Biochemical characterization and subcellular localization of the mouse retinitis pigmentosa GTPase regulator (mRprgr). *J Biol Chem* **273**:19656-63

Young RW (1984) Cell death during differentiation of the retina in the mouse. *J Comp Neurol* **229**:362-73

Zeviani M, Servidei S, Gellera C, Bertini E, DiMauro S, DiDonato S (1989) An autosomal dominant disorder with multiple deletions of mitochondrial DNA starting at the D-loop region. *Nature* **339**:309-11

Zeviani M, Bresolin N, Gellera C, Bordoni A, Pannacci M, Amati P, Moggio M, et al (1990) Nucleus-driven multiple large-scale deletions of the human mitochondrial genome: a new autosomal dominant disease. *Am J Hum Genet* **47**:904-14

Zeviani M, Muntoni F, Savarese N, Serra G, Tiranti V, Carrara F, Mariotti C, et al (1993) A MERRF/MELAS overlap syndrome associated with a new point mutation in the mitochondrial DNA tRNA(Lys) gene [published erratum appears in *Eur J Hum Genet* 1993;1(2):124]. *Eur J Hum Genet* **1**:80-7

APPENDIX A: STOCK SOLUTIONS

All reagents were purchased from BDH unless otherwise stated.

A.1 Electrophoresis solutions

10X TBE

| | |
|-------------------|------|
| Tris base | 108g |
| Boric acid | 55g |
| 0.5M EDTA, pH 8.0 | 40ml |

Made up to 1L with dH₂O

50X TAE

| | |
|-------------|-------|
| Tris base | 242g |
| Acetic acid | 57g |
| EDTA | 0.37g |

Made up to 1L with dH₂O

Agarose gels

Gels of 0.8 - 2.5% were made by addition of agarose (Gibco-BRL) to 1X TAE. The agarose was solubilised by microwaving and 1 μ l of ethidium bromide added before pouring. 1X TAE was used as the running buffer.

Urea solution

| | |
|---------|--------|
| Urea | 233.5g |
| 10X TBE | 50ml |

Made up to 500ml with dH₂O

20% denaturing acrylamide mix

| | |
|---------------|--------|
| Acrylamide | 96.5g |
| Bisacrylamide | 3.35g |
| Urea | 233.5g |
| 10X TBE | 50ml |

Made up to 500ml with dH₂O and filter sterilised

8% denaturing acrylamide gel

| | |
|--------------------------------|-------|
| 20% denaturing acrylamide mix | 31ml |
| Urea solution | 44ml |
| 10% (w/v) ammonium persulphate | 600µl |
| TEMED | 75µl |

20% non-denaturing acrylamide mix

| | |
|----------------|-------|
| Acrylamide | 96.5g |
| Bis Acrylamide | 3.35g |
| 10X TBE | 50ml |

Made up to 500ml with dH₂O and filter sterilised

8% non-denaturing acrylamide gel

| | |
|-----------------------------------|-------|
| 20% non-denaturing acrylamide mix | 31ml |
| dH ₂ O | 44ml |
| 10% (w/v) ammonium persulphate | 600µl |
| TEMED | 75µl |

5-10% glycerol was often added to the gel also for SSCP analysis

Agarose Loading Dye

| | |
|--------------------------|------|
| bromophenol blue (Sigma) | 13mg |
| xylene cyanol (Sigma) | 13mg |
| glycerol | 15ml |

Formamide Loading Dye

| | |
|--------------------------|-------|
| bromophenol blue (Sigma) | 10mg |
| xylene cyanol (Sigma) | 10mg |
| 0.5M EDTA, pH 8.0 | 0.2ml |

Made up to 10ml with formamide

A.2 Culture media and buffers

LB broth

| | |
|---------------|-----|
| NaCl | 10g |
| Bactotryptone | 10g |
| Yeast extract | 5g |

Made up to 1L with dH₂O and autoclaved

NZY broth

| | |
|--------------------------------------|-----|
| NaCl | 5g |
| MgSO ₄ .7H ₂ O | 2g |
| Yeast extract | 5g |
| NZ amine (casein hydrolysate) | 10g |

Made up to 1L with dH₂O and autoclaved

NZY top agar

| | |
|-----------|----|
| NZY broth | 1L |
| Agarose | 7g |

Made up to 1L with dH₂O and autoclaved

NZY plates

| | |
|-------------------------|-----|
| NZY broth | 1L |
| Agar (Becton Dickinson) | 15g |

Made up to 1L with dH₂O, autoclaved and poured into plates

SM buffer

| | |
|--------------------------------------|------|
| NaCl | 5.8g |
| MgSO ₄ .7H ₂ O | 2g |
| 1M Tris-HCl, pH 7.5 | 50ml |
| 2% (w/v) gelatin | 5ml |

Made up to 1L with dH₂O and autoclaved

A.3 PCR and sequencing buffers

10X PCR buffer, 15mM MgCl₂

| | |
|--------------------------|--------|
| 2M KCL | 2.5ml |
| 0.5 M Tris-HCl, pH 9.0 | 2ml |
| 1% (w/v) gelatine | 1ml |
| 10% (v/v) triton (Sigma) | 1ml |
| 1M MgCl ₂ | 0.15ml |
| Sterile H ₂ O | 3.35ml |

PCR buffers were filtered using 2µm pore Acrodisc filters (Gelman Sciences) and were stored at -20°C. Buffers of 10mM, 12.5mM, 20mM and 25mM MgCl₂ were also made for use in PCR magnesium curves.

2X sequencing buffer

| | |
|----------------------|--------|
| 1M Tris, pH 7.8 | 25µl |
| 1M MgCl ₂ | 1.25µl |
| 0.1M DTT (Gibco-BRL) | 15µl |

Made up to 500µl with sterile H₂O

Automated sequencing suspension buffer

| | |
|-------------------|-------|
| 50mM EDTA pH 8.0 | 20µl |
| formamide (Kodak) | 100µl |

A.4 Plasmid purification solutions

Lysis solution I

| | |
|---------------------|------|
| 50mM glucose | 9g |
| 1M Tris-HCl. pH 8.0 | 10ml |
| 0.5M EDTA. pH 8.0 | 8ml |

Made up to 400ml with dH₂O, autoclaved at 5 p.s.i. for 15min and 0.5g of lysozyme/100ml (Sigma) added just before use.

Lysis solution II

| | |
|--------------|------|
| NaOH pellets | 0.8g |
| SDS | 1g |

Made up to 100ml with dH₂O and kept on ice till use.

Lysis solution III

| | |
|-------|--------|
| NaOAc | 49.21g |
|-------|--------|

Made up to 150ml with dH₂O, brought to pH 5.2 using glacial acetic acid and autoclaved.

Top up solution for ultracentrifugation

| | |
|----------------------|-------|
| CsCl (Gibco-BRL) | 17.6g |
| 10mM Tris, pH 8.0 | 17.4g |
| 10mg/ml EtBr (Sigma) | 1.4g |

A.5 RNA purification solutions

Guanidinium thiocyanate solution

| | |
|---------------------------------|---------|
| Guanidinium thiocyanate (Fluka) | 236.32g |
| EDTA pH 8.0 | 0.98g |
| Tri-sodium citrate | 3.28g |
| Sarcosyl | 2.5g |

Made up to 500mls with DEPC-H₂O

RNase free H₂O

0.2ml diethyl pyrocarbonate (DEPC) (Sigma) was added to 100ml millipore H₂O in RNase free glassware. This is incubated at 37°C with shaking for at least 2 hours and then autoclaved. Other solutions (except for Tris) were treated in the same manner.

A.6 In situ hybridisation solutions

10x PBS

| | |
|---|------|
| NaCl | 80g |
| KCl | 2g |
| Na ₂ HPO ₄ .2H ₂ O | 14g |
| KH ₂ PO ₄ | 2.4g |

The pH was adjusted to 7.2 and then the solution made up to 1L with dH₂O and autoclaved

20x SSC

| | |
|---|--------|
| NaCl | 175.3g |
| Na ₃ C ₆ H ₅ O ₇ .2H ₂ O | 88.2g |

Made up to 500ml with dH₂O and autoclaved

10x DIG1 Buffer

| | |
|------|-------|
| Tris | 121g |
| NaCl | 87.7g |

The pH was adjusted to 7.6 and then the solution made up to a final volume of 1L with DEPC-H₂O and autoclaved (cannot DEPC treat Tris directly).

1x DIG2 Buffer

| | |
|------------------------|------|
| 1M Tris pH9.5 | 50ml |
| 1M NaCl | 50ml |
| 0.5M MgCl ₂ | 50ml |

Made up to 500ml with DEPC-H₂O

Prehybridisation Buffer for cryosections

| | |
|----------------------------------|------|
| 20x SSC | 5ml |
| 20mg/ml salmon sperm DNA (Sigma) | 40µl |
| Deionized formamide (Kodak) | 10ml |
| DEPC-H ₂ O | 5ml |

This solution must be stored at 4°C

Prehybridisation Buffer for paraffin sections

| | |
|-----------------------------|------|
| 20xSSC | 10ml |
| Deionized formamide (Kodak) | 50ml |
| DEPC-H ₂ O | 40ml |

This solution must be stored at 4°C.

Hybridisation Buffer for paraffin sections

| | |
|------------------------------------|-------|
| 1.5M Tris pH7.5 | 133µl |
| 100x Denhardt's solution (Sigma) | 2.5ml |
| 20xSSC | 2ml |
| 10% (w/v) SDS | 1ml |
| Deionized formamide (Kodak) | 10ml |
| 50% (w/v) Dextran Sulphate (Sigma) | 4ml |
| 10mg/ml salmon sperm DNA | 0.5ml |

This solution must be stored at -20°C

Antibody blocking solution

| | |
|---------------------|--------|
| Pig serum (Sigma) | 200µl |
| Sheep serum (Sigma) | 20µl |
| BSA (Sigma) | 0.06g |
| 1xDIG1 buffer | 1780µl |

This solution can be stored at -20°C but should not be freeze-thawed.

Detection Solution

| | |
|----------------------------|------------|
| 1x DIG2 Buffer | 10ml |
| NBT (Boehringer Mannheim) | 44 μ l |
| BCIP (Boehringer Mannheim) | 34 μ l |
| Levamisole (Sigma) | 10 μ l |

This solution must be filtered before use and may be stored at 4°C for up to a week.

APPENDIX B: PRIMER SEQUENCES

Primers were synthesized on a four column oligosynthesizer or supplied by Genosys. All primers are written in the 5' to 3' direction. An "f" in the primer name denotes a forward primer and an "r" denotes a reverse primer.

B.1 7q microsatellite primers

| | |
|-----------|----------------------------|
| D7S648f: | TCGATGGACTTCCTTGAAAA |
| D7S648r: | CTGAGGCACAAAAATTGCTT |
| D7S2471f: | ATGAATCATCTCAGTATTGGTCTGGG |
| D7S2471r: | TGCTGATCTCAAGTTGTGGGAC |
| D7S686f: | TCAAAGCCTGGTGAGAA |
| D7S686r: | TGACCCCTATATAAAAATGTAAAAT |
| D7S1874f: | TCACCTTGAGATTCCATCC |
| D7S1874r: | AACACCGTGGTCTTATCAAA |
| D7S530f: | TGCATTTTAGTGGAGCACA |
| D7S530r: | CAGGCATTGGGAACTTT |

B.2 GRM8 sequencing and SSCP primers

Primer names ending in "p" refer to PCR primers and those ending in "s" refer to sequencing primers.

Exon A primers

| | |
|--------|------------------------|
| Af1p : | TGGTAGCCTCCAGAAGGTGC |
| Af1s : | TGGTCTTGATTGCAATACCACC |
| Ar1s : | GCATGGCCTCCAGTCTGTGA |

Af2s : CCTGTCCACGCAAAGGGAGA
Ar2s : TGGATCTCCATTAGCACACCT
Af3s : TCCTCGACACGTGCTTCTAG
Ar3s : CCTGCAGTAGAGTCATAGCATT
Ar3p : ACCTGGTAACACAAAAGGGTCT

Exon B primers

Bfp : GGCTGTTTAGCTCATATGAC
Brp : CATGCATCTGTAGGAGTTCC
Bfs : CGTCAATGGGTTGAAATGAC
Brs : CCCTACAGATAAGAGAGCAC

Exon C primers

Cfp/s: TGCTCTTTCTGATCACCAC
Crp : GCAGTCTGTTATTCGAAGGC
Crs : ATGGGACACAAATCTGACCC

Exon D primers

Dfp : GTTAAACAGTGACCTACTGA
Drp : TCCTCATATTATGATACTCC
Dfs : CTTCTAAATCTGGTCTT
Drs : TTTTGCCTTTGAGTTCAG

Exon E primers

Efp : CTTTTTCATGCAGTGATCAGA
Erp : ATGATCAGGGTATGCTCAGC
Efs : CCATTCGAAAGTTCTGACAA
Ers : TGAAATAAATGCACCACAGG

Exon H primers

Hf1p : TGTA CTGTCAGCATTCTGTGA
Hr1s : AACCCGTGGCTAGATTAGGA

Hr1s : ATCCACCAGGTAGTTGTAAC
 Hf2s : TAAGCCAGGGGAGAGGAAGA
 Hr2s : GGTGGTGGCGATGATTCC
 Hf3s : AATTGGAGTGGCATTCTCCC
 Hr3s : GATTGTATCTGTGCTGCAATC
 Hf4s : CCTTAGTTACGTGCTCCTAACGG
 Hr4s : GGTGATCACCAGCTGAGATG
 Hf5s : CAAACCGTATCCACCGAATA
 Hr5s : AATGTCACACTTGAGCACTCC
 Hf6s : CATTGACTATGGAGAGCAGC
 Hr6S : GATGCAGGTGGTATACATGGT
 Hf7s : AACGAGAGGTGTCCCAGAGA
 Hr7s : AAGGAGGAAAAGCATCCTAAA
 Hr7p : ATAGCACAGACTGAAGCATC

Exon I primers

Ifp : AGCAGAGAAGCTGGAACAAT
 Irp : ACCATCATGCCCCTGGAAAC
 Ifs : CTCCTACTGTTAGGCTTACC
 Irs : TATTAGAAGTGCTCCCGCTC

Exon J primers

Jfp : ACATGCTGTAAAAGCTGG
 Jrp : TGATTGATTGTAGTCTACGG
 Jfs : AAGTCATTACAGGACTTG
 Jrs : ATCTCCAGGAGTGAATTT

B.3 “Housekeeping gene”, G3PDH primers

G3PDHf: ACCACAGTCCATGCCATCAC
 G3PDHr: TCCACCACCCTGTTGCTGTA

B.4 RT-PCR on illegitimate GRM8 transcript primers

A : GCCACTCCAATTTGATGGGGAT
B : GTTGGGGATCCAAAATAGCACC
C : TTCCCCAAACGAGCATCAATTGATGG
D : CATGTTGGGTCTCTGATCCAGA
E : CAAGTAGCTCTTTCCCATCA

B.5 DGK1 SSCP and sequencing primers

These sequence from which these primer sequences were designed was kindly provided by Dr. Steve Prescotts laboratory, The Huntsman Cancer Institute, Utah, USA.

Exon 4f: GATGTCAGGTGGGTCTTTTCCTG
Exon 4r: CAAGACGGAGCGCACACTCAC

Exon 5f: CCACCCTAAATCATGCAGATGTGG
Exon 5r: TCAGCAAACAAGAGAGTGAACGAC

Exon 6f: GAATCACCTGGGATCTCTGTTG
Exon 6r: TAAAGTCAAGTGTGCACATGTTG

Exon 7f: GCACTCCAGTGTGGGTGACAG
Exon 7r: GACAGGACTCATCTACCTCAGTTG

Exon 8f: CACGTCATTGCACTTCAGGAGGG
Exon 8r: GGAATGCCTTCTACTTCCAGGGAG

Exon 9f: GCTGCAGCATTACTCTTTGACCAG
Exon 9r: GGAATGAACTGAGGAAGCTAAGC

Exon 10f: GGTCTTACTCCCTGCCTCTCCGTG
Exon 10r: ATAACATTTCCAGGCAAGCG

Exon 11f: GCCTTACATGGAAGTCGTGTTAAG
Exon 11r: TCTTCCAAATCCTTGGGATCCTAGT

Exon 12f: TCAACTGATCCACCATGCGTCAGCC
Exon 12r: ATGGTCAGGATATACCTCACAAGG

Exon 13f: TTTCTCCAGCGGACACCACCCC
Exon 13r: TGACCACATCCCTACTTCATGGC

Exon 14f: GCTCTTGGAAGCCTCTGTTTCTC
Exon 14r: TCTTCCATTAGAACATCATGTGAT

Exon 15f: AACGGCTTGGCTCTTCCTTGCG
Exon 15r: CAGGCAGATGCTCCAGGGCTC

Exon 16f: TCCACTTTGAGTTGTGGCTGATC
Exon 16r: TAGCTCCCAGAGTCATCCTGAAG

Exon 17f: CATGGGATCTATTGGATCTGTAGG
Exon 17r: TTCTTAAGCCCAGCCATGAAACAG

Exon 18f: CCTTCCAATGACCCTCAGAATTGTC
Exon 18r: CCCAGCAACTAAGACAGTGCCTG

Exon 19f: TCACTTAAGCAGAGATAGGGCAAG
Exon 19r: GACGCACAAAACCACCAACC

Exon 20f: GCAAATGCTTCCCCTTCATTTCCC
Exon 20r: CCTGTGAATTGAATAAACTCTGTGAC

Exon 22f: GACCACTCGGTTCTTGTTTG
Exon 22r: AAATCAATGAGGCACTTCCA

Exon 23f: CGGACATATCTAAAAAACCC
 Exon 23r: CACTTCCTCTCCAAATGCATC

Exon 26af: CCTCGAGACCAAGAATACTTG
 Exon 26br: CGAACCAGACATGGATGTCAC

Exon 26bf: CTGGCAAGATTCATCTTCAG
 Exon 26br: GAGTCCTCATAATAGGGAGC

Exon 28f: TTCCTGCCCAAATGTAGACTA
 Exon 28r: CAGTFCAAGCAGGGGATGATAT

Exon 29f: TGTCCTCTAAGGCTGGAAACA
 Exon 29r: TCACTATGCCTACTTACCGTGG

Exon 31f: TGCTGCCTCCAACCCCTTTAT
 Exon 31r: GATGTCCGTGCTATGGTCACA

Exon 32f: CACGACTAGCGCTTGTGTCTAT
 Exon 32r: TTCCAGGGGAGCTGCCCAATT

B.6 λ DASH II library 7q primers

Standard PCR : D7S680f : CATCCAAGTTGGCAGTTTTT
 : D7S680r : AGATGCTGAATTCCCAGACA

Long range PCR : 680LRPf : GACGTTGACAGGAATCATAGC
 680LRPr : TCCACATGTCTGGGAATTCAG
 Lambda f : GGCGGAATTAACCCTCACTAA
 Lambda r : CCGCGTAATACGACTCACTAT

B.7 mGluR8 and cGMP RT-PCR primers

mGluR8f: GCGAATTGCACGGGATT
mGluR8r: CATTAGCTCTTCCCATCG

cGMPf: CGTTCATCGTACCTTAGGG
cGMPr: GCCTTACTGCATCCAAGTC

B.8 7q EST RT-PCR primers

7qEST34f1: TTTTAAGGACTCTTTCCGCA
7qEST34r1: ATAAGTGTTATGAAGGAAACAAAGC

7qEST34f2: GTCTTCTTTTCCAACCTTAGG
7qEST34r2: GATAGTAGTGAGATGAGTCA

7qEST35f1: TGATGGTGTATCTGTGCCTCA
7qEST35r1: ATGCTGCCTCTCACCCAAGT

7qEST35f2: GTGCCTCAAGTAAAAAGGGCGG
7qEST35r2: GATAGTTCTGTGGGTTGGCAGC

7qEST38f1: TCCATTAACACACAAATTGTACTGT
7qEST38r1: TCTGACCTCCTTCCTTGACAC

7qEST38f2: AAGGAAGGAGGTCAGAGC
7qEST38r2: GCTGCGCAGTTCTCACATTA

B.9 ISH primers

Mouse Rho f1: GGACATTAACCCTCACTAAAGGGATATGTGCCCTTCTC
CAACTG

Mouse Rho r1: GCTGTAATACGACTCACTATAGGGACGGCCAAGTTGAG
CAGGATG

Human Rho f1: GGACATTAACCCTCACTAAAGGGATACGTGCCCTTCT
CCAATGC

Human Rho r1: GCTGTAATACGACTCACTATAGGGACGGCTAGGTTG
AGCAGGATG

EST 34 f1: GAACATTAACCCTCACTAAAGGGACAACCTGTTGAAACA
CACTGT

EST 34 r1: GCTGTAATACGACTCACTATAGGGACTAGAATGAAGC
ACAAGATG

EST 35 f2: GGACATTAACCCTCACTAAAGGGAGACTTGTGCCCCAT
CAGATG

EST 35 r2: GCTGTAATACGACTCACTATAGGGAGCTTACACATGG
ATATGGC

EST 35 f3: GGACATTAACCCTCACTAAAGGGAAATTGGATGCTTAC
GATTTG

EST 35 r3: GCTGTAATACGACTCACTATAGGGAATTCAGGAGAAAA
CTATCC

EST 38 f1: GGACATTAACCCTCACTAAAGGGAGGCAATTAATACAA
CATAGG

EST 38 r1: GCTGTAATACGACTCACTATAGGGATTCCCCTTATGTCC
ACATCT

B.10 TIGR/myocilin primers

| | |
|----------|-------------------------------|
| Exon 1f: | GAA CTC GAA CAA ACC TGG GA |
| Exon 1r: | CAT GCT GCA GTA CTT ATA GCG G |
| Exon 2f: | ATA CTG CCT AGG CCA CTG GA |
| Exon 2r: | CAA TGT CCG TGT AGC CAC C |
| Exon 3f: | TGG CTA CCA CGG ACA GTT C |
| Exon 3r: | CAT TGG CGA CTG ACT GCT TA |

B.11 Mitochondrial screening primers

Forward and reverse primers grouped together were used as a pair in a PCR and one or both of the pair subsequently used to sequence the PCR product. An asterix denotes primers used in sequencing. An "s" in the primer name indicates that the primer was used as a nested primer only in sequencing. The number of the primer refers to the mitochondrial position of the first primer base.

| | |
|----------|------------------------------|
| 170f: | CGT TCA ATA TTA CAG GCG AAC* |
| 523r: | TGT GTG TGT GCT GGG TAG GAT |
| 420r(s): | GTG CAT ACC GCC AAA AGA TA* |
| 3324f: | CCT ACT CCT CAT TGT ACC CA* |
| 3617r: | AAT AGG AGG CCT AGG TTG AG* |
| 3731f: | ATG AAG TCA CCC TAG CCA TC |
| 3930r: | GAC TAG TTC GGA CTC CCC TT* |
| 4711f: | CCG GAC AAT GAA CCA TAA CC |
| 4920r: | CGT TAA GTG AGG GAG AGA TT* |
| 5148f: | CCC TAC TAC TAT CTC GCA CC |
| 5390r: | TAT GGG GAG TAG TGT GAT TG* |

5170f: GAA ACA AGC TAA CAT GAC TA
 5430r: TGG TAT GTT CAA ACT GTC AT*

5261f: GGC CAT TAT CGA AGA ATT CA*
 5490r: GGG AGA TAG GTA GGA GTA GC*

5651f: CCC TTA CTA GAC CAA TGG GA*
 5930r: AGA GAA TAG TCA ACG GTC GG*

6151f: TTC CCC TAA TAA TCG GTG CC*
 6360r: CTA GGT GTA AGG AGA AGA TG

11600f: GAC CTA AAA TCG CTC ATT GC*
 11820r: AGT GGG AGT AGA GTT TGA AG

12111f: CCG ACA TCA TTA CCG GGT TT
 12467r: AAG GTG GAT GCG ACA ATG GA
 12174f(s): GAC TGT TGT CTC CGA ATG CT*
 12420r(s): TTT GTT AGG GTT AAC GAG GG*

12628f: GGT CCA TCA TAG AAT TCT CAC*
 12870r: GCC GAT ACG GTT GTA TAG GAT

14251f: ACC AAT AGG ATC CTC CCG AA*
 14472r: GGA TAT ACT ACA GCG ATG GC

14603f: GAA GGC TTA GAA GAA AAC CC
 14753r: GGG TCA TTG GTG TTC TTG TA*

15582f: AAT TCT CCG ATC CGT CCC TA*
 15808r: TGC TAC TTG TC AAT GAT GG

B.12 MTTS2 automated sequencing primers

12111f: CCG ACA TCA TTA CCG GGT TT
12420r: TTT GTT AGG GTT AAC GAG GG

B.13 MTTS2 SSCP primers

12111f: CCG ACA TCA TTA CCG GGT TT
12467r: AAG GTG GAT GCG ACA ATG GA

B.14 ABCR PCR, SSCP and sequencing primers

These primer sequences were kindly provided by Dr. Michael Dean, NCI-Frederick Cancer Research Centre, Maryland, USA.

Exon 47f: CAC ATC CCA CAG GCA AGA G
Exon 47r: TTC CAA GTG TCA ATG GAG AAC

Exon 48f: ATT ACC TTA GGC CCA ACC AC
Exon 48r: ACA CTG GGT GTT CTG GAC C

B.15 RPE65 exon 13 primers

RPE65f: GAC TGA TTG CTT GAT TGA TTT TTC TTT CTC ACA AAC AAC
T
RPE65r: AAG GCA TCT GGG TGA GAA AC

Appendix C: Cloned and/or Mapped Genes Causing Retinal Diseases

Adapted from RetNet (Daiger *et al.*, 1999)

Listed by chromosome

| Chromosome 1 | | | | |
|---|------------|--|---|---|
| Symbol; OMIM Number | Location | Disease; Protein | Mapping Method; Comment | References |
| LCA2, RP20, RPE65; <u>204100</u> , <u>180069</u> | 1p31 | recessive Leber congenital amaurosis; recessive RP; protein: retinal pigment epithelium-specific 65 kD protein | cloned gene; accounts for 2% of recessive RP and 16% of recessive Leber congenital amaurosis; 'RP20' withdrawn; same as Swedish Briard-Beagle dog retinal degeneration | <u>Aguirre 98</u> ; <u>Gu 97</u> ; <u>Marlhens 97</u> ; <u>Morimura 98</u> ; <u>Veske 99</u> |
| STGD1, RP19, ABCR; <u>248200</u> , <u>601691</u> , <u>601718</u> | 1p21-p22 | recessive Stargardt disease, juvenile and late onset; recessive MD; recessive RP; recessive fundus flavimaculatus; recessive combined RP and cone-rod dystrophy; protein: ATP-binding cassette transporter - retinal | linkage mapping, cloned gene; may be involved in age-related macular degeneration but controversial; same as ROS1.2 and rim protein, expressed only in rod outer segment | <u>Allikmets 97</u> ; <u>Allikmets 97a</u> ; <u>Anderson 94</u> ; <u>Cremers 98</u> ; <u>Gerber 95</u> ; <u>Gerber 98</u> ; <u>Kaplan 93</u> ; <u>Kaplan 94</u> ; <u>Lewis 99</u> ; <u>Martinez-Mir 97</u> ; <u>Martinez-Mir 98</u> ; <u>Nasonkin 98</u> ; <u>Rozet 98</u> ; <u>Stone 98</u> ; <u>Sun 97</u> |
| RP18; <u>601414</u> | 1q13-q23 | dominant RP | linkage mapping; Danish family; early onset night blindness | <u>Xu 96a</u> ; <u>Xu 98</u> |
| ARMD1; <u>603075</u> | 1q25-q31 | dominant MD, age-related | linkage mapping; possible model for acquired age-related macular degeneration | <u>Klein 98</u> |
| AXPC1 | 1q31-q32 | recessive ataxia, posterior column with RP | linkage mapping | <u>Higgins 99</u> |
| RP12; <u>600105</u> , <u>268030</u> | 1q31-q32.1 | recessive RP with para-arteriolar preservation of the RPE (PPRPE) | linkage mapping; Netherlands family; close to mouse <i>rd3</i> | <u>Heckenlively 82</u> ; <u>Leutelt 95</u> ; <u>van Soest 94</u> |
| USH2A; <u>276901</u> | 1q41 | recessive Usher syndrome, type 2a; protein: novel protein with similarity to laminins and cell adhesion molecules | linkage mapping, cloned gene; may be either an extracellular-matrix protein or cell adhesion molecule; USH2B at same site; common 2314delG mutation with atypical phenotype | <u>Eudy 98</u> ; <u>Kimberling 90</u> ; <u>Kimberling 95</u> ; <u>Lewis 90</u> ; <u>Liu 99</u> ; <u>Saouda 98</u> |

| Chromosome 2 | | | | |
|--|----------|--|--|--|
| Symbol; OMIM Number | Location | Disease; Protein | Mapping Method; Comment | References |
| EFEMP1, DHRD, MTLV; <u>126600</u> | 2p16-p21 | dominant radial, macular drusen; dominant Doyme honeycomb retinal degeneration (Malattia Leventinese); protein: EGF-containing fibrillin-like extracellular matrix protein 1 | linkage mapping, cloned gene; single mutation (Arg345Trp) found in all affected individuals to date; possible model for age-related macular degeneration | <u>Edwards 98</u> ; <u>Héon 96</u> ; <u>Héon 96a</u> ; <u>Kermani 99</u> ; <u>Gregory 96</u> ; <u>Stone 99</u> |
| ALMS1, ALSS; <u>203800</u> | 2p14-p13 | recessive Alström syndrome | homozygosity and linkage mapping; symptoms include RP, deafness, obesity and diabetes (like BBS) | <u>Collin 97</u> ; <u>Macari 98</u> |
| RP28 | 2p11-p16 | recessive RP | homozygosity mapping; consanguineous Indian family | <u>Gu 98a</u> |
| ACHM2, RMCH2, CNCG3, CNGA3; <u>216900</u> , <u>600053</u> | 2q11 | recessive achromatopsia; protein: cone photoreceptor cGMP-gated cation channel, alpha subunit | homozygosity mapping, cloned gene; total color blindness and other cone-related abnormalities (rod monochromacy) | <u>Arbour 97</u> ; <u>Kohl 98</u> ; <u>Wissinger 98</u> |
| RP26 | 2q31-q33 | recessive RP | linkage mapping | <u>Bayés 98</u> |
| BBS5; <u>603650</u> | 2q31 | recessive Bardet-Biedl syndrome | linkage mapping | <u>Young 99</u> |
| SAG; <u>258100</u> , <u>181031</u> | 2q37.1 | recessive Oguchi disease; recessive RP; protein: arrestin (s-antigen) | cloned gene; CSNB and fundus palor in Japanese primarily; recessive RP in Japanese | <u>Fuchs 95</u> ; <u>Maw 95</u> ; <u>Nakazawa 98</u> ; <u>Wada 96</u> |

| Chromosome 3 | | | | |
|--|----------|--|--|--|
| Symbol; OMIM Number | Location | Disease; Protein | Mapping Method; Comment | References |
| GNAT1; <u>139330</u> | 3p22 | dominant CSNB, Nougaret type; protein: rod transducin alpha subunit | cloned gene; missense mutation in a single large French family, may affect taste perception | <u>Dryja 96</u> ; <u>Maumenee-Hussels 96</u> |
| SCA7, OPCA3, ADCA2; <u>164500</u> | 3p13-p12 | dominant spinocerebellar ataxia w/ MD or retinal degeneration; protein: SCA7 protein | linkage mapping, cloned gene; Moroccan, Belgian, French, Swedish, American and African-American families; shows anticipation with expanding CAG repeat in coding sequence of protein with unknown function | <u>Benomar 95</u> ; <u>David 97</u> ; <u>Del Favero 98</u> ; <u>Gouw 95</u> ; <u>Holmberg 95</u> |
| BBS3; | 3p13-p12 | recessive Bardet-Biedl | homozygosity and linkage | <u>Beales 97</u> ; <u>Sheffield 94</u> ; |

| | | | | |
|----------------------------|----------|--|--|--|
| <u>600151</u> | | syndrome | mapping | <u>Kwitek-Black 94; Woods 99</u> |
| <u>RP5; 180102</u> | 3q | not distinct from RHO/RP4 | linkage mapping; mapping error: was dropped | <u>Farrar 92</u> |
| <u>RHO, RP4; 180380</u> | 3q21-q24 | dominant RP; dominant CSNB; recessive RP; protein: rhodopsin | linkage mapping, cloned gene; accounts for 30 to 40% of autosomal dominant RP; more than 100 distinct mutations but RhoPro23His causes 15% of adRP in US Caucasians; 'RP4' withdrawn | <u>Dryja 90; Dryja 90a; Dryja 91; Farrar 90a; McWilliams 89; Nathans 84</u> |
| <u>USH3A, USH3; 276902</u> | 3q21-q25 | recessive Usher syndrome, type 3 | linkage mapping; USH3 withdrawn | <u>Joensuu 96; Sankila 94; Sankila 95</u> |
| <u>OPA1; 165500</u> | 3q28-q29 | dominant optic atrophy, Kjer type | linkage mapping; little or no genetic heterogeneity | <u>Bonneau 95; Brown 97a; Eiberg 94; Johnston 97; Lunkes 95; Seller 97; Votruba 97; Votruba 98</u> |

Chromosome 4

| Symbol; OMIM Number | Location | Disease; Protein | Mapping Method; Comment | References |
|-------------------------------------|----------|---|---|---|
| <u>STGD4; 603786</u> | 4p | dominant Stargardt-like macular dystrophy | linkage mapping; Caribbean family | <u>Kniazeva 99</u> |
| <u>CSNB3, PDE6B; 163500, 180072</u> | 4p16.3 | recessive RP; dominant CSNB; protein: rod cGMP phosphodiesterase beta subunit | linkage mapping, cloned gene; same as mouse <i>rd</i> , mouse <i>r</i> and <i>rd1</i> Irish Setter dog retinal degeneration | <u>Altherr 92; Bateman 92; Bayés 95; Bowes 90; Collins 92; Farber 92; Gal 94; Gal 94a; McLaughlin 93; McLaughlin 95; Piriev 98; Pittler 91; Pittler 93; Riess 92; Suber 93; Valverde 95; Weber 91</u> |
| <u>WFS1; 222300, 598500</u> | 4p16.1 | recessive Wolfram syndrome; protein: wolframin | linkage mapping, cloned gene; symptoms include diabetes, optic atrophy and deafness; often associated with multiple mitochondrial deletions | <u>Barrientos 96; Barrientos 96a; Collier 96; Inoue 98; Polymeropoulos 94; Strom 98a</u> |
| <u>CNGA1, CNCG, CNCG1; 123825</u> | 4p12-cen | recessive RP; protein: rod cGMP-gated channel alpha subunit | cloned gene; nonsense, missense and deletion mutations in four RP families | <u>Dhalla 92; Dryja 95; Griffin 93</u> |
| <u>ABL, MTP; 200100, 157147</u> | 4q24 | recessive abetalipoproteinemia; protein: microsomal triglyceride transfer protein | cloned gene; multiple lipid abnormalities including pigmentary retinal degeneration | <u>Narcisi 95; Sharp 93; Shoulders 93</u> |

Chromosome 5

| Symbol; OMIM Number | Location | Disease; Protein | Mapping Method; Comment | References |
|---------------------------------|------------|---|---|-------------------------------------|
| WGN1, ERVR; <u>143200</u> | 5q13-q14 | dominant Wagner disease and erosive vitreoretinopathy | linkage mapping | <u>Brown 95</u> |
| PDE6A; <u>180071</u> | 5q31.2-q34 | recessive RP; protein: cGMP phosphodiesterase alpha subunit | cloned gene; homozygote and compound heterozygote mutations | <u>Pittler 90</u> ; <u>Huang 95</u> |

Chromosome 6

| Symbol; OMIM Number | Location | Disease; Protein | Mapping Method; Comment | References |
|--|------------|--|---|--|
| RP14, TULP1; <u>600132</u> , <u>602280</u> | 6p21.3 | recessive RP; protein: tubby- like protein 1 | linkage mapping, cloned gene; two Dominican families and others; same as mouse <i>tub</i> which causes obesity, deafness and retinal degeneration | <u>Banerjee 97</u> ; <u>Banerjee 98</u> ; <u>Banerjee 98a</u> ; <u>Gu 98</u> ; <u>Hagstrom 98</u> ; <u>Knowles 94</u> ; <u>Shugart 95</u> |
| RDS, RP7; <u>179605</u> | 6p21.2-cen | dominant RP; dominant MD; digenic RP with ROM1; dominant adult vitelliform MD; protein: peripherin/RDS | linkage mapping, cloned gene; dominant mutations; also, compound heterozygotes with <u>ROM1</u> ; accounts for 5% of autosomal dominant RP; same as mouse <i>rds</i> ; 'RP7' withdrawn | <u>Arikawa 92</u> ; <u>Connell 90</u> ; <u>Connell 91</u> ; <u>Dryja 97</u> ; <u>Farrar 91</u> ; <u>Felbor 97a</u> ; <u>Jordan 92a</u> ; <u>Kajiwara 91</u> ; <u>Kajiwara 94</u> ; <u>Travis 91</u> ; <u>Travis 91a</u> |
| COD3, GCAP1, GUCA1A; <u>602093</u> , <u>600364</u> | 6p21.1 | dominant cone dystrophy; protein: guanylate cyclase activating protein 1A | linkage mapping, cloned gene; British family with constitutively active mutant | <u>Payne 97</u> ; <u>Payne 98</u> ; <u>Sokal 98</u> |
| CORD7; <u>603649</u> | 6q | dominant cone-rod dystrophy | linkage mapping | <u>Kelsell 98</u> |
| RP25; <u>602772</u> | 6cen-q15 | recessive RP | homozygosity mapping; Spanish families (10-20% of arRP); mapped to region containing GABA receptors | <u>Ruiz 98</u> |
| STGD3; <u>600110</u> | 6q11-q15 | dominant MD, Stargardt-like | linkage mapping; excluded from MCDR1; Griesinger 98 may be distinct | <u>Griesinger 98</u> ; <u>Stone 94</u> |
| MCDR1, PBCRA; <u>136550</u> | 6q14-q16.2 | dominant MD, North Carolina type; dominant progressive bifocal chorioretinal atrophy | linkage mapping; North Carolina, German, Belizean and British families; PBCRA is clinically distinct from MCDR1 | <u>Kelsell 95</u> ; <u>Rabb 98</u> ; <u>Sauer 97a</u> ; <u>Small 92</u> ; <u>Small 97</u> |
| RCD1; <u>180020</u> | 6q25-q26 | dominant retinal-cone dystrophy 1 | deletion mapping | <u>OMIM 98</u> |

Chromosome 7

| Symbol; OMIM Number | Location | Disease; Protein | Mapping Method; Comment | References |
|--|-----------|--|--|---|
| CYMD; <u>153880</u> | 7p21-p15 | dominant MD, cystoid | linkage mapping; distinct from RP9 | <u>Inglehearn 94a</u> ; <u>Kremer 94</u> |
| RP9; <u>180104</u> | 7p15-p13 | dominant RP | linkage mapping | <u>Inglehearn 93</u> ; <u>Inglehearn 94b</u> ; <u>Inglehearn 98</u> ; <u>Keen 95</u> ; <u>Kim 95</u> |
| PEX1, IRD; <u>266510</u> , <u>602136</u> | 7q21-q22 | recessive Refsum disease, infantile; protein: peroxisome biogenesis factor 1 | cloned gene; symptoms include RP, retardation and hearing deficit | <u>Portsteffen 97</u> ; <u>Reuber 97</u> |
| RP10; <u>180105</u> | 7q31.3 | dominant RP | linkage mapping; Spanish, Scottish and American families | <u>Daiger 97</u> ; <u>Jordan 93</u> ; <u>McGuire 95</u> ; <u>McGuire 96</u> ; <u>Millán 95</u> ; <u>Mohamed 96</u> |
| BCP, CBT; <u>190900</u> | 7q31.3-32 | dominant tritanopia; protein: blue cone opsin | cloned gene; several mutations; progressive retinopathy not observed | <u>Fitzgibbon 94</u> ; <u>Nathans 86</u> ; <u>Nathans 92</u> ; <u>Nathans 93</u> ; <u>Weitz 92</u> ; <u>Weitz 92a</u> |

Chromosome 8

| Symbol; OMIM Number | Location | Disease; Protein | Mapping Method; Comment | References |
|---------------------------|--------------|--|--|---|
| RP1; <u>180100</u> | 8q11-q13 | dominant RP; protein: RP1 protein | linkage mapping, cloned gene; causes 5 to 10% of adRP; protein is photoreceptor-specific with unknown function but similarity over short region to doublecortin; distinct from mouse <i>Rd4</i> ; large Kentucky family and others | <u>Blanton 91</u> ; <u>Daiger 97</u> ; <u>Pierce 99</u> ; <u>Roderick 97</u> ; <u>Sadler 93</u> ; <u>Sullivan 99</u> ; <u>Xu 96</u> |
| TTPA; <u>600415</u> | 8q13.1-q13.3 | recessive RP and/or recessive or dominant ataxia; protein: alpha-tocopherol-transfer protein | cloned gene; TPA mutations found in patients with vitamin E deficiency | <u>Yokota 96</u> |
| ACHM3; <u>262300</u> | 8q21-q22 | recessive achromatopsia Pingelapese | linkage mapping; includes total color blindness, photophobia and nystagmus; affects 4 to 10% of Pingelapese people on the Eastern Caroline Islands | <u>Winick 99</u> |
| VMD1; <u>153840</u> | not 8q24 | dominant MD, atypical vitelliform | linkage exclusion; linked to GPT but later excluded | <u>Daiger 97</u> ; <u>Ferrell 83</u> ; <u>Leach 96</u> ; <u>Sohocki 97</u> |

Chromosome 9

| Symbol; OMIM Number | Location | Disease; Protein | Mapping Method; Comment | References |
|---------------------------|-------------------|--|--|--------------------------------------|
| RP21; <u>601850</u> | not 9q34- qter | dominant RP with sensorineural deafness | linkage mapping; RP21 withdrawn; later mapped to <u>MTTS2</u> in mitochondrion | <u>Kenna 97</u> ; <u>Mansergh 99</u> |

Chromosome 10

| Symbol; OMIM Number | Location | Disease; Protein | Mapping Method; Comment | References |
|---|-------------------|---|--|---|
| USH1F; <u>602083</u> | 10 | recessive Usher syndrome, type 1f | homozygosity mapping; inbred Hutterite family; distinct from USH1D | <u>Wayne 97</u> |
| RDPA, PHYH, PAHX; <u>266500</u> , <u>602026</u> | 10p15.3- p12.2 | recessive Refsum disease; protein: phytanoyl-CoA hydroxylase | homozygosity mapping, cloned gene; symptoms include RP, peripheral neuropathy and cerebellar ataxia; same proteins with different names | <u>Jansen 97</u> ; <u>Jansen 97a</u> ; <u>Mihalik 97</u> ; <u>Nadal 95</u> |
| USH1D; <u>601067</u> | 10q | recessive Usher syndrome, type 1d | homozygosity mapping; Pakistani family | <u>Wayne 96</u> |
| (- - -); <u>221900</u> | 10q21 | recessive nonsyndromal congenital retinal nonattachment | homozygosity mapping; Iranian population | <u>Ghiasvand 98</u> |
| RBP4; <u>180250</u> | 10q24 | recessive RPE degeneration; protein: retinol-binding protein 4 | cloned gene; RPE atrophy with night blindness and reduced visual acuity; carrier protein for serum retinol | <u>Seeliger 99</u> |
| ONCR, PAX2; <u>120330</u> , <u>167409</u> | 10q25 | dominant renal-coloboma syndrome; protein: paired homeotic gene 2 | cloned gene; optic nerve colobomas with renal abnormalities; similar malformations in mouse <i>Pax2(1Neu)</i> mutation | <u>Favor 96</u> ; <u>Sanyanusin 95</u> ; <u>Sanyanusin 95a</u> |
| OAT; <u>258870</u> | 10q26 | recessive gyrate atrophy; protein: ornithine aminotransferase | cloned gene; many mutations reported | <u>Valle 95</u> |

Chromosome 11

| Symbol; OMIM Number | Location | Disease; Protein | Mapping Method; Comment | References |
|--|-----------|--|--|---|
| AA; <u>108985</u> | 11p15 | dominant atrophia areata; dominant chorioretinal degeneration, helicoid | linkage mapping | <u>Fossdal 95</u> |
| USH1C; <u>276904</u> | 11p15.1 | recessive Usher syndrome, Acadian | linkage mapping; possibly same as mouse <i>rd5</i> | <u>Ayyagari 95</u> ; <u>Heckenlively 95</u> ; <u>Keats 94</u> ; <u>Noun 93</u> ; <u>Nouri 94</u> ; <u>Smith 92</u> |
| BBS1; <u>209901</u> | 11q13 | recessive Bardet-Biedl syndrome | linkage mapping; approximately 40% of BBS families | <u>Beales 97</u> ; <u>Bruford 97</u> ; <u>Cornier 95</u> ; <u>Leppert 94</u> ; <u>Woods 99</u> ; <u>Wright 95</u> |
| ROM1; <u>180721</u> | 11q13 | dominant RP; digenic RP with RDS; protein: retinal outer segment membrane protein 1 | cloned gene; compound heterozygote with <u>peripherin/RDS</u> ; dominant RP is rare and doubtful | <u>Bascom 92</u> ; <u>Bascom 92a</u> ; <u>Bascom 93</u> ; <u>Bascom 93a</u> ; <u>Bascom 95</u> ; <u>Dryja 97</u> ; <u>Kajiwara 94</u> ; <u>Martinez-Mir 97a</u> ; <u>Nichols 94</u> ; <u>Sakuma 95</u> |
| VMD2; <u>153700</u> | 11q13 | dominant MD, Best type; protein: bestrophin | linkage mapping, cloned gene; bestrophin is retinal- specific, expressed in the RPE, possibly involved in metabolism/transport of polyunsaturated fatty acids | <u>Forsman 92</u> ; <u>Graff 94</u> ; <u>Petrukhin 98</u> ; <u>Marquardt 98</u> ; <u>Nichols 94</u> ; <u>Stone 92a</u> ; <u>Wadeilus 93</u> ; <u>Weber 93</u> ; <u>Weber 94a</u> ; <u>Weber 94c</u> ; <u>Zhaung 93</u> |
| EVR1, FEVR; <u>133780</u> | 11q13-q23 | dominant familial exudative vitreoretinopathy | linkage mapping; distinct from VRNI | <u>Li 92</u> ; <u>Li 92a</u> ; <u>Müller 94</u> |
| VRNI; <u>193235</u> | 11q13 | dominant neovascular inflammatory vitreoretinopathy | linkage mapping; distinct from EVR1 | <u>Stone 92</u> |
| MYO7A, DFNB2, USH1B; <u>276903</u> , <u>600060</u> | 11q13.5 | recessive Usher syndrome, type 1; recessive congenital deafness without RP; recessive atypical Usher syndrome (USH3-like); protein: myosin VIIA | linkage mapping, cloned gene; MYO7A is a common component of cilia and microvilli; same as mouse <i>sh1</i> shaker-1 (but no RP); 'USH1B' withdrawn | <u>Adato 97</u> ; <u>Bonné-Tamir 94</u> ; <u>El-Amraoui 96</u> ; <u>Gibson 95</u> ; <u>Kelley 97</u> ; <u>Kimberling 92</u> ; <u>Lévy 97</u> ; <u>Liu 97</u> ; <u>Liu 97a</u> ; <u>Liu 97b</u> ; <u>Liu 98</u> ; <u>Smith 92</u> ; <u>Weil 95</u> ; <u>Weil 97</u> ; <u>Weston 95</u> ; <u>Weston 96</u> ; <u>Wolftrum 98</u> |

Chromosome 12

| Symbol; OMIM Number | Location | Disease; Protein | Mapping Method; Comment | References |
|---------------------------------|-----------|---|--|--------------------------------------|
| RDH5, RDH1; <u>601617</u> | 12q13-q14 | recessive fundus albipunctatus; protein: 11- <i>cis</i> retinol dehydrogenase 5 | cloned gene; stationary night blindness with subretinal spots and delayed dark adaptation; protein is an RPE microsomal enzyme involved in converting 11- <i>cis</i> retinol to 11- <i>cis</i> retinal | <u>Simon 96</u> ; <u>Yamamoto 99</u> |

Chromosome 13

| Symbol; OMIM Number | Location | Disease; Protein | Mapping Method; Comment | References |
|----------------------------|----------|--|---|--|
| RB1; <u>180200</u> | 13q14.2 | dominant germline or somatic retinoblastoma; benign retinoma; pinealoma; osteogenic sarcoma; protein: retinoblastoma protein 1 | deletion mapping, cloned gene; requires 'second hit' loss of heterozygosity; 5 to 10% inherited, 20 to 30% new mutation, remainder sporadic; preferential loss of maternal chromosome; protein is cell-cycle regulatory element | <u>Dryja 89</u> ; <u>Francke 76</u> ; <u>Friend 86</u> ; <u>Knudson 71</u> ; <u>Lee 87</u> ; <u>Lohmann 96</u> ; <u>Mancini 94</u> ; <u>Sparkes 83</u> ; <u>Toguchida 93</u> |
| STGD2; <u>153900</u> | 13q34 | dominant MD, Stargardt type | linkage mapping; large American family | <u>Zhang 94</u> |
| RHOK, RK; <u>180381</u> | 13q34 | recessive CSNB, Oguchi type; protein: rhodopsin kinase | cloned gene; several mutations in Japanese | <u>Cideciyan 98</u> ; <u>Khani 98</u> ; <u>Maw 98</u> ; <u>Yamamoto 97</u> |

Chromosome 14

| Symbol; OMIM Number | Location | Disease; Protein | Mapping Method; Comment | References |
|----------------------------------|----------|---|---|--|
| (RP16) | 14 | recessive RP (possibly) | linkage mapping | <u>Bruford 94</u> |
| ACHM1, RMCH; <u>216900</u> | 14 | recessive rod monochromacy or achromatopsia | uniparental isodisomy; total color blindness or 'day blindness' | <u>Pentao 92</u> |
| NRL, RP27; <u>162080</u> | 14q11.2 | dominant RP; protein: neural retina luciferase zipper | linkage mapping, cloned gene; NRL is a retinal transcription factor which interacts with <u>CRX</u> and promotes transcription of rhodopsin and other retinal genes | <u>Bessant 99</u> ; <u>Farjo 97</u> ; <u>Rehemtulla 96</u> ; <u>Swaroop 92</u> ; <u>Yang-Feng 92</u> |
| LCA3 | 14q24 | recessive Leber congenital amaurosis | homozygosity mapping; consanguineous Saudi Arabian family | <u>Stockton 98</u> |

| | | | | |
|----------------------------------|-------|-------------------------------------|--------------------------------|--|
| USH1A, USH1; <u>276900</u> | 14q32 | recessive Usher syndrome, French | linkage mapping; was 'USH1' | <u>Kaplan 91</u> ; <u>Larget-Piet 94</u> |
|----------------------------------|-------|-------------------------------------|--------------------------------|--|

Chromosome 15

| Symbol; OMIM Number | Location | Disease; Protein | Mapping Method; Comment | References |
|------------------------------------|-------------|---|---|--|
| BBS4; <u>600374</u> | 15q22.3-q23 | recessive Bardet-Biedl syndrome | homozygosity and linkage mapping; approximately 30% of BBS families | <u>Beales 97</u> ; <u>Bruford 97</u> ; <u>Carmi 95</u> |
| MRST; <u>602685</u> | 15q24 | recessive retardation, spasticity and retinal degeneration | linkage mapping; inbred Pakistani family | <u>Mitchell 98</u> |
| RLBP1, CRALBP; <u>180090</u> | 15q26 | recessive RP; recessive Bothnia dystrophy; recessive retinitis punctata albescens; protein: cellular retinaldehyde-binding protein | cloned gene; consanguineous Indian family, Swedish families and others | <u>Burstedt 99</u> ; <u>Maw 97</u> ; <u>Morimura 99</u> |

Chromosome 16

| Symbol; OMIM Number | Location | Disease; Protein | Mapping Method; Comment | References |
|---------------------------------|-------------------|---|---|---|
| CLN3, JNCL; <u>204200</u> | 16p12.1 | recessive Batten disease (ceroid-lipofuscinosis, neuronal 3), juvenile; protein: Batten disease protein | linkage mapping, cloned gene; symptoms include early-onset retinal pigmentary degeneration with later mental deteriation | <u>Batten Disease 95</u> ; <u>Eiberg 89</u> ; <u>Gardiner 90</u> ; <u>Mitchison 95</u> ; <u>Mitchison 95a</u> ; <u>Mitchison 97</u> ; <u>Munroe 97</u> |
| RP22; <u>602594</u> | 16p12.1- p12.3 | recessive RP | homozygosity mapping; Indian families | <u>Finckh 98</u> |
| BBS2; <u>209900</u> | 16q21 | recessive Bardet-Biedl syndrome, type 2 | linkage mapping; Bedouin family; approximately 20% of BBS families | <u>Beales 97</u> ; <u>Bruford 97</u> ; <u>Kwitek-Black 93</u> ; <u>Kwitek- Black 94</u> ; <u>Kwitek-Black 96</u> ; <u>Woods 99</u> ; <u>Wright 95</u> |

Chromosome 17

| Symbol; OMIM Number | Location | Disease; Protein | Mapping Method; Comment | References |
|---|-----------|---|---|---|
| CORD5, RCD2; 600977 , 601251 | 17p13-p12 | dominant cone dystrophy, progressive; recessive cone- rod dystrophy | linkage mapping; several families with dominant CORD map to this region, as does a family with recessive CORD -- these may or may not be allelic | Balciuniene 95 ; Payne 99 ; Small 95 ; Small 96 |
| CACD; 215500 | 17p13 | dominant central areolar choroidal dystrophy | linkage mapping | Hughes 98 ; Lotery 96 |
| RP13; 600059 | 17p13.3 | dominant RP | linkage mapping; South African and English families; not recoverin | Goliath 95 ; Greenberg 94 ; Kojis 96 ; Inglehearn 98 ; Tarttelin 96 |
| GUCY2D, CORD6, LCA1, RETGC1; 204000 , 600179 , 601777 | 17p13.1 | recessive Leber congenital amaurosis; dominant cone- rod dystrophy; protein: retinal-specific guanylate cyclase | linkage mapping, cloned gene; North African families and several mutations; same as chicken <i>rd/rd</i> | Camuzat 95 ; Camuzat 96 ; Kelsell 97 ; Kelsell 98a ; Perrault 96 ; Perrault 98 ; Semple-Rowland 98 |
| CORD4 | 17q | cone-rod dystrophy | association with neurofibromatosis; presumed dominant like NF | Klystra 93 |
| PDE6G, PDEG; 180073 | 17q21.1 | mouse recessive retinal degeneration; protein: cGMP phosphodiesterase gamma subunit | cloned gene; targeted disruption transgene | Dollfus 93 ; Tsang 95 |
| RP17; 600852 | 17q22 | dominant RP | linkage mapping; South African and Dutch families; PDEG excluded; same location as dog <i>prcd</i> progressive rod-cone degeneration | Acland 98 ; Bardien 95 ; Bardien 97 ; den Hollander 99 ; Inglehearn 98 |

Chromosome 18

| Symbol; OMIM Number | Location | Disease; Protein | Mapping Method; Comment | References |
|----------------------------------|-------------------|--|--|---|
| CORD1; 600624 | 18q21.1- q21.3 | cone-rod dystrophy; de Grouchy syndrome | deletion mapping; isolated case; symptoms include COD, retardation and hearing impairment | Manhant 95 ; Warburg 91 |

Chromosome 19

| Symbol; OMIM Number | Location | Disease; Protein | Mapping Method; Comment | References |
|---------------------------|----------|---------------------|----------------------------|------------|
|---------------------------|----------|---------------------|----------------------------|------------|

| | | | | |
|---------------------------------|-------------------|--|---|---|
| OPA3, MGA3; <u>258501</u> | 19q13.2- q13.3 | recessive optic atrophy with ataxia and 3-methylglutaconic aciduria | linkage mapping; Iraqi-Jewish families | <u>Nystuen 98</u> |
| CORD2, CRX; <u>120970</u> | 19q13.3 | dominant cone-rod dystrophy; recessive, dominant and 'de novo' Leber congenital amaurosis; dominant RP; protein: cone-rod otx-like photoreceptor homeobox transcription factor | linkage mapping, cloned gene; meiotic drive suggested; CRX also activates pineal genes; interacts with <u>NRL</u> | <u>Bellingham 97</u> ; <u>Evans 94</u> ; <u>Evans 95</u> ; <u>Freund 97</u> ; <u>Freund 98</u> ; <u>Gregory 94</u> ; <u>Li 98</u> ; <u>Sohocki 98</u> ; <u>Swain 97</u> ; <u>Swaroop 99</u> |
| RP11; <u>600138</u> | 19q13.4 | dominant RP | linkage mapping; distinct from CORD2; high frequency in British Isles (21%), highly variable; some cases may involve protein kinase C gamma (PRKCG) | <u>Al-Maghtheh 94</u> ; <u>Al-Maghtheh 96</u> ; <u>Al-Maghtheh 98</u> ; <u>Inglehearn 98</u> ; <u>McGee 97</u> ; <u>Nakazawa 95</u> ; <u>Vithana 98</u> |

Chromosome 20

| Symbol; OMIM Number | Location | Disease; Protein | Mapping Method; Comment | References |
|---------------------------------|----------|---|---|-----------------------------------|
| AGS, PLCB4; <u>600810</u> | 20p12 | dominant Alagille syndrome; protein: phospholipase-C-beta-4 | deletion mapping, cloned gene; multiple affected organs; same as <i>Drosophila norpA</i> retinal mutant | <u>Alvarez 95</u> ; <u>Rao 95</u> |

Chromosome 21

| Symbol; OMIM Number | Location | Disease; Protein | Mapping Method; Comment | References |
|---------------------------|----------|----------------------------------|----------------------------|-----------------|
| USH1E; <u>602097</u> | 21q21 | recessive Usher syndrome, type 1 | linkage mapping | <u>Chäib 97</u> |

Chromosome 22

| Symbol; OMIM Number | Location | Disease; Protein | Mapping Method; Comment | References |
|--|-------------------|---|---|---|
| SFD, TIMP3; <u>136900</u> , <u>188826</u> | 22q12.1- q13.2 | dominant Sorsby's fundus dystrophy; protein: tissue inhibitor of metalloproteinases-3 | linkage mapping, cloned gene; model for ARMD; common British mutation; vitamin A reverses night blindness | <u>Felbor 95</u> ; <u>Felbor 97</u> ; <u>Jacobson 95</u> ; <u>Peters 95</u> ; <u>Stöhr 95</u> ; <u>Weber 94</u> ; <u>Weber 94b</u> ; <u>Wijesuriya 96</u> |

X Chromosome

| Symbol; OMIM Number | Location | Disease; Protein | Mapping Method; Comment | References |
|---|--------------------|---|--|--|
| RP23 | Xp22 | X-linked RP | linkage mapping; distinct from RP2 and RP3 | <u>Hardcastle 99a</u> |
| RS1, XLR51; <u>312700</u> | Xp22.2 | retinoschisis; protein: X-linked retinoschisis 1 protein | linkage mapping, cloned gene | <u>Bergen 93a</u> ; <u>Huopaniemi 97</u> ; <u>Retinoschisis 98</u> ; <u>Sauer 97</u> ; <u>Sieving 90</u> |
| RP15; <u>300029</u> | Xp22.13- p22.11 | X-linked RP, dominant | linkage mapping; distinct from COD1, RP2, RP3, RP6 and RS | <u>McGuire 95a</u> |
| (- - -) | Xp21-q21 | RP with mental retardation | linkage mapping; may be contiguous gene syndrome including RP2 | <u>Aldred 94</u> |
| RP6; <u>312612</u> | Xp21.3- p21.2 | X-linked RP | linkage mapping | <u>Musarella 90</u> ; <u>Ott 90</u> |
| DMD; <u>310200</u> | Xp21.2 | Oregon eye disease (probable cause); protein: dystrophin | cloned gene; exons 20-28 involved in retinal disease | <u>D'Souza 95</u> ; <u>Pillers 93</u> ; <u>Ray 92</u> |
| RPGR, RP3; <u>312610</u> | Xp21.1 | X-linked RP; X-linked CSNB (possibly); protein: retinitis pigmentosa GTPase regulator | linkage mapping, cloned gene; RPGR mutations are found in roughly 20% of RP3 cases; protein homologous to RCC1 and binds PDE-delta; mutations may affect protein localization | <u>Andréasson 97</u> ; <u>Buraczynska 97</u> ; <u>Fujita 97</u> ; <u>Hermann 96</u> ; <u>Linari 99</u> ; <u>Meindl 96</u> ; <u>Musarella 90</u> ; <u>Ott 90</u> ; <u>Roepman 96</u> ; <u>Roepman 96a</u> |
| AIED, OA2; <u>300600</u> | Xp11.4-q21 | Åland island eye disease | linkage mapping | <u>Alitalo 91</u> ; <u>Glass 93</u> ; <u>Schwartz 91</u> |
| CSNB4; <u>300071</u> | Xp11.4- p11.3 | X-linked CSNB | linkage mapping; distinct from RP2, RP3, CSNB1 and CSNB2; overlaps with COD1; 'CSNB4' also refers to rhodopsin | <u>Bergen 95</u> ; <u>Berger 95</u> ; <u>Hardcastle 97</u> |
| CSNB1; <u>310500</u> | Xp11.4- p11.3 | X-linked CSNB | linkage mapping | <u>Aldred 92</u> ; <u>Bech-Hansen 92</u> ; <u>Boycott 98</u> ; <u>Gal 89</u> ; <u>Musarella 89</u> |
| OPA2; <u>311050</u> | Xp11.4- p11.2 | X-linked optic atrophy | linkage mapping; large Dutch family | <u>Assink 97</u> |
| COD1; <u>304020</u> | Xp11.4 | X-linked cone dystrophy, 1 | linkage mapping; RP2 and RP3 excluded | <u>Bartley 89</u> ; <u>Bergen 93</u> ; <u>Dash-Modi 96</u> ; <u>Hong 94</u> ; <u>Meire 94</u> ; <u>Seymour 98</u> |
| PRD; <u>312550</u> | Xp11.3- p11.23 | retinal dysplasia, primary | linkage mapping; linked to Norrie disease, may be same locus | <u>Ravia 93</u> |
| NDP, EVR2; <u>310600</u> , <u>305390</u> | Xp11.3 | Norrie Disease; familial exudative vitreoretinopathy; protein: Norrie disease protein | linkage mapping, cloned gene; expressed in multiple tissues, function unknown; some mutations cause FEVR but evidence of genetic heterogeneity; associated with retinopathy of prematurity | <u>Berger 92</u> ; <u>Berger 92a</u> ; <u>Chen 92</u> ; <u>Chen 93</u> ; <u>Chen 93a</u> ; <u>Fuchs 94</u> ; <u>Fuchs 96</u> ; <u>Fullwood 93</u> ; <u>Isashiki 95</u> ; <u>Meindl 92</u> ; <u>Meindl 95</u> ; <u>Rehm 97</u> ; <u>Schuback 95</u> ; <u>Shastry 95</u> ; <u>Shastry 97</u> ; <u>Shastry 97a</u> ; <u>Shastry 97b</u> ; |

| | | | | |
|---|--------------|--|--|---|
| | | | | <u>Strasberg 95</u> |
| RP2; <u>312600</u> | Xp11.3 | X-linked RP; protein: novel protein with similarity to human cofactor C | linkage mapping, cloned gene; human cofactor C is involved in beta-tubulin folding; accounts for 10% of XIRP | <u>Bhattacharya 84</u> ; <u>Hardcastle 99</u> ; <u>Schwahn 98</u> ; <u>Teague 94</u> ; <u>Thiselton 96</u> |
| CSNB2, CSNBX2, CACNA1F; <u>300071</u> , <u>300110</u> | Xp11.23 | X-linked CSNB, incomplete; protein: L-type voltage-gated calcium channel, alpha-1 subunit | linkage mapping, cloned gene; distinct from CSNB1; includes large Mennonite family; CACNA1F is retinal-specific | <u>Bech-Hansen 98</u> ; <u>Bech-Hansen 98a</u> ; <u>Bergen 94</u> ; <u>Bergen 95</u> ; <u>Bergen 96</u> ; <u>Boycott 98</u> ; <u>Strom 98</u> |
| PGK1; <u>311800</u> | Xq13.3 | RP with myopathy; protein: phosphoglycerate kinase | cloned gene; one case only - RP is not usually found with PGK deficiency | <u>Tonin 93</u> |
| CHM, REP1; <u>303100</u> | Xq21.1-q21.3 | choroideremia; protein: geranylgeranyl transferase Rab escort protein 1 | linkage mapping, cloned gene; ubiquitously expressed protein (REP2 can substitute); attaches isoprenoids to Rab (e.g. Rab 27) proteins | <u>Andres 93</u> ; <u>Beaufrère 96</u> ; <u>Cremers 90</u> ; <u>Seabra 93</u> ; <u>van Bokhoven 94</u> ; <u>van Bokhoven 94a</u> ; <u>van den Hurk 92</u> ; <u>van den Hurk 97</u> |
| RP24; <u>300155</u> | Xq26-q27 | X-linked RP | linkage mapping; single large family; RP2, RP3 and RP15 excluded | <u>Gieser 98</u> |
| COD2, XLPCD; <u>300085</u> | Xq27 | X-linked progressive cone dystrophy, 2 | linkage mapping | <u>Bergen 97</u> |
| CBP, RCP; <u>303900</u> | Xq28 | protanopia and rare dystrophy in blue cone monochromacy; protein: red cone opsin | cloned gene; Ala180Ser polymorphism with spectral shift | <u>Nathans 86</u> ; <u>Nathans 92</u> |
| CBD, GCP; <u>303800</u> | Xq28 | deuteranopia and rare retinal dystrophy in blue cone monochromacy; protein: green cone opsin | cloned gene; one to five copies 3' to red pigment gene or more complex organization | <u>Nathans 86</u> ; <u>Nathans 92</u> ; <u>Neitz 95</u> ; <u>Winderickx 92</u> |

Mitochondrion

| Symbol; OMIM Number | Location | Disease; Protein | Mapping Method; Comment | References |
|---|---------------|---|--|---|
| KSS; <u>535000</u> | mitochondrion | Kearns-Sayre syndrome including retinal pigmentary degeneration | sequencing; mutations in ATPase subunit 6 or multiple large deletions | <u>OMIM 98</u> ; <u>Puattu 93</u> ; <u>Wallace 92</u> |
| LHON; <u>535000</u> | mitochondrion | Leber hereditary optic neuropathy; protein: several mitochondrial proteins | sequencing; three mutations (nt 3460, 11778 and 14484) account for 95% of European cases and one (11778) for 80% of Japanese cases; penetrance influenced by mtDNA haplotype; uncertain role of rare variants; spontaneous recovery possible | <u>Brown 92</u> ; <u>Brown 97</u> ; <u>Hofmann 97</u> ; <u>Howell 97</u> ; <u>Howell 98</u> ; <u>Huoponen 93</u> ; <u>Mashima 93</u> ; <u>Nikoskelainen 96</u> ; <u>OMIM 98</u> ; <u>Riordan-Eva 95</u> ; <u>Torroni 97</u> ; <u>Wallace 88</u> |
| MTTL1, DMDF; <u>520000</u> , <u>590050</u> | mitochondrion | macular pattern dystrophy with type II diabetes and deafness; protein: leucine tRNA 1 (UUA/G) | sequencing; one of two mitochondrial leucine tRNAs; often caused by heteroplasmic A3243G mutation; other mutations can cause a similar disease | <u>Bonte 97</u> ; <u>Harrison 97</u> ; <u>Massin 95</u> ; <u>van den Ouweland 92</u> |
| MTTS2; <u>590085</u> , <u>601850</u> , <u>180103</u> | mitochondrion | RP with progressive sensorineural hearing loss; protein: serine tRNA 2 (AGU/C) | linkage mapping, sequencing; one of two mitochondrial serine tRNAs; Irish family; previously mapped to 9q as <u>RP21</u> | <u>Mansergh 99</u> |